2003

# Mechanistic study of oxygen atom transfer catalyzed by rhenium compounds

Xiaopeng Shan
*Iowa State University*

# Mechanistic study of oxygen atom transfer catalyzed by rhenium compounds

by

Xiaopeng Shan

A dissertation submitted to the graduate faculty

in partial fulfillment of the requirements for the degree of

DOCTOR OF PHILOSOPHY

Major: Inorganic Chemistry

Program of Study Committee:
James H. Espenson, Major Professor
Douglas K. Finnemore
William S. Jenks
John G. Verkade
Keith Woo

Iowa State University

Ames, Iowa

2003

ProQuest Information and Learning Company
300 North Zeeb Road
P.O. Box 1346
Ann Arbor, MI 48106-1346

Graduate College
Iowa State University

This is to certify that the doctoral dissertation of

Xiaopeng Shan

has met the dissertation requirements of Iowa State University

Signature was redacted for privacy.

Major Professor

Signature was redacted for privacy.

For the Major Program

## TABLE OF CONTENTS

# GENERAL INTRODUCTION

## Introduction

Oxygen atom transfer (OAT) catalyzed by transition metal complexes has received extensive attention from inorganic and bioinorganic chemists for decades due to its contribution to biochemistry and industrial applications.[1-3] Molybdenum(IV/VI) and tungsten(IV/VI) complexes have been widely explored because of their important roles in oxo-transferases.[2,4-6] To the contrary, rhenium(V/VII), as a neighbor, only has been explored only to a limited extent.[7]

A rhenium(V) dimer, $\{MeReO(mtp)\}_2$, a model of a proposed intermediate for sulfur transfer reaction, was synthesized from methyltrioxorhenium(VII), abbreviated MTO, and $mtpH_2$, 2-(mercaptomethyl) thiophenol ($o$-$HSC_6H_4CH_2SH$).[8] Lewis bases, pyridines and phosphanes, were found to monomerize $\{MeReO(mtp)\}_2$, giving rise to MeReO(mtp)L (L = Lewis base).[9-11] All of these rhenium(V) complexes are able to catalyze OAT reactions, especially $MeReO(mtp)PPh_3$, showing remarkable reactivity for reaction between pyridine N-oxides and phsophanes in eq 1.[12-14]

$$PyO + PZ_3 \rightarrow Py + OPZ_3 \qquad (1)$$

A notable feature of these rhenium(V) complexes is the five-coordinate distorted square pyramidal structure in chart 1. The rhenium atom is surrounded by the terminal oxo group at the axial position and a basal plane defined by a methyl, two thiolate and one thioether sulfur atom for the dimer, or a Lewis base for monomers. There is vacant position trans to the terminal oxo group, from which substrates access rhenium as well as the departure of the products.

**Chart 1**

| | |
|---|---|
| 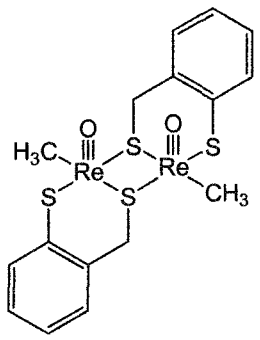 | 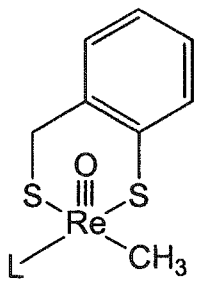 |
| {MeReO(mtp)}$_2$ | MeReO(mtp)L |

Aside from studies on OAT, in Chapter I, we described an unique methyl transfer from rhenium to thiolate sulfur, which occurs during the oxidation of $MeReO(edt)PPh_3$ with sulfoxides and the reaction of MTO with 1,2-ethanedithiol as well. Only a few precedents exist for this type of methyl transfer. An example is the conversion of D,L-homocystein, $HS(CH_2)_2CHNH_2CO_2H$, to L-methionine, $MeS(CH_2)_2CHNH_2CO_2H$ with methylcobalamin and methylcobinamide, which is catalyzed by Vitamin $B_{12}$, modeled by methyl-bis(dimethylglyoximato)cobalt(III) and related complexes which are able to convert thiols to thioethers. The new reactions of rhenium complexes, reported in Chapter I, give sound evidence for the analogous conversion, which affords further mechanistic understanding of methyl transfer. Although the structure of $ReO(\kappa^2\text{-edt})(\kappa^2\text{-edtMe})$ was unsolved, evidence from NMR, UV spectra for oxidation products by $H_2O_2$ and structure of further ligand displacement product of $ReO(\kappa^2\text{-edt})(\kappa^1\text{-edtMe})TPA$ all proved that the methyl group, originally on rhenium in $MeReO(edt)PPh_3$ or MTO, transfers to thiolate sulfur. On the basis of kinetic information and a literature study, a reductive methyl transfer mechanism was proposed.

Often a monoanionic bidentate ligand is employed for the study of the coordination chemistry of rhenium for the radiotherapeutic applications of the β-emitting isotopes $^{186}Re$

and $^{188}Re$, containing a $\{Re^{V}O\}$ core without methyl group. Typical donor atom pairs are P,O (HPO = phosphinocarboxylic acid); N,O (HNO = e.g., picolinic acid or 8-hydroxyquinoline); and N,S (HNS = 2-mercaptoquinoline). In Chapter II, we described syntheses and characterization of four methyloxorhenium(V) complexes: $MeReO(PA)_2$, $MeReO(HQ)_2$, $MeReO(MQ)_2$, and $MeReO(DPPB)_2$ (in which PAH = 2-picolinic acid, HQH = 8-hydroxyquinoline, MQH = 8-mercaptoquinoline, and DPPBH = diphenylphosphinobenzoic acid). These compounds catalyze the sulfoxidation of thioethers by pyridine N-oxides and sulfoxides. Here we report kinetic and mechanistic studies of the latter reaction. The trapping of a transient dioxorhenium(VII) species was performed.

To extend our exploration of rhenium catalysts, in Chapter III we describe the formation and characterization of three methyl(oxo)rhenium(V) complexes; two contain the anion $MeReO(edt)(SPh)^-$ with the cations 2-picolinium and 2,6-lutidinium, and the third is a neutral rhenium compound, MeReO(edt)(tmtu), where edt stands for 1,2-ethanedithiolate and tmtu for 1,1,3,3-tetramethylthiourea. To understand the OAT process catalyzed by $MeReO(mtp)PPh_3$, which is described early, it is important to investigate the steps of OAT from pyridine N-oxides to rhenium catalyst separately, including a study of the intermediates MeReO(edt)PyO from ligand displacement and $MeReO_2(edt)PyO$ from oxidation. An especially the striking feature is that nucleophiles assist oxidation by incorporation of a second molecule of pyridine N-oxide in the transition state. The ionic compound was found to be suitable for this purpose because formation of both intermediates can be clearly separated and kinetically investigated. To extend an understanding of ligand displacement, the non-oxidizing ligands pyridines and $PPh_3$ were employed as well. An unanticipated assistance of ligand displacement of ionic compound by Brønsted bases was discovered and studied.

As an essential step in OAT and an important part of rhenium chemistry, ligand displacement has attracted our attention. In Chapters IV and V, kinetic and equilibrium studies of ligand displacements of MeReO(dithiolato)Py and $ReO(\kappa^2\text{-edt})(\kappa^2\text{-edtMe})$ were performed. In Chapter IV, equilibrium and rate constants have been determined for this family of ligand displacement reactions of previously-prepared five-coordinate, square-pyramidal rhenium(V) complexes:

$$MeReO(dt)Py + PZ_3 = MeReO(dt)(PZ_3) + Py \quad (2)$$

In this equation, $PZ_3$ denotes a generalized phosphane (Z = aryl, alkyl), often $P(C_6H_4\text{-}4\text{-}Y)_3$ with subsituent Y, Py is a generalized pyridine, $4\text{-}X\text{-}C_5H_4N$ with subsituent X and dt represents either 1,2-ethanedithiolate or 1,3-propanedithiolate. We have evaluated equilibrium constants for reaction 2, and correlated them by a two-variable linear free-energy relationship. The rate constants for eq 2 were also evaluated, but their interpretation was less straightforward. A multiple-substituent correlation analysis, authenticated for certain organic reactions, was not particularly satisfactory. The answer lies in a multiple step mechanism, in which the rate controlling step may vary with the influence of the substituent on the entering ligand.

In Chapter V, we report the kinetics and mechanism of ligand (phosphane) displacement (eq 3) of the thioether sulfur to generate a phosphane-rhenium(V) compound.

$$ReO(\kappa^2\text{-edt})(\kappa^2\text{-edtMe}) + PZ_3 = ReO(\kappa^2\text{-edt})(\kappa^1\text{-edtMe})(PZ_3) \quad (3)$$

Hammett analysis for both equilibrium and rate constants revealed that an early transition state was involved in the reaction. Also, sulfur inversion of the thioether ligand has been observed as a line-broadening effect of proton residual of the methyl on thiolate sulfur. A planar intermediate was proposed for sulfur inversion, derived from the comparison of activation energy parameters of ligand displacement and sulfur inversion.

The study of OAT catalyzed by rhenium(V) complexes revealed that the oxidation of rhenium(V) complexes to rhenium(VII) is an essential step in the catalytic cycle. Steric demand is always an important issue for such catalysts. Different ligands for rhenium(V) complexes have been employed, especially those with "3+1", "3+2" and "3+1+1" coordination shells, where "3", "2", "1" represent tri-, bi-, and mono-dentate ligands. They differ in geometry as well as coordination number. In Chapter VI, we describe the syntheses and characterization of four new rhenium(V) compounds with tridentate chelating ligands: 2-mercaptoethyl thioether, 2-mercaptoethyl ether, thioldiglycolic acid and 2-(salicylideneamino)benzoic acid, abbreviated as HSSSH, HSOSH, HOSOH and HONOH respectively. Compounds MeReO(SSS) and MeReO(SOS) have a five-coordinate distorted pentagonal pyramidal geometry about rhenium. To the contrary, $MeReO(OSO)(PZ_3)$ and $MeReO(ONO)(PPh_3)$ are six-coordinate compounds with distorted octahedral structures. The

oxidation of three of these compounds was investigated and followed different rate laws. These mechanistic differences have been interpreted as reflecting the different steric demands of five- and six-coordination shells.

During the period 1998-2003, around two dozen rhenium complexes were synthesized and characterized in our group. In Chapter VII, we summarized the syntheses of rhenium complexes including some unpublished results. The criteria for syntheses were discussed as well, which lie in two issues. First, rhenium(VII) in MTO needs to be reduced to rhenium(V). Usually thiols, phosphanes and even sulfides were employed as reducing reagent. Second, suitable ligands must be used to stabilize rhenium(V). As is well known, methyldioxorhenium(V) does not persist in solution, but it can be readily oxidized by oxidants such as dioxygen, pyridine N-oxides, sulfoxides, nitrate and even perchlorate etc.[15,16] Without an oxidant, a black precipitate was observed as the product of polymerization of methyldioxorhenium(V).[17]

**Dissertation Organization**

This dissertation consists of seven Chapters. Chapter I has been published in *Angewandte Chemie International Edition*. Chapter II has been published in *Inorganic Chemistry*. Chapter III has been submitted to *Inorganic Chemistry*. Chapter IV has been submitted to *Dalton transactions*. Chapter V has been published in *Organometallics*. Chapter VI has been published in *Inorganic Chemistry*. Chapter VII contains part of a manuscript submitted to *Inorganic Synthesis*. Each Chapter is self-contained with its own equations, figures, tables, references, and supporting information. Following the last Chapter are general conclusions. Except for the X-ray structural analysis and several synthetic procedures in Chapter VII, all the work in this dissertation was performed by the author of this thesis, Xiaopeng Shan.

**References**

(1) Bernadou, J.; Meunier, B. *Chem. Commun.* **1998**, 2167-2173.

(2) Young, C. G.; Wedd, A. G. *Chem. Commun.* **1997**, 1251-1257.

(3) Holm, R. H. *Chem. Rev.* **1987**, *87*, 1401-1449.

(4) Hille, R. *Trends Biochem. Sci.* **2002**, *27*, 360-367.

(5) Holm, R. H. *Coord. Chem. Rev.* **1990**, *100*, 183-221.

(6) Arzoumanian, H. *Coord. Chem. Rev.* **1998**, *178-180*, 191-202.

(7) Arias, J.; Newlands, C. R.; Abu-Omar, M. M. *Inorg. Chem.* **2001**, *40*, 2185-2192.

(8) Jacob, J.; Guzei, I. A.; Espenson, J. H. *Inorg. Chem.* **1999**, *38*, 1040-1041.

(9) Lente, G.; Shan, X.; Guzei, I. A.; Espenson, J. H. *Inorg. Chem.* **2000**, *39*, 3572-3576.

(10) Lente, G.; Guzei, I. A.; Espenson, J. H. *Inorg. Chem.* **2000**, *39*, 1311-1319.

(11) Jacob, J.; Lente, G.; Guzei, I. A.; Espenson, J. H. *Inorg. Chem.* **1999**, *38*, 3762-3763.

(12) Wang, Y.; Espenson, J. H. *Inorg. Chem.* **2002**, *41*, 2266-2274.

(13) Wang, Y.; Espenson, J. H. *Org. Lett.* **2000**, *2*, 3525-3526.

(14) Lente, G.; Espenson, J. H. *Inorg. Chem.* **2000**, *39*, 4809-4814.

(15) Abu-Omar, M. M.; Espenson, J. H. *Inorg. Chem.* **1995**, *34*, 6239-6240.

(16) Abu-Omar, M. M.; Appelman, E. H.; Espenson, J. H. *Inorg. Chem.* **1996**, *35*, 7751-7757.

(17) Espenson, J. H.; Yiu, D. T. Y. *Inorg. Chem.* **2000**, *39*, 4113-4118.

# CHAPTER I. METHYL TRANSFER FROM RHENIUM TO COORDINATED THIOLATE GROUPS

A communication published in *Angewandte Chemie International Edition*

Xiaopeng Shan, Arkady Ellern and James H. Espenson

A prominent reaction of Vitamin $B_{12}$ is the conversion of D,L-homocystein, $HS(CH_2)_2CHNH_2CO_2H$, to L-methionine, $MeS(CH_2)_2CHNH_2CO_2H$ with methylcobalamin and methylcobinamide.[1-4] Methyl-bis(dimethylglyoximato)cobalt(III) and related complexes also convert thiols to thioethers.[5]

$$Co^{III}\text{–}CH_3 + RSH \rightarrow [Co^{I}]^- + RSCH_3 + H^+ \qquad (1)$$

There are, however, a lack of precedents in the literature that do not involve organocobalt complexes. In this work, new reactions of rhenium complexes have been examined, and sound evidence for the analogous conversion has now been obtained.

**Chart 1**

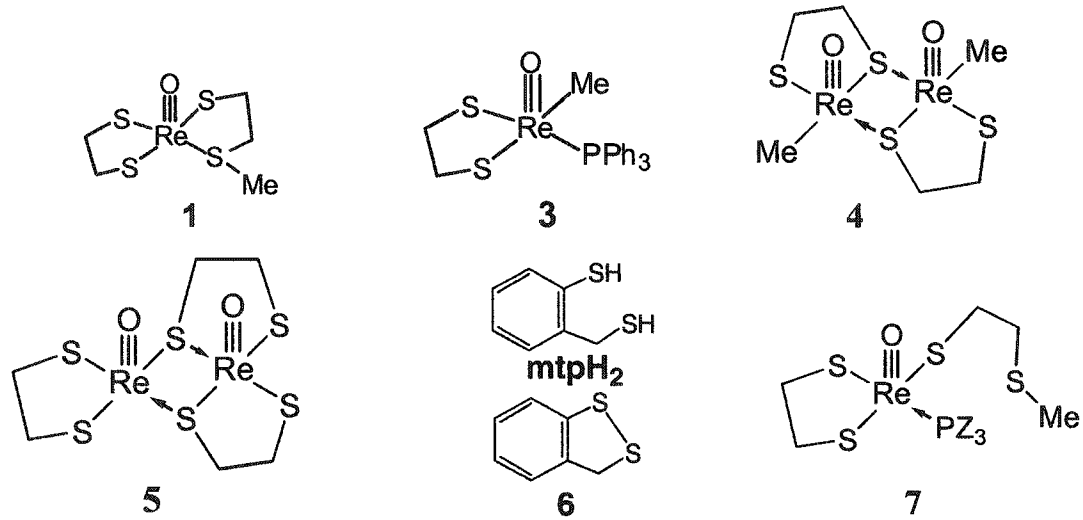


$MeReO_3$ (MTO, **2**)[6] reacts with the readily-oxidized $mtpH_2$, 2-(mercaptomethyl)-thiophenol ($mtpH_2$), to yield a disulfide (eq. 2):

$$2\ MeReO_3 + 4\ mtpH_2 \rightarrow 4 + 2\ (\mathbf{6}) + 4\ H_2O \qquad (2)$$

With 1,2-ethanedithiol, however, a quite different result was obtained. As $Re^{VII}$ was reduced to $Re^{V}$, one $edtH_2$ molecule was transformed to $HS(CH_2)_2SMe$, which remains coordinated to rhenium(V) through both sulfur atoms in a $\kappa^2$ fashion (eq. 3):

$$MeReO_3 + 2\ edtH_2 \rightarrow\ 1 + 2\ H_2O \qquad (3)$$

Details of the synthesis and characterization of the dark red compound **1** are given in the Experimental Section. A similar reaction starting with [MeReO(edt)($PPh_3$)], **3**,[7] gave the same product in lower yield. Crystals of **1** suitable for x-ray diffraction could not be obtained. We have formulated composition of **1** as ReO($\kappa^2$-edt)($\kappa^2$-edtMe) on the basis of the elemental analysis and spectroscopic data. An alternative formulation as an organorhenium(VII) compound, $MeReO(edt)_2$, could not be ruled out by these data, although there was faint evidence in favor of structure **1**, in that the $CH_3$ resonance appeared at $\delta$ 1.90 ppm, which is further downfield than would be expected for a methyl group coordinated to a $Re^{VII}$ center. Indeed, the proposed mechanism suggests that $MeReO(edt)_2$ lies on the pathway to **1**.

Chemical methods were therefore used to obtain information about the molecular structure of **1**, particularly with respect to whether the Me–Re interaction present in the starting materials is retained. Its reaction of **1** with $H_2O_2$ in wet acetonitrile gave $ReO_4^-$ ions, which are easily recognized from its characteristic UV spectrum. The same product was obtained from **5**, another compound that lacks a Me–Re bond. In contrast, several compounds that do contain a Me–Re group (**2**, **3** and **4**) clearly reacted with hydrogen peroxide to form [MeReO($\kappa^2$-$O_2$)$_2$($OH_2$)], with a characteristic absorption maximum at 360 nm ($\varepsilon$ = 1200). Thus, these results suggest that no Me-Re bond exists in **1**.[8]

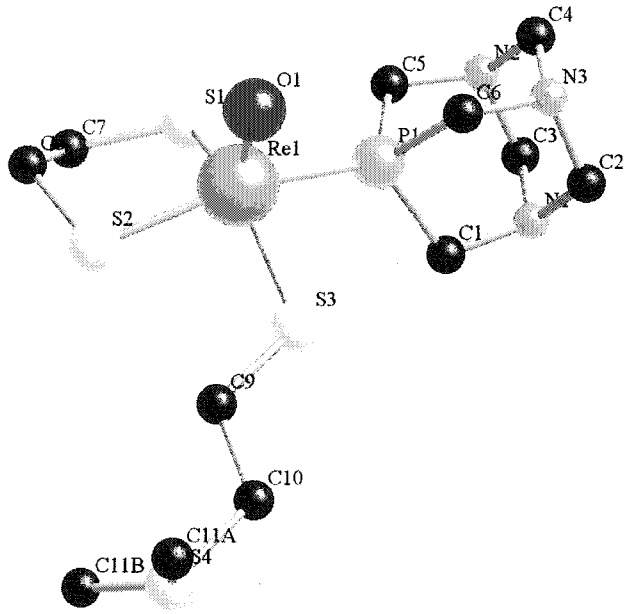


**Figure 1**. The molecular structure of [ReO($\kappa^2$-edt)($\kappa^1$-edtMe)(PTA)]. The methyl group at $S_4$ was disordered; the structure was refined at 50% occupancy of the two sites. Selected bond lengths (pm) and angles (°) are: Re–O, 170.05(5); Re–S(3), 230.54(17); Re–P, 242.25(18); S(4)–C(10), 181.0(9); S(4)–C11A, 175.6(17); S(4)–C(11B), 184.0(4). O–Re–S(3), 110.68(19); O–Re–P, 97.3(2); S(2)–Re–P, 153.94(6); S(1)–Re–S(3), 133.58(7); C(10)–S(4)–C(11A), 102.7(7); C(10)–S(4)–C(11B), 104.3(17); C(11A)–S(4)–C(11B), 133.1(14). The structure was drawn with the program CrystalMaker.[14]

The reaction of compound **1** with phosphanes ($PZ_3$, in general) yields a new series of compounds, [ReO($\kappa^2$-edt)($\kappa^1$-edtMe)($PZ_3$)] (**7**) in which the thioether arm has been displaced. One such compound, where $PZ_3$ = 1,3,5-triaza-phosphaadmantane (PTA),[9] has been characterized crystallographically; the molecular structure is displayed in Figure 1. Phosphanes are generally much stronger Lewis bases than thioethers and will, to a great extent, displace RSR' group. In keeping with this fact, the equilibrium constant for $PPh_3$ ($K_4$,

eq. 4) is $6 \times 10^5$ ($C_6H_6$, 25 °C),[10] whereas that for eq. 5 is 8.0 under the same conditions. The large difference in theses values arises from the chelate effect, and illustrates its very substantial importance in this case.

$$MeReO(edt)(Me_2S) + PPh_3 \rightarrow MeReO(edt)PPh_3 + Me_2S \qquad K_4 \ (4)$$

$$\mathbf{1} + PPh_3 = ReO(\kappa^2\text{-edt})(\kappa^1\text{-edtMe})(PPh_3) \qquad K_5 \ (5)$$

The formation of **1**, as shown in reaction (3), follows the net 1:2 stoichiometry given. It is a sequential process that obeys the rate law (eq. 6):

$$d[\mathbf{1}]/dt = k \times [\mathbf{2}] \times [edtH_2] \qquad (6)$$

with $k = 7.3 \times 10^{-2}$ L mol$^{-1}$ s$^{-1}$ ($Me_2SO$, 25 °C). Clearly the first condensation step is rate determining, as the methylation step occurs more rapidly and is not manifest in the kinetics. The sequential mechanism proposed is given in Scheme 1. The final step appears to involve nucleophilic attack of the coordinated thiolate sulfur on the methyl group of the intermediate. Precedents for this mechanism, aside from those found in organocobalt systems, are rare. While the transfer of a phenyl group to an oxo group of an intermediate species ($[TpRe(O)_2Ph]^+$, Tp = hydrotris(1-pyrazoly)borate) represents a distantly related example;[11] a more relevant case is the thermal decomposition of $[MeReO(\kappa^2\text{-}O_2)_2(OH_2)]$, which yields MeOOH and $HReO_4$.[12]

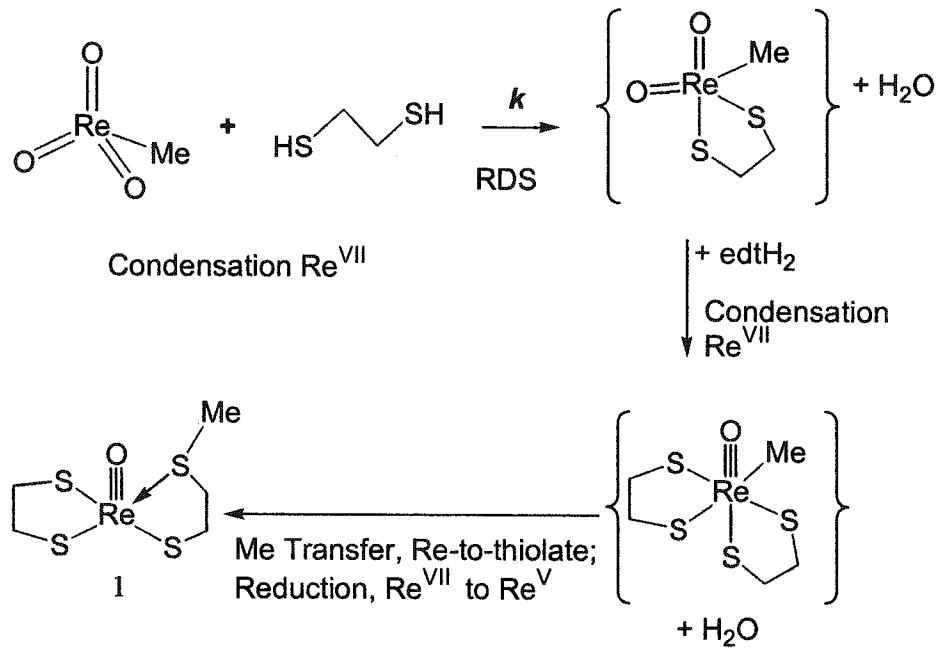


**Scheme 1**. Proposed mechanism for the formation of **1** (RDS = rate-determining step)

In summary, a novel transformation of MeRe(edt) complex to give a Re(thiolate-methylthioether) complex (**1**) has been discovered and established. This transformation is without precedent, aside from the homocystein-to-methionine transformation found for Vitamin $B_{12}$ and its mimics. Furthermore, the thioether group can be replaced by a phosphane; the derivative with PTA was characterized crystallographically. All of these reactions proceed to equilibrium, but owing to the chelate effect, the equilibrium constants are smaller by a factor of $10^5$ than the analogous values of K for the displacement of a nonchelated RSR' group.

**Experimental Section**

Synthesis of [ReO($\kappa^2$-edt)($\kappa^2$-edtMe)], **1**. Dimethylsulfoxide (0.2 mmol) was added to 5 mL of toluene containing 0.5 mmol of **2**. 1,2-Ethane dithiol (0.5 mmol) was added, whereupon the mixed solution turned red. After 4 h, 10 mL of hexanes was layered on top resulting in a deep red solid (87% yield) which was purified by recrystallization from methylene chloride-hexanes. Elemental analysis, $C_5H_{11}OReS_4$. Found C: 15.16 (14.95 calcd.), H: 2.82 (2.76); S: 32.09 (31.94). $^1$H NMR: (400 MHz, [$D_6$]benzene, 25 °C): $\delta$=3.55(m, 1H; $CH_2$), 3.36(m, 1H; CH), 2.70(m, 1H; $CH_2$), 2.51(m, 2H, $CH_2$), 2.11(m, 1H; $CH_2$), 1.92(m, 1H; $CH_2$), 1.90(s, 3H, $CH_3$), 0.84(m, 1H; $CH_2$); $^{13}$C NMR(400 MHz, [$D_6$]benzene, 25 °C): $\delta$= 45.6, 45.0, 43.5, 36.2, 22.3; UV/Vis (benzene): $\lambda_{max}$ ($\varepsilon$) = 510 nm (16$\tilde{6}$), 389 nm (3400).

Synthesis of [ReO($\kappa^2$-edt)($\kappa^1$-edtMe)(PTA)]. A 1:1 reaction between **1** and PTA in toluene gave dark, shiny single crystals after recrystallization from toluene-hexanes. Elemental Analysis: $C_{11}H_{23}ON_3PReS_4$. C: 23.57 (23.65 calcd), H: 4.12 (4.15), N: 7.55 (7.52), S: 23.25 (22.96), P: 5.61 (5.54). $^1$H NMR (400 MHz, [$D_6$]benzene, 25 °C), $\delta$ = 4.34(m, 1H; $CH_2$), 4.21(m, 7H; $CH_2$), 3.86(m, 6H; $CH_2$); 3.43(m, 1H; $CH_2$), 3.34(m, 1H; $CH_2$), 3.20(m, 1H; $CH_2$), 2.97(m, 1H; $CH_2$), 2.41(m, 2H; $CH_2$), 1.98(s, 3H; $CH_3$); $^{13}$C NMR(400 MHz, [$D_6$]benzene, 25 °C): $\delta$= 72.5(d, J(C, P) = 7 Hz), 51.9(d, J(C, P) = 16 Hz), 43.6(d, J(C, P) = 8 Hz), 42.0(s), 37.2(s), 35.5(d, J(C, P) = 9 Hz), 15.3(s); $^{31}$P NMR(400 MHz, [$D_6$]benzene, 25 °C): $\delta$= –74.0; UV/Vis (benzene) $\lambda_{max}$ ($\varepsilon$) = 386 nm (1900), 318 nm (1600; sh), 262 nm (3$\tilde{8}$).

**References:**


(1) J. R. Guest, S. Friedman, D. D. Woods, E. L. Smith, *Nature* **1962**, *195*, 340.

(2) J. R. Guest, S. Friedman, M. J. Dilworth, D. D. Woods, *Ann. New York Acad. Sci.* **1964**, *112*, 774.

(3) M. L. Ludwig, R. G. Matthews, *Annu. Rev. Biochem.* **1997**, *66*, 269-313.

(4) R. G. Matthews, *Acc. Chem. Res* **2001**, *34*, 681-689.

(5) G. N. Schrauzer, R. J. Windgassen, *J. Am. Chem. Soc.* **1968**, *89*, 3067.

(6) W. A. Herrmann, R. M. Kratzer, R. W. Fischer, *Angew. Chem. Int. Ed. Engl.* **1997**, *36*, 2652-2654.

(7) G. Lente, X. Shan, I. A. Guzei, J. H. Espenson, *Inorg. Chem.* **2000**, *39*, 3572-3576.

(8) Each compound was treated with 30% hydrogen peroxide to give a final concentration of 38 mM $H_2O_2$ in acetonitrile. The final spectra from these procedures confirming the two indicated Re(VII) products are given in the Supporting Information.

(9) D. J. Darensbourg, T. J. Decuir, J. H. Reibenspies, *NATO ASI Ser., Ser. 3* **1995**, *5*, 61-80.

(10) This equilibrium constant applies to the analogue of **3**, with mtp instead of edt, where $mtpH_2$ is 2-(mercaptomethyl)thiophenol. The terms contributing to $K_1$ are given in the Supporting Information.

(11) S. N. Brown, J. M. Mayer, *J. Am. Chem. Soc.* **1996**, *118*, 12119-12133.

(12) W.-D. Wang, J. H. Espenson, *Inorg. Chem.* **1997**, *36*, 5069-5075.

(13) D. Palmer, CrystalMaker, 2.0 ed., Hollywell Press, Bicester, Oxfordshire, **1999**.

**Supporting Information**



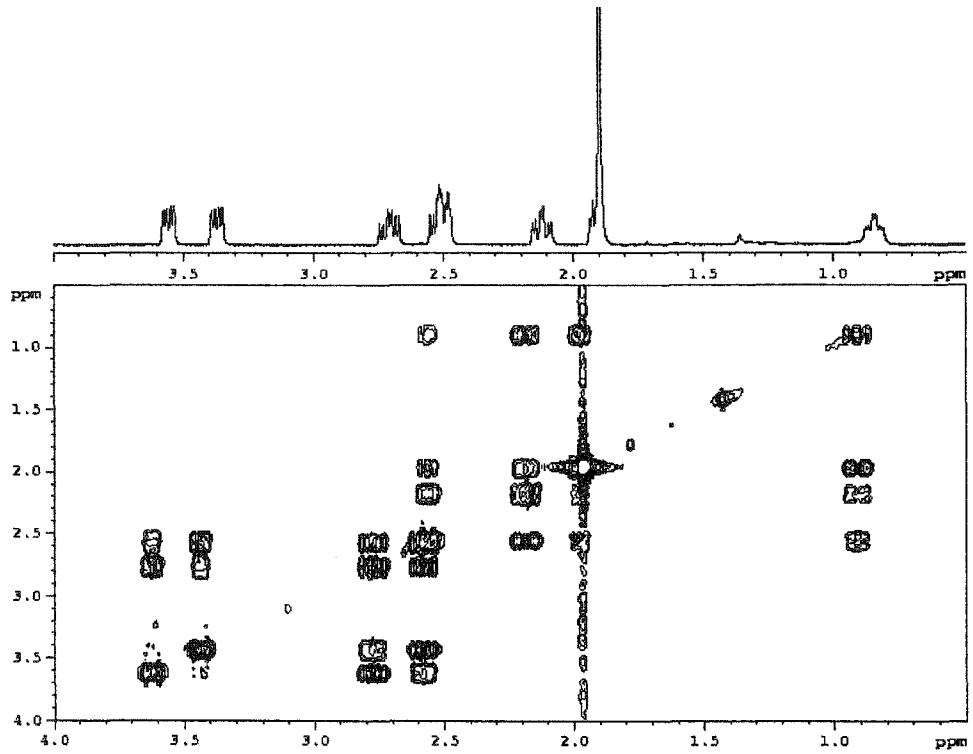


Figure S-1. NMR spectrum of $ReO(\kappa^2\text{-edt})(\kappa^2\text{-edtMe})$

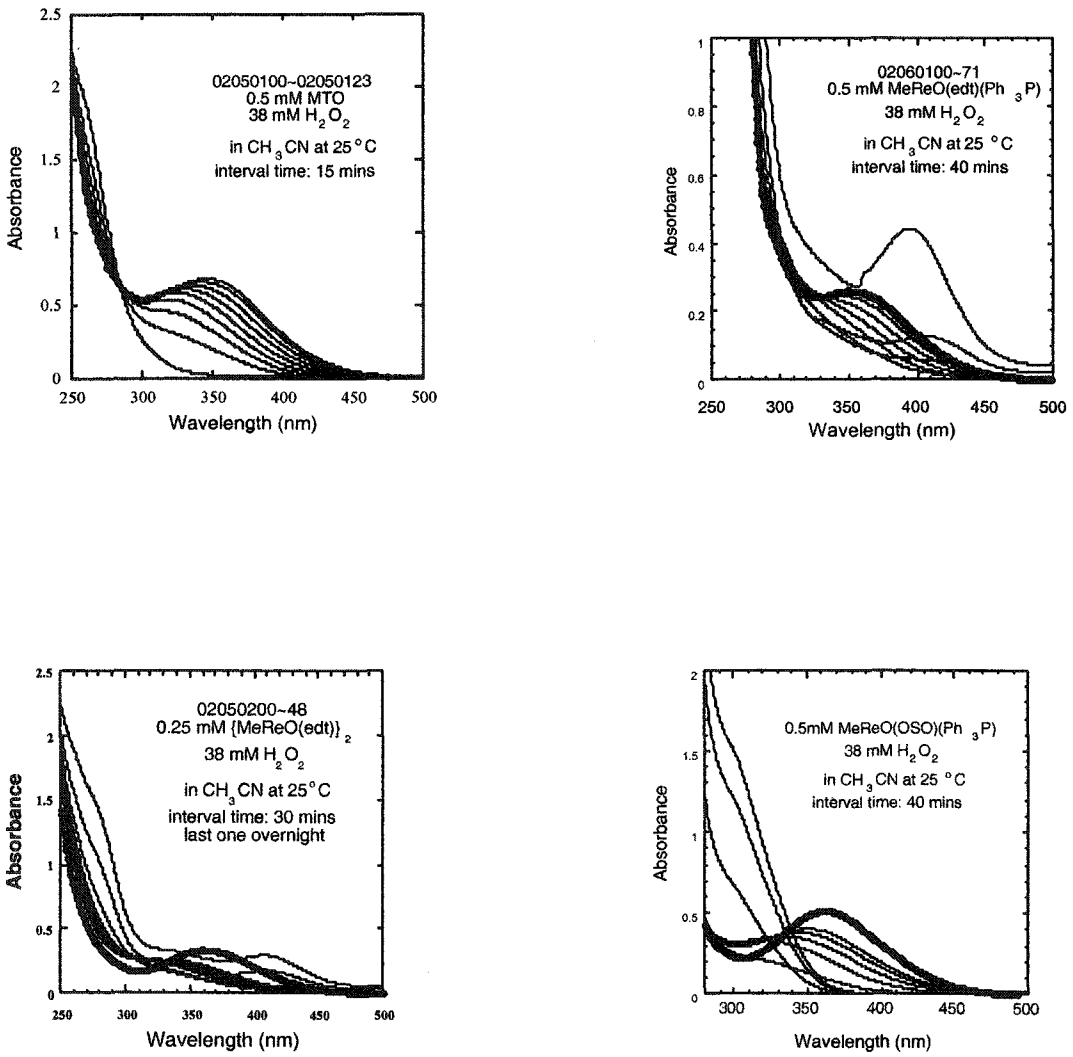


Figure S-2. A. Verification of the formation of [MeReO($\kappa^2$-$O_2$)$_2$($H_2O$)] by its maximum at 360 nm upon addition of $H_2O_2$ to different compounds containing a Me–Re bond. The final spectrum in each case is shown by the heavy line.

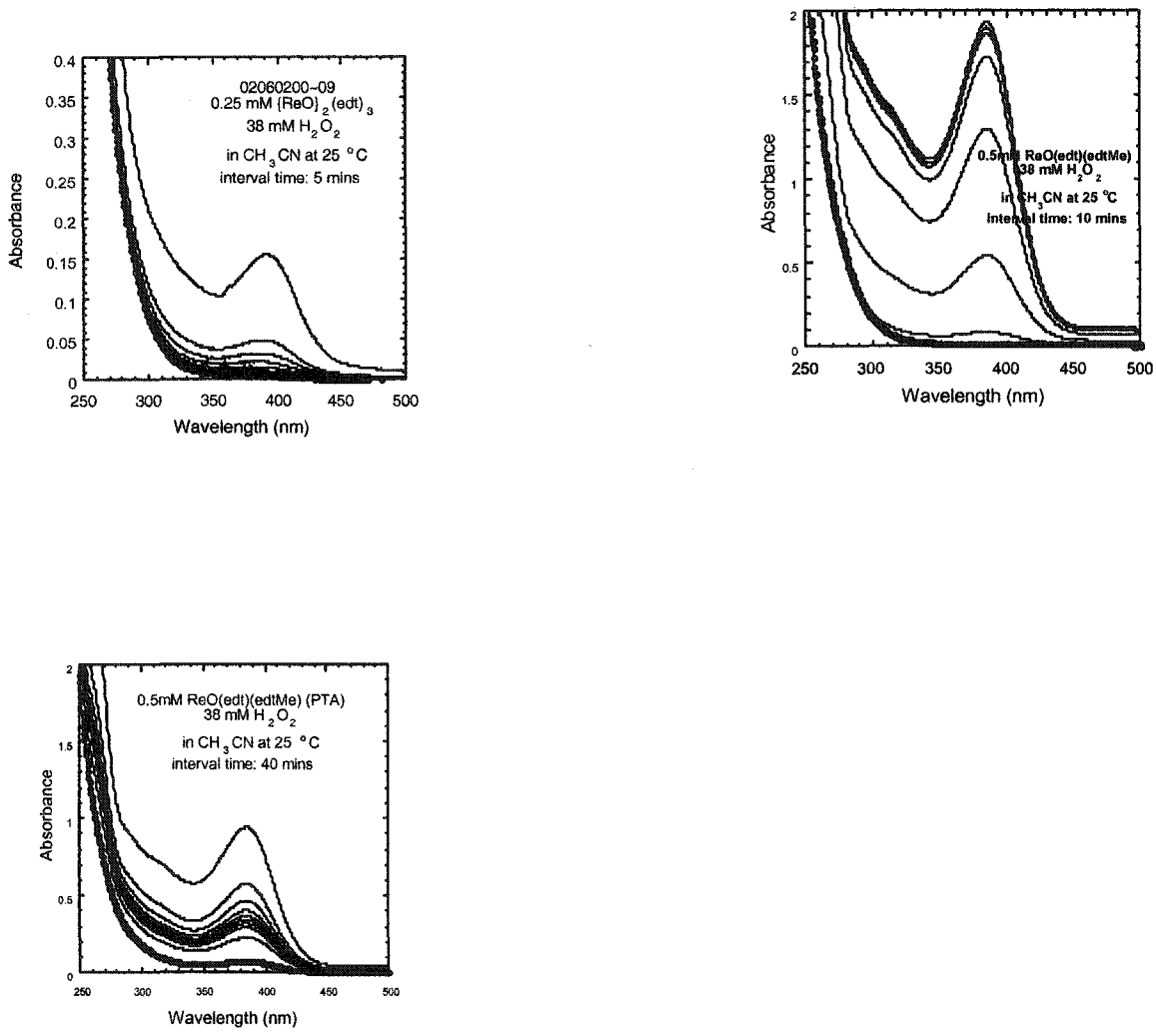


Figure S-2. B. Lack for formation of $[MeReO(\kappa^2\text{-}O_2)_2(H_2O)]$ upon addition of $H_2O_2$ to a compound lacking a Me–Re bond (left), to the compound under investigation, $ReO(\kappa^2\text{-}edt)(\kappa^2\text{-}edtMe)$, and to $[ReO(\kappa^2\text{-}edt)(\kappa^1\text{-}edtMe)(PTA)]$.

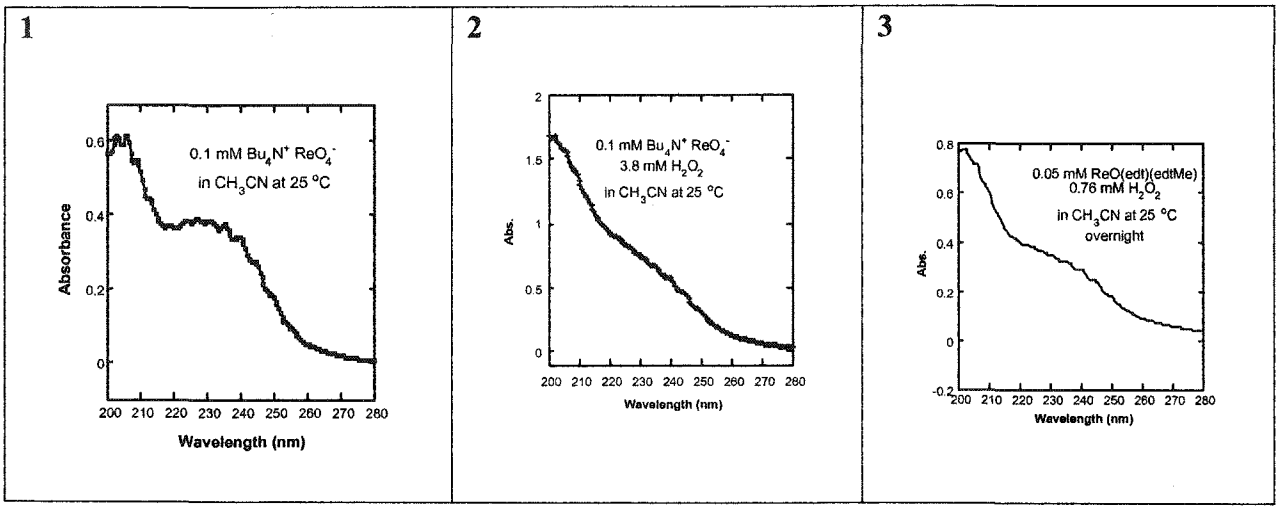


Figure S-2. C. Verification of $ReO_4^-$ from the reactions of $\{ReO\}_2(edt)_3$ and $ReO(\kappa^2\text{-edt})(\kappa^2\text{-edtMe})$ with $H_2O_2$. The UV spectrum is characteristic of $ReO_4^-$ treated with peroxide. (1) $ReO_4^-$ alone; (2) $ReO_4^-$ with $H_2O_2$; (3) 1 with $H_2O_2$

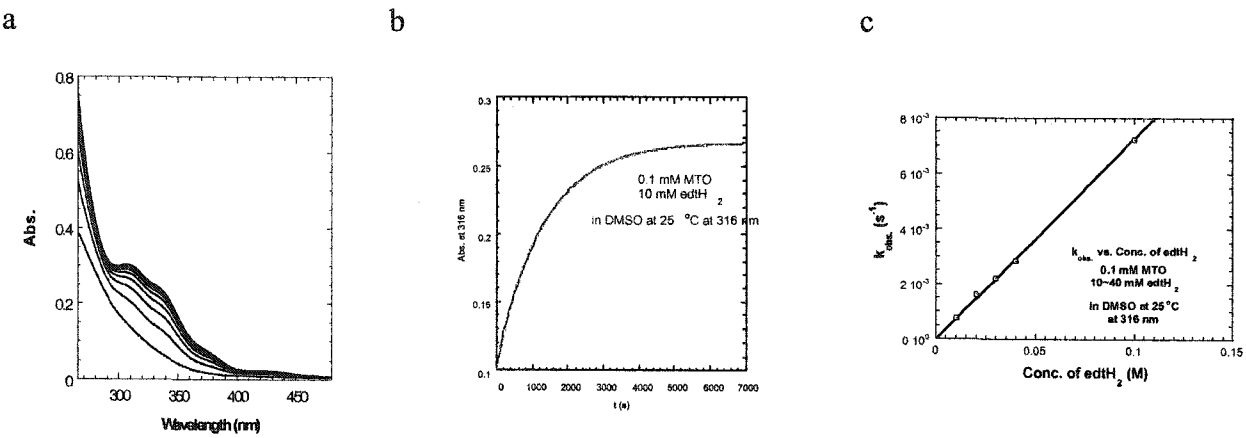


Figure S-3. Kinetic data for the reaction between $MeReO_3$ and $edtH_2$. (a) repetitive scans; (b) absorbance-time data; (c) plot of $k_\Psi$ against $[edtH_2]$.

Table S–1. Crystallographic data for ReO(edt)(edtMe)(PTA)

Part A. Crystal data and structure refinement for ReO(edt)(edtMe)(PTA).

| | |
|---|---|
| Identification code | ReO(edt)(edtMe)(PTA) |
| Empirical formula | $C_{11}H_{23}N_3OPReS_4$ |

| | | |
|---|---|---|
| Formula weight | 558.73 | |
| Temperature | 293(2) K | |
| Wavelength | 0.71073 Å | |
| Crystal system | Triclinic | |
| Space group | P-1 | |
| Unit cell dimensions | a = 6.4459(4) Å | α= 89.6710(10)°. |
| | b = 10.6334(7) Å | β= 84.4990(10)°. |
| | c = 13.4904(8) Å | γ = 77.3490(10)°. |
| Volume | 897.94(10) $Å^3$ | |
| Z | 2 | |
| Density (calculated) | 2.067 $Mg/m^3$ | |
| Absorption coefficient | 7.321 $mm^{-1}$ | |
| F(000) | 544 | |
| Crystal size | 0.20 × 0.18 × 0.05 $mm^3$ | |
| Theta range for data collection | 1.96 to 28.27°. | |
| Index ranges | $-8 \le h \le 5$, $-13 \le k \le 13$, $-17 \le l \le 17$ | |
| Reflections collected | 6486 | |
| Independent reflections | 3977 [R(int) = 0.0636] | |
| Completeness to theta = 28.27° | 89.2 % | |
| Absorption correction | Empirical | |
| Max. and min. transmission | 0.69 and 0.40 | |
| Refinement method | Full-matrix least-squares on $F^2$ | |
| Data / restraints / parameters | 3977 / 0 / 192 | |
| Goodness-of-fit on $F^2$ | 1.060 | |
| Final R indices [I>2sigma(I)] | R1 = 0.0570, wR2 = 0.1637 | |
| R indices (all data) | R1 = 0.0580, wR2 = 0.1653 | |
| Largest diff. peak and hole | 2.777 and -1.652 $e.Å^{-3}$ | |

---

$R1 = \Sigma \, | \, |F_o| - |F_c| \, | \, / \, \Sigma \, |F_o|$ and $wR2 = \{ \, \Sigma \, [ \, w(F_o^2 - F_c^2)^2 \, ] \, / \, \Sigma \, [ \, w(F_o^2)^2 \, ] \, \}^{1/2}$

Part B. Atomic coordinates ( $\times 10^4$) and equivalent isotropic displacement parameters ($Å^2 \times 10^3$) for ReO(edt)(edtMe)(PTA). U(eq) is defined as one third of the trace of the orthogonalized $U_{ij}$ tensor.

| | x | y | z | U(eq) |
|---|---|---|---|---|
| Re(1) | 1012(1) | 3752(1) | 8352(1) | 15(1) |
| S(1) | -2138(3) | 3148(2) | 8799(1) | 22(1) |
| S(2) | 2425(3) | 1573(2) | 8115(1) | 23(1) |
| S(3) | 2738(3) | 4151(2) | 6845(1) | 23(1) |
| S(4) | 7940(4) | 1716(3) | 4887(2) | 38(1) |
| P(1) | -1434(3) | 5764(2) | 8049(1) | 16(1) |
| C(1) | -1843(12) | 6386(7) | 6786(5) | 24(2) |
| C(2) | -2071(13) | 8586(7) | 7326(6) | 25(2) |
| C(3) | -5266(11) | 7784(7) | 7362(6) | 22(1) |
| C(4) | -4099(12) | 8383(7) | 8888(6) | 23(2) |
| C(5) | -4221(10) | 6141(7) | 8603(5) | 19(1) |
| C(6) | -476(11) | 7110(7) | 8565(5) | 20(1) |
| C(7) | -1601(13) | 1371(7) | 8799(7) | 28(2) |
| C(8) | 655(12) | 832(7) | 8957(6) | 23(1) |
| C(9) | 4931(14) | 2817(9) | 6412(6) | 31(2) |
| C(10) | 5790(15) | 3029(10) | 5364(6) | 35(2) |
| C(11A) | 10080(30) | 1933(17) | 5532(13) | 55(6) |
| C(11B) | 6640(60) | 350(40) | 4770(30) | 87(10) |
| N(1) | -3129(11) | 7704(6) | 6829(5) | 23(1) |
| N(2) | -5235(10) | 7500(6) | 8428(5) | 21(1) |
| N(3) | -1956(10) | 8351(6) | 8396(5) | 22(1) |
| O(1) | 2136(9) | 4286(5) | 9311(4) | 26(1) |

Atom C11 was refined as disordered by two positions C11A and C11B with occupancy factors 0.5.

Part C. Bond lengths [Å] and angles [°] for ReO(edt)(edtMe)(PTA).

| | | | |
|---|---|---|---|
| Re(1)-O(1) | 1.700(5) | P(1)-C(1) | 1.845(7) |
| Re(1)-S(1) | 2.2868(17) | C(1)-N(1) | 1.462(10) |
| Re(1)-S(3) | 2.3054(17) | C(2)-N(3) | 1.470(10) |
| Re(1)-S(2) | 2.3081(18) | C(2)-N(1) | 1.473(10) |
| Re(1)-P(1) | 2.4225(18) | C(3)-N(2) | 1.470(10) |
| S(1)-C(7) | 1.845(8) | C(3)-N(1) | 1.477(10) |
| S(2)-C(8) | 1.830(7) | C(4)-N(3) | 1.468(9) |
| S(3)-C(9) | 1.823(9) | C(4)-N(2) | 1.483(9) |
| S(4)-C(11A) | 1.756(17) | C(5)-N(2) | 1.477(9) |
| S(4)-C(10) | 1.810(9) | C(6)-N(3) | 1.480(10) |
| S(4)-C(11B) | 1.84(4) | C(7)-C(8) | 1.477(11) |
| P(1)-C(5) | 1.838(7) | C(9)-C(10) | 1.502(11) |
| P(1)-C(6) | 1.843(7) | | |

| | | | |
|---|---|---|---|
| O(1)-Re(1)-S(1) | 114.66(19) | C(5)-P(1)-Re(1) | 122.1(2) |
| O(1)-Re(1)-S(3) | 110.68(19) | C(6)-P(1)-Re(1) | 109.3(3) |
| S(1)-Re(1)-S(3) | 133.58(7) | C(1)-P(1)-Re(1) | 122.8(2) |
| O(1)-Re(1)-S(2) | 108.6(2) | N(1)-C(1)-P(1) | 111.0(5) |
| S(1)-Re(1)-S(2) | 85.06(6) | N(3)-C(2)-N(1) | 113.7(6) |
| S(3)-Re(1)-S(2) | 89.85(6) | N(2)-C(3)-N(1) | 114.0(6) |
| O(1)-Re(1)-P(1) | 97.3(2) | N(3)-C(4)-N(2) | 113.8(6) |
| S(1)-Re(1)-P(1) | 81.19(6) | N(2)-C(5)-P(1) | 110.5(5) |
| S(3)-Re(1)-P(1) | 83.86(6) | N(3)-C(6)-P(1) | 110.3(5) |
| S(2)-Re(1)-P(1) | 153.94(6) | C(8)-C(7)-S(1) | 110.3(5) |
| C(7)-S(1)-Re(1) | 108.1(3) | C(7)-C(8)-S(2) | 110.4(5) |
| C(8)-S(2)-Re(1) | 103.2(3) | C(10)-C(9)-S(3) | 110.9(6) |
| C(9)-S(3)-Re(1) | 112.7(3) | C(9)-C(10)-S(4) | 112.8(7) |
| C(11A)-S(4)-C(10) | 102.7(7) | C(1)-N(1)-C(2) | 111.3(6) |
| C(11A)-S(4)-C(11B) | 133.1(14) | C(1)-N(1)-C(3) | 111.9(6) |
| C(10)-S(4)-C(11B) | 104.3(13) | C(2)-N(1)-C(3) | 108.3(6) |

| | | | |
|---|---|---|---|
| C(5)-P(1)-C(6) | 100.1(3) | C(3)-N(2)-C(5) | 112.2(6) |
| C(5)-P(1)-C(1) | 99.3(3) | C(3)-N(2)-C(4) | 108.4(6) |
| C(6)-P(1)-C(1) | 98.9(3) | C(5)-N(2)-C(4) | 110.8(6) |
| C(2)-N(3)-C(4) | 110.0(6) | C(4)-N(3)-C(6) | 111.0(6) |
| C(2)-N(3)-C(6) | 111.0(6) | | |

Part D. Anisotropic displacement parameters ($Å^2 \times 10^3$) for ReO(edt)(edtMe)(PTA). The anisotropic displacement factor exponent takes the form: $-2\pi^2[ h^2 a^{*2} U_{11} + ... + 2 h k a^* b^* U_{12} ]$

| | $U_{11}$ | $U_{22}$ | $U_{33}$ | $U_{23}$ | $U_{13}$ | $U_{12}$ |
|---|---|---|---|---|---|---|
| Re(1) | 15(1) | 17(1) | 15(1) | 1(1) | -1(1) | -7(1) |
| S(1) | 17(1) | 20(1) | 29(1) | 3(1) | 0(1) | -9(1) |
| S(2) | 24(1) | 18(1) | 26(1) | 2(1) | 5(1) | -5(1) |
| S(3) | 24(1) | 24(1) | 20(1) | 4(1) | 4(1) | -4(1) |
| S(4) | 28(1) | 55(2) | 28(1) | -11(1) | 4(1) | -5(1) |
| P(1) | 16(1) | 17(1) | 16(1) | 1(1) | -2(1) | -6(1) |
| C(1) | 26(4) | 22(4) | 20(3) | 1(3) | -1(3) | -1(3) |
| C(2) | 27(4) | 21(4) | 28(4) | 7(3) | -1(3) | -11(3) |
| C(3) | 18(3) | 24(4) | 24(4) | 3(3) | -8(3) | -3(3) |
| C(4) | 23(4) | 21(4) | 25(4) | -7(3) | 4(3) | -9(3) |
| C(5) | 12(3) | 21(3) | 24(3) | 2(3) | -2(2) | -5(2) |
| C(6) | 20(3) | 19(3) | 24(3) | 0(3) | 1(3) | -12(3) |
| C(7) | 29(4) | 18(4) | 39(5) | 4(3) | -3(3) | -11(3) |
| C(8) | 21(3) | 18(3) | 28(4) | 5(3) | 2(3) | -6(3) |
| C(9) | 34(4) | 34(4) | 22(4) | 8(3) | 6(3) | -3(3) |
| C(10) | 33(4) | 49(5) | 18(4) | 4(3) | 6(3) | -2(4) |
| N(1) | 22(3) | 25(3) | 21(3) | 2(2) | -2(2) | -6(2) |
| N(2) | 18(3) | 26(3) | 20(3) | -2(2) | -2(2) | -10(2) |
| N(3) | 22(3) | 21(3) | 23(3) | 0(2) | 0(2) | -10(2) |
| O(1) | 28(3) | 29(3) | 24(3) | 2(2) | -4(2) | -14(2) |

| | | | | | | |
|---|---|---|---|---|---|---|
| Re(1) | 15(1) | 17(1) | 15(1) | 1(1) | -1(1) | -7(1) |
| S(1) | 17(1) | 20(1) | 29(1) | 3(1) | 0(1) | -9(1) |

Part E. Hydrogen coordinates ( $\times 10^4$) and isotropic displacement parameters ($Å^2 \times 10^3$) for ReO(edt)(edtMe)(PTA).

| | x | y | z | U(eq) |
|---|---|---|---|---|
| H(1A) | -468 | 6369 | 6419 | 28 |
| H(1B) | -2556 | 5834 | 6436 | 28 |
| H(2A) | -633 | 8499 | 7005 | 29 |
| H(2B) | -2839 | 9465 | 7238 | 29 |
| H(3A) | -6123 | 8645 | 7288 | 26 |
| H(3B) | -5953 | 7184 | 7051 | 26 |
| H(4A) | -4948 | 9256 | 8872 | 27 |
| H(4B) | -3979 | 8157 | 9581 | 27 |
| H(5A) | -5008 | 5579 | 8313 | 23 |
| H(5B) | -4262 | 5989 | 9314 | 23 |
| H(6A) | -376 | 6993 | 9274 | 24 |
| H(6B) | 937 | 7120 | 8250 | 24 |
| H(7A) | -2525 | 1089 | 9323 | 34 |
| H(7B) | -1907 | 1058 | 8167 | 34 |
| H(8A) | 984 | -93 | 8838 | 27 |
| H(8B) | 884 | 988 | 9642 | 27 |
| H(9A) | 6064 | 2739 | 6847 | 38 |
| H(9B) | 4432 | 2020 | 6439 | 38 |
| H(10A) | 6303 | 3821 | 5344 | 42 |
| H(10B) | 4640 | 3130 | 4936 | 42 |
| H(11A) | 9867 | 1669 | 6210 | 82 |
| H(11B) | 10146 | 2826 | 5522 | 82 |
| H(11C) | 11389 | 1422 | 5219 | 82 |

| | | | | |
|---|---|---|---|---|
| H(11D) | 5751 | 509 | 4227 | 130 |
| H(11E) | 5790 | 267 | 5374 | 130 |

Derivation S-1. Evaluation of K for the equilibrium

| Reaction | K | Ref |
|---|---|---|
| $MeReO(mtp)SMe_2 + PPh_3 = MeReO(mtp)PPh_3 + Me_2S$ | $K_1$ | |
| Given these data: | | |
| $\{MeReO(mtp)\}_2 + 2\ Py = 2\ MeReO(mtp)Py$ | $K_2 = 1.74 \times 10^2$ | 1 |
| $\{MeReO(mtp)\}_2 + 2\ Me_2S = 2\ MeReO(mtp)SMe_2$ | $K_3 = 4.2 \times 10^{-4}$ | 2 |
| $MeReO(mtp)Py + PPh_3 = MeReO(mtp)PPh_3 + Py$ | $K_4 = 9.0 \times 10^2$ | 1 |

$$K_1 = K_4 \times \sqrt{\frac{K_2}{K_3}} = 6 \times 10^5$$

(1) Lente, G.; Guzei, I. A.; Espenson, J. H. *Inorg. Chem.* 2000, 39, 1311-1319.

(2) Shan, X.; Espenson, J. H., unpublished results.

# CHAPTER II. METHYLOXORHENIUM(V) COMPLEXES WITH TWO BIDENTATE LIGANDS: SYNTHESES AND REACTIVITY STUDIES

A manuscript published in *Inorganic Chemistry*

Xiaopeng Shan, Arkady Ellern, James H. Espenson

**Abstract**

Four new methyloxorhenium(V) complexes were synthesized: $MeReO(PA)_2$ (**1**), $MeReO(HQ)_2$ (**2**), $MeReO(MQ)_2$ (**3**), and MeReO(diphenylphosphinobenzoate)$_2$ (**4**) (in which PAH = 2-picolinic acid, HQH = 8-hydroxyquinoline and MQH = 8-mercaptoquinoline). Although only one geometric structure has been identified crystallographically for **1**, **2** and **3**, two isomers of **3** and **4** in solution were detected by NMR spectroscopy. These compounds catalyze the sulfoxidation of thioethers by pyridine N-oxides and sulfoxides. The rate law for the reaction between pyridine N-oxides and thioethers, catalyzed by **1**, shows a first-order dependence on the concentrations of pyridine N-oxide and **1**. The second order rate constants of series of para substituted pyridine N-oxides fall in the range of 0.27–7.5 L $mol^{-1}$ $s^{-1}$. Correlation of these rate constants by the Hammett LFER method gave a large negative reaction constant, $\rho = -5.2$. The next and rapid step does not influence the kinetics, but it could be explored with competition experiments carried out with a pair of methyl aryl sulfides, $MeSC_6H_4$-*p*-Y. The value of each rate was expressed relative to the reference compound that has Y = H. A Hammett analysis of $k_Y/k_H$ gave $\rho = -1.9$. Oxygen-18 labeled **1** was used in a single turnover experiment for 4-picoline N-oxide and dimethyl sulfide. No $^{18}O$ labeled DMSO was found. We suggest that the reaction proceeds by way of two intermediates that were not observed during the reaction. The first intermediate contains an opened PA-chelate ring; this allows the pyridine N-oxide to access the primary coordination sphere of rhenium. The second intermediate is a *cis*-dioxorhenium(VII) species, which the thioether then attacks. Oxygen-18 experiments were used to show that the two oxygens of this intermediate are not equivalent; only the "new" oxygen is attacked by, and transferred to, $SR_2$. Water inhibits the reaction because it hydrolyzes the rhenium(VII) intermediate.

**Introduction**

Certain aspects of the coordination chemistry of rhenium have been widely developed because of the radiotherapeutic applications of the β-emitting isotopes $^{186}$Re and $^{188}$Re.[1-3] Most of these rhenium complexes contain a {Re$^{V}$O} core.[4-7] Often a monoanionic bidentate ligand is present. Typical donor atom pairs such as P,O (HPO = phosphinocarboxylic acid),[8,9] N,O (HNO = e.g., picolinic acid or 8-hydroxyquinoline),[10-13] and N,S (HNS = 2-mercaptoquinoline).[12] Molybdenum complexes have been extensively investigated owing to interest in their oxotransferase activity,[14-18] In comparison, only a few rhenium complexes have been investigated.[19-23] This research focuses on compounds containing a methyl(oxo)-rhenium(V) core, {MeRe$^{V}$O}.[24-27]

We have now extended our exploration of rhenium catalysts[28-33] by the preparation and characterization of four new [2+2]methyl-oxorhenium compounds, Chart 1. These reactions are catalyzed by them:

$$RSR' + XC_5H_4NO \xrightarrow{[Re]} RS(O)R' + C_5H_4N \quad (1)$$

$$R_2S + R'_2SO \rightleftharpoons R_2S(O) + R'_2S \quad (2)$$

**Chart 1.** Structural Formulas of [2+2] Methyloxorhenium(V) Compounds

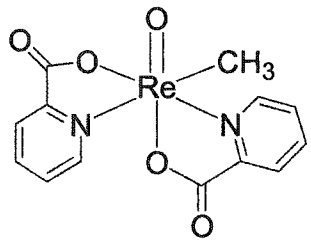

MeReO(PA)$_2$ **1**

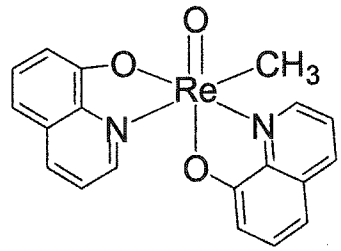

MeReO(HQ)$_2$ **2**

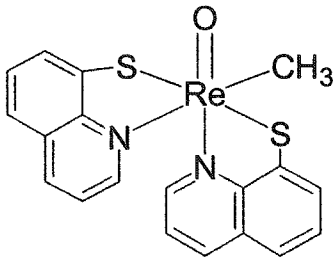

MeReO(MQ)$_2$ **3a**

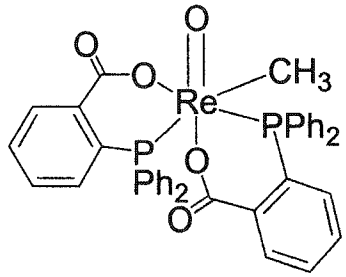

MeReO(diphenylphos-phinobenzoate)$_2$ **4a**

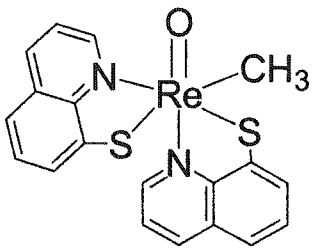

MeReO(MQ)$_2$ **3b**

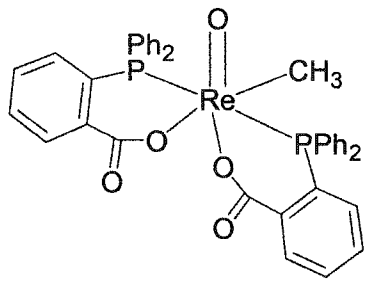

MeReO(diphenylphos-phinobenzoate)$_2$ **4b**

Kinetic studies were carried out with **1**, the most effective catalyst. Our goal has been to identify the steps in the mechanism, including the formulation of chemically-reasonable reaction intermediates. This includes the trapping of a transient dioxorhenium(VII) species.

## Experimental Section

**Reagents and Instrumentation.** Methyltrioxorhenium(VII), $CH_3ReO_3$ or MTO, was prepared from sodium perrhenate, tetramethyl tin and chlorotrimethylsilane.[34] The chelating

ligands were purchased from commercial sources and used as received. Anhydrous methylene chloride was the solvent for UV/Visible spectrophotometry. $D_1$-chloroform for NMR studies was dried over 4A molecular sieves (Fisher) for 24 h at 200 °C.

UV/Vis data were obtained with a Shimadzu Model 2501 spectrophotometer. Least-squares kinetic fits were carried out with KaleidaGraph software. Bruker DRX-400 MHz and AC200 spectrometers were used to record $^1H$, $^{13}C$ and $^{31}P$ NMR spectra. The chemical shift for $^1H$ was defined relative to that of the residual $CHCl_3$ in the solvent, δ 7.27 ppm. Infrared spectra were recorded by a Nicolet-500 spectrometer. GC-MS spectra were recorded by Finnegan MAT MAGNUM mass spectrometer. Elemental analysis was performed by Desert Analytics Laboratory.

**Syntheses**. Compounds **1-3** were prepared from MTO (50 mg, 0.2 mmol), the bidentate ligand (0.4 mmol), and the reducing agent triphenylphosphine (53 mg, 0.2 mmol) in 20 mL of $CH_2Cl_2$. After stirring the mixture for 12 h, 20 mL of hexanes was layered the top of the resulting solution and the mixture placed in a freezer at ca. –12 °C. After 24 h a black powder had deposited; it was filtered and rinsed with hexanes. A crystal suitable for x-ray diffraction analysis was obtained by recrystallization from methylene chloride-hexanes. Dimethyl sulfide (19 mg, 0.3 mmol) could also be used as the reducing agent for the preparation of **1** provided anhydrous sodium sulfate was added as a drying agent to complete the reaction. If the acidic form of the monoanionic ligand is written as H(X,Y), where X and Y are the donor atoms, the chemical equation for the syntheses is

$$MeReO_3 + 2\ H(X,Y) + PPh_3/Me_2S \rightarrow MeRe(O)(X,Y)_2 + H_2O + Ph_3PO/Me_2SO \qquad (3)$$

**1** was obtained in 83% yield from triphenylphosphine, 53% from dimethyl sulfide. NMR $^1H$: δ 8.84 (d, 1H), 8.52 (d, 1H), 8.44 (m, 1H), 8.29 (m, 1H), 8.19 (d, 1H), 7.77 (m, 3H), 4.43 (s, 3H); $^{13}C$: 180, 163, 153, 150, 148, 146, 143, 130, 126, 125, 53, 29, 11. IR ($CHCl_3$): 1003 $cm^{-1}$ and, for the $^{18}O$-labeled compound, 951 $cm^{-1}$. The two agree precisely with the predicted $(18/16)^{1/2}$ ratio. UV-Vis ($CHCl_3$), $\lambda_{max}$/nm (log ε/L $mol^{-1}$ $cm^{-1}$): 568 (2.3), 396.5 (3.83) and 260 (4.14). Elemental Analysis: $C_{13}H_{11}N_2O_5Re$, Found (Calcd.) C 33.85 (33.84), H 2.48 (2.40), N 6.06 (6.07).

**2** was obtained in 80% yield. NMR $^1H$: δ 8.56 (d, 1H), 8.36 (m, 1H), 8.21 (m, 1H), 7.66 (m, 4H), 7.40 (m, 3H), 7.07 (d, 1H) 6.46 (d, 1H), 4.53 (s, 3H). $^{13}C$: too insoluble. IR ($CHCl_3$):

980 $cm^{-1}$. UV-Vis ($CHCl_3$), $\lambda_{max}$/nm (log ε/L $mol^{-1}$ $cm^{-1}$): 470 (sh), 417 (3.70) and 360 (sh). Elemental Analysis: $C_{19}H_{15}N_2O_3Re$, Found (Calcd.): C 44.64 (45.14), H 2.92 (2.99), N 5.29 (5.54).

**3** was obtained in 50% yield. Two sets of $^1H$ NMR resonance peaks were found in solution with a ratio 3:1. Two geometric isomers were assigned to these peaks according to the x-ray structure and an earlier study of pyridine exchange reactions.[35] In solution, the major species is **3a**, NMR $^1H$: δ 10.88 (d, 1H), 8.39 (d, 1H), 8.34 (d, 2H), 8.06 (d, 2H), 7.80 (t, 1H), 7.74 (d, 1H), 7.58 (m, 1H), 7.74 (d, 1H), 7.41 (t, 1H), 6.95 (d, 1H), 6.75 (m, 1H), 4.95 (s, 3H). The minor solution species is **3b**. Only three peaks are available due to broadening and overlap with peaks from **3a**. NMR $^1H$: δ 9.40 (s, 1H), 8.65 (s, 1H), 5.14 (s, 3H) ppm. $^{13}C$: too insoluble. IR ($CHCl_3$): **3a**, 985.46 $cm^{-1}$; **3b**, 999 $cm^{-1}$. UV-Vis ($CHCl_3$), $\lambda_{max}$/nm (log ε/L $mol^{-1}$ $cm^{-1}$): 699 (2.6), 432 (3.78) and 267.5 (4.43). Elemental Analysis: $C_{19}H_{15}N_2OReS_2$, Found (Calcd.): C 42.16 (42.44), H 2.54 (2.81), N 5.13 (5.21), S 11.37 (11.93).

**4** was prepared by adding MTO (50 mg, 0.2 mmol) into 20 mL of $CH_2Cl_2$ containing 2-diphenylphosphinobenzoic acid (184 mg, 0.6 mmol), which served both as the reducing agent and the new ligand. The color of the solution changed to violet. After 12 h stirring the mixture was layered with hexanes and put into the freezer. A dark powder was isolated by filtration 24 h later and rinsed with hexanes. It consisted of two geometric isomers, **4a** and **4b**, in a total yield of 65%. The two could not be separated, but their NMR spectra in $CDCl_3$ were resolved and assigned as explained later. **4a** $^1H$ NMR: δ 6.5–8.5 (m, 14H), 3.39 (t, 3H); $^{31}P$ NMR: –0.34 (d, $J_{PP}$ = 9 Hz), –3.07 (d, $J_{PP}$ = 9 Hz); **4b**: 6.5–8.5 (m, 14H), 4.12 (t, 3H); $^{31}P$ NMR: 6.64 (d, $J_{PP}$ = 262 Hz), –5.28 (d, $J_{PP}$ = 262 Hz).

**X-ray studies.** Crystals for **1**, **2** and **3a** were selected under ambient conditions. Each crystal was mounted and centered in the X-ray beam by use of a video camera. The crystal evaluation and data collection were performed on a Bruker CCD-1000 diffractometer with Mo $K_\alpha$ (λ = 0.71073 Å) radiation and a detector-to-crystal distance of 4.98 cm. The initial cell constants were obtained from three series of ω scans at different starting angles. Each series consisted of 30 frames collected at intervals of 0.3° in a 10° range about ω with the exposure time of 10 s per frame. The reflections were successfully indexed by an automated indexing routine built into the SMART program. The final cell constants were calculated

from a set of strong reflections from the actual data collection. The data were collected using the full sphere routine for high redundancy. The data were corrected for Lorentz and polarization effects. The absorption correction was based on fitting a function to the empirical transmission surface as sampled by multiple equivalent measurements[36] using SADABS software.[37]

The position of the heavy atom was found by the Patterson method. The remaining atoms were located in an alternating series of least-squares cycles and difference Fourier maps. All non-hydrogen atoms were refined in full-matrix an isotropic approximation. All hydrogen atoms were placed at calculated idealized positions and were allowed to ride on the neighboring atoms with relative isotropic displacement coefficients. The ORTEP diagrams were drawn at 50% probability level.

**Kinetics**. Reactions of pyridine N-oxides and dimethyl sulfide were monitored by following the decrease in absorbance from 275 to 310 nm according to which pyridine N-oxide was being studied. Owing to the large values of their molar absorptivities, a cell with a path length of 0.05 cm in a cylindrical cell holder thermostated at 25.0 ± 0.2 °C was used. Dimethyl sulfide was added in at least ten-fold excess, allowing the absorbance–time data to be fitted to pseudo-first-order kinetics, according to eq 2.

$$\mathrm{Abs}_t = \mathrm{Abs}_\infty + (\mathrm{Abs}_0 - \mathrm{Abs}_\infty) \times \exp(-k_{\mathrm{obs}} t) \tag{4}$$

**Competition kinetics.** A different aspect of the reaction scheme was studied by this method. A pair of methyl aryl sulfides with different para substituents at concentrations ten times higher than that of 4-picoline N-oxide. The concentrations of the two starting sulfides and of the sulfoxides formed were determined by NMR spectroscopy 15 min after the beginning of the reaction. The rate constant ratio for $MeSC_6H_4Y$ as compared to MeSPh is given simply as the product of two concentration ratios at a given time because the sulfide concentrations are nearly invariant during the initial reaction period.

$$\frac{k_Y}{k_H} = \frac{d[MeS(O)C_6H_4Y] / dt}{d[MeS(O)Ph] / dt} = \frac{[MeS(O)C_6H_4Y]_t}{[MeS(O)Ph]_t} \times \frac{[MeSPh]_0}{[MeSC_6H_4Y]_0} \tag{5}$$

**Oxygen-18 labeling**. Equilibration between MTO and 30 times the molar ratio of $H_2{}^{18}O$ (90% enrichment) was allowed to proceed for 20 min in anhydrous methylene chloride,

which was sufficient for oxygen exchange between MTO and water.[38] The resulting solution was vacuum dried. The same procedure was repeated three times, yielding a sample of $MeRe^{18}O_3$, enriched to ca. 50% $^{18}O$ content. It used to prepare **1** by the $PPh_3$ method. The $^{18}O$ content of **1** was ca. 50% by IR spectroscopy. A reaction was carried out in anhydrous methylene chloride with 4-picoline N-oxide (10 mM), dimethyl sulfide (20 mM) and **1** (10 mM) to guarantee the formation of enough sulfoxides. The isotopic content of the resulting solution was determined by GC-MS.

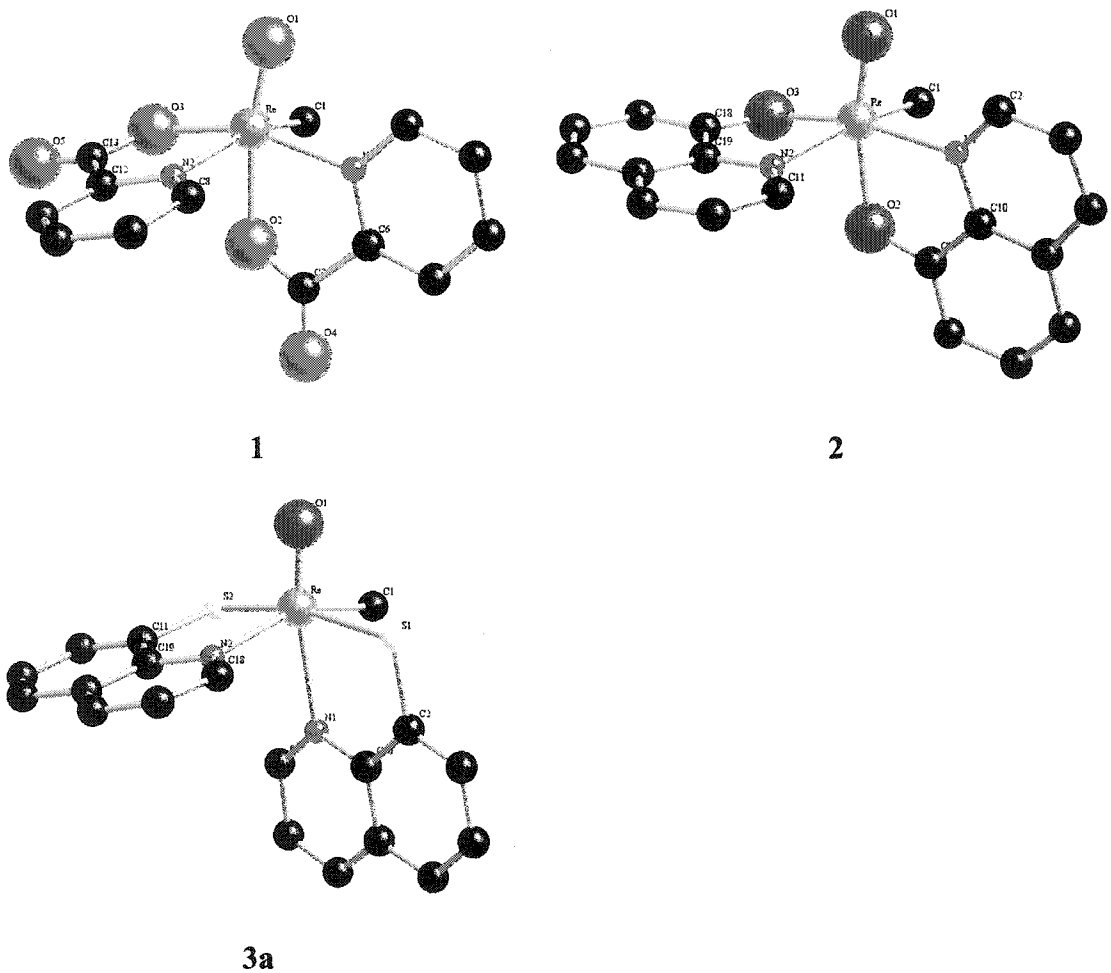

**1** **2**

**3a**

**Figure 1**. Crystallographically-determined molecular structures of compounds **1**, **2** and 3a. Table 2 shows the selected bond lengths and angles.

**Table 1.** Experimental Data for the X-ray Diffraction Studies of **1**, **2**, and **3a**.

| Compound | **1** | **2** | **3a** |
|---|---|---|---|
| empirical formula | $C_{13}H_{11}N_2O_5Re$ | $C_{19}H_{15}N_2O_3Re$ | $C_{19}H_{15}N_2OReS_2$ |
| formula wt | 461.44 | 505.53 | 537.65 |
| a, Å | 28.466(7) | 9.233(2) | 8.4428(14) |
| b, Å | 7.0933(17) | 9.724(2) | 9.1357(15) |
| c, Å | 15.186(4) | 10.780(2) | 12.531(2) |
| α, deg | | 101.054(3) | 85.504(3) |
| β, deg | 111.892(4) | 103.955(3) | 89.214(3) |
| γ, deg | | 112.402(4) | 64.825(3) |
| volume, Å3 | 2845.3(12) | 823.8(3) | 871.8(3) |
| Z | 8 | 2 | 2 |
| space group | C2/c | P-1 | P-1 |
| temp, K | 298(2) | 298(2) | 298(2) |
| Wavelength | 0.71073 Å | 0.71073 Å | 0.71073 Å |
| $\rho_{calcd}$, g cm-3 | 2.154 | 2.038 | 2.048 |
| μ, mm-1 | 8.564 | 7.396 | 7.218 |
| R indices | R1 = 0.0821, | R1 = 0.0354 | R1 = 0.0681 |
| (all data)a | wR2 = 0.1686 | wR2 = 0.0832 | wR2 = 0.1566 |

[a] $R1 = \Sigma \, | \, |F_o| - |F_c| \, | \, / \, \Sigma \, |F_o|$; $wR2 = \{ \Sigma [ w(F_o^2 - F_c^2)^2 ] / \Sigma [ w(F_o^2)^2 ] \}^{1/2}$.

**Table 2.** Selected Bond lengths (pm) and Angles[a] (deg) of **1**, **2** and **3a** Complexes.

| | **1** | **2** | **3a** |
|---|---|---|---|
| Re–O(1) | 166.2(8) | 167.7(4) | 167.4(8) |
| Re–C(1) | 211.1(13) | 211.1(6) | 211.3(12) |
| Re–N(1) | 211.3(9) | 212.5(4) | 238.3(9) |
| Re–N(2) | 216.3(9) | 220.1(4) | 214.8(9) |
| Re–O(2) | 210.0(7) | 203.7(4) | |
| Re–O(3) | 201.4(8) | 198.6(4) | |
| Re–S(1) | | | 244.7(3) |
| Re–S(2) | | | 231.3(3) |
| O(1)–Re–C(1) | 98.8(5) | 97.9(3) | 102.5(4) |
| O(1)–Re–N(1) | 90.9(4) | 87.47(17) | *165.6(4)* |
| O(1)–Re–N(2) | 103.9(4) | 99.02(17) | 103.6(4) |
| C(1)–Re–N(1) | 88.6(5) | 89.3(2) | 78.8(4) |
| C(1)–Re–N(2) | 156.3(4) | 81.66(15) | 153.6(4) |
| N(2)–Re–N(1) | 97.9(3) | 100.12(16) | 76.9(3) |
| O(1)–Re–O(2) | *165.3(4)* | *162.86(17)* | - |
| N(1)–Re–O(3) | 159.4(4) | 166.48(15) | - |
| C(1)–Re–O(2) | 84.1(5) | 84.8(2) | - |
| S(1)–Re–N(2) | - | - | 95.9(3) |
| S(1)–Re–S(2) | - | - | 165.66(10) |
| C(1)–Re–S(2) | - | - | 87.2(4) |

[a] Italicized entries: *trans*-[Oxo-Re-donor atom] angles

## Results

**Structures**. Table 1 shows the crystallographic parameters for **1**, **2** and **3a**, and Figure 1 displays their molecular structures drawn by the program CrystalMaker.[39] In all three compounds the rhenium(V) atom occupies the center of a distorted octahedron defined by its axial ligands, the terminal oxo group and one donor atom of one bidentate ligand. The three remaining donor atoms and the methyl group occupy the equatorial plane. Table 2 lists the

important bond distances and angles. In all of these compounds the Re ≡ O distances are virtually identical at 167 pm, as are the Re–C distances at 211 pm. The values of ν(Re–O) from the IR studies fall in the range 985-1003 $cm^{-1}$ for **1-4**, relatively insensitive to the ligand environment. In every case, the donor atom trans to the terminal oxo group lies at a longer distance than its counterpart in the equatorial plane; this comes as no surprise, reflecting extensive $\pi$ back-bonding from oxo to rhenium(V). In keeping with that, the *trans*(O≡ Re–donor atom) angles lie in the range 162.9–165.5°, notably less than 180°.

All of **1–4** should exist as four geometrical isomers. No evidence for structures of **1** or **2**, other than the ones characterized, was obtained. Even the solution NMR in deuterated chloroform from the original preparation prior to product isolation showed the single isomer. Two isomers in ca. 3:1 ratio were found for **3** in solution, but only the major one, **3a**, was isolated. The minor isomer, **3b**, is characterized by δ(Me–Re) 5.14. The hydrogen signals from the MQ ligand are somewhat broadened, which is not the case for **3a** or free MQH. This suggests an internal process, and brings to mind the exchange between Py and five-coordinate MeReO(edt)Py ($edtH_2$ = 1,2-ethane dithiol). For it, the transition state is six-coordinate and features a turnstile rotation that interchanges the Me group and the two Py ligands.[35,40] Such an exchange, if it occurs within **3b**, could well give rise to signal broadening.

Compound **4** exists as ca. equimolar amounts of two isomers, the structures of which are presented in Chart 1. The basis for these assignments is the widely different coupling constants in the $^{31}P$ NMR spectra. $J_{P-P}$ = 9 Hz in **4a** and 262 Hz in **4b**. According to the literature[41-43] the very high coupling constant suggests a structure for **4b** in which the two phosphorus donor atoms lie trans to one another.

The donor atoms are N and O for PA and HQ; we surmise the heterocyclic nitrogen is the more weakly bound when both are equatorial; consequently **1** and **2** adopt structures with an axial O-donor atom. Whatever atom is trans to the oxo group is the most weakly bound of all, irrespective of the inherent Lewis basicity. The same rule applies to ligand MQ, which gives rise to the minor isomer **3b**, because a thiolate sulfur is a better Lewis base than a ring nitrogen. In that sense, **3a** is similar insofar as the MQ ligand that spans an axial and an equatorial position. The two isomers differ only in regards to the orientation of the in-plane

ligand, which may be a factor of less consequence. Again, the two isomers of **4** differ in the same way as do the two isomers of **3**. Both isomers of **4** have an O-donor atom trans to the oxo group; that donor is a weaker Lewis base than a phosphine towards Re(V). The comparable abundances of **4a** and **4b** may reflect the steric influence of the bulky phosphine ligand.

**Oxygen atom transfer: Sulfoxide to sulfide.** The following nearly isoenergetic reaction,[19] occurred when any of the compounds **1–4** was used in catalytic quantity with a 10-fold excess of dimethyl sulfide:

$$Ph_2SO + Me_2S \rightarrow Ph_2S + Me_2SO \qquad (6)$$

Unlike some oxorhenium(V) compounds that catalyze this reaction efficiently, such as $[(hoz)_2Re(O)(OH_2)][OTf]$[19] and MeReO(dithiolatte)$PPh_3$,[32,33] none of these compounds led to a rapid reaction for reasons that will be presented later. We therefore turned our attention to a catalytic system where efficient reactions could be observed.

**Oxygen atom transfer: pyridine N-oxides to thioethers.** Kinetic studies of these reactions in anhydrous methylene chloride were carried out:

$$XC_5H_4NO + RSR' \rightarrow XC_5H_4N + RS(O)R' \qquad (7)$$

Studies were limited to catalyst **1** because **2** and **3** react more slowly and **4** is not available as a single compound. A sample repetitive scan spectrum (X = 4-Me; $Me_2S$) is presented in Figure 2.

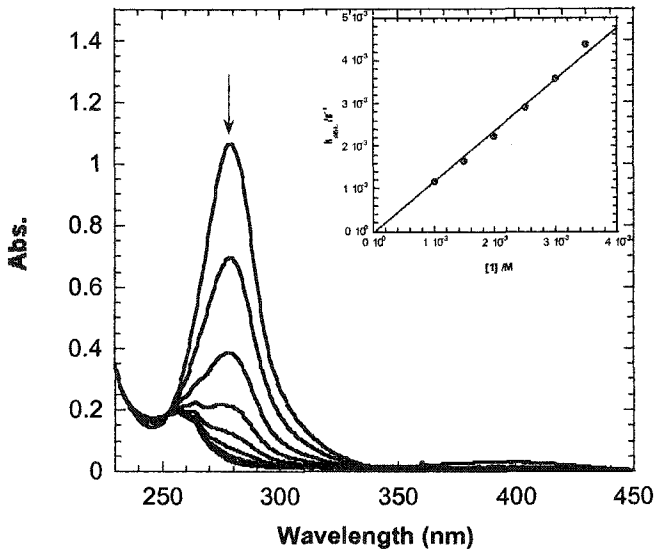


**Figure 2.** Repetitive scans of 10 mM 4-picoline N-oxide, 100 mM dimethyl sulfide and 2 mM **1** in anhydrous methylene chloride at 25 °C. The inset shows the plot of $k_{cat}$ against the concentration of the catalyst.

The absorbance-time decrease, which shows the greatest amplitude at 279 nm, follows first-order kinetics. The values of $k_{obs}$ so obtained are linear functions of the total catalyst concentration, designated as $[\mathbf{1}]_T$, to reflect the fact that at various points during the cycle **1** exists in different forms present at low concentrations.

$$-\frac{d[XC_5H_4NO]}{dt} = k_{cat}[XC_5H_4NO][\mathbf{1}]_T \qquad (8)$$

The kinetic determinations employed a ≥10-fold excess of sulfide over pyridine N-oxide. Varying the sulfide concentration gave the same rate constant, $k_{cat}$ = 1.23 ± 0.01 (10 mM $Me_2S$) and 1.20 ± 0.05 L $mol^{-1}$ $s^{-1}$ (100 mM $Me_2S$). Different thioethers also gave the same value of $k_{cat}$/L $mol^{-1}$ $s^{-1}$: 1.20 ± 0.05 ($Me_2S$), 1.22 ± 0.01 (pentamethylene sulfide) and 1.28 ± 0.07 (*tert*-butyl methyl sulfide. For a range of pyridine N-oxides, the identity of X exerts a strong influence on the value of $k_{cat}$, as can be seen from Table 3.

**Table 3.** Kinetics of Sulfoxidation Reactions Catalyzed by **1**

Part A. UV spectra of $XC_5H_4NO$ and $k_{cat}$ [b]

| X | $\lambda_{max}$/nm ($\varepsilon/10^4$ L mol$^{-1}$cm$^{-1}$) | $k_{cat}$/L mol$^{-1}$ s$^{-1}$ |
|---|---|---|
| 4-MeO | 280 (0.415) | 7.5 |
| 4-Me | 279 (1.07) | 1.23 |
| 2-Me | 272 (1.04) | 0.57 |
| 3-Me | 278 (0.920) | 0.43 |
| 4-Ph | 310 (1.54) | 0.36 |
| 4-H | 277 (0.615) | 0.27 |

Part B. Relative Rate Constants for **5** and methyl aryl sulfides [c]

| Y | $k_Y/k_H$ |
|---|---|
| 4-MeO | 5.1 |
| 4-Me | 2.4 |
| 4-H | 1.00 (rel.) |
| 4-Cl | 0.44 |
| 4-Br | 0.37 |
| 4-$HO_2C$ | 0.18 |
| 4-MeC(O) | 0.11 |
| 4-CN | 0.078 |

[a] In anhydrous dichloromethane at 25 °C; [b] Conditions: 10 mM $XC_5H_4NO$, 100 mM $Me_2S$, 2–8 mM **1**; [c] At 25 °C in $D_1$-chloroform with 10 mM 4-$MeC_5H_4NO$, 2 mM **1**, and 50 mM each of MeSPh and $MeSC_6H_4Y$.

**Competition experiments**. The foregoing reveals that the sulfide enters the catalytic cycle at a stage later than the step(s) that determine the rate and the value of $k_{cat}$. That is, RSR' reacts with an active rhenium intermediate in a fast subsequent step. To evaluate the effects of thioethers it was therefore useful to take the thioethers in pairs, for which purpose

$MeSC_6H_4Y$ and MeSPh were employed. The design of the experiment is presented in this diagram:

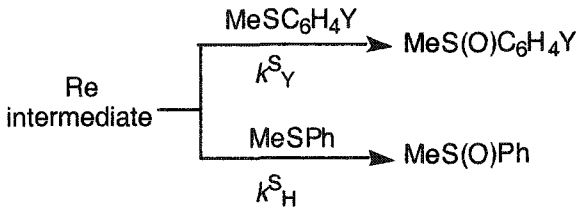


The NMR data were analyzed to determine the ratio $k^S_Y/k^S_H$ for the different aryl groups on sulfide according to eq 5. Table 3B presents the results of such determinations. For reasons to be presented later, it was deemed essential to determine the same ratio for two other pyridine N-oxides. These data are also given in Table 3.

**Oxygen-18 labeling**. Stoichiometric amounts of **1** and 4-picoline N-oxide and twice as much $Me_2S$ were employed in the case where $MeRe^{18}O(PA)_2$ was employed in anhydrous dichloromethane. The solution was analyzed by GC-MS after two h reaction time. Although ample $Me_2S^{16}O$ was detected, $Me_2S^{18}O$ proved absent.

## Discussion

**Thermochemical and electronic considerations**. Sulfoxide-to-sulfide transfer of an oxygen atom is nearly isoenergetic;. $\Delta G° = -2.9$ kJ for reaction 6 between diphenyl sulfoxide and dimethyl sulfide in methylene chloride.[19] The use of pyridine N-oxides provides a system with a considerably greater driving force. From thermochemical data for $C_5H_4NO$ and $Me_2S$,[44-47] we estimate $\Delta G° \cong \Delta H° = -63$ kJ $mol^{-1}$.

The value of $k_{cat}$ depends strongly on the electronic properties of the substituent on the pyridine N-oxide ring. For the five entries in 3 with substituents in the 4- and 3-positions, an analysis according to Hammett's method gives $\rho_{cat} = -5.2$ in Figure 3. This is an exceptionally negative value, most reasonably interpreted in terms of two composite effects that enter in the same direction. More will be said about this in what follows.

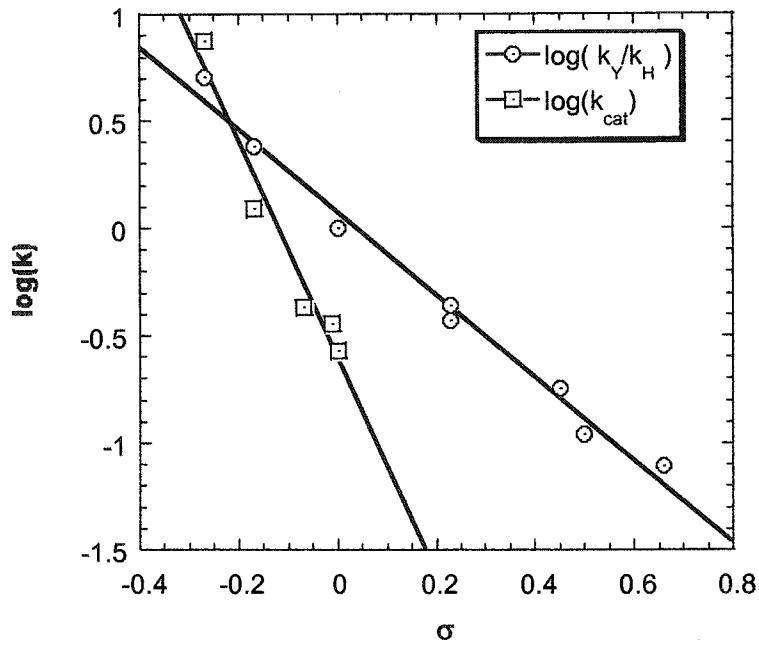


**Figure 3.** LFER correlations. (1) of $k_{cat}$ values for reactions between $XC_5H_4NO$ and 100 mM $Me_2S$ in presence of 2~8 mM **1** in anhydrous $CH_2Cl_2$ at 25 °C; (2) of relative rate constants $k_Y/k_H$ determined by competition kinetics for reactions of $MeSC_6H_4Y$ reactions between 10 mM 4-picoline N-oxide and 50 mM each of $MeSC_5H_4Y$ and 50 mM $C_6H_5SCH_3$ in the presence of 2 mM **1** in $CDCl_3$ at 25 °C.

A similar analysis was carried out on the rate constant ratio $k^S_Y/k^S_H$. The fact that this quantity is a ratio and not an absolute rate constant does not compromise the answer in the least. From the data in Table 3, we find $\rho_S = -1.9$, as shown in Figure 3.

**Substrate binding**. It seems self-evident that activation of a pyridine N-oxide requires its coordination to rhenium(V) for the catalyst to exert its effect. In systems studied earlier, this has not appeared to pose a significant part of the overall barrier, because five-coordinate catalysts such as MeReO(dithiolate)$PPh_3$ permit its ready entry. For **1**, however, one must propose either that PyO attacks **1** as it is, giving rise to a seven-coordinate intermediate, or that ring-opening of one arm of one PA ligand precedes entry of PyO. We surmise the N donor atom is preferentially released to avoid the presumably unfavorable $[Re]^+O^-$ in dichloromethane.

We have argued strongly against any dissociative process for complexes such as MeReO(dithiolate)L.[35,40] Thus it seems we must also consider direct ligand displacement as the route to **5**. We discount this mechanism, however; because the parent is not a *five-coordinate* complex from which ligand dissociation becomes unlikely, but a *six-coordinate* one in which the weakness of a rhenium–ligand trans to the oxo group has been well established.

By whichever pathway the **1** = **5** reaction occurs, the net process is an equilibrium that can be represented by an equilibrium constant $K_{15}$, the value of which varies with the X-group of $XC_5H_4NO$ according to its Lewis basicity. Because this step remains at equilibrium, its mechanism, while of intrinsic interest in its own right, remains immaterial in the kinetic analysis. Stronger Lewis bases are more strongly coordinated in **5**, which provides one factor contributing to the negative reaction constant $\rho_{cat}$ found for $k_{cat}$. That contribution is designated $\rho_{15}$, and it is one component of $\rho_{cat}$.

**The rate-controlling step (RCS).** The rate law indicates that the thioether is not involved in the mechanism until after the RCS, because the rate remains independent of variations in the concentration and identity of RSR'. We therefore conclude that intermediate **5** undergoes unimolecular cleavage of the N–O bond of coordinated pyridine N-oxide:

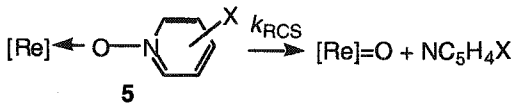


**5**

The experimental rate constant $k_{cat}$ is therefore a composite: $k_{cat} = K_{15} \times k_{RCS}$. The large negative reaction constant $\rho_{cat} = -5.2$ allows us to argue that the substituent effects on each component must have the same sign, lest cancellation of the effects take place. Because $K_{15}$ represents a Lewis acid-base equilibrium, $\rho_{15}$ will therefore be negative, as argued previously. The negative reaction constant $\rho_{RCS}$ indicates that electron flow from the oxygen of the coordinate pyridine N-oxide provides the principal barrier at the transition state:

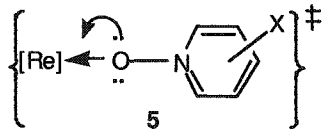


**5**

**The thioether step and its oxo-group selectivity.** A direct reaction occurs between intermediate **6** and RSR'. Because it occurs rapidly compared to the RCS, kinetic competition

experiments were employed. The rate constants relative to MeSPh are given in Table 3B. The reaction constant is $\rho_S = -1.9$, which indicates nucleophilic attack of the thioether on one oxygen of dioxorhenium(VII) intermediate **6**. This forms the next intermediate, **7**, that might best be viewed as being or becoming a sulfoxide complex of rhenium(V).

What is astonishing, however, is the high selectivity the thioether exhibits as to which of the two oxo groups of **6** it attacks. Data obtained with the catalyst **1** as $MeRe(^{18}O)(PA)_2$ (oxygen-18 content, 50%) gave, in combination with an equimolar quantity of 4-$MeC_5H_4N^{16}O$ and dimethyl sulfide, only $Me_2S^{16}O$. Had the thioether reacted non-selectively, the enrichment level of the sulfoxide would have corresponded to 25% $Me_2S^{18}O$.

Examination of the plausible structure of **6** is helpful in this regard. As shown in Scheme 1, intermediate **7a** appears to be a dead-end because displacement of sulfoxide by the dangling pyridine arm of PA is impossible. On the other hand, unimolecular displacement within **7b** restores **1** directly and forms $Me_2S^{16}O$ exclusively.

**Scheme 1:** Oxo-group selectivity at the thioether step

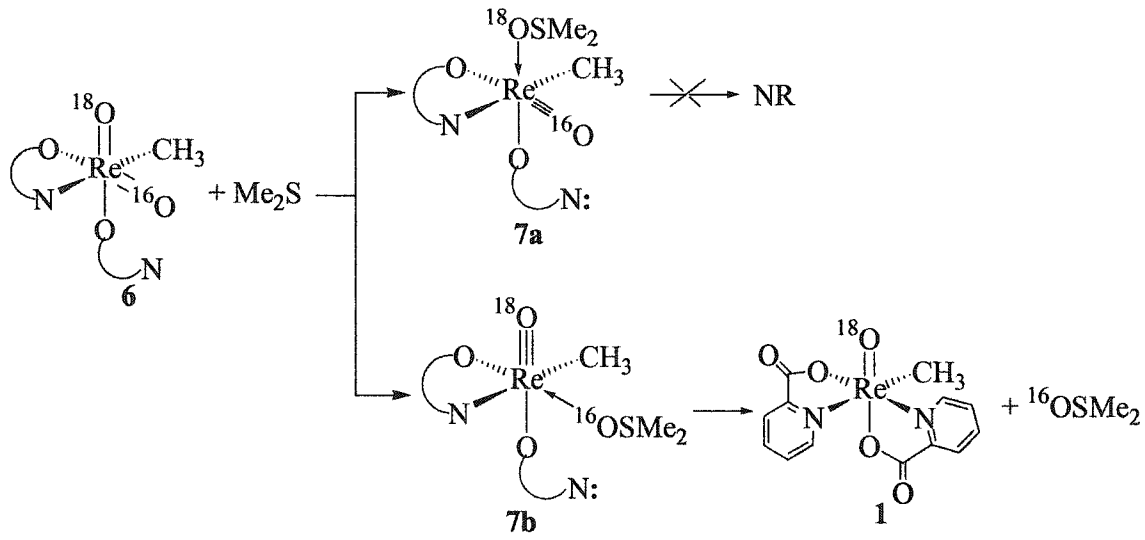


**Conclusion**. Four new rhenium(V) complexes with monoanionic bidentate ligands, PA, HQ, MQ, and DPPB, were synthesized and characterized. All of them catalyze oxygen atom transfer from milder oxidants, pyridine N-oxides or sulfoxides, to thioethers. Based on

kinetic and mechanistic studies, a multi-step mechanism has been proposed with involvement of several unobserved but plausible intermediates to account for the reaction at each stage.

**References**

(1) Blower, P. J.; Prakash, S. *Perspectives on Bioinorganic Chemistry* **1999**, *4*, 91-143.

(2) Hashimoto, K.; Yoshihara, K. *Top. Curr. Chem.* **1996**, *176*, 275-291.

(3) Blaeuenstein, P. *New J. Chem.* **1990**, *14*, 405-407.

(4) Bandoli, G.; Tisato, F.; Refosco, F.; Gerber, T. I. A. *Revs. Inorg. Chem.* **1999**, *19*, 187-210.

(5) Romão, C. C.; Kühn, F. E.; Herrmann, W. A. *Chem. Rev.* **1997**, *97*, 3197-3246.

(6) Herrmann, W. A.; Kuehn, F. E. *Acc. Chem. Res.* 1997; Vol. 30, p 169-180.

(7) Herrmann, W. A. *J. Organomet. Chem.* **1986**, *300*, 111-137.

(8) Correia, J. D. G.; Domingos, A.; Santos, I.; Bolzati, C.; Refosco, F.; Tisato, F. *Inorg. Chim. Acta* **2001**, *315*, 213-219.

(9) Bolzati, C.; Tisato, F.; Refosco, F.; Bandoli, G.; Dolmella, A. *Inorg. Chem.* **1996**, *35*, 6221-6229.

(10) Harris, T. A.; McKinney, T. M.; Wu, W.; Fanwick, P. E.; Walton, R. A. *Polyhedron* **1996**, *15*, 3289-3298.

(11) Dorsett, T. E.; Walton, R. A. *J. Organomet. Chem.* **1976**, *114*, 127-134.

(12) Leeaphon, M.; Rohl, K.; Thomas, R. J.; Fanwick, P. E.; Walton, R. A. *Inorg. Chem.* **1993**, *32*, 5562-5568.

(13) Wilcox, B. E.; Heeg, M. J.; Deutsch, E. *Inorg. Chem.* **1984**, *23*, 2962-2967.

(14) Coucouvanis, D. *Acc. Chem. Res.* **1991**, *24*, 1-8.

(15) Holm, R. H.; Berg, J. M. *Acc. Chem. Res.* **1986**, *19*, 363-370.

(16) Holm, R. H. *Coord. Chem. Rev.* **1990**, *100*, 183-221.

(17) Thapper, A.; Lorber, C.; Fryxelius, J.; Behrens, A.; Nordlander, E. *J. Inorg. Bioch.* **2000**, *79*, 67-74.

(18) Young, C. G. *J. Biol. Inorg. Chem* **1997**, *2*, 810-816.

(19) Arias, J.; Newlands, C. R.; Abu-Omar, M. M. *Inorg. Chem.* **2001**, *40*, 2185-2192.

(20) Huang, R.; Espenson, J. H. *J. Mol. Catal. A:* **2001**, *168*, 39-46.

(21) Arterburn, J. B.; Perry, M. C. *Organic Letters* **1999**, *1*, 769-771.

(22) Abu-Omar, M. M.; Khan, S. I. *Inorg. Chem.* **1998**, *37*, 4979-4985.

(23) Arterburn, J. B.; Nelson, S. L. *J. Org. Chem.* **1996**, *61*, 2260-2261.

(24) Espenson, J. H.; Shan, X.; Wang, Y.; Huang, R.; Lahti, D. W.; Dixon, J.; Lente, G.; Ellern, A.; Guzei, I. A. *Inorg. Chem.* **2002**, *41*, 2583-2591.

(25) Jacob, J.; Guzei, I. A.; Espenson, J. H. *Inorg. Chem.* **1999**, *38*, 3266-3267.

(26) Jacob, J.; Guzei, I. A.; Espenson, J. H. *Inorg. Chem.* **1999**, *38*, 1040-1041.

(27) Lente, G.; Shan, X.; Guzei, I. A.; Espenson, J. H. *Inorg. Chem.* **2000**, *39*, 3572-3576.

(28) Jacob, J.; Lente, G.; Guzei, I. A.; Espenson, J. H. *Inorg. Chem.* **1999**, *38*, 3762-3763.

(29) Lente, G.; Guzei, I. A.; Espenson, J. H. *Inorg. Chem.* **2000**, *39*, 1311-1319.

(30) Lente, G.; Jacob, J.; Guzei, I. A.; Espenson, J. H. *Inorg. React. Mechs.* **2000**, *2*, 169-177.

(31) Lente, G.; Espenson, J. H. *Inorg. Chem.* **2000**, *39*, 4809-4814.

(32) Wang, Y.; Espenson, J. H. *Inorg. Chem.* **2002**, *41*, 2266-2274.

(33) Wang, Y.; Espenson, J. H. *Organic Letters* **2000**, *2*, 3525-3526.

(34) Herrmann, W. A.; Kratzer, R. M.; Fischer, R. W. *Angew. Chem., Int. Ed.* **1997**, *36*, 2652-2654.

(35) Espenson, J. H.; Shan, X.; Lahti, D. W.; Rockey, T. M.; Saha, B.; Ellern, A. *Inorg. Chem.* **2001**, *40*, 6717-6724.

(36) Blessing, R. H. *Acta Cryst. Sect. A* **1995**, *51*, 33-38.

(37) All software and sources of the scattering factors are contained in the SHELXTL (version 5.1) program library (G. Sheldrick, B. A. X.-R. S., Madison, WI)..

(38) Herrmann, W. A.; Kuchler, J. G.; Weichselbaumer, G.; Herdtweck, E.; Kiprof, P. *J. Organomet. Chem.* **1989**, *372*, 351-370.

(39) Palmer, D.; CrystalMaker, 2.0 ed.; Hollywell Press: Bicester, Oxfordshire, 1999.

(40) Lahti, D. W.; Espenson, J. H. *J. Amer. Chem. Soc.* **2001**, *123*, 6014-6024.

(41) Bennett, M. A.; Robertson, G. B.; Rokicki, A.; Wickramasinghe, W. A. *J. Am. Chem. Soc.* **1988**, *110*, 7098-7105.

(42) Cotton, F. A.; Dikarev, E. V.; Herrero, S. *Inorg. Chem.* **2000**, *39*, 609-616.

(43) Cowan, R. L.; Trogler, W. C. *J. Am. Chem. Soc.* **1989**, *111*, 4750-4761.

(44) Shaofeng, L.; Pilcher, G. *J. Chem. Thermo.* **1988**, *20*, 463-465.

(45) Ribeiro da Silva, M. D. M. C.; Agostinha, M.; Matos, R.; Vaz, M. C.; Santos, L. M. N. B. F.; Pilcher, G.; Acree, W. E., Jr.; Powell, J. R. *J. Chem. Thermo.* **1998**, *30*, 869-878.

(46) Jenks, W. S.; Matsunaga, N.; Gordon, M. *J. Org. Chem.* **1996**, *61*, 1275-1283.

(47) Mackle, K. *Tetrahedron* 1963, *19*, 1159-1170.

**Supporting Information**

S-1. Crystal data for compound **1**.

Part A. Crystal data and structure refinement for **1**.

| | | |
|---|---|---|
| Identification code | 1 | |
| Empirical formula | $C_{13}H_{11}N_2O_5Re$ | |
| Formula weight | 461.44 | |
| Temperature | 298(2) K | |
| Wavelength | 0.71073 Å | |
| Crystal system | Monoclinic | |
| Space group | C2/c | |
| Unit cell dimensions | a = 28.466(7) Å | α= 90°. |
| | b = 7.0933(17) Å | β= 111.892(4)°. |
| | c = 15.186(4) Å | γ = 90°. |
| Volume | 2845.3(12) $Å^3$ | |
| Z | 8 | |
| Density (calculated) | 2.154 $Mg/m^3$ | |
| Absorption coefficient | 8.564 $mm^{-1}$ | |
| F(000) | 1744 | |
| Crystal size | 0.4 × 0.4 × 0.1 $mm^3$ | |
| Theta range for data collection | 2.72 to 26.38°. | |
| Index ranges | $-35 \le h \le 35, -8 \le k \le 8, -18 \le l \le 18$ | |
| Reflections collected | 11350 | |
| Independent reflections | 2900 [R(int) = 0.1399] | |
| Completeness to theta = 26.38° | 99.6 % | |
| Absorption correction | Empirical | |
| Max. and min. transmission | 1 and 0.38 | |
| Refinement method | Full-matrix least-squares on $F^2$ | |
| Data / restraints / parameters | 2900 / 0 / 190 | |
| Goodness-of-fit on $F^2$ | 0.978 | |

| | |
|---|---|
| Final R indices [I>2sigma(I)] | R1 = 0.0656, wR2 = 0.1567 |
| R indices (all data) | R1 = 0.0821, wR2 = 0.1686 |
| Largest diff. peak and hole | 3.453 and -4.686 e.Å$^{-3}$ |

$R1 = \Sigma \, | \, |F_o| - |F_c| \, | \, / \, \Sigma \, |F_o|$ and $wR2 = \{ \, \Sigma \, [ \, w(F_o^2 - F_c^2)^2 \, ] \, / \, \Sigma \, [ \, w(F_o^2)^2 \, ] \, \}^{1/2}$

Part B. Atomic coordinates ( $\times 10^4$) and equivalent isotropic displacement parameters (Å$^2 \times 10^3$) for 1. U(eq) is defined as one third of the trace of the orthogonalized $U_{ij}$ tensor.

| | x | y | z | U(eq) |
|---|---|---|---|---|
| Re | 4062(1) | 1212(1) | 10101(1) | 35(1) |
| C(1) | 4738(5) | 2510(20) | 10999(9) | 61(3) |
| C(2) | 4313(5) | 2244(19) | 8360(8) | 52(3) |
| C(3) | 4319(6) | 3420(30) | 7628(9) | 72(5) |
| C(4) | 4124(5) | 5220(20) | 7536(10) | 68(4) |
| C(5) | 3905(5) | 5803(19) | 8145(10) | 59(4) |
| C(6) | 3906(4) | 4612(15) | 8867(8) | 42(3) |
| C(7) | 3657(4) | 5083(16) | 9551(9) | 45(3) |
| C(8) | 2952(5) | 693(17) | 8615(9) | 48(3) |
| C(9) | 2428(5) | 370(20) | 8335(10) | 61(3) |
| C(10) | 2237(5) | -90(20) | 9005(10) | 62(3) |
| C(11) | 2553(6) | -152(18) | 9965(11) | 57(3) |
| C(12) | 3068(4) | 232(13) | 10190(8) | 36(2) |
| C(13) | 3445(5) | 171(17) | 11185(9) | 50(3) |
| N(1) | 4099(4) | 2849(12) | 8966(6) | 39(2) |
| N(2) | 3257(3) | 647(12) | 9523(6) | 35(2) |
| O(1) | 4312(4) | -626(13) | 9754(7) | 60(2) |
| O(2) | 3730(3) | 3807(9) | 10200(6) | 43(2) |
| O(3) | 3923(3) | 526(12) | 11268(6) | 51(2) |
| O(4) | 3416(4) | 6532(13) | 9466(10) | 83(4) |

| | | | | |
|---|---|---|---|---|
| O(5) | 3335(4) | -160(16) | 11858(7) | 74(3) |

Part C. Bond lengths [Å] and angles [°] for **1**.

| | | | |
|---|---|---|---|
| Re-O(1) | 1.662(8) | C(6)-C(7) | 1.495(16) |
| Re-O(3) | 2.014(8) | C(7)-O(4) | 1.215(14) |
| Re-O(2) | 2.100(7) | C(7)-O(2) | 1.297(13) |
| Re-C(1) | 2.111(13) | C(13)-O(5) | 1.198(13) |
| Re-N(1) | 2.113(9) | C(13)-O(3) | 1.343(14) |
| Re-N(2) | 2.163(9) | C(13)-C(12) | 1.492(17) |
| C(2)-N(1) | 1.350(14) | C(12)-N(2) | 1.346(13) |
| C(2)-C(3) | 1.393(18) | C(12)-C(11) | 1.402(18) |
| C(3)-C(4) | 1.38(2) | C(11)-C(10) | 1.40(2) |
| C(4)-C(5) | 1.36(2) | C(10)-C(9) | 1.357(18) |
| C(5)-C(6) | 1.384(16) | C(9)-C(8) | 1.410(17) |
| C(6)-N(1) | 1.351(15) | C(8)-N(2) | 1.328(15) |

| | | | |
|---|---|---|---|
| O(1)-Re-O(3) | 109.7(4) | O(4)-C(7)-O(2) | 126.4(12) |
| O(1)-Re-O(2) | 165.3(4) | O(4)-C(7)-C(6) | 120.7(11) |
| O(3)-Re-O(2) | 84.7(3) | O(2)-C(7)-C(6) | 112.9(10) |
| O(1)-Re-C(1) | 98.8(5) | O(5)-C(13)-O(3) | 122.3(12) |
| O(3)-Re-C(1) | 88.2(4) | O(5)-C(13)-C(12) | 123.5(12) |
| O(2)-Re-C(1) | 84.1(5) | O(3)-C(13)-C(12) | 114.2(9) |
| O(1)-Re-N(1) | 90.9(4) | N(2)-C(12)-C(11) | 122.3(11) |
| O(3)-Re-N(1) | 159.4(4) | N(2)-C(12)-C(13) | 115.5(10) |
| O(2)-Re-N(1) | 74.8(3) | C(11)-C(12)-C(13) | 122.2(11) |
| C(1)-Re-N(1) | 88.6(5) | C(10)-C(11)-C(12) | 117.0(12) |
| O(1)-Re-N(2) | 103.9(4) | C(9)-C(10)-C(11) | 120.5(13) |
| O(3)-Re-N(2) | 77.7(3) | C(10)-C(9)-C(8) | 119.1(13) |
| O(2)-Re-N(2) | 75.8(3) | N(2)-C(8)-C(9) | 121.3(11) |

| | | | |
|---|---|---|---|
| C(1)-Re-N(2) | 156.3(4) | C(6)-N(1)-C(2) | 119.1(10) |
| N(1)-Re-N(2) | 97.9(3) | C(6)-N(1)-Re | 117.2(7) |
| N(1)-C(2)-C(3) | 119.8(13) | C(2)-N(1)-Re | 123.6(8) |
| C(4)-C(3)-C(2) | 120.6(13) | C(8)-N(2)-C(12) | 119.8(10) |
| C(5)-C(4)-C(3) | 119.0(13) | C(8)-N(2)-Re | 127.0(8) |
| C(4)-C(5)-C(6) | 119.2(14) | C(12)-N(2)-Re | 113.2(7) |
| N(1)-C(6)-C(5) | 122.2(11) | C(7)-O(2)-Re | 120.4(7) |
| N(1)-C(6)-C(7) | 114.1(9) | C(13)-O(3)-Re | 119.2(7) |
| C(5)-C(6)-C(7) | 123.5(12) | | |

Part D. Anisotropic displacement parameters ($Å^2 \times 10^3$) for **1**. The anisotropic displacement factor exponent takes the form: $-2\pi^2[ h^2 a^{*2} U_{11} + ... + 2 h k a^* b^* U_{12} ]$

| | $U_{11}$ | $U_{22}$ | $U_{33}$ | $U_{23}$ | $U_{13}$ | $U_{12}$ |
|---|---|---|---|---|---|---|
| Re | 32(1) | 33(1) | 46(1) | 1(1) | 21(1) | 5(1) |
| C(1) | 40(8) | 80(10) | 59(7) | -5(7) | 15(6) | 2(6) |
| C(2) | 50(8) | 62(8) | 51(6) | -16(6) | 28(6) | -6(6) |
| C(3) | 73(11) | 113(14) | 43(7) | -19(8) | 35(7) | -45(10) |
| C(4) | 57(10) | 87(12) | 62(9) | 16(8) | 25(7) | -18(9) |
| C(5) | 47(8) | 48(7) | 74(9) | 19(6) | 15(7) | -12(6) |
| C(6) | 44(7) | 36(6) | 51(6) | -2(5) | 21(5) | -12(5) |
| C(7) | 36(7) | 36(6) | 68(7) | 6(5) | 28(6) | -2(5) |
| C(8) | 51(8) | 43(6) | 60(7) | -3(5) | 33(6) | -2(5) |
| C(9) | 38(7) | 77(10) | 66(8) | -2(7) | 17(6) | -3(7) |
| C(10) | 47(8) | 61(8) | 79(9) | -5(7) | 24(7) | -2(6) |
| C(11) | 66(9) | 33(6) | 87(9) | 2(6) | 45(8) | 5(6) |
| C(12) | 42(6) | 22(5) | 51(6) | 3(4) | 24(5) | 9(4) |
| C(13) | 60(8) | 47(7) | 59(7) | 12(6) | 38(6) | 9(6) |
| N(1) | 41(5) | 37(5) | 37(4) | -8(4) | 13(4) | -4(4) |
| N(2) | 39(5) | 29(4) | 45(5) | 4(4) | 24(4) | 6(4) |

| | | | | | | |
|---|---|---|---|---|---|---|
| O(1) | 64(6) | 39(4) | 92(7) | -1(4) | 45(5) | 13(4) |
| O(2) | 40(5) | 37(4) | 60(5) | -5(3) | 29(4) | 2(3) |
| O(3) | 48(5) | 55(5) | 52(4) | 13(4) | 22(4) | 2(4) |
| O(4) | 69(7) | 41(5) | 166(12) | 26(6) | 73(8) | 17(5) |
| O(5) | 75(7) | 89(8) | 74(6) | 27(6) | 45(5) | 6(6) |

Part E. Hydrogen coordinates ( $\times 10^4$) and isotropic displacement parameters ($Å^2 \times 10^3$) for **1**.

| | x | y | z | U(eq) |
|---|---|---|---|---|
| H(1A) | 5017 | 2039 | 10856 | 91 |
| H(1B) | 4792 | 2242 | 11648 | 91 |
| H(1C) | 4712 | 3853 | 10900 | 91 |
| H(2) | 4457 | 1049 | 8431 | 62 |
| H(3) | 4456 | 2980 | 7198 | 87 |
| H(4) | 4142 | 6016 | 7064 | 82 |
| H(5) | 3758 | 6990 | 8078 | 70 |
| H(8) | 3086 | 945 | 8155 | 58 |
| H(9) | 2215 | 457 | 7700 | 73 |
| H(10) | 1894 | -354 | 8824 | 75 |
| H(11) | 2427 | -438 | 10433 | 69 |

**S-2.** Crystal data for compound **2**.

Part A. Crystal data and structure refinement for **2**.

| | |
|---|---|
| Identification code | 2 |
| Empirical formula | $C_{19}H_{15}N_2O_3Re$ |
| Formula weight | 505.53 |
| Temperature | 298(2) K |
| Wavelength | 0.71073 Å |
| Crystal system | Triclinic |

| | | |
|---|---|---|
| Space group | P-1 | |
| Unit cell dimensions | a = 9.233(2) Å | α= 101.054(3)°. |
| | b = 9.724(2) Å | β= 103.955(3)°. |
| | c = 10.780(2) Å | γ = 112.402(4)°. |
| Volume | 823.8(3) $Å^3$ | |
| Z | 2 | |
| Density (calculated) | 2.038 $Mg/m^3$ | |
| Absorption coefficient | 7.396 $mm^{-1}$ | |
| F(000) | 484 | |
| Crystal size | 0.36 × 0.28 × 0.25 $mm^3$ | |
| Theta range for data collection | 2.05 to 28.24°. | |
| Index ranges | $-11 \le h \le 11, -12 \le k \le 12, -14 \le l \le 14$ | |
| Reflections collected | 7383 | |
| Independent reflections | 3718 [R(int) = 0.0338] | |
| Completeness to theta = 28.24° | 91.3 % | |
| Absorption correction | Empirical | |
| Max. and min. transmission | 1 and 0.644 | |
| Refinement method | Full-matrix least-squares on $F^2$ | |
| Data / restraints / parameters | 3718 / 0 / 226 | |
| Goodness-of-fit on $F^2$ | 1.019 | |
| Final R indices [I>2sigma(I)] | R1 = 0.0323, wR2 = 0.0819 | |
| R indices (all data) | R1 = 0.0354, wR2 = 0.0832 | |
| Largest diff. peak and hole | 2.355 and -1.956 $e.Å^{-3}$ | |

---

$R1 = \Sigma \, | \, |F_o| - |F_c| \, | \, / \, \Sigma \, |F_o|$ and $wR2 = \{ \, \Sigma \, [ \, w(F_o^2 - F_c^2)^2 \, ] \, / \, \Sigma \, [ \, w(F_o^2)^2 \, ] \, \}^{1/2}$

Part B. Atomic coordinates ( × $10^4$) and equivalent isotropic displacement parameters ($Å^2$ ×

$10^3$) for **2**. U(eq) is defined as one third of the trace of the orthogonalized $U_{ij}$ tensor.

| | x | y | z | U(eq) |
|---|---|---|---|---|
| Re | 2291(1) | -850(1) | 2890(1) | 28(1) |
| C(1) | -193(8) | -1670(8) | 2859(7) | 53(2) |
| C(2) | 3624(7) | 1864(7) | 5578(5) | 35(1) |
| C(3) | 3918(8) | 3299(7) | 6365(5) | 44(1) |
| C(4) | 3421(8) | 4254(7) | 5806(6) | 46(1) |
| C(5) | 2631(7) | 3768(6) | 4393(6) | 37(1) |
| C(6) | 2057(8) | 4633(7) | 3661(7) | 47(1) |
| C(7) | 1377(8) | 4047(7) | 2297(6) | 46(1) |
| C(8) | 1195(7) | 2604(7) | 1550(6) | 39(1) |
| C(9) | 1718(6) | 1717(6) | 2239(5) | 32(1) |
| C(10) | 2420(6) | 2309(6) | 3655(5) | 30(1) |
| C(11) | 5888(7) | 1100(6) | 2683(5) | 38(1) |
| C(12) | 7200(7) | 1239(7) | 2212(6) | 44(1) |
| C(13) | 7016(7) | 1(8) | 1236(6) | 43(1) |
| C(14) | 5528(7) | -1401(7) | 720(5) | 36(1) |
| C(15) | 5201(8) | -2784(8) | -255(6) | 44(1) |
| C(16) | 3717(8) | -4061(7) | -666(6) | 45(1) |
| C(17) | 2424(7) | -4088(6) | -183(5) | 36(1) |
| C(18) | 2699(6) | -2753(6) | 780(5) | 29(1) |
| C(19) | 4252(6) | -1416(6) | 1231(4) | 28(1) |
| N(1) | 2897(5) | 1350(5) | 4245(4) | 31(1) |
| N(2) | 4449(5) | -184(5) | 2205(4) | 29(1) |
| O(1) | 3070(5) | -1308(5) | 4236(4) | 39(1) |
| O(2) | 1649(5) | 346(4) | 1677(3) | 35(1) |
| O(3) | 1528(4) | -2701(4) | 1299(4) | 33(1) |

Part C. Bond lengths [Å] and angles [°] for **2**.

| | | | |
|---|---|---|---|
| Re-O(1) | 1.677(4) | C(9)-O(2) | 1.325(6) |
| Re-O(2) | 2.037(4) | C(9)-C(10) | 1.409(7) |
| Re-O(3) | 1.986(4) | C(10)-N(1) | 1.369(6) |
| Re-C(1) | 2.111(6) | C(11)-N(2) | 1.322(7) |
| Re-N(1) | 2.125(4) | C(11)-C(12) | 1.394(9) |
| Re-N(2) | 2.201(4) | C(12)-C(13) | 1.362(9) |
| C(2)-N(1) | 1.330(6) | C(13)-C(14) | 1.403(8) |
| C(2)-C(3) | 1.373(8) | C(14)-C(19) | 1.411(7) |
| C(3)-C(4) | 1.357(9) | C(14)-C(15) | 1.415(8) |
| C(4)-C(5) | 1.414(8) | C(15)-C(16) | 1.347(9) |
| C(5)-C(10) | 1.401(7) | C(16)-C(17) | 1.406(8) |
| C(5)-C(6) | 1.417(8) | C(17)-C(18) | 1.391(7) |
| C(6)-C(7) | 1.356(9) | C(18)-O(3) | 1.344(6) |
| C(7)-C(8) | 1.403(9) | C(18)-C(19) | 1.408(7) |
| C(8)-C(9) | 1.385(7) | C(19)-N(2) | 1.354(6) |

| | | | |
|---|---|---|---|
| O(1)-Re-O(3) | 106.04(17) | N(1)-C(10)-C(5) | 123.0(5) |
| O(1)-Re-O(2) | 162.86(17) | N(1)-C(10)-C(9) | 114.3(4) |
| O(3)-Re-O(2) | 90.91(15) | C(5)-C(10)-C(9) | 122.7(5) |
| O(1)-Re-C(1) | 97.9(3) | N(2)-C(11)-C(12) | 122.6(5) |
| O(3)-Re-C(1) | 88.7(2) | C(13)-C(12)-C(11) | 119.2(5) |
| O(2)-Re-C(1) | 84.8(2) | C(12)-C(13)-C(14) | 120.4(5) |
| O(1)-Re-N(1) | 87.47(17) | C(13)-C(14)-C(19) | 116.4(5) |
| O(3)-Re-N(1) | 166.48(15) | C(13)-C(14)-C(15) | 125.9(5) |
| O(2)-Re-N(1) | 75.59(15) | C(19)-C(14)-C(15) | 117.7(5) |
| C(1)-Re-N(1) | 89.3(2) | C(16)-C(15)-C(14) | 120.3(5) |
| O(1)-Re-N(2) | 99.02(17) | C(15)-C(16)-C(17) | 122.8(5) |
| O(3)-Re-N(2) | 78.20(15) | C(18)-C(17)-C(16) | 118.7(5) |
| O(2)-Re-N(2) | 81.66(15) | O(3)-C(18)-C(17) | 121.9(5) |
| C(1)-Re-N(2) | 160.9(2) | O(3)-C(18)-C(19) | 118.9(4) |

| | | | |
|---|---|---|---|
| N(1)-Re-N(2) | 100.12(16) | C(17)-C(18)-C(19) | 119.1(5) |
| N(1)-C(2)-C(3) | 122.9(5) | N(2)-C(19)-C(18) | 115.7(4) |
| C(4)-C(3)-C(2) | 120.7(5) | N(2)-C(19)-C(14) | 122.8(5) |
| C(3)-C(4)-C(5) | 119.0(5) | C(18)-C(19)-C(14) | 121.5(5) |
| C(10)-C(5)-C(4) | 116.9(5) | C(2)-N(1)-C(10) | 117.4(5) |
| C(10)-C(5)-C(6) | 117.3(5) | C(2)-N(1)-Re | 127.8(4) |
| C(4)-C(5)-C(6) | 125.7(6) | C(10)-N(1)-Re | 114.8(3) |
| C(7)-C(6)-C(5) | 119.4(6) | C(11)-N(2)-C(19) | 118.6(5) |
| C(6)-C(7)-C(8) | 123.5(5) | C(11)-N(2)-Re | 130.8(4) |
| C(9)-C(8)-C(7) | 118.4(5) | C(19)-N(2)-Re | 110.1(3) |
| O(2)-C(9)-C(8) | 125.5(5) | C(9)-O(2)-Re | 118.8(3) |
| O(2)-C(9)-C(10) | 115.9(4) | C(18)-O(3)-Re | 115.7(3) |
| C(7)-C(9)-C(10) | 118.6(5) | | |

Part D. Anisotropic displacement parameters ($Å^2 \times 10^3$) for **2**. The anisotropic displacement factor exponent takes the form: $-2\pi^2[\, h^2 a^{*2} U_{11} + \ldots + 2\, h\, k\, a^*\, b^*\, U_{12}\,]$

| | $U_{11}$ | $U_{22}$ | $U_{33}$ | $U_{23}$ | $U_{13}$ | $U_{12}$ |
|---|---|---|---|---|---|---|
| Re | 29(1) | 25(1) | 33(1) | 9(1) | 11(1) | 14(1) |
| C(1) | 38(3) | 52(4) | 70(4) | 13(3) | 27(3) | 20(3) |
| C(2) | 36(3) | 40(3) | 33(2) | 11(2) | 11(2) | 23(2) |
| C(3) | 47(3) | 43(3) | 36(3) | 6(2) | 12(2) | 21(3) |
| C(4) | 54(3) | 32(3) | 48(3) | 5(2) | 20(3) | 19(3) |
| C(5) | 40(3) | 27(3) | 51(3) | 15(2) | 21(2) | 17(2) |
| C(6) | 52(3) | 33(3) | 71(4) | 24(3) | 26(3) | 28(3) |
| C(7) | 47(3) | 43(3) | 66(4) | 36(3) | 24(3) | 27(3) |
| C(8) | 32(3) | 43(3) | 49(3) | 25(2) | 14(2) | 19(2) |
| C(9) | 30(2) | 32(3) | 38(2) | 16(2) | 12(2) | 15(2) |
| C(10) | 27(2) | 29(3) | 40(2) | 13(2) | 14(2) | 16(2) |
| C(11) | 37(3) | 26(3) | 42(3) | 13(2) | 7(2) | 10(2) |

| | | | | | | |
|---|---|---|---|---|---|---|
| C(12) | 32(3) | 39(3) | 55(3) | 21(3) | 11(2) | 9(3) |
| C(13) | 29(3) | 50(4) | 56(3) | 24(3) | 19(2) | 18(3) |
| C(14) | 33(3) | 46(3) | 39(2) | 21(2) | 15(2) | 23(2) |
| C(15) | 48(3) | 57(4) | 47(3) | 19(3) | 26(3) | 35(3) |
| C(16) | 58(4) | 40(3) | 45(3) | 9(2) | 25(3) | 29(3) |
| C(17) | 39(3) | 28(3) | 39(2) | 7(2) | 10(2) | 16(2) |
| C(18) | 33(2) | 28(2) | 32(2) | 12(2) | 13(2) | 18(2) |
| C(19) | 31(2) | 28(2) | 31(2) | 13(2) | 10(2) | 16(2) |
| N(1) | 31(2) | 32(2) | 33(2) | 12(2) | 12(2) | 18(2) |
| N(2) | 29(2) | 27(2) | 34(2) | 15(2) | 10(2) | 14(2) |
| O(1) | 51(2) | 33(2) | 48(2) | 22(2) | 20(2) | 28(2) |
| O(2) | 38(2) | 34(2) | 33(2) | 10(1) | 8(1) | 20(2) |
| O(3) | 28(2) | 25(2) | 41(2) | 6(1) | 12(1) | 8(2) |

Part E. Hydrogen coordinates ( $\times 10^4$) and isotropic displacement parameters ($Å^2 \times 10^3$) for **2**.

| | x | y | z | U(eq) |
|---|---|---|---|---|
| H(1A) | -205 | -1616 | 3755 | 79 |
| H(1B) | -838 | -2737 | 2281 | 79 |
| H(1C) | -665 | -1031 | 2527 | 79 |
| H(2) | 3948 | 1224 | 5996 | 42 |
| H(3) | 4464 | 3620 | 7290 | 52 |
| H(4) | 3598 | 5214 | 6344 | 55 |
| H(6) | 2147 | 5596 | 4110 | 56 |
| H(7) | 1010 | 4633 | 1833 | 55 |
| H(8) | 735 | 2251 | 615 | 47 |
| H(11) | 6030 | 1944 | 3359 | 45 |
| H(12) | 8190 | 2165 | 2560 | 53 |
| H(13) | 7881 | 86 | 910 | 51 |

| | | | | |
|---|---|---|---|---|
| H(15) | 6014 | -2813 | -613 | 53 |
| H(16) | 3541 | -4963 | -1295 | 54 |
| H(17) | 1404 | -4982 | -503 | 43 |

**S-3.** Crystal data for compound **3a**.

Part A. Crystal data and structure refinement for **3a**.

| | | |
|---|---|---|
| Identification code | 3a | |
| Empirical formula | $C_{19}H_{15}N_2OReS_2$ | |
| Formula weight | 537.65 | |
| Temperature | 298(2) K | |
| Wavelength | 0.71073 Å | |
| Crystal system | Triclinic | |
| Space group | P-1 | |
| Unit cell dimensions | a = 8.4428(14) Å | α= 85.504(3)°. |
| | b = 9.1357(15) Å | β= 89.214(3)°. |
| | c = 12.531(2) Å | γ = 64.825(3)°. |
| Volume | 871.8(3) $Å^3$ | |
| Z | 2 | |
| Density (calculated) | 2.048 $Mg/m^3$ | |
| Absorption coefficient | 7.218 $mm^{-1}$ | |
| F(000) | 516 | |
| Crystal size | 0.3 × 0.3 × 0.2 $mm^3$ | |
| Theta range for data collection | 1.63 to 28.26°. | |
| Index ranges | $-10 \le h \le 11, -11 \le k \le 11, -16 \le l \le 16$ | |
| Reflections collected | 7758 | |
| Independent reflections | 3926 [R(int) = 0.0273] | |
| Completeness to theta = 28.26° | 90.8 % | |
| Absorption correction | Empirical | |
| Max. and min. transmission | 1 and 0.52 | |

| | |
|---|---|
| Refinement method | Full-matrix least-squares on $F^2$ |
| Data / restraints / parameters | 3926 / 0 / 226 |
| Goodness-of-fit on $F^2$ | 1.099 |
| Final R indices [I>2sigma(I)] | R1 = 0.0633, wR2 = 0.1540 |
| R indices (all data) | R1 = 0.0681, wR2 = 0.1566 |
| Largest diff. peak and hole | 6.437 and -2.618 e.Å$^{-3}$ |
| | (both about 0.6A from Re atom) |

$R1 = \Sigma \, | \, |F_o| - |F_c| \, | \, / \, \Sigma \, |F_o|$ and $wR2 = \{ \Sigma [ w(F_o^2 - F_c^2)^2 ] / \Sigma [ w(F_o^2)^2 ] \}^{1/2}$

Part B. Atomic coordinates ( × $10^4$) and equivalent isotropic displacement parameters (Å$^2$ × $10^3$) for **3a**. U(eq) is defined as one third of the trace of the orthogonalized $U_{ij}$ tensor.

| | x | y | z | U(eq) |
|---|---|---|---|---|
| Re | 59(1) | 7351(1) | 7378(1) | 33(1) |
| S(1) | 451(4) | 4579(4) | 7159(3) | 44(1) |
| S(2) | 378(4) | 9740(3) | 7405(2) | 38(1) |
| C(1) | -238(16) | 7815(16) | 5697(10) | 45(3) |
| C(2) | 2586(14) | 3606(13) | 6737(8) | 33(2) |
| C(3) | 3275(16) | 2003(14) | 6506(10) | 42(3) |
| C(4) | 5006(18) | 1167(15) | 6199(10) | 48(3) |
| C(5) | 6082(15) | 1938(15) | 6104(10) | 44(3) |
| C(6) | 5455(13) | 3581(14) | 6306(8) | 34(2) |
| C(7) | 6489(14) | 4441(16) | 6218(9) | 41(3) |
| C(8) | 5801(15) | 6022(16) | 6422(9) | 41(3) |
| C(9) | 4033(15) | 6783(15) | 6726(10) | 40(2) |
| C(10) | 3680(13) | 4427(12) | 6636(7) | 29(2) |
| C(11) | 1460(14) | 9439(13) | 8640(8) | 34(2) |
| C(12) | 1886(18) | 10603(16) | 9031(10) | 48(3) |
| C(13) | 2760(20) | 10314(19) | 10019(11) | 56(3) |
| C(14) | 3167(19) | 8940(20) | 10632(11) | 57(4) |

| | | | | |
|---|---|---|---|---|
| C(15) | 2766(17) | 7683(17) | 10271(9) | 46(3) |
| C(16) | 3150(20) | 6190(20) | 10863(11) | 61(4) |
| C(17) | 2690(20) | 5080(20) | 10479(12) | 63(4) |
| C(18) | 1897(18) | 5395(16) | 9462(10) | 48(3) |
| C(19) | 1925(14) | 7952(14) | 9261(9) | 36(2) |
| N(1) | 3019(11) | 6033(10) | 6836(7) | 30(2) |
| N(2) | 1518(12) | 6781(11) | 8862(7) | 37(2) |
| O(1) | -1993(10) | 7806(10) | 7764(7) | 43(2) |

Part C. Bond lengths [Å] and angles [°] for **3a**.

| | | | |
|---|---|---|---|
| Re-O(1) | 1.674(8) | C(7)-C(8) | 1.353(18) |
| Re-C(1) | 2.113(12) | C(8)-C(9) | 1.414(16) |
| Re-N(2) | 2.148(9) | C(9)-N(1) | 1.304(14) |
| Re-S(2) | 2.313(3) | C(10)-N(1) | 1.373(13) |
| Re-N(1) | 2.383(9) | C(11)-C(12) | 1.383(15) |
| Re-S(1) | 2.447(3) | C(11)-C(19) | 1.412(16) |
| S(1)-C(2) | 1.733(11) | C(12)-C(13) | 1.40(2) |
| S(2)-C(11) | 1.750(11) | C(13)-C(14) | 1.33(2) |
| C(2)-C(3) | 1.380(15) | C(14)-C(15) | 1.43(2) |
| C(2)-C(10) | 1.416(15) | C(15)-C(16) | 1.41(2) |
| C(3)-C(4) | 1.396(18) | C(15)-C(19) | 1.412(16) |
| C(4)-C(5) | 1.365(19) | C(16)-C(17) | 1.35(2) |
| C(5)-C(6) | 1.407(17) | C(17)-C(18) | 1.398(19) |
| C(6)-C(7) | 1.400(16) | C(18)-N(2) | 1.336(15) |
| C(6)-C(10) | 1.435(14) | C(19)-N(2) | 1.383(15) |

| | | | |
|---|---|---|---|
| O(1)-Re-C(1) | 102.5(4) | C(7)-C(8)-C(9) | 119.0(11) |
| O(1)-Re-N(2) | 103.6(4) | N(1)-C(9)-C(8) | 123.4(11) |
| C(1)-Re-N(2) | 153.6(4) | N(1)-C(10)-C(2) | 119.5(9) |

| | | | |
|---|---|---|---|
| O(1)-Re-S(2) | 105.2(3) | N(1)-C(10)-C(6) | 120.8(9) |
| C(1)-Re-S(2) | 87.2(4) | C(2)-C(10)-C(6) | 119.7(10) |
| N(2)-Re-S(2) | 82.3(3) | C(12)-C(11)-C(19) | 118.6(11) |
| O(1)-Re-N(1) | 165.6(4) | C(12)-C(11)-S(2) | 122.4(10) |
| C(1)-Re-N(1) | 78.8(4) | C(19)-C(11)-S(2) | 119.0(8) |
| N(2)-Re-N(1) | 76.9(3) | C(11)-C(12)-C(13) | 120.7(13) |
| S(2)-Re-N(1) | 89.1(2) | C(14)-C(13)-C(12) | 121.8(12) |
| O(1)-Re-S(1) | 89.0(3) | C(13)-C(14)-C(15) | 120.1(12) |
| C(1)-Re-S(1) | 88.3(4) | C(16)-C(15)-C(19) | 117.6(12) |
| N(2)-Re-S(1) | 95.9(3) | C(16)-C(15)-C(14) | 124.1(12) |
| S(2)-Re-S(1) | 165.66(10) | C(19)-C(15)-C(14) | 118.3(12) |
| N(1)-Re-S(1) | 76.6(2) | C(17)-C(16)-C(15) | 120.5(13) |
| C(2)-S(1)-Re | 104.2(4) | C(16)-C(17)-C(18) | 119.4(13) |
| C(11)-S(2)-Re | 101.2(4) | N(2)-C(18)-C(17) | 122.5(13) |
| C(3)-C(2)-C(10) | 118.1(10) | N(2)-C(19)-C(11) | 118.5(10) |
| C(3)-C(2)-S(1) | 121.0(9) | N(2)-C(19)-C(15) | 121.1(11) |
| C(10)-C(2)-S(1) | 120.9(8) | C(11)-C(19)-C(15) | 120.4(11) |
| C(2)-C(3)-C(4) | 122.4(12) | C(9)-N(1)-C(10) | 118.9(9) |
| C(5)-C(4)-C(3) | 120.2(11) | C(9)-N(1)-Re | 122.3(8) |
| C(4)-C(5)-C(6) | 120.4(11) | C(10)-N(1)-Re | 118.7(6) |
| C(7)-C(6)-C(5) | 123.1(10) | C(18)-N(2)-C(19) | 118.7(10) |
| C(7)-C(6)-C(10) | 117.7(10) | C(18)-N(2)-Re | 122.1(8) |
| C(5)-C(6)-C(10) | 119.2(10) | C(19)-N(2)-Re | 118.9(7) |
| C(8)-C(7)-C(6) | 120.1(10) | | |

Part D. Anisotropic displacement parameters ($Å^2 \times 10^3$) for **3a**. The anisotropic displacement factor exponent takes the form: $-2\pi^2[\, h^2 a^{*2} U_{11} + \ldots + 2\, h\, k\, a^* b^* U_{12}\,]$

| | $U_{11}$ | $U_{22}$ | $U_{33}$ | $U_{23}$ | $U_{13}$ | $U_{12}$ |
|---|---|---|---|---|---|---|

| | | | | | | |
|---|---|---|---|---|---|---|
| Re | 31(1) | 32(1) | 36(1) | -4(1) | -1(1) | -12(1) |
| S(1) | 33(1) | 38(1) | 68(2) | -16(1) | 8(1) | -19(1) |
| S(2) | 45(2) | 32(1) | 35(1) | 0(1) | -4(1) | -15(1) |
| C(1) | 37(6) | 54(7) | 42(6) | -16(5) | 1(5) | -15(5) |
| C(2) | 30(5) | 37(5) | 29(5) | -4(4) | -1(4) | -11(4) |
| C(3) | 44(6) | 37(6) | 45(6) | -8(5) | 4(5) | -16(5) |
| C(4) | 52(7) | 35(6) | 47(7) | -9(5) | 0(6) | -6(5) |
| C(5) | 33(6) | 44(6) | 44(6) | -7(5) | 3(5) | -4(5) |
| C(6) | 28(5) | 45(6) | 21(4) | -1(4) | -3(4) | -10(4) |
| C(7) | 27(5) | 61(7) | 33(5) | -3(5) | 1(4) | -16(5) |
| C(8) | 31(5) | 58(7) | 41(6) | -1(5) | -1(5) | -26(5) |
| C(9) | 37(6) | 46(6) | 44(6) | -6(5) | 0(5) | -23(5) |
| C(10) | 29(5) | 34(5) | 21(4) | -1(4) | -5(4) | -9(4) |
| C(11) | 37(5) | 36(5) | 33(5) | -11(4) | 7(4) | -18(4) |
| C(12) | 62(8) | 49(7) | 45(7) | -18(6) | 13(6) | -32(6) |
| C(13) | 65(9) | 71(9) | 50(7) | -26(7) | 12(6) | -44(8) |
| C(14) | 57(8) | 86(11) | 37(6) | -22(7) | 6(6) | -36(8) |
| C(15) | 45(7) | 64(8) | 28(5) | -3(5) | 2(5) | -23(6) |
| C(16) | 64(9) | 79(10) | 32(6) | 11(6) | -5(6) | -27(8) |
| C(17) | 74(10) | 68(9) | 46(7) | 21(7) | -9(7) | -33(8) |
| C(18) | 58(8) | 48(7) | 43(6) | 10(5) | 3(6) | -30(6) |
| C(19) | 32(5) | 42(6) | 33(5) | -6(4) | 3(4) | -14(5) |
| N(1) | 28(4) | 31(4) | 31(4) | -2(3) | -1(3) | -12(3) |
| N(2) | 37(5) | 38(5) | 34(5) | 3(4) | 1(4) | -17(4) |
| O(1) | 35(4) | 49(5) | 46(5) | -17(4) | 10(3) | -17(4) |

Part E. Hydrogen coordinates ( $\times 10^4$) and isotropic displacement parameters ($Å^2 \times 10^3$) for **3a**.

| | x | y | z | U(eq) |
|---|---|---|---|---|
| H(1A) | -432 | 8917 | 5502 | 67 |
| H(1B) | -1221 | 7648 | 5460 | 67 |
| H(1C) | 803 | 7092 | 5365 | 67 |
| H(3) | 2560 | 1459 | 6556 | 51 |
| H(4) | 5428 | 82 | 6060 | 58 |
| H(5) | 7237 | 1373 | 5903 | 53 |
| H(7) | 7651 | 3925 | 6019 | 49 |
| H(8) | 6481 | 6601 | 6364 | 50 |
| H(9) | 3569 | 7874 | 6855 | 49 |
| H(12) | 1589 | 11588 | 8631 | 58 |
| H(13) | 3060 | 11104 | 10254 | 67 |
| H(14) | 3714 | 8795 | 11297 | 68 |
| H(16) | 3727 | 5970 | 11524 | 73 |
| H(17) | 2892 | 4124 | 10888 | 75 |
| H(18) | 1626 | 4606 | 9194 | 57 |

# CHAPTER III. LIGAND DISPLACEMENT AND OXIDATION REACTIONS OF METHYLOXORHENIUM(V) COMPLEXES

A manuscript submitted to *Inorganic Chemistry*

Xiaopeng Shan, Arkady Ellern, Ilia A. Guzei, James H. Espenson


## Abstract

Compounds containing the anion MeReO(edt)(SPh)$^-$ (**3**) were prepared with the counter-cations 2-picolinium (**PicH$^+$3$^-$**) and 2,6-lutidinium (**LutH$^+$3$^-$**), where edt is 1,2-ethanedithiolate, were synthesized. **PicH$^+$3$^-$** and MeReO(edt)(tmtu) (**4**) were crystallographically characterized (tmtu is 1,1,3,3-tetramethylthiourea). The rhenium atom in these compounds exists in a five-coordinate distorted square pyramid. In the solid state, **PicH$^+$3$^-$** contains an anion with a hydrogen bonded (N–H···S) interaction to the cation. Displacement of PhSH by $PPh_3$ followed second-order kinetics, whereas with pyridines the reaction was second-order with respect to [Py] and first-order in [**PicH$^+$3$^-$**] in chloroform. To account for this unusual kinetics, the structure formula of **PicH$^+$3$^-$** in chloroform was proposed to be the molecular species MeReO(edtH)SPh, which can react with a Brönsted base to accelerate ligand displacement. When PicH$^+$**3**$^-$ reacts with pyridine N-oxides, a three-stage reaction was observed, consistent with ligand replacement of SPh$^-$ by PyO, N–O bond cleavage of the PyO assisted by another PyO, and eventual decomposition of $MeReO_2$(edt)PyO to $MeReO_3$. Each of first two steps showed a large substituent effects, $\rho$ = –5.3 and $\rho$ = –4.3.


## Introduction

Our exploration of oxorhenium(V) catalysts[1-7] for oxygen atom transfer (OAT) reactions has been extended. The stoichiometric reactions and certain mechanistic aspects are analogous to those catalyzed by molybdenum oxotranferases.[8-10] Three new methyl(oxo)rhenium(V) complexes have been prepared and characterized; two contain the anion MeReO(edt)(SPh)$^-$ (**3**) with the cations 2-picolinium (**PicH$^+$3$^-$**) and 2,6-lutidinium (**LutH$^+$3$^-$**), and the third is a neutral rhenium compound, MeReO(edt)(tmtu) (**4**), where edt

stands for 1,2-ethanedithiolate and tmtu for 1,1,3,3-tetramethylthiourea. Their structural formulas are shown in Chart 1.

**Chart 1**. Structural formulas of **1-4**

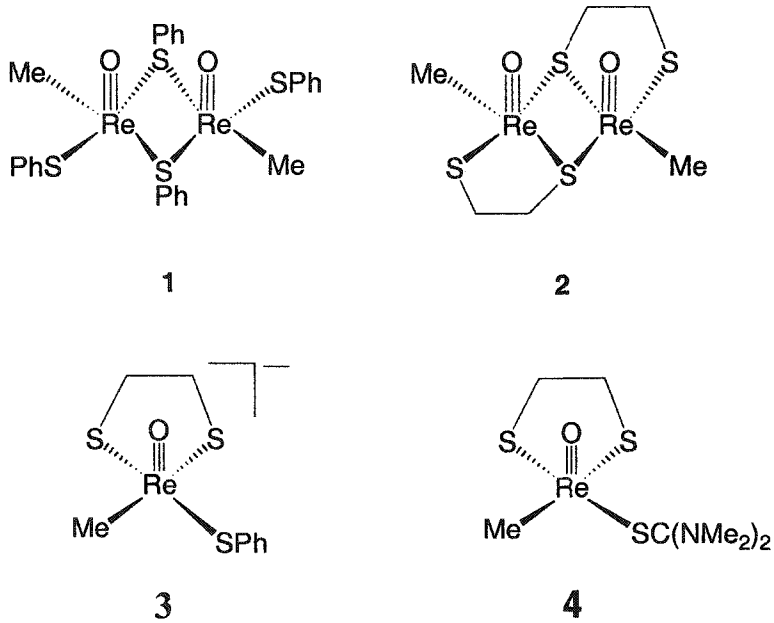


Our goal has been to characterize the steps of OAT from pyridine N-oxides to triphenylphosphine, eq 1, including a study of the intermediates MeReO(edt)PyO from ligand displacement and $MeReO_2$(edt)PyO from oxidation, especially the striking feature that nucleophiles assist oxidation by incorporation of a second molecule of pyridine N-oxide in the transition state. To extend understanding of ligand displacement, the non-oxidizing ligands pyridines and $PPh_3$ were employed as well. An unanticipated assistance of ligand displacement of **3** by Brønsted bases was discovered and studied.

$$PyO + PPh_3 \rightarrow Py + Ph_3PO \qquad (1)$$

**Experimental Section**

**Reagents and instrumentation.** {MeReO(edt)}$_2$ (**2**) was synthesized from 1,2-ethanedithiol and {MeReO(benzenethiolate)}$_2$ (**1**),[11] the later prepared according to the literature.[12] Other chemical reagents were purchased from Aldrich and used as received. Acetonitrile-$d_3$, benzene-$d_6$ and chloroform-$d_1$ were employed as solvents for NMR

spectroscopy. Chloroform from Fisher Scientific was used as solvent for UV/Visible and IR spectrophotometry and for kinetics.

UV/Visible spectra and kinetic data were obtained with Shimadzu Model 3101 and OLIS RSM stopped-flow spectrophotometers. A circulating water thermostatic system controlled the temperature variation to within ±0.2 °C was used for the stopped-flow instrument and an electronic thermostatic holder that maintained the temperature of the cell to ±0.2 °C was used for the UV/visible spectrophotometer. IR spectra were collected with a Nicolet-500 spectrometer. A Bruker DRX-400 MHz spectrophotometer was used to record $^{1}H$ and $^{13}C$ NMR spectra. The chemical shift for $^{1}H$ was calculated relative to the residual proton of the solvent, δ 1.94 for acetonenitrile-$d_3$, 7.16 for benzene-$d_6$, and 7.27 for chloroform-$d_1$. Elemental analyses were performed by Desert Analytics Laboratory.

**Kinetics.** Reactions of **2**, **PicH$^+$3$^-$**, **LutH$^+$3$^-$**, **4** with $PPh_3$ and pyridines were followed by the increase in absorbance from 380 to 420 nm from the products MeReO(edt)$PPh_3$ and MeReO(edt)Py. The concentrations of the ligands were in at least 10-fold excess over rhenium. Thus the absorbance-time data could be fitted to pseudo-first-order kinetics,

$$Abs_t = Abs_\infty + (Abs_0 - Abs_\infty) \times e^{-k\psi \cdot t} \quad (2)$$

Reactions of **2**, **3** and **4** with pyridine N-oxides were monitored by the change in absorbance from 400 to 500 nm according to the identities of pyridine N-oxides and rhenium compounds. In most case, the concentrations of pyridine N-oxides were at least 100 times larger than those of rhenium compounds. Multiple-phase absorbance changes were observed; reactions with **2** and **3** displayed a three-stage absorbance change: a fast rise and fall followed by a slow decrease. Kinetic traces of the first and second phases can be fitted to consecutive pseudo-first-order kinetics,

$$Abs_t = Abs_\infty + \alpha \times e^{-k\alpha \cdot t} + \beta \times e^{-k\beta \cdot t} \quad (3)$$

The third phase was too sluggish to be studied. In contrast, reaction with compound **4** was a simplified version of reactions with **2** and **3**; only two-stage absorbance change was observed: a fast rise and slow decrease, the former can be fitted to eq 5 and the latter, which spans almost same period of time as the third stage of reactions of **2** and **3**, is not suitable for kinetic study.

**Preparation of Salts of MeReO(edt)(SPh)$^-$ (3).** 1,2-Ethanedithiol (18.8 mg, 16.8 μL, 0.2 mmol) was added to a mixture of **1** (87 mg, 0.1 mmol) and 2-picoline for PicH$^+$**3**$^-$ or 2,6-lutidine for **LutH**$^+$**3**$^-$ (0.2 mmol) in 20 mL of toluene. The resulting solution was stirred for 2 h as a dark red solid deposited. The product was collected by filtration, rinsed by hexanes, and dried under vacuum.

**PicH**$^+$**3**$^-$ was obtained in 97% yield. A crystal suitable for x-ray diffraction analysis was obtained by recrystallization from methylene chloride-hexanes. NMR (acetonitrile-$d_3$) $^1$H: δ 8.48 (d, 1H), 8.41 (m, 1H), 7.81 (m, 2H), 7.57 (m, 2H), 7.23 (t, 2H), 7.10 (t, 1H), 2.88 (m, 1H), 2.73 (s, 3H), 2.67 (m, 2H), 2.49 (m, 1H), 2.18 (s, 3H); $^{13}$C: 150.0, 147.0, 133.9, 128.3, 127.5, 124.8, 124.7, 43.6, 43.4, 19.3, 7.2. IR ($CHCl_3$): 1003 cm$^{-1}$. UV-Vis($CHCl_3$), $\lambda_{max}$/nm (log ε): 337(sh), 397(3.48). Elemental analysis: $C_{15}H_{20}NOReS_3$, Found (Calcd.) C: 35.30 (35.14), H: 4.05 (3.93), N: 2.71 (2.73), S: 19.08 (18.76).

**LutH**$^+$**3**$^-$ was obtained in 90% yield. NMR (acetonitrile-$d_3$) $^1$H: δ 8.26 (t, 1H), 7.57 (m, 4H), 7.23 (m, 2H), 7.11 (m, 1H), 2.88 (m, 1H), 2.69 (m, 2H), 2.67 (s, 6H), 2.17 (s, 3H); $^{13}$C: 146.5, 133.9, 127.4, 125.0, 124.7, 43.6, 43.4, 18.8, 6.5. UV-Vis($CHCl_3$), $\lambda_{max}$/nm (log ε): 337(sh), 369(3.48).

**Preparation of MeReO(edt)(tmtu) (4).** Tetramethylthiourea (24.6 mg, 0.2 mmol) was mixed with **2** (61.9 mg, 0.1 mmol) in 20 mL of toluene. After stirring the mixture for 4 h, color of the solution changed from brown to violet and 20 mL of hexanes was layered on the top. After one day, black crystals appeared; they were filtered and rinsed by hexanes. The yield was 76%. Crystal suitable for x-ray diffraction analysis were obtained. NMR (benzene-$d_6$) $^1$H: δ 3.58 (m, 1H), 3.25 (s, 3H), 3.13 (m, 1H), 3.04 (m, 1H), 2.69 (m, 1H), 2.38 (sb, 12H); $^{13}$C: 46.2, 43.2, 6.8. IR ($CHCl_3$): 976 cm$^{-1}$. UV-Vis($CHCl_3$), $\lambda_{max}$/nm (log ε/L mol$^{-1}$ cm$^{-1}$): 300(sh). Elemental analysis: $C_7H_{19}N_2OReS_3$, Found (Calcd.) C: 21.71 (21.76), H: 4.12 (4.34), N: 6.34 (6.34), S: 21.80 (21.78).

**X-ray Crystallography.** Crystals of **PicH**$^+$**3**$^-$ and **4**, selected under ambient conditions, were mounted and centered in the X-ray beam by using a video camera. The crystal evaluation and data collection were performed on a Bruker CCD-1000 diffractometer with Mo $K_\alpha$ ($\lambda$ = 0.71073 Å) radiation and the detector to crystal distance of 4.90 cm. The cell constants were calculated from a set of certain amount of strong reflections from the actual

data collection. The data were collected by using the full sphere routine. This data set was corrected for Lorentz and polarization effects. The absorption correction was based on fitting a function to the empirical transmission surface as sampled by multiple equivalent measurements[13] using SADABS software.[14]

The position of the Re atom was found by the Patterson method. The remaining atoms were located in an alternating series of least-squares cycles and difference Fourier maps. All non-hydrogen atoms were refined in full-matrix anisotropic approximation. All hydrogen atoms were placed in the structure factor calculation at idealized positions and were allowed to ride on the neighboring atoms with relative isotropic displacement coefficients.

**Results**

**Structures.** Table 1 shows the crystallographic parameters for **PicH$^+$3$^-$** and **4** and Figure 1 depicts their molecular structures. In both compounds, the rhenium(V) atom lies in the center of a distorted square pyramid defined by the apical terminal oxo group and a basal plane occupied by a methyl group and three sulfur atoms from edt and SPh or tmtu. Important bond lengths and angles are summarized in Table 2. Irrespective of the negative charge on **PicH$^+$3$^-$**, the Re≡O distances are identical at 169 pm for **PicH$^+$3$^-$** and **4**, as are the values of $\nu$(Re–O) from the IR studies, which fall in the narrow range of 976-1003 cm$^{-1}$, indicating that the ionic charge does not influence the Re≡O bond. Re–C distances differ slightly, 215 pm in **PicH$^+$3$^-$** and 213 pm in **4**. Also, the chemical shifts of $^{13}$C for $CH_3$, δ 7.2 for **PicH$^+$3$^-$**, 6.8 for **4**; the $CH_3$ $^1$H resonance is more sensitive to the ligand environment, being δ 2.38 for PicH$^+$**3**$^-$ and 3.25 for **4**.

**Table 1**. Experimental Data for the X-ray Diffraction Studies of **PicH$^+$3$^-$** and **4**.

| | **PicH$^+$3$^-$** | **4** |
|---|---|---|
| Empirical formula | $C_{15}H_{20}NOReS_3$ | $C_7H_{19}N_2OReS_3$ |
| formula weight | 512.72 | 441.64 |
| *a*, Å | 7.3826(5) | 8.7615(12) |
| *b*, Å | 9.7701(6) | 16.426(3) |
| *c*, Å | 12.8309(8) | 10.0210(15) |
| $\alpha$, deg | 94.362(1) | |
| $\beta$, deg | 102.414(1) | 93.768(4) |
| $\gamma$, deg | 99.639(1) | |
| *V*, Å$^3$ | 885.02(10) | 1439.1(4) |
| *Z* | 2 | 4 |
| space group | P-1 | P2(1) |
| *T*, K | 173(2) | 293(2) |
| Wavelength, Å | 0.71073 | 0.71073 |
| $\rho_{calcd}$, g cm$^{-3}$ | 1.924 | 2.038 |
| $\mu$, mm$^{-1}$ | 7.216 | 8.859 |
| R indices | R1 = 0.0237, | R1 = 0.0340 |
| (all data)[a] | wR2 = 0.0575 | wR2 = 0.0711 |

[a] $R1 = \Sigma \, | \, |F_0| - |F_c| \, | \, / \, \Sigma \, |F_0|$; $wR2 = \{ \, \Sigma \, [ \, w(F_0^2 - F_c^2)^2 \, ] \, / \, \Sigma \, [ \, w(F_0^2)^2 \, ] \, \}^{1/2}$.

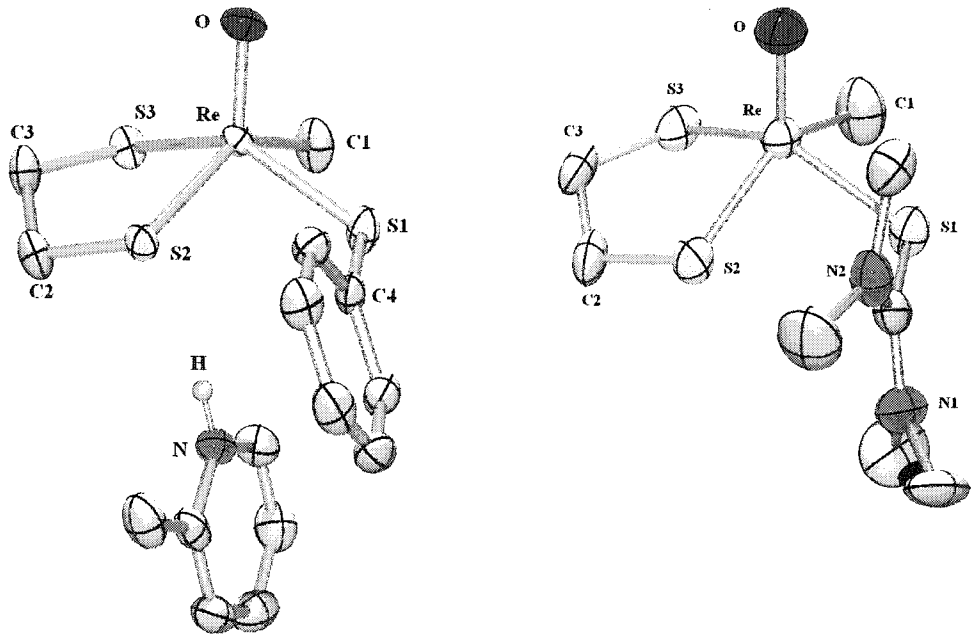


**Figure 1.** Crystallographically-determined structures of **PicH$^+$3$^-$** and **4**.

**Table 2**. Selected Bond Lengths (pm) and Angles (deg) of **PicH$^+$3$^-$** and **4**.

| | PicH$^+$**3**$^-$ | **4** |
|---|---|---|
| Re–O | 169.2(3) | 168.0(8) |
| Re–C(1) | 215.4(4) | 212.8(11) |
| Re–S(1) | 233.49(10) | 236.6(3) |
| Re–S(2) | 232.49(9) | 230.2(3) |
| Re–S(3) | 229.65(9) | 226.4(3) |
| O–Re–C(1) | 107.14(16) | 107.6(4) |
| O–Re–S(1) | 109.48(10) | 107.4(3) |
| O–Re–S(3) | 108.59(10) | 109.2(3) |
| C(1)–Re–S(2) | 139.72(14) | 137.3(3) |
| S(1)–Re–S(3) | 140.85(4) | 142.54(11) |

It is worth noting that **PicH$^+$3$^-$** is a salt in the solid state. The 2 pm elongations of Re–S(2) and Re–S(3) can be attributed to the negative charge on PicH$^+$**3**$^-$. Based on the

orientation of N–H and the N···S(2) nonbonded distance, 319 pm, we assume a hydrogen bond (N–H···S) interaction between N and S(2). Raper and co-workers discovered a such interaction between a bridging thionate sulfur and a thioamide nitrogen in a copper complex with a N···S distance of 349 pm.[15] Francois and co-workers found two types of N–H···S hydrogen bonds in $(TACN)_2Fe_2S_6$: a "strong" interaction with $d_{SH}$ = 231 pm and a "weak" interaction with $d_{SH}$ = 265 pm.[16] In our case, the calculated position of H gives an angle of 170.3° for N–H···S(2) and $d_{SH}$ = 232 pm. Compared with the literature values, we conclude that a "strong" hydrogen bond interaction exists in **PicH$^+$3$^-$**.

**Reactions with $PPh_3$.** $PPh_3$ reacts with **PicH$^+$3$^-$** and **4** to yield $MeReO(edt)PPh_3$, eq 4-5. The product was identified by $^1H$ NMR.[17] The reaction of PicH$^+$**3**$^-$ gave rise to benzenethiol and 2-picoline (2-Pic) according to the (aqueous) acidity of PhSH and 2-picolinium (2-PicH$^+$): $pK_a$ = 6.62 for PhSH and $pK_a$ = 6.00 for 2-PicH$^+$; the reaction of **4** generates free tmtu (eq 5).

$$PicH^+\mathbf{3}^- + PPh_3 \rightarrow MeReO(edt)PPh_3 + PhSH + 2\text{-}Pic \quad (4)$$

$$\mathbf{4} + PPh_3 \rightarrow MeReO(edt)PPh_3 + tmtu \quad (5)$$

Both reactions are first-order with respect to the concentrations of rhenium complexes and $PPh_3$. The second-order rate constants are 2.57 ± 0.02 L mol$^{-1}$ s$^{-1}$ for PicH$^+$**3**$^-$ and (8.20 ± 0.06) × $10^{-2}$ L mol$^{-1}$ s$^{-1}$ for **4** (Figure 2) in chloroform at 25.0 °C. The thirty-fold slower reaction of **4** can be attributed to the steric hindrance of tmtu. Both rate constants are relatively small compared with the reaction of MeReO(edt)Py with $PPh_3$, with k = 127 L mol$^{-1}$ s$^{-1}$ in $C_6H_6$.[18]

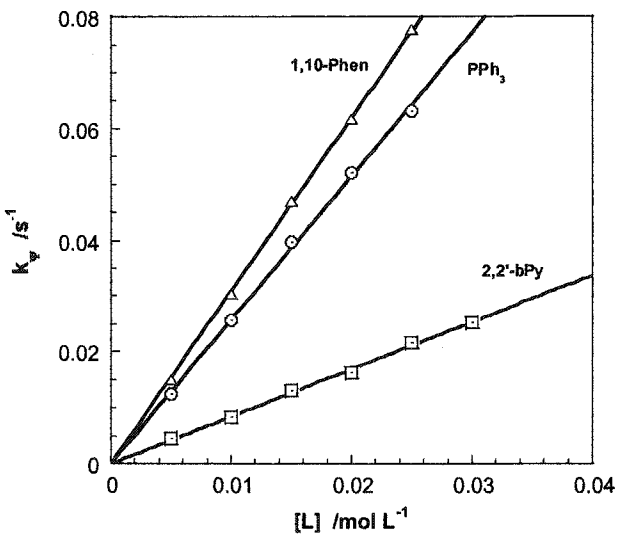


(a)

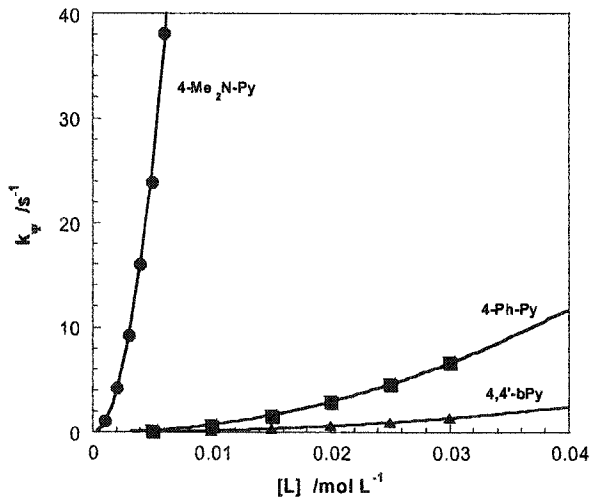


(b)

**Figure 2.** Plots of the pseudo-first-order rate constants in $CHCl_3$ at 25 °C for the reactions of **PicH$^+$3$^-$** against the concentrations of ligands; (a) $PPh_3$, 2,2'-bpy, and 1,10-Phen; and (b) 4-$Me_2N$-Py, 4-Ph-Py, and 4,4'-bpy.

**Reactions with Pyridines.** The reactions of **PicH$^+$3$^-$** and **4** with pyridines produce MeReO(edt)Py, eq 6-7. The reactions of **PicH$^+$3$^-$** show a second-order dependence on the concentration of pyridines (Figure 2b). Two pyridines, 4-$Me_2N$-Py and 4-Ph-Py, gave third-order rate constants, $1.02(2) \times 10^6$ and $7.4(1) \times 10^3$ $L^2$ $mol^{-2}$ $s^{-1}$ respectively. The two order of magnitude difference between these rate constants indicates a substantial electronic effect from the substituents on pyridine. The electronic effect is cumulative because two molecules of pyridine are involved in the third-order reactions. No reaction has been observed with the less basic pyridine, 4-cyano pyridine (4-NC-Py), or with the sterically hindered pyridine, 2-Me-Py. Unlike the case of **PicH$^+$3$^-$**, first-order kinetics was observed when **4** reacts with excess 4-$Me_2N$-Py, giving $k = 20.1(2)$ L $mol^{-1}$ $s^{-1}$. To rule out the involvement of the dimer, an experiment with $\{MeReO(edt)\}_2$ (**2**) and 4-Ph-Py was carried out; the reaction shows a second-order dependence on [Py], with $k = 2.76(3) \times 10^4$ $L^2$ $mol^{-2}$ $s^{-1}$, which is four times bigger than the rate constant for **PicH$^+$3$^-$**.

$$\textbf{PicH}^+\textbf{3}^- + Py \rightarrow MeReO(edt)Py + PhSH + 2\text{-}Pic \quad (6)$$

$$\textbf{4} + Py \rightarrow MeReO(edt)Py + tmtu \quad (7)$$

**Reactions with Bidentate Ligands.** The chelating ligands, 2,2'-bpy and 1,10-phen react with **PicH$^+$3$^-$** to produce six-coordinate complexes with first-order dependences on the concentrations of **PicH$^+$3$^-$** and the ligand (Figure 2a). Second-order rate are $k = 0.84(2)$ L $mol^{-1}$ $s^{-1}$ for 2,2'-bpy and 3.14(3) L $mol^{-1}$ $s^{-1}$ for 1,10-phen. Reaction of **PicH$^+$3$^-$** with the nonchelating ligand 4,4'-bipyridine follows second-order kinetics with respect to ligand concentration, Figure 2b, with $k = 1.53(2) \times 10^3$ $L^2$ $mol^{-2}$ $s^{-1}$.

**Base Assistance in Ligand Displacement**. Although the Brønsted bases (**B**) 4-NC-Py and 2-Pic do not react with **PicH$^+$3$^-$**, they do accelerate the reaction of **PicH$^+$3$^-$** with $PPh_3$. It is important to point out that MeReO(edt)**B** was not observed. When [$PPh_3$] was kept constant at 10 mM, the pseudo-first order rate constant rises with [**B**] and saturates at the high concentration, Figure 3. The data, including that of the reactions without Brønsted bases, were fitted to eq 8 by using the computer program Scientist,[19] affording $K = 240(40)$, $k_2 = 3.1(1)$ L $mol^{-1}$ $s^{-1}$ for 4-NC-Py, and $K = 23(8)$, $k_2 = 1.7(9)$ L $mol^{-1}$ $s^{-1}$ for 2-Pic, and $k_1 = 2.58(5)$ L $mol^{-1}$ $s^{-1}$, the same for both. The latter agrees with the directly-determined value, 2.57(2) L $mol^{-1}$ $s^{-1}$.

$$k_\psi = k_1[PPh_3] + \frac{k_2K[B]}{1+K[B]}[PPh_3] \quad (8)$$

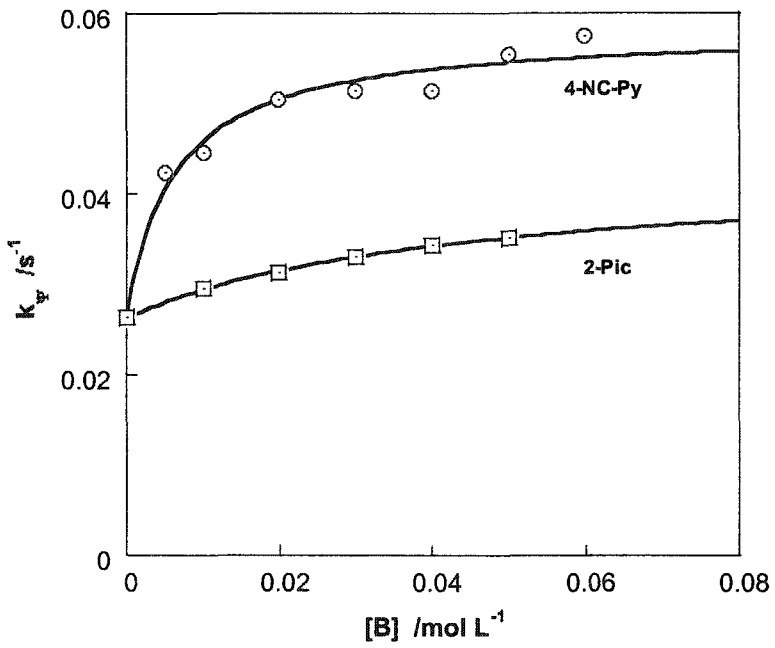


**Figure 3.** Plots of the pseudo-first-order rate constants for reactions of **PicH$^+$3$^-$** with $PPh_3$ in the presence of the added Brønsted bases 4-NC-Py and 2-Me-Pic against [**B**] in $CHCl_3$ at 25 °C.

Similarly, 4-NC-Py and 2-Pic accelerated the reaction of **PicH$^+$3$^-$** with 4-$Me_2$N-Py, but without rate saturation was even at high [**B**]. The rate is given by

$$v = k_m \cdot [\mathbf{3}\text{-Pic}] \cdot [Me_2NPy] \cdot [\mathbf{B}] \quad (9)$$

with $k_m = 5.8(1) \times 10^4$ (4-NC-Py) and 88(18) $L^2\ mol^{-2}\ s^{-1}$ (2-Me-Py).

Brønsted bases like 4-Ph-Py, that react with **PicH$^+$3$^-$** with $k = 7.37(5) \times 10^3\ L^2\ mol^{-2}\ s^{-1}$, show an additional effect when added to the $PPh_3$ reaction, where biphasic kinetics was observed. The intermediate MeReO(edt)(4-Ph-Py) formed and vanished during the course of the reaction. With excess 4-Ph-Py and $PPh_3$, the two-phase absorbance change could be fitted to eq 3, giving pseudo-first –order rate constants, $k_\alpha$ for the formation of MeReO(edt)(4-Ph-

Py) and $k_\beta$ for its disappearance. Keeping [$PPh_3$] constant (10 mmol/L) during the course of the reaction, $k_\alpha$ shows a second-order dependence on [4-Ph-Py], giving $k_1 = 6.8(1) \times 10^3$ $L^2$ $mol^{-2}$ $s^{-1}$; similarly, with [4-Ph-Py] = 30 mM, $k_\beta$ depends linearly on [$PPh_3$], giving $k_2 = 98(1)$ L $mol^{-1}$ $s^{-1}$. Both rate constants agree with the independent values from the direct study of the two steps, $k_\alpha = 7.4(1) \times 10^3$ $L^2$ $mol^{-2}$ $s^{-1}$ and $k_\beta = 96(1)$ L $mol^{-1}$ $s^{-1}$.

Again, the acceleration was observed when pyridines were introduced into the reaction of **4** with $PPh_3$. When [$PPh_3$] was kept constant, the rate varied linear according to [4-NC-Py] and [2-Pic], giving the second-order rate constants 0.095(1) and 0.0103(3) L $mol^{-1}$ $s^{-1}$ for 4-NC-Py and 2-Pic respectively. With the most basic pyridine, 4-$Me_2$N-Py, biphasic kinetics was observed and intermediate MeReO(edt)(4-$Me_2$N-Py) formed and disappeared during the course of the reaction. The rate constants for the two phases were obtained by fitting the kinetic trace to eq 3, giving $k_\alpha$ and $k_\beta$, which are linearly dependent on [4-$Me_2$N-Py] and [$PPh_3$] respectively, $k_\alpha = k_1$[4-$Me_2$N-Py] and $k_\beta = k_2$[$PPh_3$], with $k_1 = 19.2(3)$ and $k_2 = 33(1)$ L $mol^{-1}$ $s^{-1}$. The consistency of these rate constants is acceptable, compared with the independent values, 20.1(2) L $mol^{-1}$ $s^{-1}$ and 28.0(5) L $mol^{-1}$ $s^{-1}$.

**Influence of the Cation.** This factor was investigated by using $LutH^+\mathbf{3}^-$ in reactions with $Ph_3P$ and 4-Ph-Py. The results are identical with those for $\mathbf{PicH^+3^-}$, with k = 2.53(3) L $mol^{-1}$ $s^{-1}$ and 7.14(9) $\times 10^3$ $L^2$ $mol^{-2}$ $s^{-1}$ for $LutH^+\mathbf{3}^-$, as compared with 2.57(2) and 7.37(5) $\times 10^3$ for $\mathbf{PicH^+3^-}$. An excess of pyridinium ions was added to the reaction system and it had no effect on the kinetics. This clearly indicates that the counter-cation is not involved.

The reactions and rate constants are summarized in Table 4.

**Table 4**. Summary of Kinetic Data for **PicH$^+$3$^-$** and **4**

| | | **PicH$^+$3$^-$** | **4** |
|---|---|---|---|
| L | $[L]^n$ | $k/L^{n-1}\ mol^{1-n}\ s^{-1}$ | $k/L^{n-1}\ mol^{1-n}\ s^{-1}$ |
| | n = | | |
| 4,4'-Bpy | 1 | $1.53(2) \times 10^3$ | |
| 1,10-Phen | 1 | 3.14(3) | |
| $PPh_3$ | 1 | 2.57(2) | $8.20(6) \times 10^{-2}$ |
| 2,2'-Bpy | 1 | 0.84(2) | |
| 4-$Me_2$N-Py | 2 | $1.02(6) \times 10^6$ | 20.1(2), n = 1 |
| 4-Ph-Py | 2 | $7.4(1) \times 10^3$ | |
| 4-NC-Py | – | NR | |
| 2-Me-Py | – | NR | |
| 4-$Me_2$N-Py + 4-NC-Py | 1+ 1 | $5.8(1) \times 10^4$ | |
| 4-$Me_2$N-Py + 2-Me-Py | 1 + 1 | 88(2) | |
| $PPh_3$ + 4-NC-Py | eq 8 | $K = 2.4(4) \times 10^2$, $k_2 = 3.1(1)$ | |
| $PPh_3$ + 2-Me-Py | eq 8 | $K = 23.8(1)$, $k_2 = 1.7(9)$ | |

**Reactions with Pyridine N-oxides.** When **PicH$^+$3$^-$** reacts with pyridine N-oxides, a three-stage absorbance change was observed. Those changes are consistent with the scheme: (1) the first pyridine N-oxide replaces the $SPh^-$ ligand to form MeReO(edt)OPy; (2) a second pyridine N-oxide coordinates to rhenium trans to the oxo group, where it assists the cleavage of the N–O bond of the first pyridine N-oxide to yield a Re(VII) intermediate, $MeRe(O)_2$(edt)OPy; (3) the slow decomposition of that intermediate completes the sequence. The UV/Vis spectra of these species are given in Figure 4.

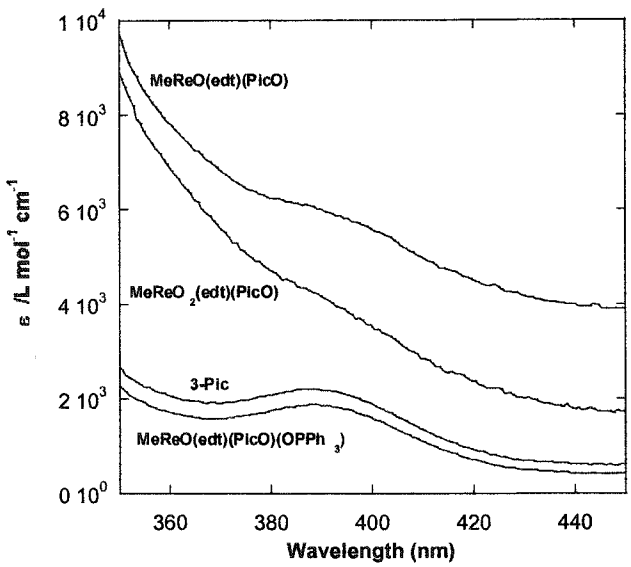


**Figure 4.** Spectra of $\mathbf{PicH^+3^-}$ and the intermediates MeReO(edt)(OPic) and $MeRe(O)_2(edt)$, and the product from the reaction of the latter with $PPh_3$, $MeReO(edt)(OPic)(OPPh_3)$.

The last stage of decomposition was too sluggish for kinetic study. The first two stages of absorbance change were fitted to eq 3, giving two pseudo-first-order rate constants, designated $k_\alpha$ and $k_\beta$ ($k_\alpha > k_\beta$). Figure 5 depicts the plots of the pseudo-first-order rate constants for oxidation of $\mathbf{PicH^+3^-}$ against concentrations of pyridine N-oxides.

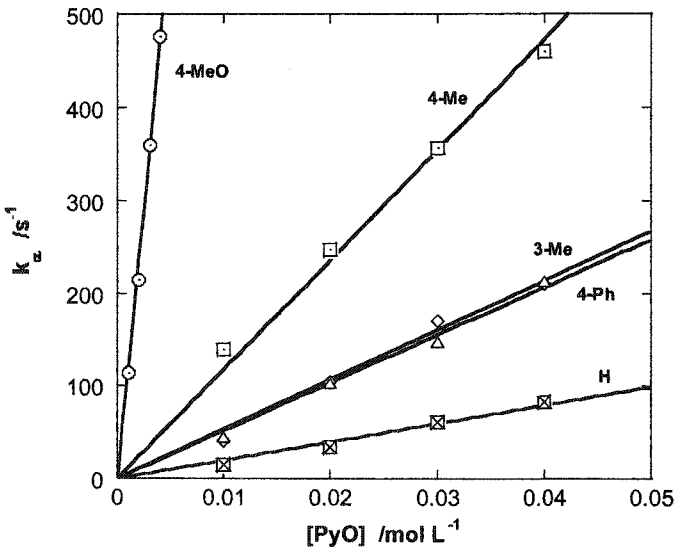


(a)

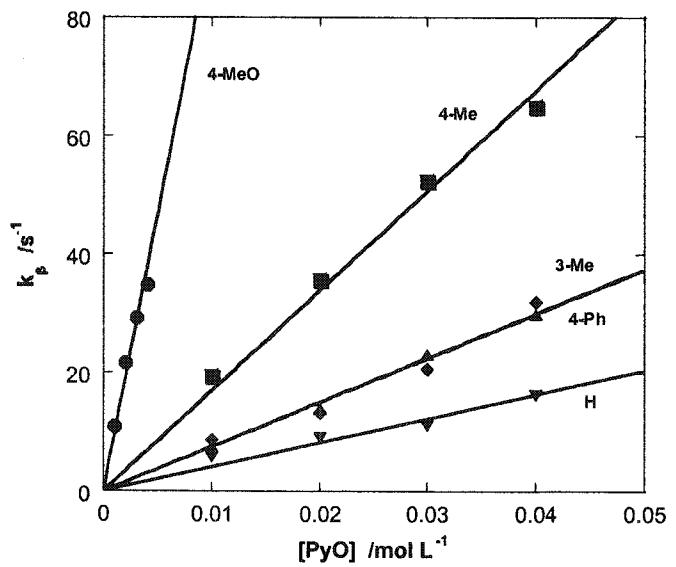


(b)

**Figure 5**. Plots of (a) $k_\alpha$, (b) $k_\beta$ against [PyO] for the reaction between **PicH$^+$3**$^-$ and pyridine N-oxides in $CHCl_3$ at 25 °C.

Both rate constants vary linearly with [PyO]. Rate constants of oxidation of **PicH$^+$3$^-$** by pyridine N-oxides are summarized in Table 5. The rate constants of the first stage span a range of $2.3 \times 10^3$ - $1.2 \times 10^5$ L mol$^{-1}$ s$^{-1}$; those of the second stage lie in the range of $3 \times 10^2$ - $8 \times 10^3$ L mol$^{-1}$ s$^{-1}$. The Hammett analysis for **PicH$^+$3$^-$** shows large reaction constants, $\rho_1$ = –5.3 and $\rho_2$ = –4.3, as illustrated in Figure 6.

**Table 5**. Rate constants for the oxidation of **PicH$^+$3$^-$** and **4** by pyridine N-oxides.

| X-$C_5H_4NO$ | **PicH$^+$3$^-$** | | **4** |
|---|---|---|---|
| X = | $k_1$ / $10^3$ L mol$^{-1}$ s$^{-1}$ | $k_2$ / $10^3$ L mol$^{-1}$ s$^{-1}$ | $k_1$ / L mol$^{-1}$ s$^{-1}$ |
| 4-MeO | 123(6) | 7.9(8) | 20.5(5) |
| 4-Me | 10.7(1) | 1.53(6) | 3.58(3) |
| 3-Me | 5.8(4) | 0.78(11) | 1.27(2) |
| 4-Ph | 5.5(3) | 0.77(4) | 1.34(2) |
| H | 2.3(1) | 0.34(4) | 0.84(1) |

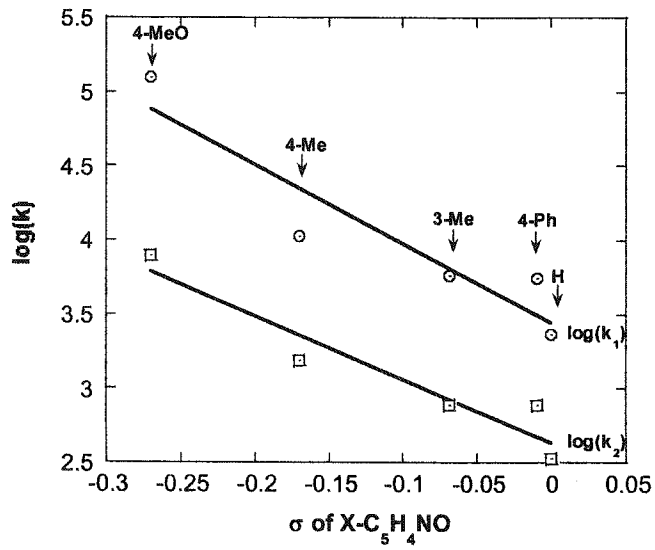


**Figure 6**. Analysis of the kinetic effects of pyridine N-oxide substituents on the rate constants for oxidation of **PicH$^+$3$^-$** by the Hammett equation.

To identify the rate constant for the first two steps, **2** was used to react with 4-MeO-PyO and 4-Ph-PyO. Three-stage absorbance changes were observed, like those for **PicH$^+$3$^-$**. The first two stages were fitted to eq 3, affording $k_\alpha$ and $k_\beta$. Varying the concentrations of two PyO, $k_\alpha$ shows mixed first-order and second-order dependences on [PyO], $k_\alpha = k_{1a}[PyO] + k_{1b}[PyO]^2$, affording $k_{1a} = 1.27(8) \times 10^4$ L mol$^{-1}$ s$^{-1}$ and $k_{1a} = 8(6) \times 10^4$ L$^2$ mol$^{-2}$ s$^{-1}$ for 4-MeO-PyO and $k_{1a} = 6.5(3) \times 10^3$ L mol$^{-1}$ s$^{-1}$ and $k_{1a} = 1.4(2) \times 10^5$ L$^2$ mol$^{-2}$ s$^{-1}$ for 4-Ph-PyO. Unlike $k_\alpha$, $k_\beta$ varies linearly with [PyO], giving second-order rate constants, $1.70(3) \times 10^4$ L mol$^{-1}$ s$^{-1}$ for 4-MeO-PyO and $1.32(1) \times 10^3$ for 4-Ph-PyO. The monomerization of **2** follows mixed first-order and second-order kinetics.[11,20] Although the complexity of the reaction of **2** with pyridine N-oxides causes the difference between the second-order rate constants from $k_\beta$ and that of **3**, we can assign $k_\alpha$ to ligand displacement and $k_\beta$ to oxidation.

The reaction of **4** with PyO is much slower than that of **PicH$^+$3$^-$**; the absorbance change occurs in two stages, the second corresponds to the third stage of the **PicH$^+$3$^-$** reaction, namely the decomposition of $MeRe(O)_2(edt)OPy$. The first stage shows a first-order dependence on [PyO], affording second-order rate constants in the range of 0.8-23 L mol$^{-1}$ s$^{-1}$, as listed in Table 4. A Hammett analysis gave $\rho = -4.7 \pm 0.7$, indicative of an unusually large substituent effect.

Although the decomposition of $MeRe(O)_2(edt)OPy$ is too sluggish for kinetics, the relative rate can be estimated by the time for complete reaction. The rate did not depend on [PyO], but did depend on the identity of pyridine N-oxides. The rate for 4-Ph-PyO is about two times slower than that for 4-PicO. When $PPh_3$ was added to the solution of $MeReO_2(edt)OPy$, the absorbance changed instantaneously, as the catalytic cycle transfers an oxygen atom from PyO to $PPh_3$ according to the stoichiometric reaction of eq 1. Figure 4 depicts the spectrum of $MeReO(edt)(4\text{-}OPic)(OPPh_3)$, the product from this reaction. The weak ligand $Ph_3PO$ can be readily replaced by PyO in the system. Although this metastable species was not structurally characterized, certain comparison compounds has been found in the literature, involving Re-$OPPh_3$ interaction..[21-24] $Re(O)Cl_3(OPPh_3)(Me_2S)$ was used as a catalyst for oxygenation of thiols.[21] $[(HCpz_3)ReCl_2(OPPh_3)]Cl$ and $(HBpz_3)ReCl2(OPPh_3)$ was formed from the oxygen abstraction of $PPh_3$ from corresponding rhenium(V) complexes, $(HCpz_3)ReOCl_2$ and $(HBpz_3)ReOCl_2$.[24] Analogous Mo and W compounds were also found

and structurally characterized, such as $[LMo^{IV}(OPR_3)(p\text{-}OC_6H_4\text{-}OC_2H_5)_2]^+$ and anti-$Cl_2O(Ph_3PO)W(\mu\text{-}S\text{-}i\text{-}Bu)_2W(Ph_3PO)Cl_2O$.[22,23] The reaction of $MeRe(O)_2(edt)OPy$ with $PPh_3$ is too fast for stopped-flow kinetics, giving a conservative limit on the second-order rate constant $k > 6\times10^5$ L mol$^{-1}$ s$^{-1}$.

## Discussion

**The N–H···S Hydrogen Bond.** This interaction has been recognized in metalloproteins, electron-transfer iron-sulfur proteins,[25-29] and cytochrome P450 compounds containing thiolate-metal coordination.[30-32] This weak interaction plays an important role in maintaining structures and modulating redox potentials of metal centers. Model compounds containing Fe, Co, Mo were synthesized and a variety of N–H···S hydrogen bonds were discovered and characterized.[33-37] Most of them contain a bent hydrogen bond with an N–H···S angle <180°.[33-36] In only a few cases has an angle close to 180° been observed.[37] To our knowledge, the N–H···S hydrogen bond in $\mathbf{PicH^+3^-}$ is the first case of this interaction in a rhenium complex. Another point of significance can be seen from the crystal structure of $\mathbf{PicH^+3^-}$: the N–H···S hydrogen bond could arise from the reaction of partially protonated $edtH^-$ with the Brϕnsted base 2-Pic. This reaction enters into the interpretation of the Brϕnsted base-assisted ligand displacement.

**Ligand Displacement**. First-order kinetics with respect to the concentration of entering ligand is a common feature of well-known ligand displacement reactions of methyl(oxo)rhenium(V) complexes.[38-40] The reaction of $\mathbf{PicH^+3^-}$ with $PPh_3$ and the reactions of **4** with $PPh_3$ and pyridines exactly follow this behavior. Strikingly, the reactions of $\mathbf{PicH^+3^-}$ with pyridines displayed second-order dependences on [Py]. Noting that the monomerization of dimeric methyl(oxo)rhenium(V) complexes with pyridine also shows a second-order dependence on [Py] owing to their two metal centers,[11,20] we presumed that $\mathbf{PicH^+3^-}$ in solution has two reaction centers. One can be attacked by $PPh_3$ and Py, another can be attacked only by the Brønsted base, Py. This proposal was confirmed by the finding that the added Brønsted bases, 4-NC-Py and 2-Pic, which themselves are not able to replace the $SPh^-$ ligand, accelerate the reactions of $\mathbf{PicH^+3^-}$ with $PPh_3$ and Py. Again, the first-order kinetic dependence on the entering ligand for $\mathbf{PicH^+3^-}$ with the chelating bidentate ligands

2,2'-bpy and 1,10-phen confirms the existence of two reaction centers and further indicates that those two centers are relatively rigid and close to one another, because the reaction with 4,4'-bpy, which does not have two N atoms close to one another, is second-order with respect to [4,4'-bpy].

Thus, we presume that the resulting species that exists in chloroform is MeReO(edtH)SPh, **5**, with the structural formula

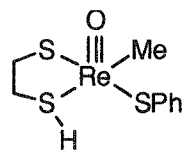


**5**

This is a neutral complex that contains two reaction centers: a rhenium atom that can be attacked by a Lewis base, $PPh_3$ and Py, and a proton attached to sulfur that can be abstracted by a Brønsted base. This proposal was also based on the fact that the same rate constants were obtained for $\mathbf{PicH^+3^-}$, $LutH^+\mathbf{3}^-$, and $\mathbf{PicH^+3^-} + PyH^+$.

The Lewis base $PPh_3$ can attack only the rhenium atom of $\mathbf{PicH^+3^-}$ to yield $MeReO(edt)PPh_3$. This reaction is first-order with respect to $[PPh_3]$. This mechanism was displayed in Scheme **1**, pathway **a**. In the presence of a Brønsted base **B**, = 4-NC-Py or 2-Me-Py, the reaction was accelerated to a saturation level in [**B**], clearly indicating that a prior equilibrium between $\mathbf{PicH^+3^-}$ and pyridine was established before the replacement of $SPh^-$ with $PPh_3$ (pathway **b**). An intermediate with the same structure, containing an N–H···S hydrogen bond, was proposed in accord with the kinetic observations.

**Scheme 1**. Alternative pathways **a-c** for displacement of $SPh^-$ by $PPh_3$, assisted by Py

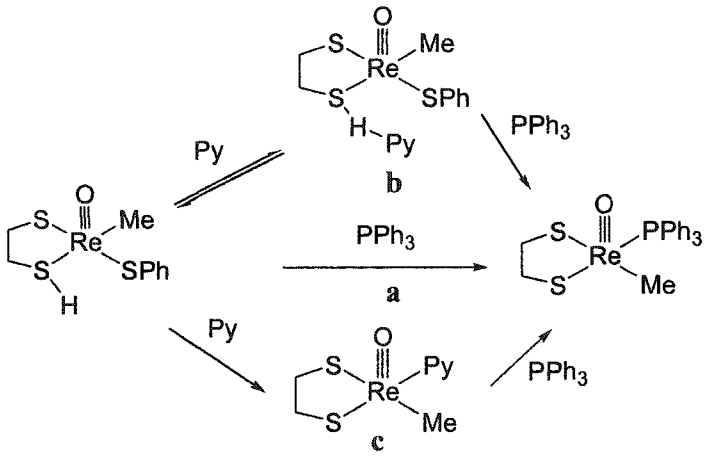


Given that Py can react with $\mathbf{PicH^+3^-}$ to form MeReO(edt)Py, it seems plausible that there will be yet another possible pathway (**c**) by which 4-NC-Py and 2-Pic might assist ligand displacement from $\mathbf{PicH^+3^-}$ with $PPh_3$. It is through an intermediate, MeReO(edt)Py, which might be formed from more basic and less sterically hindered pyridines. But in the cases of 4-NC-Py and 2-Pic, there is no direct reaction between these pyridines and $\mathbf{PicH^+3^-}$; one can presume that the equilibrium between $\mathbf{PicH^+3^-}$ and MeReO(edt)Py is unfavorable with K<<1. This is totally opposite to the data obtained from the kinetic study, K = 240 ± 40 for 4-NC-Py and K = 23 ± 8 for 2-Me-Py. For 4-Ph-Py, however, which is capable of replacing $SPh^-$, pathway **c** becomes available, especially at a high (30 mM) concentration of 4-Ph-Py; indeed, MeReO(edt)(4-Ph-Py) was detected spectrophotometrically and the rate constants for the biphasic kinetics were obtained. These values were in good agreement with those from the independently-studied reactions between $\mathbf{PicH^+3^-}$ with 4-Ph-Py and MeReO(edt)(4-Ph-Py) with $PPh_3$.

As was already mentioned, pyridine, both a Brønsted and a Lewis base, can attack both reaction sites in $\mathbf{PicH^+3^-}$, affording the second-order kinetics with respect to [Py]. The two pathways in Scheme 2 are potentially consistent with the kinetic data. In pathway **d**, a prior equilibrium was proposed as in **b**, followed by an attack of second Py on rhenium from the position trans to oxo group. In **e**, Py approaches rhenium from the lower empty position and

equilibrates quickly; then second Py attacks the proton on sulfur, followed by a fast step to yield the final product MeReO(edt)Py.

Pathway **d** can be ruled out by the following analysis. Since the prior equilibrium in **d** is as same as that in scheme 1 pathway **b**, the same rate saturation should be observed as that in the Py assisted reaction of $\mathbf{PicH^+3^-}$ with $PPh_3$. But in experiments no saturation was ever observed with single or mixed pyridines. To the contrary, for **e**, the prior equilibrium for formation of six-coordinate rhenium species is unfavorable. Indeed, no $MeReO(edt)L_2$, where L is a monodentate ligand, has ever been observed. The clear implication is that the equilibrium constant is small and can not lead to saturation. On the other hand, it is reasonable to postulate the formation of intermediate six-coordinate rhenium species because they are known with chelating ligands.[39] The reason for requirement of the second Py possibly lies on that the abstraction of proton from sulfur increases the electron density on sulfur, and further on rhenium; the scission of Re–S bond requires the shift of electron from Re to S.

**Scheme 2.** Alternative pathways **d-e** for the two-stage displacement of $SPh^-$ by Py

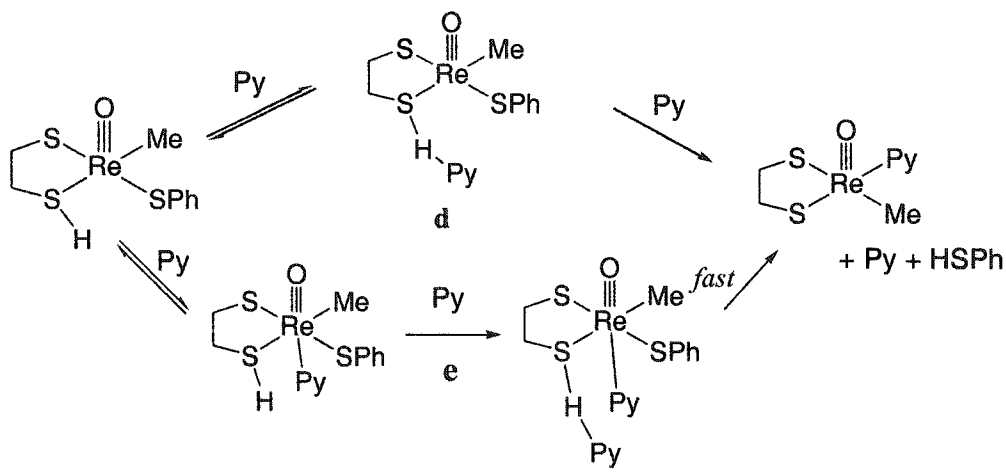


In contrast to **3**, **4** only has one reaction site, the rhenium atom. Displacement of tmtu in **4** by Py and $PPh_3$ is a simplified version of the reactions of **3**. Since there is no proton on the sulfur atom of **4**, pathway **b**, **d** and **e** are not suitable for the reactions of **4** any more. But pathways **a** and **c** are adaptable. Scheme 3 depicts two pathways for the reactions of **4** which can account for of the kinetic data. Pathway **f** stands for a common ligand displacement mechanism, affording a second-order kinetics, first-order dependence on both rhenium

complex and the entering ligand. Pathway **g** is a two-step scheme. For 4-$Me_2N$-Py, the reaction stops at the first step. For the Py assisted reaction of **4** with $PPh_3$, the reaction goes through two steps, the formation of intermediate MeReO(edt)Py and the generation of final product MeReO(edt)$PPh_3$. For the case of 4-$Me_2N$-Py, the formation and disappearance of MeReO(edt)(4-$Me_2N$-Py) was observed and the kinetic curve was fitted to the biphasic kinetics. When 4-NC-Py and 2-Pic were used, the first step becomes very slow compared the rate of the second step. Thus the biphasic kinetics changes to a single-phase kinetics. That is, the first step becomes the rate-controlling step, which is first-order dependence on [4-NC-Py] and [2-Pic].

**Scheme 3**. Alternative pathways **f, g** for displacement of tmtu by $PPh_3$, assisted by Py

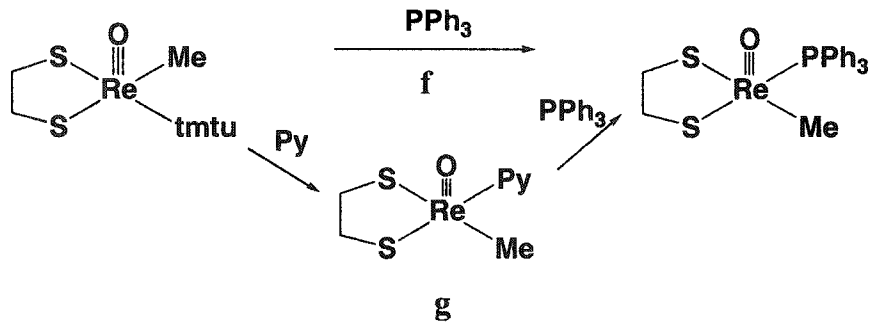


**g**

**Oxidation of Rhenium Complexes**. The nucleophilic assistance on the severing of the O–Py bond was first discovered in the reduction of pyridine N-oxides with the catalyst MeReO(mtp)$PPh_3$.[6,7] In the case of oxidation of **PicH$^+$3$^-$**, the three-stage absorbance change corresponded to the mechanism proposed in Scheme 4. The first stage is a common ligand displacement since pyridine N-oxide acts well as Lewis base,[41-44] showed first-order dependence on [PyO]. By using series of substituted pyridine N-oxides, a large substituent effect, $\rho = -5.3$, was found, which is possibly caused by the change of the charge on rhenium during the first step.

**Scheme 4**. Oxidation of $PiCH^{+}3^{-}$

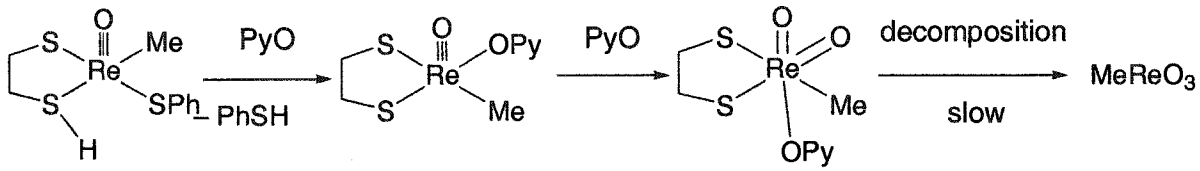


The scission of the O–N bond of PyO coordinated to rhenium occurs in the second step with the assistance of a second PyO. Two reasonable species can be assigned as the transient oxidation product, $MeRe(O)_2(edt)$ and $MeRe(O)_2(edt)OPy$. The former is a five coordinated rhenium(VII) complex with two terminal oxo groups. An analogous compound, $\{MeRe(O)_2\}_2\{SCH_2CH(O)CH(O)CH_2S\}$, was discovered with a distorted trigonal bipyramidal structure that contained two identical oxo groups.[11] The reaction of $MeRe(O)_2(OCH_2CH_2S)$ with $PPh_3$ occurs at relatively slow rate.[1] Similar to these rhenium compounds, five-coordinate Mo(VI) complexes with two terminal oxo groups were recognized as key models for sulfite oxidase, which has been widely studied and characterized.[45-49] The later species is a six-coordinate rhenium complex containing one PyO trans to one of the oxo groups. With 8-hydroxyqulinoline as ligand, a six-coordinate dirhenium complex was synthesized from the condensation of methyltrioxorhenium(VII) with free ligands.[50] Similarly, the condensation of methyltrioxorhenium(VII) with diols and diamines affords dioxorhenium(VII) complexes with an extra Lewis base as the sixth ligand.[12,51,52] Both of these compounds have two oxo groups cis to each other. In the catalytic OAT reaction, six-coordinate dioxorhenium species were proposed as the immediate oxidation product.[4,53] The dependence on the identity of PyO of the decomposition of this species indicates that PyO is coordinated. Thus $MeRe(O)_2(edt)OPy$ is the product from the scission of the O–N bond.

As to why nucleophilic assistance is necessary, we note that the scission of O-N bond requires electron transfer from O to N. With coordination of another PyO, the electron density on rhenium is enriched; as is it on the O atom. Another possibility is that the coordinated PyO stabilizes the oxidation product, dioxorhenium(VII), which would direct the

reaction through a nucleophile-assisted pathway. Electron-rich ligands are known to stabilize and lower the reactivity of Re=O bond.[54]

The first step of the oxidation of **4** by pyridine N-oxides is much slower than the second, which is as same as the second step of oxidation of $\mathbf{PicH^+3^-}$. So the reactions simplify into two stages, ligand displacement and decomposition of $MeRe(O)_2(edt)OPy$.

**Conclusion**

Two ionic and one neutral methyl(oxo)rhenium(V) compounds were synthesized and structurally characterized. They were compared in reactivity towards the ligands triphenylphosphane, pyridines, pyridine N-oxides. Assistance from Brønsted bases was found on ligand displacement of ionic rhenium compounds as well as nucleophile assistance on oxidation of all of compounds. From the kinetic data, crystal structures, and an analysis of the intermediates, a structural formula of $\mathbf{PicH^+3^-}$ and mechanisms of ligand displacement and oxidation were proposed.

**Acknowledgment.** This research was supported by the U.S. Department of Energy, Office of Basic Energy Sciences, Division of Chemical Sciences under Contract W-7405-Eng-82 with Iowa State University of Science and Technology.

**Supporting Information Available:** X-ray crystallographic tables and plots of kinetic data. This material is available free of charge via the Internet at http://pubs.acs.org.

**References**

(1) Dixon, J.; Espenson, J. H. *Inorg. Chem.* **2002**, *41*, 4727-4731.

(2) Espenson, J. H. *Chem. Commun.* **1999**, 479-488.

(3) Lente, G.; Espenson, J. H. *Inorg. Chem.* **2000**, *39*, 4809-4814.

(4) Shan, X.; Ellern, A.; Espenson, J. H. *Inorg. Chem.* **2002**, *41*, 7136-7142.

(5) Shan, X.; Ellern, A.; Guzei, I. A.; Espenson, J. H. *Inorg. Chem.* **2003**, *42*, 2362-2367.

(6) Wang, Y.; Espenson, J. H. *Organic Letters* **2000**, *2*, 3525-3526.

(7) Wang, Y.; Espenson, J. H. *Inorg. Chem.* **2002**, *41*, 2266-2274.

(8) Coucouvanis, D. *Acc. Chem. Res.* **1991**, *24*, 1-8.

(9) Holm, R. H.; Berg, J. M. *Acc. Chem. Res.* **1986**, *19*, 363-370.

(10) Holm, R. H. *Coord. Chem. Rev.* **1990**, *100*, 183-221.

(11) Espenson, J. H.; Shan, X.; Wang, Y.; Huang, R.; Lahti, D. W.; Dixon, J.; Lente, G.; Ellern, A.; Guzei, I. A. *Inorg. Chem.* **2002**, *41*, 2583-2591.

(12) Takacs, J.; Cook, M. R.; Kiprof, P.; Kuchler, J. G.; Herrmann, W. A. *Organometallics* **1991**, *10*, 316-320.

(13) Blessing, R. H. *Acta Cryst.* **1995**, *51*, 33-38.

(14) All software and sources of the scattering factors are contained in SHELXTL (version 5.1) program library (Sheldrick, G. M. S., Version 5.1; Bruker Analytical X-ray Systems: Madison, WI, 1997)..

(15) Raper, E. S.; Creighton, J. R.; Clegg, W.; Cucurull-Sanchez, L.; Hill, M. N. S.; Akrivos, P. D. *Inorg. Chim. Acta* **1998**, *271*, 57-64.

(16) Francois, S.; Rohmer, M.-M.; Benard, M.; Moreland, A. C.; Rauchfuss, T. B. *J. Amer. Chem. Soc.* **2000**, *122*, 12743-12750.

(17) Lente, G.; Shan, X.; Guzei, I. A.; Espenson, J. H. *Inorg. Chem.* **2000**, *39*, 3572-3576.

(18) Shan, X.; Espenson, J. H.,, Unpublished information.

(19) Scientist; 2.0 ed.; Micromath Software: 1995.

(20) Lente, G.; Guzei, I. A.; Espenson, J. H. *Inorg. Chem.* **2000**, *39*, 1311-1319.

(21) Abu-Omar, M. M.; Khan, S. I. *Inorg. Chem.* **1998**, *37*, 4979-4985.

(22) Ball, J. M.; Boorman, P. M.; Richardson, J. F. *Inorg. Chem.* **1986**, *25*, 3325-3327.

(23) Nemykin, V. N.; Davie, S. R.; Mondal, S.; Rubie, N.; Kirk, M. L.; Somogyi, A.; Basu, P. *J. Amer. Chem. Soc.* **2002**, *124*, 756-757.

(24) Seymore, S. B.; Brown, S. N. *Inorg. Chem.* **2000**, *39*, 325-332.

(25) Bertini, I.; Felli, I.; Kastrau, D. H. W.; Luchinat, C.; Piccioli, M.; Viezzoli, M. S. *European Journal of Biochemistry* **1994**, *225*, 703-714.

(26) Blake, P. R.; Park, J. B.; Adams, M. W. W.; Summers, M. F. *J. Amer. Chem. Soc.* **1992**, *114*, 4931-4933.

(27) Denke, E.; Merbitz-Zahradnik, T.; Hatzfeld, O. M.; Snyder, C. H.; Link, T. A.; Trumpower, B. L. *J. Biol. Chem.* **1998**, *273*, 9085-9093.

(28) Nakamura, A.; Ueyama, N. *Adv. Inorg. Chem.* **1989**, *33*, 39-67.

(29) Sheridan, R. P.; Allen, L. C.; Carter, C. W., Jr. *J. Biol. Chem.* **1981**, *256*, 5052-5057.

(30) Sundaramoorthy, M.; Terner, J.; Poulos, T. L. *Structure* **1995**, *3*, 1367-1377.

(31) Crane, B. R.; Arvai, A. S.; Gachhui, R.; Wu, C.; Ghosh, D. K.; Getzoff, E. D.; Stuehr, D. J.; Tainer, J. A. *Science* **1997**, *278*, 425-431.

(32) Cupp-Vickery, J. R.; Poulos, T. L. *Nature Structural Biology* **1995**, *2*, 144-153.

(33) Huang, J.; Ostrander, R. L.; Rheingold, A. L.; Leung, Y.; Walters, M. A. *J. Amer. Chem. Soc.* **1994**, *116*, 6769-6776.

(34) Walters, M. A.; Dewan, J. C.; Min, C.; Pinto, S. *Inorg. Chem.* **1991**, *30*, 2656-2662.

(35) Okamura, T.-A.; Takamizawa, S.; Ueyama, N.; Nakamura, A. *Inorg. Chem.* **1998**, *37*, 18-28.

(36) Ueyama, N.; Nishikawa, N.; Yamada, Y.; Okamura, T.-a.; Nakamura, A. *J. Amer. Chem. Soc.* **1996**, *118*, 12826-12827.

(37) Suzuki, N.; Higuchi, T.; Urano, Y.; Kikuchi, K.; Uekusa, H.; Ohashi, Y.; Uchida, T.; Kitagawa, T.; Nagano, T. *J. Amer. Chem. Soc.* **1999**, *121*, 11571-11572.

(38) Shan, X.; Espenson, J. H. *Organometallics* **2003**, *22*, 1250-1254.

(39) Espenson, J. H.; Shan, X.; Lahti, D. W.; Rockey, T. M.; Saha, B.; Ellern, A. *Inorg. Chem.* **2001**, *40*, 6717-6724.

(40) Lahti, D. W.; Espenson, J. H. *J. Amer. Chem. Soc.* **2001**, *123*, 6014-6024.

(41) Batigalhia, F.; Zaldini-Hernandes, M.; Ferreira, A. G.; Malvestiti, I.; Cass, Q. B. *Tetrahedron* **2001**, *57*, 9669-9676.

(42) Herrmann, W. A.; Correia, J. D. G.; Rauch, M. U.; Artus, G. R. J.; Kuehn, F. E. *J. Mol. Catal. A:* **1997**, *118*, 33-45.

(43) Lichtenhan, J. D.; Ziller, J. W.; Doherty, N. M. *Inorg. Chem.* **1992**, *31*, 4210-4212.

(44) Sensato, F. R.; Cass, Q. B.; Longo, E.; Zukerman-Schpector, J.; Custodio, R.; Andres, J.; Hernandes, M. Z.; Longo, R. L. *Inorg. Chem.* **2001**, *40*, 6022-6025.

(45) Garrett, R. M.; Rajagopalan, K. V. *J. Biol. Chem.* **1996**, *271*, 7387-7391.

(46) George, G. N.; Garrett, R. M.; Prince, R. C.; Rajagopalan, K. V. *J. Amer. Chem. Soc.* **1996**, *118*, 8588-8592.

(47) George, G. N.; Kipke, C. A.; Prince, R. C.; Sunde, R. A.; Enemark, J. H.; Cramer, S. P. *Biochemistry* **1989**, *28*, 5075-5080.

(48) Kisker, C.; Schindelin, H.; Pacheco, A.; Wehbi, W. A.; Garrett, R. M.; Rajagopalan, K. V.; Enemark, J. H.; Rees, D. C. *Cell* **1997**, *91*, 973-983.

(49) Peariso, K.; McNaughton, R. L.; Kirk, M. L. *J. Amer. Chem. Soc.* **2002**, *124*, 9006-9007.

(50) Takacs, J.; Kiprof, P.; Kuchler, J. G.; Herrmann, W. A. *J. Organomet. Chem.* **1989**, *369*, C1-C5.

(51) Takacs, J.; Kiprof, P.; Riede, J.; Herrmann, W. A. *Organometallics* **1990**, *9*, 782-787.

(52) Wang, W.-D.; Ellern, A.; Guzei, I. A.; Espenson, J. H. *Organometallics* **2002**, *21*, 5576-5582.

(53) Arias, J.; Newlands, C. R.; Abu-Omar, M. M. *Inorg. Chem.* **2001**, *40*, 2185-2192.

(54) Gangopadhyay, J.; Sengupta, S.; Bhattacharyya, S.; Chakraborty, I.; Chakravorty, A. *Inorg. Chem.* **2002**, *41*, 2616-2622.

**Supporting Information**

Table of contents:

S-1. Plot of $k_\Psi$ against the Concentration of Triphenylphosphine (10~50 mM) with 0.1 mM **4** in $CHCl_3$ at 25 °C.

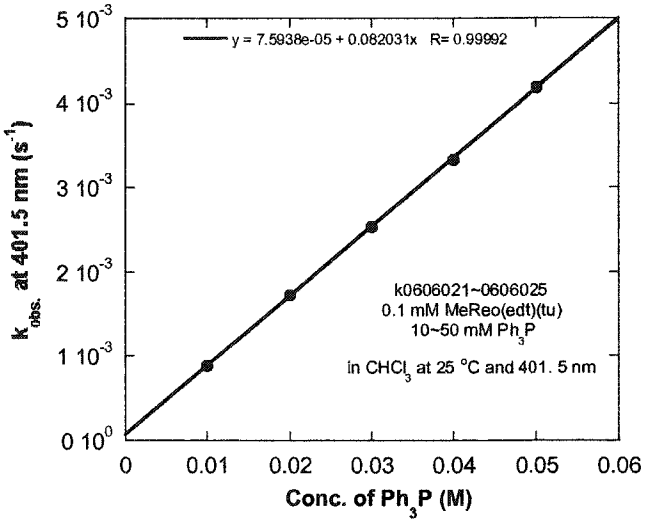


S-2. Plot of $k_\Psi$ against the Concentrations of 4-Picoline N-oxide (5~25 mM) in the Reaction with 0.1 mM **4** in $CHCl_3$ at 25 °C.

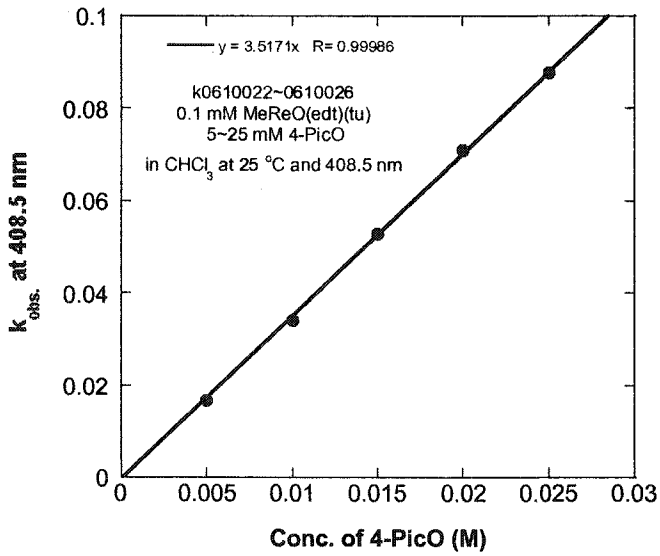

S-3. Plot of $k_\Psi$ against the Concentrations of 4-Phenylpyridine (5~30 mM) in the Reaction with 0.025 mM **2** in $CHCl_3$ at 25 °C.

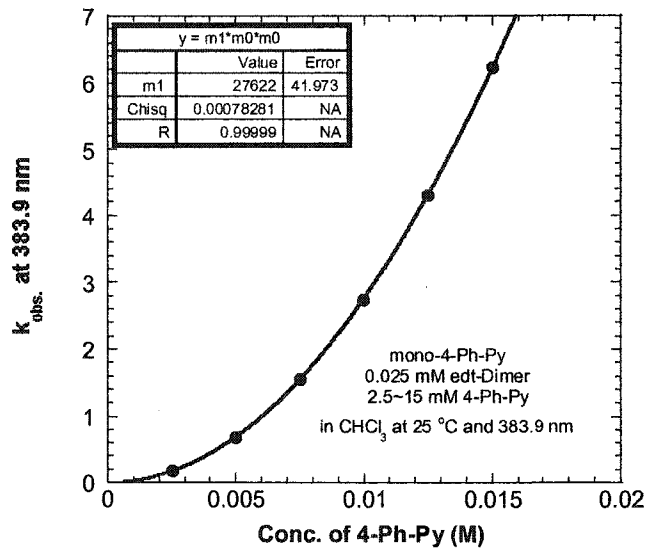


S-4. Plot of $k_\Psi$ against the Concentrations of 4-Phenylpyridine N-oxide (2.5~15 mM) in the Reaction with 0.025 mM **2** in $CHCl_3$ at 25 °C.

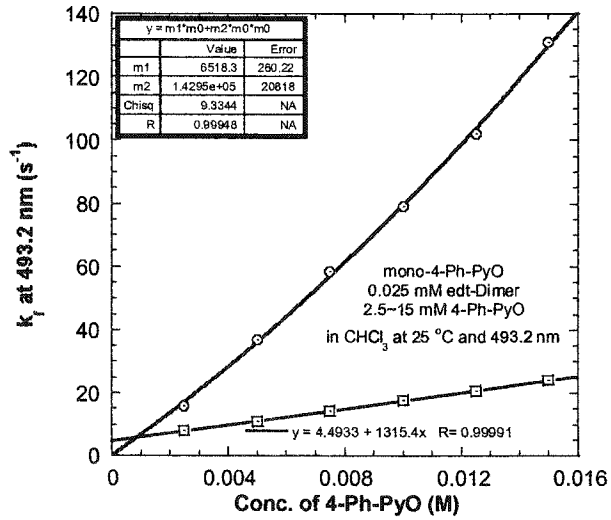

S-5. Plot of $k_\Psi$ against the Concentrations of 4-Picoline N-oxide (2.5~15 mM) in the Reaction with 0.025 mM **2** in $CHCl_3$ at 25 °C.

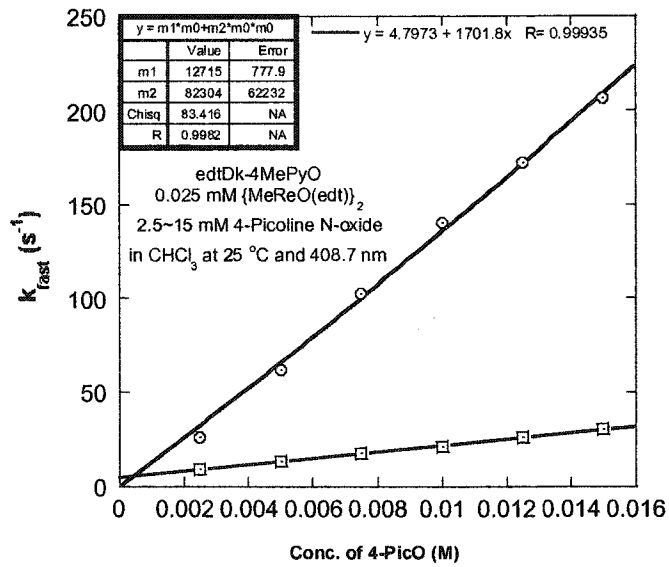


S-6. Crystal data of compound **3**.

A. Crystal data and structure refinement for **3**.

| | | |
|---|---|---|
| Identification code | **$PicH^+$ $3^-$** | |
| Empirical formula | $C_{15}H_{20}NOPReS_3$ | |
| Formula weight | 512.70 | |
| Temperature | 173(2) K | |
| Wavelength | 0.71073 Å | |
| Crystal system | Triclinic | |
| Space group | $P\bar{1}$ | |
| Unit cell dimensions | a = 7.3826(5) Å | α= 94.362(1)°. |
| | b = 9.7701(6) Å | β= 102.414(1)°. |
| | c = 12.8309(8) Å | γ = 99.639(1)°. |
| Volume | 885.02(10) $Å^3$ | |
| Z | 2 | |
| Density (calculated) | 1.924 $Mg/m^3$ | |
| Absorption coefficient | 7.216 $mm^{-1}$ | |

| | |
|---|---|
| F(000) | 496 |
| Crystal size | 0.38 × 0.35 × 0.15 $mm^3$ |
| Theta range for data collection | 2.13 to 26.37°. |
| Index ranges | -9<=h<=8, -12<=k<=12, 0<=l<=16 |
| Reflections collected | 7878 |
| Independent reflections | 3581 [R(int) = 0.0226] |
| Completeness to theta = 26.37° | 99.0 % |
| Absorption correction | Empirical with SADABS |
| Max. and min. transmission | 0.4107 and 0.1702 |
| Refinement method | Full-matrix least-squares on $F^2$ |
| Data / restraints / parameters | 3581 / 0 / 203 |
| Goodness-of-fit on $F^2$ | 1.020 |
| Final R indices [I>2sigma(I)] | R1 = 0.0219, wR2 = 0.0567 |
| R indices (all data) | R1 = 0.0237, wR2 = 0.0575 |
| Largest diff. peak and hole | 1.489 and –1.227 e.$Å^{-3}$ |

B. Atomic coordinates ( × $10^4$) and equivalent isotropic displacement parameters ($Å^2$ × $10^3$) for **3**. U(eq) is defined as one third of the trace of the orthogonalized $U_{ij}$ tensor.

| | x | y | z | U(eq) |
|---|---|---|---|---|
| Re | 841(1) | 2795(1) | 7240(1) | 23(1) |
| S(1) | -478(1) | 4719(1) | 6719(1) | 35(1) |
| S(2) | 3193(1) | 4311(1) | 8505(1) | 27(1) |
| S(3) | 3231(1) | 1660(1) | 7002(1) | 33(1) |
| O | -657(4) | 1743(3) | 7797(2) | 35(1) |
| N | 4468(4) | 6609(3) | 7034(3) | 33(1) |
| C(1) | -28(6) | 2229(5) | 5527(3) | 45(1) |
| C(2) | 5400(5) | 3625(5) | 8628(3) | 39(1) |
| C(3) | 4995(5) | 2087(5) | 8277(3) | 39(1) |

| | | | | |
|---|---|---|---|---|
| C(4) | 37(5) | 6156(4) | 7740(3) | 27(1) |
| C(5) | -75(5) | 6014(4) | 8790(3) | 31(1) |
| C(6) | 328(5) | 7175(4) | 9549(3) | 36(1) |
| C(7) | 814(6) | 8482(4) | 9276(4) | 41(1) |
| C(8) | 913(6) | 8666(4) | 8246(4) | 42(1) |
| C(9) | 531(5) | 7510(4) | 7467(3) | 35(1) |
| C(10) | 5693(7) | 8117(5) | 8718(4) | 48(1) |
| C(11) | 5491(5) | 7846(4) | 7542(3) | 34(1) |
| C(12) | 6261(6) | 8756(4) | 6909(4) | 45(1) |
| C(13) | 5974(7) | 8407(5) | 5826(4) | 49(1) |
| C(14) | 4897(6) | 7121(5) | 5343(4) | 48(1) |
| C(15) | 4142(5) | 6233(4) | 5967(3) | 41(1) |

C. Bond lengths [Å] and angles [°] for **3**.

| | | | |
|---|---|---|---|
| Re-O | 1.692(3) | C(4)-C(5) | 1.384(5) |
| Re-C(1) | 2.154(4) | C(4)-C(9) | 1.404(5) |
| Re-S(3) | 2.2965(9) | C(5)-C(6) | 1.386(5) |
| Re-S(2) | 2.3249(9) | C(6)-C(7) | 1.360(6) |
| Re-S(1) | 2.3349(10) | C(7)-C(8) | 1.363(6) |
| S(1)-C(4) | 1.777(4) | C(8)-C(9) | 1.398(6) |
| S(2)-C(2) | 1.844(4) | C(10)-C(11) | 1.482(6) |
| S(3)-C(3) | 1.829(4) | C(11)-C(12) | 1.383(6) |
| N-C(15) | 1.349(5) | C(12)-C(13) | 1.367(7) |
| N-C(11) | 1.846(5) | C(13)-C(14) | 1.389(7) |
| C(2)-C(3) | 1.496(6) | C(14)-C(15) | 1.356(6) |

| | | | |
|---|---|---|---|
| O-Re-C(1) | 107.14(16) | C(5)-C(4)-C(9) | 118.0(3) |
| O-Re-S(3) | 108.59(10) | C(5)-C(4)-S(1) | 123.3(3) |
| C(1)-Re-S(3) | 80.80(12) | C(9)-C(4)-S(1) | 118.7(3) |
| O-Re-S(2) | 113.10(10) | C(4)-C(5)-C(6) | 120.7(4) |

| | | | |
|---|---|---|---|
| C(1)-Re-S(2) | 139.72(14) | C(7)-C(6)-C(5) | 120.8(4) |
| S(3)-Re-S(2) | 84.83(3) | C(6)-C(7)-C(8) | 120.3(4) |
| O-Re-S(1) | 109.48(10) | C(7)-C(8)-C(9) | 120.1(4) |
| C(1)-Re-S(1) | 79.71(12) | C(8)-C(9)-C(4) | 120.2(4) |
| S(3)-Re-S(1) | 140.85(4) | N-C(11)-C(12) | 116.4(4) |
| S(2)-Re-S(1) | 88.55(3) | N-C(11)-C(10) | 117.9(4) |
| C(4)-S(1)-Re | 114.43(12) | C(12)-C(11)-C(10) | 125.7(4) |
| C(2)-S(2)-Re | 107.97(14) | C(13)-C(12)-C(11) | 121.0(4) |
| C(3)-S(3)-Re | 104.70(13) | C(12)-C(13)-C(14) | 120.1(4) |
| C(15)-N-C(11) | 124.2(3) | C(15)-C(14)-C(13) | 118.6(4) |
| C(3)-C(2)-S(2) | 111.0(3) | N-C(15)-C(14) | 119.6(4) |
| C(2)-C(3)-S(3) | 110.8(3) | | |

D. Anisotropic displacement parameters ($Å^2 \times 10^3$) for **3**. The anisotropic displacement factor exponent takes the form: $-2\pi^2[ h^2 a^{*2} U_{11} + ... + 2 h k a^* b^* U_{12} ]$

| | $U_{11}$ | $U_{22}$ | $U_{33}$ | $U_{23}$ | $U_{13}$ | $U_{12}$ |
|---|---|---|---|---|---|---|
| Re | 23(1) | 21(1) | 23(1) | -2(1) | 4(1) | 2(1) |
| S(1) | 39(1) | 33(1) | 28(1) | -3(1) | -6(1) | 12(1) |
| S(2) | 26(1) | 26(1) | 27(1) | -1(1) | 0(1) | 2(1) |
| S(3) | 33(1) | 37(1) | 30(1) | -2(1) | 10(1) | 10(1) |
| O | 35(1) | 24(1) | 46(2) | -1(1) | 14(1) | -2(1) |
| N | 33(2) | 26(2) | 38(2) | 1(1) | 10(1) | 3(1) |
| C(1) | 49(2) | 50(3) | 29(2) | -11(2) | -2(2) | 15(2) |
| C(2) | 26(2) | 50(3) | 36(2) | 0(2) | 0(2) | 7(2) |
| C(3) | 31(2) | 50(3) | 37(2) | 2(2) | 3(2) | 19(2) |
| C(4) | 25(2) | 26(2) | 29(2) | 2(1) | 0(1) | 10(1) |
| C(5) | 31(2) | 28(2) | 35(2) | 7(2) | 9(2) | 7(2) |
| C(6) | 36(2) | 37(2) | 36(2) | -4(2) | 9(2) | 12(2) |
| C(7) | 34(2) | 35(2) | 52(3) | -10(2) | 5(2) | 11(2) |

| | | | | | | |
|---|---|---|---|---|---|---|
| C(8) | 34(2) | 24(2) | 68(3) | 8(2) | 10(2) | 8(2) |
| C(9) | 36(2) | 35(2) | 36(2) | 10(2) | 7(2) | 11(2) |
| C(10) | 41(2) | 49(3) | 47(3) | -12(2) | -2(2) | 7(2) |
| C(11) | 24(2) | 34(2) | 44(2) | -4(2) | 6(2) | 7(2) |
| C(12) | 32(2) | 30(2) | 72(3) | 2(2) | 15(2) | 3(2) |
| C(13) | 50(3) | 41(30 | 69(3) | 18(2) | 32(2) | 13(2) |
| C(14) | 45(3) | 59(3) | 45(3) | 5(2) | 16(2) | 15(2) |
| C(15) | 45(2) | 39(2) | 38(2) | -1(2) | 13(2) | 3(2) |

E. Hydrogen coordinates ( $\times 10^4$) and isotropic displacement parameters ($Å^2 \times 10^3$) for**3**.

| | x | y | z | U(eq) |
|---|---|---|---|---|
| H(1A) | 386 | 1360 | 5337 | 67 |
| H(1B) | 542 | 2977 | 5164 | 67 |
| H(1C) | -1407 | 2092 | 5299 | 67 |
| H | 3981 | 6008 | 7424 | 39 |
| H(2A) | 6180 | 4114 | 8181 | 46 |
| H(2B) | 6128 | 3810 | 9385 | 46 |
| H(3A) | 4526 | 1578 | 8834 | 47 |
| H(3B) | 6174 | 1782 | 8194 | 47 |
| H(5) | -432 | 5110 | 8993 | 37 |
| H(6) | 263 | 7058 | 10270 | 43 |
| H(7) | 1086 | 9269 | 9804 | 49 |
| H(8) | 1242 | 9581 | 8057 | 50 |
| H(9) | 607 | 7641 | 6750 | 42 |
| H(10A) | 4482 | 7778 | 8895 | 73 |
| H(10B) | 6080 | 9124 | 8945 | 73 |
| H(10C) | 6652 | 7630 | 9092 | 73 |
| H(12) | 7002 | 9637 | 7232 | 54 |
| H(13) | 6512 | 9045 | 5403 | 59 |

| | | | | |
|---|---|---|---|---|
| H(14) | 4693 | 6869 | 4592 | 58 |
| H(15) | 3389 | 5352 | 5655 | 49 |

S-7. Crystal data of Compound **4**.

A. Crystal data and structure refinement for **4**.

| | | |
|---|---|---|
| Identification code | **4** | |
| Empirical formula | $C_8H_{19}N_2OReS_3$ | |
| Formula weight | 441.63 | |
| Temperature | 293(2) K | |
| Wavelength | 0.71073 Å | |
| Crystal system | Monoclinic | |
| Space group | P2(1) | |
| Unit cell dimensions | a = 8.7615(12) Å | α= 90°. |
| | b = 16.426(3) Å | β= 93.768(4)°. |
| | c = 10.0210(15) Å | γ = 90°. |
| Volume | 1439.1(4) $Å^3$ | |
| Z | 4 | |
| Density (calculated) | 2.038 $Mg/m^3$ | |
| Absorption coefficient | 8.859 $mm^{-1}$ | |
| F(000) | 848 | |
| Crystal size | 0.22 × 0.18 × 0.08 $mm^3$ | |
| Theta range for data collection | 2.04 to 24.72°. | |
| Index ranges | $-10 \le h \le 3, -18 \le k \le 15, -8 \le l \le 11$ | |
| Reflections collected | 4488 | |
| Independent reflections | 3787 [R(int) = 0.0233] | |
| Completeness to theta = 24.72° | 89.4 % | |
| Absorption correction | Empirical | |
| Max. and min. transmission | 0.68 and 0.26 | |

| | |
|---|---|
| Refinement method | Full-matrix least-squares on $F^2$ |
| Data / restraints / parameters | 3787 / 1 / 271 |
| Goodness-of-fit on $F^2$ | 0.962 |
| Final R indices [I>2sigma(I)] | R1 = 0.0303, wR2 = 0.0698 |
| R indices (all data) | R1 = 0.0340, wR2 = 0.0711 |
| Absolute structure parameter | 0.003(12) |
| Largest diff. peak and hole | 1.805 and -1.062 e.Å$^{-3}$ |

$R1 = \Sigma \, | \, |F_o| - |F_c| \, | \, / \, \Sigma \, |F_o|$ and $wR2 = \{ \Sigma [ w(F_o^2 - F_c^2)^2 ] / \Sigma [ w(F_o^2)^2 ] \}^{1/2}$

B. Atomic coordinates ( $\times 10^4$) and equivalent isotropic displacement parameters (Å$^2 \times 10^3$) for **4**. U(eq) is defined as one third of the trace of the orthogonalized $U_{ij}$ tensor.

| | x | y | z | U(eq) |
|---|---|---|---|---|
| Re(1) | 8331(1) | 989(1) | 9873(1) | 32(1) |
| Re(2) | 4183(1) | 9011(1) | 5076(1) | 38(1) |
| S(1) | 9233(4) | -44(2) | 8587(3) | 55(1) |
| S(2) | 8741(4) | 99(2) | 11583(3) | 48(1) |
| S(3) | 9602(3) | 1907(2) | 8503(3) | 40(1) |
| S(4) | 2758(4) | 8197(2) | 6356(3) | 49(1) |
| S(5) | 2023(3) | 9086(2) | 3650(3) | 46(1) |
| S(6) | 5614(3) | 8976(2) | 3164(3) | 47(1) |
| C(1) | 9252(14) | 1840(7) | 11311(11) | 43(3) |
| C(2) | 8768(17) | -918(7) | 10839(13) | 60(4) |
| C(3) | 9360(30) | -963(9) | 9608(15) | 120(9) |
| C(4) | 9744(13) | 1469(6) | 6918(12) | 38(3) |
| C(5) | 12515(15) | 1426(9) | 7309(15) | 70(4) |
| C(6) | 11364(15) | 1384(9) | 5018(13) | 65(4) |
| C(7) | 8493(17) | 554(8) | 5226(14) | 60(4) |
| C(8) | 6935(13) | 1544(8) | 6414(14) | 55(4) |
| C(9) | 5944(16) | 8180(9) | 5738(17) | 79(5) |

| | | | | |
|---|---|---|---|---|
| C(10) | 794(14) | 8513(7) | 5941(13) | 50(3) |
| C(11) | 465(13) | 8597(7) | 4498(14) | 50(3) |
| C(12) | 4661(13) | 9477(7) | 1804(12) | 42(3) |
| C(13) | 5038(14) | 10803(7) | 2863(12) | 51(3) |
| C(14) | 2967(16) | 10621(9) | 1122(15) | 72(4) |
| C(15) | 4256(19) | 9437(9) | -676(12) | 70(5) |
| C(16) | 4220(20) | 8168(8) | 596(17) | 89(5) |
| N(1) | 11114(11) | 1393(6) | 6450(10) | 44(3) |
| N(2) | 8487(11) | 1238(5) | 6196(10) | 40(2) |
| N(3) | 4295(10) | 10261(6) | 1863(10) | 45(2) |
| N(4) | 4328(12) | 9067(7) | 684(10) | 50(3) |
| O(1) | 4589(10) | 9891(5) | 5957(9) | 60(2) |
| O(2) | 6447(9) | 1174(5) | 9636(9) | 49(2) |

C. Bond lengths [Å] and angles [°] for **4**.

| | | | |
|---|---|---|---|
| Re(1)-O(2) | 1.680(8) | S(6)-C(12) | 1.756(13) |
| Re(1)-C(1) | 2.128(11) | C(2)-C(3) | 1.372(18) |
| Re(1)-S(2) | 2.264(3) | C(4)-N(1) | 1.323(14) |
| Re(1)-S(1) | 2.302(3) | C(4)-N(2) | 1.333(14) |
| Re(1)-S(3) | 2.366(3) | C(5)-N(1) | 1.453(16) |
| Re(2)-O(1) | 1.718(8) | C(6)-N(1) | 1.465(14) |
| Re(2)-C(9) | 2.133(14) | C(7)-N(2) | 1.486(14) |
| Re(2)-S(4) | 2.281(3) | C(8)-N(2) | 1.479(14) |
| Re(2)-S(5) | 2.298(3) | C(10)-C(11) | 1.463(18) |
| Re(2)-S(6) | 2.359(3) | C(12)-N(4) | 1.325(15) |
| S(1)-C(3) | 1.823(14) | C(12)-N(3) | 1.330(14) |
| S(2)-C(2) | 1.830(13) | C(13)-N(3) | 1.460(14) |
| S(3)-C(4) | 1.756(12) | C(14)-N(3) | 1.463(15) |
| S(4)-C(10) | 1.819(13) | C(15)-N(4) | 1.491(16) |
| S(5)-C(11) | 1.839(11) | C(16)-N(4) | 1.481(17) |

| | | | |
|---|---|---|---|
| O(2)-Re(1)-C(1) | 107.6(4) | C(11)-S(5)-Re(2) | 107.2(5) |
| O(2)-Re(1)-S(2) | 109.2(3) | C(12)-S(6)-Re(2) | 111.6(4) |
| C(1)-Re(1)-S(2) | 83.0(3) | C(3)-C(2)-S(2) | 115.5(10) |
| O(2)-Re(1)-S(1) | 115.1(3) | C(2)-C(3)-S(1) | 116.5(11) |
| C(1)-Re(1)-S(1) | 137.3(3) | N(1)-C(4)-N(2) | 121.1(11) |
| S(2)-Re(1)-S(1) | 84.51(12) | N(1)-C(4)-S(3) | 118.7(10) |
| O(2)-Re(1)-S(3) | 107.4(3) | N(2)-C(4)-S(3) | 120.2(8) |
| C(1)-Re(1)-S(3) | 78.6(3) | C(11)-C(10)-S(4) | 112.0(8) |
| S(2)-Re(1)-S(3) | 142.54(11) | C(10)-C(11)-S(5) | 113.2(9) |
| S(1)-Re(1)-S(3) | 87.35(10) | N(4)-C(12)-N(3) | 119.4(12) |
| O(1)-Re(2)-C(9) | 104.9(6) | N(4)-C(12)-S(6) | 119.1(10) |
| O(1)-Re(2)-S(4) | 107.8(3) | N(3)-C(12)-S(6) | 121.6(10) |
| C(9)-Re(2)-S(4) | 82.1(4) | C(4)-N(1)-C(5) | 122.4(10) |
| O(1)-Re(2)-S(5) | 114.1(3) | C(4)-N(1)-C(6) | 123.0(11) |
| C(9)-Re(2)-S(5) | 141.0(5) | C(5)-N(1)-C(6) | 114.0(10) |
| S(4)-Re(2)-S(5) | 85.54(12) | C(4)-N(2)-C(8) | 123.9(10) |
| O(1)-Re(2)-S(6) | 109.6(3) | C(4)-N(2)-C(7) | 122.1(10) |
| C(9)-Re(2)-S(6) | 79.9(4) | C(8)-N(2)-C(7) | 113.4(10) |
| S(4)-Re(2)-S(6) | 141.48(12) | C(12)-N(3)-C(13) | 121.5(10) |
| S(5)-Re(2)-S(6) | 87.49(10) | C(12)-N(3)-C(14) | 123.7(11) |
| C(3)-S(1)-Re(1) | 107.9(5) | C(13)-N(3)-C(14) | 114.0(10) |
| C(2)-S(2)-Re(1) | 106.7(4) | C(12)-N(4)-C(16) | 124.6(12) |
| C(4)-S(3)-Re(1) | 109.1(4) | C(12)-N(4)-C(15) | 124.1(11) |
| C(10)-S(4)-Re(2) | 104.4(4) | C(16)-N(4)-C(15) | 110.7(12) |

D. Anisotropic displacement parameters ($Å^2 \times 10^3$) for **4**. The anisotropic displacement factor exponent takes the form: $-2\pi^2[ h^2 a^{*2} U_{11} + ... + 2 h k a^* b^* U_{12} ]$

| | $U_{11}$ | $U_{22}$ | $U_{33}$ | $U_{23}$ | $U_{13}$ | $U_{12}$ |
|---|---|---|---|---|---|---|

| | | | | | | |
|---|---|---|---|---|---|---|
| Re(1) | 38(1) | 28(1) | 32(1) | -1(1) | 11(1) | 2(1) |
| Re(2) | 43(1) | 37(1) | 35(1) | 2(1) | 5(1) | -3(1) |
| S(1) | 99(3) | 31(2) | 38(2) | -1(2) | 30(2) | 8(2) |
| S(2) | 63(2) | 43(2) | 41(2) | 7(2) | 17(2) | 8(1) |
| S(3) | 53(2) | 33(2) | 35(2) | -4(1) | 12(1) | -12(1) |
| S(4) | 61(2) | 48(2) | 39(2) | 8(2) | 10(2) | -5(2) |
| S(5) | 41(1) | 58(2) | 38(2) | 7(2) | 5(1) | -4(1) |
| S(6) | 43(1) | 54(2) | 44(2) | 8(2) | 10(1) | 5(1) |
| C(1) | 60(8) | 45(7) | 23(7) | -3(5) | -1(6) | -2(6) |
| C(2) | 99(10) | 31(7) | 53(9) | 12(7) | 24(7) | 5(7) |
| C(3) | 280(30) | 26(8) | 67(11) | 18(9) | 83(14) | 24(13) |
| C(4) | 51(7) | 20(6) | 43(8) | 5(5) | 8(6) | 4(5) |
| C(5) | 47(8) | 87(11) | 78(12) | -11(9) | 14(8) | 5(7) |
| C(6) | 58(8) | 75(10) | 66(11) | 6(7) | 23(7) | -4(7) |
| C(7) | 75(10) | 47(8) | 58(10) | -16(7) | 5(8) | -5(7) |
| C(8) | 38(6) | 52(8) | 73(11) | 0(7) | -5(6) | 6(5) |
| C(9) | 64(9) | 82(11) | 91(13) | 21(10) | 5(9) | 13(8) |
| C(10) | 57(7) | 45(7) | 52(9) | -9(6) | 28(7) | -1(5) |
| C(11) | 40(6) | 46(7) | 67(10) | -8(6) | 25(6) | -6(5) |
| C(12) | 37(6) | 52(8) | 37(8) | -1(6) | 7(5) | -14(5) |
| C(13) | 56(7) | 47(8) | 50(8) | -2(6) | 13(6) | 3(5) |
| C(14) | 63(9) | 91(11) | 59(10) | 16(8) | -14(8) | 9(8) |
| C(15) | 93(11) | 89(11) | 25(8) | -2(7) | -7(8) | -44(9) |
| C(16) | 127(15) | 40(9) | 102(14) | 4(9) | 18(11) | -19(8) |
| N(1) | 51(6) | 45(6) | 39(6) | -2(5) | 23(5) | -1(4) |
| N(2) | 47(5) | 40(6) | 34(6) | -6(4) | 6(5) | -1(4) |
| N(3) | 37(5) | 50(6) | 47(7) | 12(5) | 4(5) | 4(4) |
| N(4) | 68(6) | 45(6) | 38(6) | 1(6) | 8(5) | -21(5) |
| O(1) | 67(6) | 51(5) | 64(7) | -21(5) | 12(5) | -15(4) |
| O(2) | 49(4) | 42(6) | 55(6) | 9(4) | -1(4) | 0(3) |

E. Hydrogen coordinates ( $\times 10^4$) and isotropic displacement parameters ($Å^2 \times 10^3$) for3.

| | x | y | z | U(eq) |
|---|---|---|---|---|
| H(1A) | 8979 | 1681 | 12186 | 64 |
| H(1B) | 8847 | 2372 | 11104 | 64 |
| H(1C) | 10346 | 1851 | 11291 | 64 |
| H(2A) | 9356 | -1275 | 11449 | 72 |
| H(2B) | 7728 | -1124 | 10757 | 72 |
| H(3A) | 8846 | -1400 | 9108 | 144 |
| H(3B) | 10434 | -1113 | 9741 | 144 |
| H(5A) | 12268 | 1424 | 8228 | 105 |
| H(5B) | 13064 | 1915 | 7127 | 105 |
| H(5C) | 13139 | 962 | 7140 | 105 |
| H(6A) | 10395 | 1363 | 4513 | 98 |
| H(6B) | 11959 | 914 | 4815 | 98 |
| H(6C) | 11901 | 1868 | 4789 | 98 |
| H(7A) | 9527 | 384 | 5126 | 90 |
| H(7B) | 8040 | 730 | 4377 | 90 |
| H(7C) | 7917 | 107 | 5550 | 90 |
| H(8A) | 7007 | 1989 | 7036 | 82 |
| H(8B) | 6338 | 1115 | 6767 | 82 |
| H(8C) | 6454 | 1728 | 5579 | 82 |
| H(9A) | 5787 | 8009 | 6634 | 118 |
| H(9B) | 6921 | 8443 | 5718 | 118 |
| H(9C) | 5917 | 7714 | 5158 | 118 |
| H(10A) | 103 | 8115 | 6286 | 60 |
| H(10B) | 612 | 9030 | 6371 | 60 |
| H(11A) | -460 | 8916 | 4335 | 60 |
| H(11B) | 277 | 8062 | 4113 | 60 |
| H(13A) | 5888 | 10526 | 3315 | 76 |

| | | | | |
|---|---|---|---|---|
| H(13B) | 4318 | 10956 | 3500 | 76 |
| H(13C) | 5396 | 11281 | 2431 | 76 |
| H(14A) | 2539 | 10234 | 484 | 108 |
| H(14B) | 3278 | 11100 | 662 | 108 |
| H(14C) | 2212 | 10765 | 1733 | 108 |
| H(15A) | 4316 | 10019 | -598 | 104 |
| H(15B) | 3310 | 9289 | -1152 | 104 |
| H(15C) | 5097 | 9242 | -1155 | 104 |
| H(16A) | 4294 | 7940 | 1480 | 134 |
| H(16B) | 5036 | 7963 | 99 | 134 |
| H(16C) | 3255 | 8019 | 152 | 134 |

# CHAPTER IV. INTRCONVERSION OF MeReO(dithiolate)($NC_5H_4$-X) AND MeReO(dithiolate)($PAr_3$) COMPLEXES: THE EQUILIBRIUM CONSTANTS FOLLOW THE HAMMETT EQUATION BUT THE RATE CONSTANTS DO NOT

A manuscript submitted to *Dalton transactions*

Xiaopeng Shan and James H. Espenson

Equilibration occurs among the species MeReO(dithiolate)Py, MeReO(dithiolate)($PZ_3$), Py, and $PZ_3$ where the chelating dithiolate ligand is 1,2-ethanedithiol (edt) or 1,3-propanedithiol (pdt), Py stands for $NC_5H_4$-4-X and $PZ_3$ for both $P(C_6H_4\text{-}4\text{-}Y)_3$ and $P(alkyl)_n(Ph)_{3-n}$. Equilibrium constants in the pdt series were evaluated directly; values of K generally favor phosphane coordination and range from $4.8 \times 10^{-2}$ (X = $NMe_2$, Y = Cl) to $3.2 \times 10^4$ (X = CN, Y = OMe). The values of K are well correlated by the Hammett equation with $\rho_X^K = 2.7(3)$ and $\rho_Y^K = -2.0(3)$. Kinetic data were determined with the stopped-flow method for 65 reactions of the edt and pdt complexes, and resolved into forward and reverse components by use of the equilibrium constants. Values of $k_{for}$ deviate markedly from Hammett behavior, especially along any series with a given X substituent, where plots of log $k_{for}$ against $3\cdot\sigma_Y$ take on a V-shaped appearance. This pattern has been interpreted in terms of a two step mechanism for ligand substitution reactions of these complexes. The rate constants for those phosphanes that are the better Lewis bases are governed by Re–P bond formation. The rate constants for those phosphanes that are weaker Lewis bases, on the other hand, are governed by the second step in which an initial $\psi$-octahedral complex rotates towards a transition state that is an approximate trigonal prism. In so doing, the prior Re–P interaction is weakened, which gives rise to an increase in log $k_{for}$ with $\sigma_Y$.

## Introduction

Ligand substitution reactions of five-coordinate, square-pyramidal methyl(oxo)rhenium(V) dithiolate complexes can be represented by the equation[1,2]

$$MeReO(dt)L^i + L^j = MeReO(dt)L^j + L^i \qquad (1)$$

In this notation, dt represents 1,2-ethanedithiolate (edt), 1,3-propanedithiolate (pdt), or 2-(mercaptomethyl)thiophenolate (mtp) and the ligands $L^i$ and $L^j$ may be, for example, phosphines or pyridines.[3-8] Structural formulas are shown in Chart 1.

Our interest in this family of reactions has been sustained by two factors. First, they are intimately involved in the mechanism of rhenium-catalyzed oxygen-atom transfer reactions ($YO + X \rightarrow Y + XO$).[2,9-13] Second, they present a fundamental issue of mechanism that appears unique to this structure, in that no direct route is available to the symmetric transition state that is necessary for an associative mechanism for substitution which also satisfies the principle of microscopic reversibility. This unusual aspect was explored in our earlier research,[14] and it will be amplified in the Discussion Section, on the basis of the new results and their mechanistic analysis.

Two examples of this reaction have been explored previously. The seemingly simpler one is pure exchange itself, between $MeReO(edt)Py^i$ and $Py^i$. These are rapid reactions that were studied by NMR line broadening. In every case, pyridine exchange follows second-order kinetics and proceeds with an associative mechanism.[15] A more telling example of ligand substitution (which further established that the Py exchange process does not proceed in a single-step) is provided by reactions between $MeReO(mtp)(PZ_3)$ and $PY_3$, where Z and Y include aryl and alkyl groups. In this case substitution proceeded in two steps with the intervention of easily detected concentrations of the intermediate $[MeReO(mtp)(PY_3)]^*$, a geometric isomer of the final product.[14]

In the present study we have turned to reaction of complexes bearing edt and pdt ligands, to avoid sequential reactions of geometrical isomers. Important as this aspect was in the mtp case, the complicating factor of observable sequential reactions can be eliminated by use of a symmetric dithiolate. This study thus entailed direct equilibrium and kinetic measurements on the reaction

$$MeReO(dt)(Py) + PZ_3 = MeReO(dt)(PZ_3) + Py \qquad (2)$$

where $PZ_3$ denotes a generalized phosphane (Z = aryl, alkyl; often $P(C_6H_4\text{-}4\text{-}Y)_3$), Py a generalized pyridine, $NC_5H_4$-4-X, and the dithiolates edt or pdt. The symmetry of the intermediate precludes a second step being detectable, $[MeReO(dt)(PY_3]^*$ and $[MeReO(dt)(PY_3)]$ being enantiomers not geometrical isomers. Nonetheless, there will still

be two steps in reaching the transition state. They respond differently to substituent groups X and Y on the ligands, however, which gives rise to non-Hammett behavior as one step or the other becomes rate-controlling.

**Chart 1**. Structural formulas of Methyl(oxo)rhenium(V) dithiolates

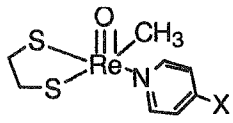

MeReO(edt)($NC_5H_4$-4-X)

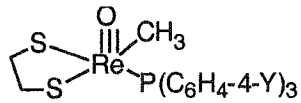

MeReO(edt)P($C_6H_4$-4-Y)$_3$

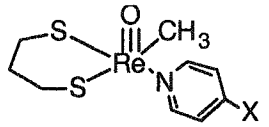

MeReO(pdt)($NC_6H_4$-4-X)

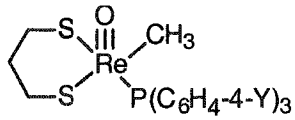

MeReO(pdt)P($C_6H_4$-4-Y)$_3$

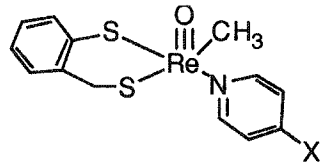

MeReO(mtp)($NC_6H_4$-4-X)

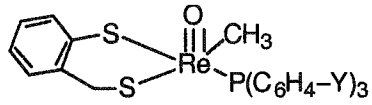

MeReO(mtp)P($C_6H_4$-4-Y)$_3$

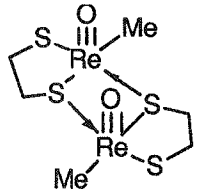

{MeReO(edt)}$_2$

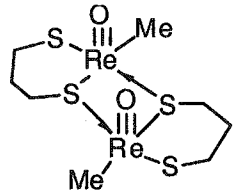

{MeReO(pdt)}$_2$

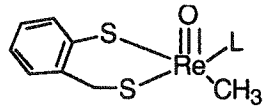

[MeReO(mtp)L]*

## Experimental Section

### General

Methyl(oxo)rhenium(V) dithiolate dimers, {MeReO(edt)}$_2$ and {MeReO(pdt)}$_2$, were synthesized according to literature procedures[4] from 1,2-ethanedithiol ($edtH_2$) or 1,3-propanedithiol ($pdtH_2$) and {MeReO($SPh)_2$}$_2$. The latter compound was prepared from $MeReO_3$ and PhSH, as reported.[16] Pyridines and phosphanes were purchased (Aldrich or Strem) and used as received. Benzene (ACS grade, Aldrich) was used as the solvent for UV-visible spectroscopy. Solutions of either MeReO(dt)($NC_5H_4$-4-X) complex in $C_6H_6$ or $C_6D_6$ were prepared by adding an excess of that pyridine in a solution of the dimer. An excess of pyridine was maintained to ensure that the no dimeric compound remained.[6,17] The mononuclear complexes were identified by NMR spectroscopy in comparison with spectra determined previously.[4]

**Equilibrium studies**

Values of $K_1$ were determined by UV-visible spectrophotometric titration only for the pdt complexes. A concentration in the range of 10-500 mM of the given Py ligand was placed in a 1-cm path UV-visible cell containing 0.05 mM $\{MeReO(pdt)\}_2$. The spectrum was recorded using a Shimadzu UV 3101PC spectrophotometer after the addition of each 10-μL portion of a solution of $PAr_3$. This procedure was repeated until the spectra remained unchanged with further addition of $PAr_3$. The software PSEQUAD[18] was used to analyze the multi-wavelength absorbance data to obtain the equilibrium constant. These calculations are based on the net absorbance change from beginning to end of the addition of $PAr_3$. Typically, absorbance readings were recorded at 10 different wavelengths in the 400-600 nm range; this set of values was used in a global fit to extract the equilibrium constant for selected pyridine and phosphane derivative.

**Kinetics**

Rate constants for reaction 2 were obtained by the use of an OLIS stopped-flow instrument equipped with a Rapid Scanning Monochromator system set for the range 350–500 nm. The absorbance readings monitor the decrease of absorbance at 350-395 nm, in the particular instance of $C_5H_5N$ and $PPh_3$, where $\varepsilon_{RePy} > \varepsilon_{RePAr3}$ and the simultaneous increase at 395–415 nm, where the reverse inequality holds. A persistent isosbestic point for this pair was found at 395 nm which showed that no intermediate attains an appreciable concentration during the reaction. The same was true for the other pyridine-phosphine combinations, save for small differences in the wavelengths cited. Circulating thermostated water was used to control the temperature at 25.0 ± 0.2 °C.

In a typical experiment, equal volumes of 20.0 mM $PPh_3$ solution in $C_6H_6$ was mixed with 0.1 mM $MeReO(edt)(NC_5H_5)$ solution containing 20.0 mM $C_5H_5N$. The excess of pyridine was used to prevent formation of the parent dimer, $\{MeReO(edt)\}_2$. The rapid-scan spectra for this particular experiment are shown in Figure 1. Reaction 2 proceeds nearly to completion with these concentrations.

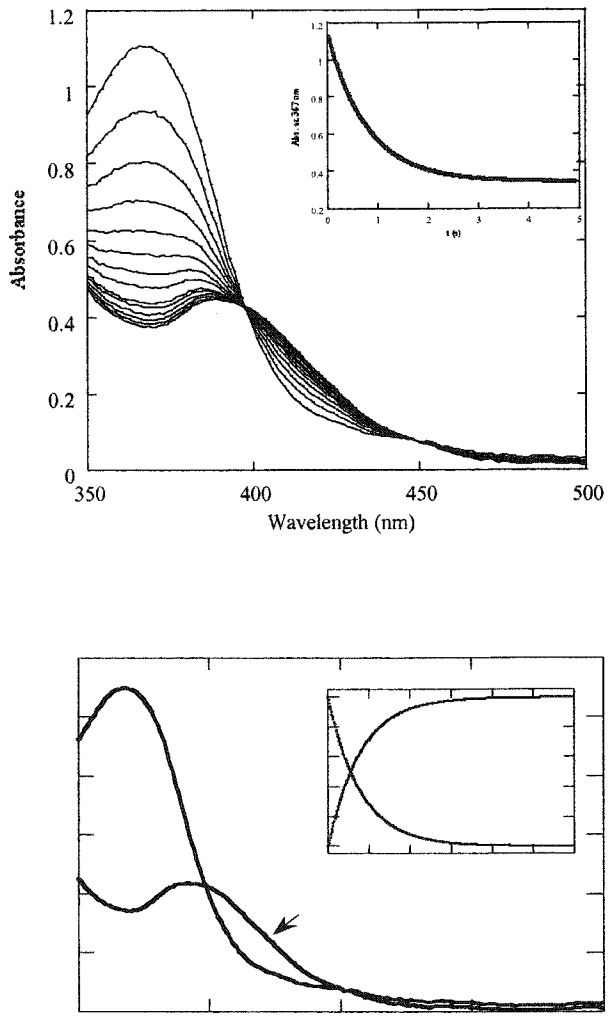


**Fig. 1** Upper: Stopped flow kinetic data showing repetitive scans of reaction **1** with these conditions: 0.05 mM MeReO(edt)($NC_5H_5$), 10.0 mM $PPh_3$ and 10.0 mM Py in $C_6H_6$ at 25 °C. Data were collected over a total time of 5.0 s at intervals of 0.0125 s; for sake of clarity only scans at 0.1 s intervals are shown. The inset shows a fit to first-order kinetics of the data extracted at 367 nm. Lower: The results of a global fit of the kinetic data by the singular value decomposition method, showing the spectra of reactant and product separately resolved by this analysis and an inset in which the spectra have been resolved into their reactant and product components, expressed as molar ratios.

**Results and discussion**

**Equilibrium constants**

Values of K were determined for 11 reactions of the pdt complexes for ten pairs of Py and $PZ_3$ derivatives: (X = $NMe_2$, Y = OMe), (X = $NMe_2$, Y = Me), (X = OMe, Y = Me), ( X = OMe, Y = H), (X = Me, Y = H), (X = Me, Y = F), (X = H, Y= F), (X = H, Y = Cl), (X = CHO, Y = Cl), (X = Ac, Y = Cl), (X = CN, Y = Cl). The values of K, which have been determined to a precision of ca. 10%, are given in Table 1. The remaining 24 values of K are redundant and were calculated directly or indirectly from these eleven experimental values. To illustrate the procedure, consider this particular equilibrium:

$$[Re]NC_5H_4CHO + P(C_6H_4Me)_3 = [Re]P(C_6H_4Me)_3 + NC_5H_4CHO \quad (3)$$

where [Re] stands for the core, MeReO(pdt). The equilibrium constant for reaction 3, K(CHO, Me) is arrived at in these steps:

$$K(Me,Me) = \frac{K(Me,H) \times K(OMe,Me)}{K(OMe,H)} = \frac{17 \times 78}{15} = 88 \quad (4)$$

$$K(H,Me) = \frac{K(Me,Me) \times K(H,F)}{K(Me,F)} = \frac{88 \times 22}{5.9} = 330 \quad (5)$$

$$K(CHO,Me) = \frac{K(H,Me) \times K(CHO,Cl)}{K(H,Cl)} = \frac{330 \times 27}{7.4} = 1200 \quad (6)$$

Not surprisingly, the largest K is $3.2 \times 10^4$ for $NC_5H_4CN$, which has the most electron-withdrawing substituent, in combination with $P(C_6H_4OMe)$, with the most electron releasing substituent. Likewise, the smallest K value is 0.048 for the reaction between $[Re]NC_5H_4NMe_2$ and $P(C_6H_4Cl)_3$.

**Table 1.** Equilibrium constants [a] for reactions between MeReO(pdt)($NC_5H_4$-4-X) and $P(C_6H_4$-4-Y$)_3$ in $C_6H_6$ at 25 °C.

| | | | K | | |
|---|---|---|---|---|---|
| X↓ Y→ | OMe | Me | H | F | Cl |
| $NMe_2$ | **8.2 ± 0.8** | **2.1 ± 0.2** | 0.40 | 0.14 | 0.048 |
| OMe | 300 | **78 ± 7** | **15 ± 1** | 5.2 | 1.8 |
| Me | 340 | 88 | **17 ± 1** | **5.9 ± 0.6** | 2.0 |
| H | 1300 | 330 | 63 | **22 ± 2** | **7.4 ± 0.7** |
| CHO | 4700 | 1200 | 230 | 80 | **27 ± 2** |
| Ac | 3700 | 930 | 180 | 62 | **21 ± 2** |
| CN | 32000 | 8000 | 1500 | 530 | **180 ± 20** |

[a] Experimental values are given in boldface; the others are redundant values of K calculated from them according to eq 4-6 as explained in the text.

**Kinetic Data**

Reaction 2 was studied with an excess of the pyridine present, usually at a concentration of 10 mmol $L^{-1}$, to prevent complications arising from the presence of the dimer $\{MeReO(pdt)\}_2$, were the following equilibrium to proceed to the right to any substantial extent,

$$2\ MeReO(pdt)Py = \{MeReO(pdt)\}_2 + 2\ Py \qquad (7)$$

The phosphanes were also used in excess over rhenium, such that both [Py] and $[PAr_3]$ remained constant in any experiment. The rate of approach to equilibrium is reaction 2 can be written as follows, with (Re) standing for MeReO(pdt)

$$-\frac{d[(Re)Py]}{dt} = k_{for}[(Re)Py]\cdot[PAr_3] - k_{rev}[(Re)PAr_3]\cdot[Py] \qquad (8)$$

The rate constant for equilibration thus becomes

$$k_e = k_{for}[PAr_3] + k_{rev}[Py] \qquad (9)$$

With explicit incorporation of K from Table 1, this expression is obtained

$$k_e = k_{for} \times \{[PAr_3] + [Py]\cdot K^{-1}\} \qquad (10)$$

which represents the equation of a straight line that passes through the origin. The least-squares fit to eq 10 gave values of $k_{for}$ that are summarized in Table 2.

**Table 2.** Rate constants ($k_{for}$/L mol$^{-1}$ s$^{-1}$) for reactions between MeReO(pdt)($NC_5H_4$-4-X) and P(4-$YC_6H_4$)$_3$ in $C_6H_6$ at 25 °C.

| X↓ Y→ | OMe | Me | H | F | Cl |
|---|---|---|---|---|---|
| $NMe_2$ | — | — | 28.8 ± 0.3 | — | — |
| OMe | 157 ± 2 | 91 ± 1 | 78 ± 1 | 137 ± 2 | 156 ± 2 |
| Me | 137 ± 2 | 82 ± 1 | 71 ± 1 | 121 ± 2 | 136 ± 2 |
| H | 190 ± 2 | 114 ± 2 | 103 ± 1 | 166 ± 2 | 182 ± 3 |
| CHO | 368 ± 5 | 235 ± 2 | 171 ± 2 | 162 ± 3 | 179 ± 5 |
| C(O)Me | 340 ± 7 | 201 ± 2 | 154 ± 2 | 166 ± 4 | 197 ± 3 |
| CN | 760 ± 20 | 477 ± 5 | 401 ± 6 | 251 ± 3 | 281 ± 3 |

Values of $k_{for}$ were obtained by fitting $k_e$ to eq 10 with K from Table 1.

Reactions of MeReO(edt)Py required a different analysis because K was not independently evaluated. Eq 10 was also used for the data analysis, but with both $k_{for}$ and K treated as adjustable parameters. The values of $K_{for}$ are given in Table 3. The equilibrium constant is often so large that the second term in eq 10 does not contribute. For the case where $k_{rev}$ does contribute, K could be determined, as given in Table 4.

**Table 3.** Rate constants ($k_{for}$/L mol$^{-1}$ s$^{-1}$) for reactions between MeReO(edt)($NC_5H_4$-4-X) and P(4-$YC_6H_4$)$_3$ in $C_6H_6$ at 25 °C.

| X↓ Y→ | OMe | Me | H | F | Cl |
|---|---|---|---|---|---|
| $NMe_2$ | 91 ± 1[a] | 50.5 ± 0.7[a] | 39.9 ± 0.4[b] | 150 ± 20[b] | — |
| OMe | 227 ± 5[a] | 120 ± 2[a] | 96 ± 2[b] | 143 ± 2[b] | 186 ± 1[a] |
| Me | 205 ± 6[a] | 111 ± 2[a] | 91 ± 1[b] | 133 ± 2[b] | 148 ± 5[a] |
| H | 300 ± 20[a] | 152 ± 2[a] | 128 ± 2[b] | 179 ± 2[a] | 160 ± 10[b] |
| CHO | 530 ± 20[a] | 284 ± 3[a] | 208 ± 2[a] | 168 ± 2[a] | 189 ± 4[a] |
| Ac | 480 ± 10[a] | 258 ± 6[a] | 195 ± 2[a] | 174 ± 2[a] | 211 ± 2[a] |
| CN | 1190 ± 40[a] | 591 ± 6[a] | 480 ± 8[a] | 279 ± 8[a] | 251 ± 3[a] |

[a] Values of $k_e$ were analyzed according to eq 10, with the term $[Py]\cdot K^{-1}$ omitted; [b] The term $[Py]\cdot K^{-1}$ of eq 10 was retained.

**Table 4.** Equilibrium constants for reactions of MeReO(edt)($NC_5H_4$-4-X) with P($C_6H_4$-4-Y)$_3$ at 25 °C in benzene.[a]

| X↓ Y→ | H | F | Cl |
|---|---|---|---|
| $Me_2N$ | 2.5 ± 0.2 | 3.0 ± 1.8 | — |
| MeO | 7 ± 4 | 18 ± 5 | — |
| Me | 36 ± 29 | 38 ± 12 | 11 ± 4 |
| H | — | — | 8 ± 4 |

[a] From fitting of kinetic data to eq 10.

Reactions of a selected group of other phosphanes were also studied, with the results presented in Table 5. Presented along with the rate constants are the cone angles and $pK_a$ values of the conjugate acids of the phosphanes.[19] Although $PMePh_2$ and P($C_6H_4$-4-OMe)$_3$ have the same value of $pK_a$, the rate constant of ligand substitution of the former is 55 times faster than that of the latter owing to the effect of steric hindrance, as indicated by a bigger cone angle, 145 degree.

**Table 5.** Rate constants of reactions between MeReO(edt)($NC_5H_5$) and other phosphanes in $C_6H_6$ at 25 °C.

| $PZ_3$ | θ (degrees) | $pK_a$ | k (L $mol^{-1}$ $s^{-1}$) |
|---|---|---|---|
| $PCyPh_2$ | 153 | 5.05 | $2.30 \times 10^2$ |
| $PCy_2Ph$ | 162 | - | $3.01 \times 10^1$ |
| $PMePh_2$ | 136 | 4.57 | $1.42 \times 10^4$ |
| $P(C_6H_4\text{-}4\text{-}OMe)_3$ | 145 | 4.57 | $2.57 \times 10^2$ |
| $P(MeO)_3$ | 107 | 2.60 | $> 4 \times 10^4$ |

**Temperature Profiles.** The temperature dependence of the reaction between MeReO(edt)Py and $PPh_3$ was studied over the temperature range of 283-323 K. Activation parameters were calculated from the least-squares fit ln (k/T) to 1/T giving $\Delta H^{\ddagger} = 24.0 \pm 0.5$ kJ $mol^{-1}$ and $\Delta S^{\ddagger} = -124 \pm 2$ J $mol^{-1}$ $K^{-1}$. The large negative activation entropy indicates an associative pathway,[20-23] which is compatible with earlier findings.[14]

**Substituent Effects**

**Equilibrium Constant.** One must take into account the effects of variations of substituents X on Py and Y on $PAr_3$, which act in concert. According to studies of multiple-substituent effects in organic chemistry,[24-27] a correlation was made using the Hammett substituent constants for X and Y in the overall expression:

$$\log K(X,Y) = \log K_{ref} + \rho_X^K \times \sigma_X + \rho_Y^K \times (3\sigma_Y) \qquad (11)$$

The factor $\sigma_Y$ includes a multiplying factor of three for $P(C_6H_4Y)_3$. The fitted reaction constants for K are symbolized by $\rho_X^K$ and $\rho_Y^K$. For this analysis only the 11 experimental data from Table 1 were used, because the remaining values of K were calculated ones whose inclusion would not enhance the analysis. The reaction constants were obtained by use of the least-square program SCIENTIST[28] which allows for the use of two independent variables. from the fit are $\rho_X^K = 2.2 \pm 0.3$ and $\rho_Y^K = -1.5 \pm 0.3$. These parameters have opposite signs, of course, because pyridine is coordinated to the reactant, phosphane to the product. In this calculation log K(H,H) was also allowed to float, the refined value being $1.58 \pm 0.09$, as

compared to the experimental value 1.80 ± 0.11. Given the error, the internal consistency is adequate. In a second treatment, K was fixed at the experimental value, which resulted in these reaction constants, $\rho_X^K = 2.7 \pm 0.3$ and $\rho_Y^K = -2.0 \pm 0.3$, which is not a significant difference. The reaction constants reflect the entering and leaving groups. Including the calculated but no less valid values of K in Table 1, the entire range of equilibrium constants spans a factor of $6.7 \times 10^5$, which indicates that the difference between reactant and product is quite sensitive to substituents.

**Rate Constants.** The entries in Tables 2 and 3 indicate that factors other than simple electronic effects on a single rate constant come into play. For one thing, the span of rate constant values for the same X, Y substituent pair is considerably narrower than that for K. For example, values of $k_{for}$ in Table 2 vary by but a factor of 30, as compared to a range of $8 \times 10^4$ in K. Further, the span of the rate constants with variation of the Y substituent is narrower than that for the variation of X substituent, which reverses the trends for the equilibrium constants.

Even more strikingly, the $k_{for}$ values show unusual trends. The small reversal of the ordering of rate constants in each column of Table 2 is barely significant. But the falling and rising of the values in each row with variation of Y is rather pronounced. The same pattern held for every Y group. Put another way, a plot of log $k_{for}$ versus $\sigma_Y$, for any given substituent X on Py, shows a distinctive V-shape. Figure 2 depicts these nonlinear Hammett plots for a few of the reactions.

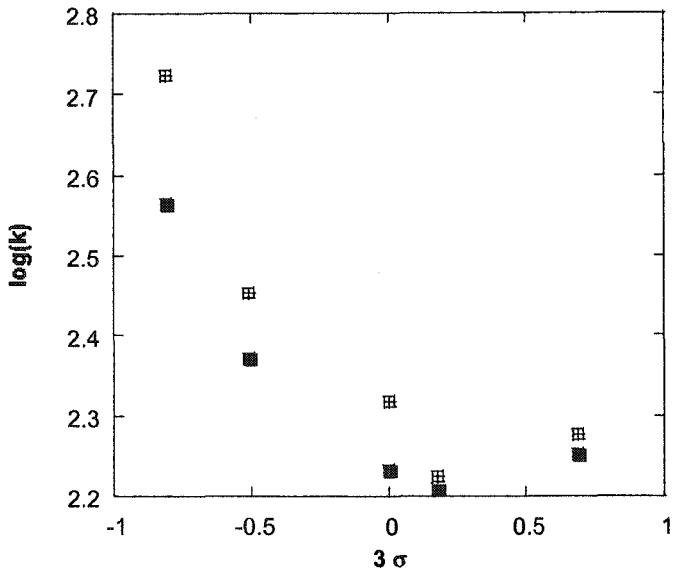


**Fig. 2** Hammett plots of log k for the reactions of MeReO(dt)[$NC_5H_4$-4-CHO) with different $P(C_6H_4\text{-}4\text{-}Y)_3$ compounds for dt = edt (hatched squares) and pdt (filled squares) showing the non-linear relationship indicative of a sequential-step mechanism.

In the introduction, a complex mechanism was mentioned. Our depiction of that mechanism is given in Scheme 1, involving multiple steps: $PZ_3$ approaches the rhenium from the vacant axial position to form six-coordinate intermediate A; a Bailar twist transfers A to its geometric isomer B; Py departs from B to generate the final product.[29,30] The coordination number of rhenium complexes can easily vary from five to six. The Bailar twist has been already proved to be a common isomerization pathway for certain six-coordinate transition metal complexes.[31-36] The justification for such an elaborate scheme, and the data that support it (which include the spectroscopic detection of intermediate A) have been presented earlier.[14] Given this mechanism as a premise, the expression for the rate constant is

$$k_{for} = \frac{k_1}{1 + k_{-1}/k_2} \tag{12}$$

**Scheme 1**. Two step mechanism for ligand substitution

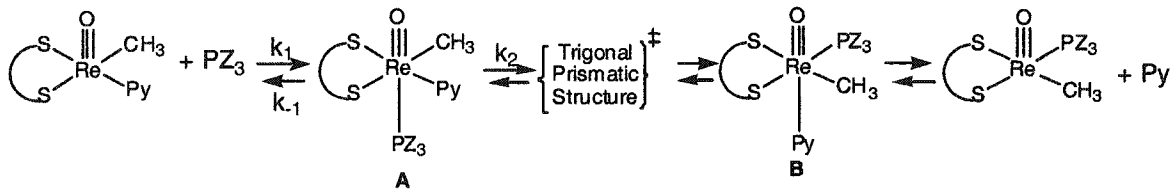


There are two limiting forms of eq 1. One identifies $k_{for}$ as $k_1$, which will be the case when $k_2 >> k_{-1}$. In that case the first step is rate-controlling, and the second much more rapid in comparison. Whether the limit is actually realized is not the major issue; whether it is, or nearly is, the rate will be governed by bond-making between Re and the incoming phosphane ligand. As such, the "ordinary" nucleophilic effect will be seen, and the more electron-donating Y is, the faster the reaction. This is evidently the case for Y = MeO and Me, for example.

The other limit has $k_{for} = (k_1/k_{-1})\cdot k_2$, in which case the first step is at equilibrium and the second is rate-controlling. When $P(C_6H_4\text{-}4\text{-}Y)_3$ is less nucleophilic, as with Y = F and Cl, then the first step will feature a small binding constant, $k_1/k_{-1} << 1$; moreover, the weakly-bound phosphine will leave more rapidly than the turnstile rotation step; that is, $k_{-1} >> k_2$. Because $k_2$ governs the substituent effect under those circumstances, the reaction constant will show a rising effect with $\sigma_Y$ as coordination of the bulky phosphane group weakens as the molecule approaches the configuration of a trigonal prism because the ligands must rotate past one another. Again, the equilibrium constants for the same reaction conform to an ordinary Hammett relationship because only the initial and final states of the system come under consideration, not the special intermediate.

**Acknowledgement**

This research was supported by the U.S. Department of Energy, Office of Basic Energy Sciences, Division of Chemical Sciences under Contract W-7405-Eng-82 with Iowa State University of Science and Technology.

**References**

(1) Lente, G.; Espenson, J. H. *Inorg. Chem.* 2000, **39**, 4809-4814.

(2) Wang, Y.; Espenson, J. H. *Inorg. Chem.* 2002, **41**, 2266-2274.

(3) Jacob, J.; Guzei, I. A.; Espenson, J. H. *Inorg. Chem.* 1999, **38**, 1040-1041.

(4) Espenson, J. H.; Shan, X.; Wang, Y.; Huang, R.; Lahti, D. W.; Dixon, J.; Lente, G.; Ellern, A.; Guzei, I. A. *Inorg. Chem.* 2002, **41**, 2583-2591.

(5) Jacob, J.; Guzei, I. A.; Espenson, J. H. *Inorg. Chem.* 1999, **38**, 3266-3267.

(6) Jacob, J.; Lente, G.; Guzei, I. A.; Espenson, J. H. *Inorg. Chem.* 1999, **38**, 3762-3763.

(7) Lente, G.; Jacob, J.; Guzei, I. A.; Espenson, J. H. *Inorg. Reac. Mechs.* 2000, **2**, 169-177.

(8) Lente, G.; Shan, X.; Guzei, I. A.; Espenson, J. H. *Inorg. Chem.* 2000, **39**, 3572-3576.

(9) Wang, Y.; Espenson, J. H. *Organic Letters* 2000, **2**, 3525-3526.

(10) Wang, Y.; Lente, G.; Espenson, J. H. *Inorg. Chem.* 2002, **41**, 1272-1280.

(11) Arias, J.; Newlands, C. R.; Abu-Omar, M. M. *Inorg. Chem.* 2001, **40**, 2185-2192.

(12) Bhattacharyya, S.; Chakraborty, I.; Dirghangi, B. K.; Chakravorty, A. *Inorg. Chem.* 2001, **40**, 286-293.

(13) Gable, K. P.; Brown, E. C. *Organometallics* 2000, **19**, 944-946.

(14) Lahti, D. W.; Espenson, J. H. *J. Amer. Chem. Soc.* 2001, **123**, 6014-6024.

(15) Espenson, J. H.; Shan, X.; Lahti, D. W.; Rockey, T. M.; Saha, B.; Ellern, A. *Inorg. Chem.* 2001, **40**, 6717-6724.

(16) Herrmann, W. A.; Kratzer, R. M.; Fischer, R. W. *Angew. Chem., Int. Ed.* 1997, **36**, 2652-2654.

(17) Lente, G.; Guzei, I. A.; Espenson, J. H. *Inorg. Chem.* 2000, **39**, 1311-1319.

(18) Zékány, L.; Nagypál, I. in *Computational methods for the determination of formation constants*; Leggett, D., Ed.: New York, 1985; p We are grateful to Gábor Lente for assistance in its implementation.

(19) Dias, P. B.; Minas de Piedade, M. E.; Martinho Simoes, J. A. *Coord. Chem. Rev.* 1994, **135**, 737-807.

(20) Kayran, C.; Kozanoglu, F.; Ozkar, S.; Saldamli, S.; Tekkaya, A.; Kreiter, C. G. *Inorg. Chim. Acta* 1999, **284**, 229-236.

(21) Lugovskoy, A.; Paur-Afshari, R.; Schultz, R. H. *J. Phys. Chem. A* 2000, **104**, 10587-10593.

(22) Meng, Q.; Huang, Y.; Ryan, W. J.; Sweigart, D. A. *Inorg. Chem.* 1992, **31**, 4051-4052.

(23) Shen, J.-K.; Kubas, G. J.; Rheingold, A. L. *Inorg. Chim. Acta* 1995, **240**, 99-104.

(24) Argile, A.; Ruasse, M. F. *J. Org. Chem.* 1983, **48**, 209-214.

(25) Dubois, J. E.; Ruasse, M. F.; Argile, A. *J. Am. Chem. Soc.* 1984, **106**, 4840-4845.

(26) Lee, I.; Park, Y. K.; Huh, C.; Lee, H. W. *J. Phys. Org. Chem.* 1994, **7**, 555-560.

(27) Lee, I. *J. Phys. Org. Chem.* 1994, **7**, 448-454.

(28) *Scientist*; 2.0 ed.; Micromath Software:, 1995.

(29) Cook, M. R.; Herrmann, W. A.; Kiprof, P.; Takacs, J. *J. Chem. Soc., Dalton Trans.* 1991, 797-804.

(30) Herrmann, W. A.; Kuehn, F. E.; Roesky, P. W. *JOURNAL OF ORGANOMETALLIC CHEMISTRY* 1995, **485**, 243-251.

(31) Abugideiri, F.; Fettinger, J. C.; Pleune, B.; Poli, R.; Bayse, C. A.; Hall, M. B. *Organometallics* 1997, **16**, 1179-1185.

(32) Alvarez, S.; Pinsky, M.; Avnir, D. *Eur. J. Inorg. Chem.* 2001, 1499-1503.

(33) Bayse, C. A.; Couty, M.; Hall, M. B. *J. Amer. Chem. Soc.* 1996, **118**, 8916-8919.

(34) Kakaliou, L.; Scanlon, W. J.; Qian, B.; Baek, S. W.; Smith, M. R., III; Motry, D. H. *Inorg. Chem.* 1999, **38**, 5964-5977.

(35) Kane-Maguire, N. A. P.; Hanks, T. W.; Jurs, D. G.; Tollison, R. M.; Heatherington, A. L.; Ritzenthaler, L. M.; McNulty, L. M.; Wilson, H. M. *Inorg. Chem.* 1995, **34**, 1121-1124.

(36) Rahim, M.; Taylor, N. J.; Xin, S.; Collins, S. *Organometallics* 1998, **17**, 1315-1323.

**Supporting Information**

Table of contents

**Figure S-1**. Plots of the rate constants as functions of [$PZ_3$]: 0.025 mM **5**, 5 mM Pyridine, 10-70 mM $CyPh_2P$ or $Cy_2PhP$ in $C_6H_6$ at 25 °C

**Figure S-2**. Plots of the pseudo-first-order rate constants against the concentrations of $PPh_3$ for its reactions with MeReO(pdt)($NC_5H_4$-4-X) at 25 °C in benzene.

**Figure S-3**. Spectrophotometric titration of MeReO(pdt)($NC_5H_4$-4-X) with $P(C_6H_4$-Y-4)$_3$ at 25 °C in benzene.

**Table S-1**. Rate constants of reaction between MeReO(edt)($C_5H_5N$) and $Ph_3P$ in $C_6H_6$ at 283~323 K.

**Table S-2**. Pseudo-first-order rate constants of reaction between MeReO(dt)(4-X-$C_5H_4N$) and $P(C_6H_4$-4-Y) in $C_6H_6$ at 25 °C.

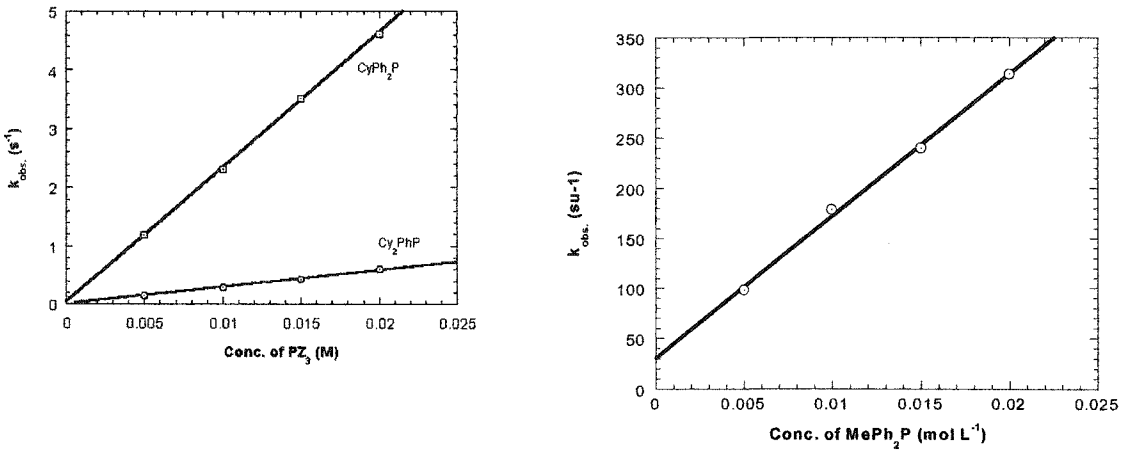


**Figure S-1**. Plots of the rate constants as functions of [$PZ_3$]: 0.025 mM **5**, 5 mM Pyridine, 10-70 mM $CyPh_2P$ or $Cy_2PhP$ in $C_6H_6$ at 25 °C

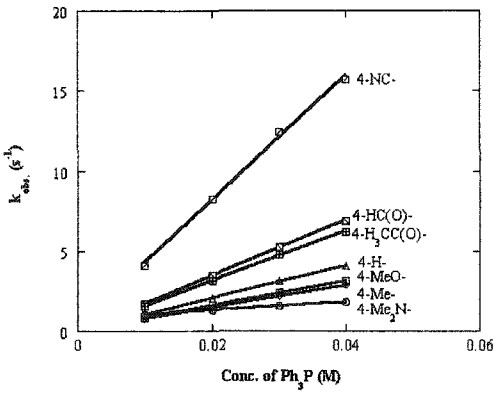


Figure **S-2**. Plots of the pseudo-first-order rate constants against the concentrations of $PPh_3$ for its reactions with MeReO(pdt)($NC_5H_4$-4-X) at 25 °C in benzene.

**Figure S-3**. Spectrophotometric titration of MeReO(pdt)($NC_5H_4$-4-X) with $P(C_6H_4$-Y-4)$_3$ at 25 °C in benzene.

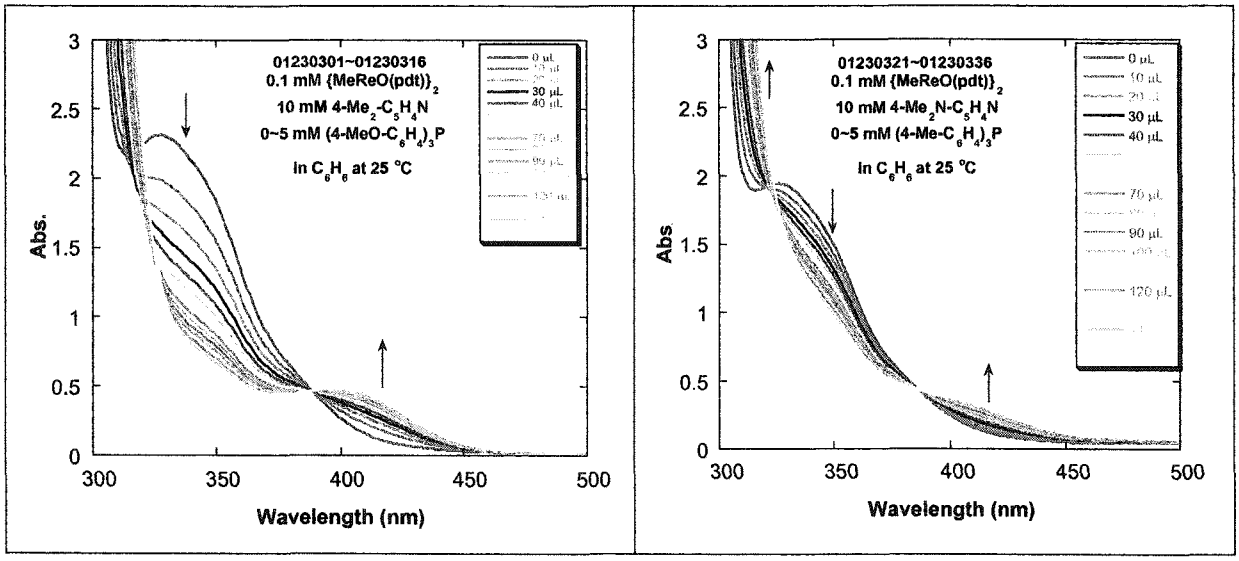

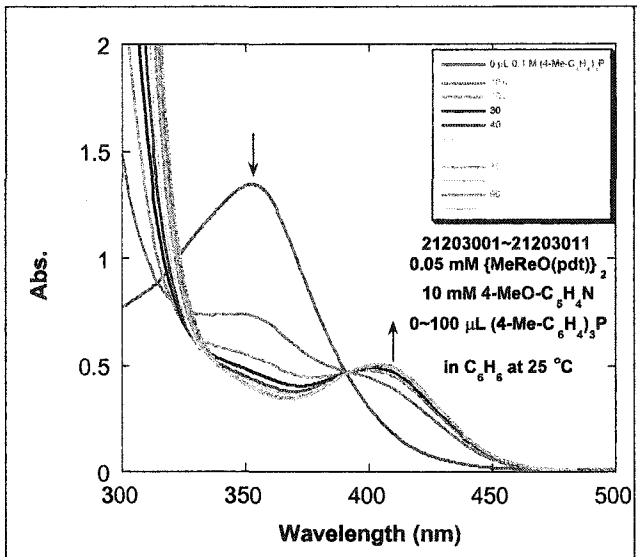
Abs.
Wavelength (nm)
21203001~21203011
0.05 mM {MeReO(pdt)}2
10 mM 4-MeO-C5H4N
0~100 μL (4-Me-C6H4)3P
in C6H6 at 25 °C

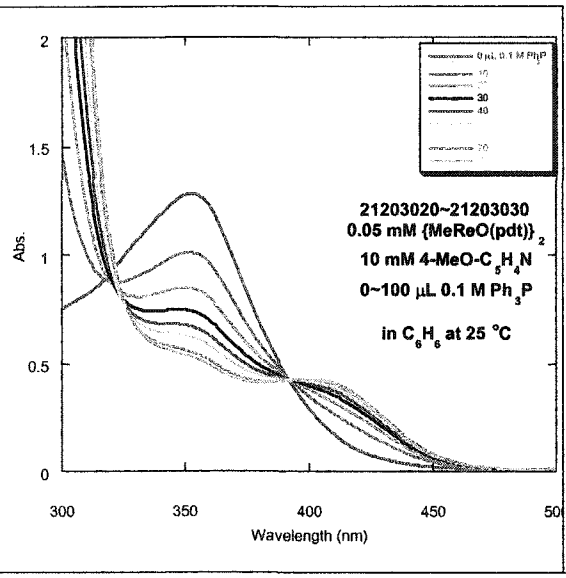
Abs.
Wavelength (nm)
21203020~21203030
0.05 mM {MeReO(pdt)}2
10 mM 4-MeO-C5H4N
0~100 μL 0.1 M Ph3P
in C6H6 at 25 °C

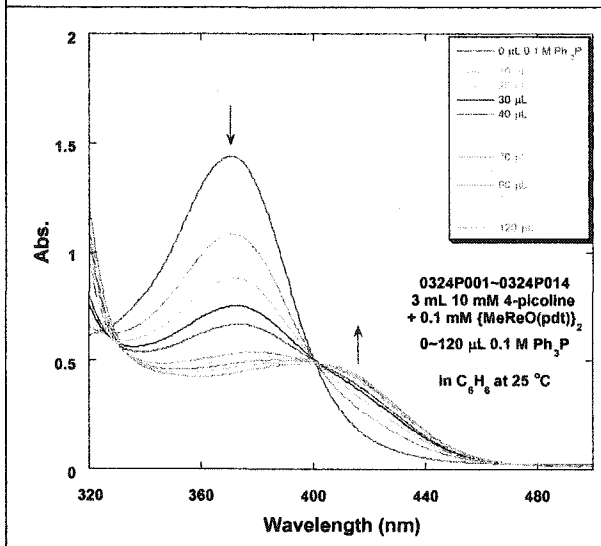
Abs.
Wavelength (nm)
0324P001~0324P014
3 mL 10 mM 4-picoline
+ 0.1 mM {MeReO(pdt)}2
0~120 μL 0.1 M Ph3P
in C6H6 at 25 °C

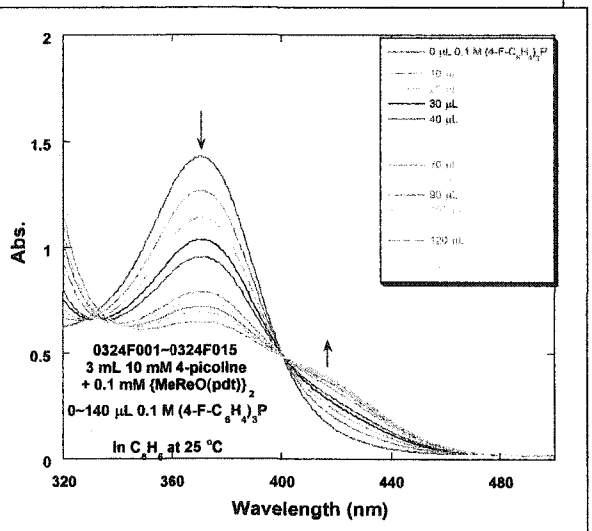
Abs.
Wavelength (nm)
0324F001~0324F015
3 mL 10 mM 4-picoline
+ 0.1 mM {MeReO(pdt)}2
0~140 μL 0.1 M (4-F-C6H4)3P
in C6H6 at 25 °C

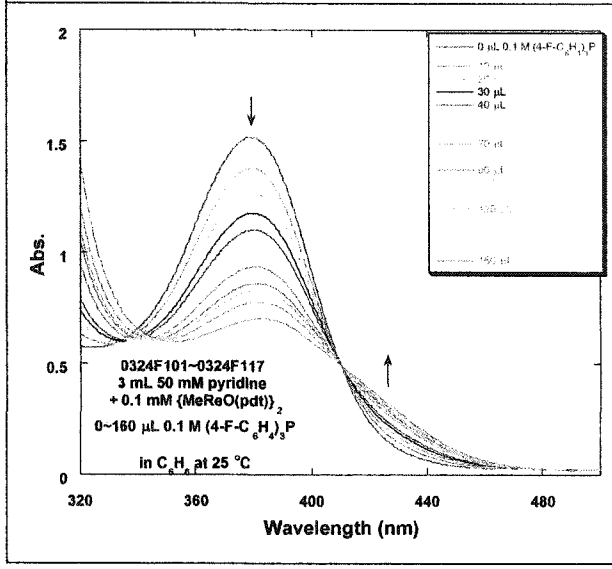
Abs.
Wavelength (nm)
0324F101~0324F117
3 mL 50 mM pyridine
+ 0.1 mM {MeReO(pdt)}2
0~160 μL 0.1 M (4-F-C6H4)3P
in C6H6 at 25 °C

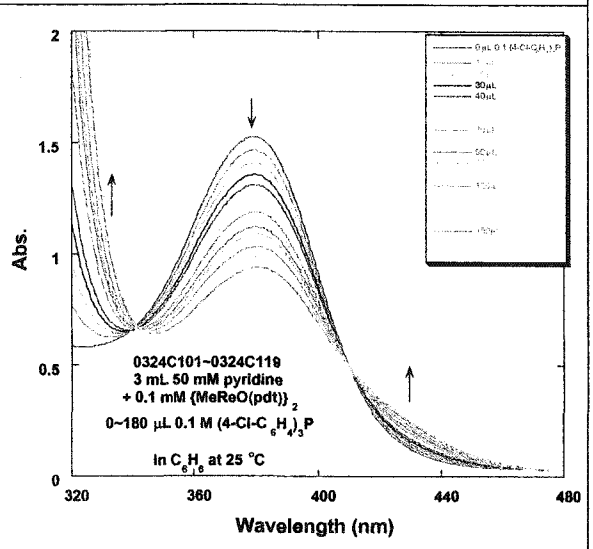
Abs.
Wavelength (nm)
0324C101~0324C119
3 mL 50 mM pyridine
+ 0.1 mM {MeReO(pdt)}2
0~180 μL 0.1 M (4-Cl-C6H4)3P
in C6H6 at 25 °C

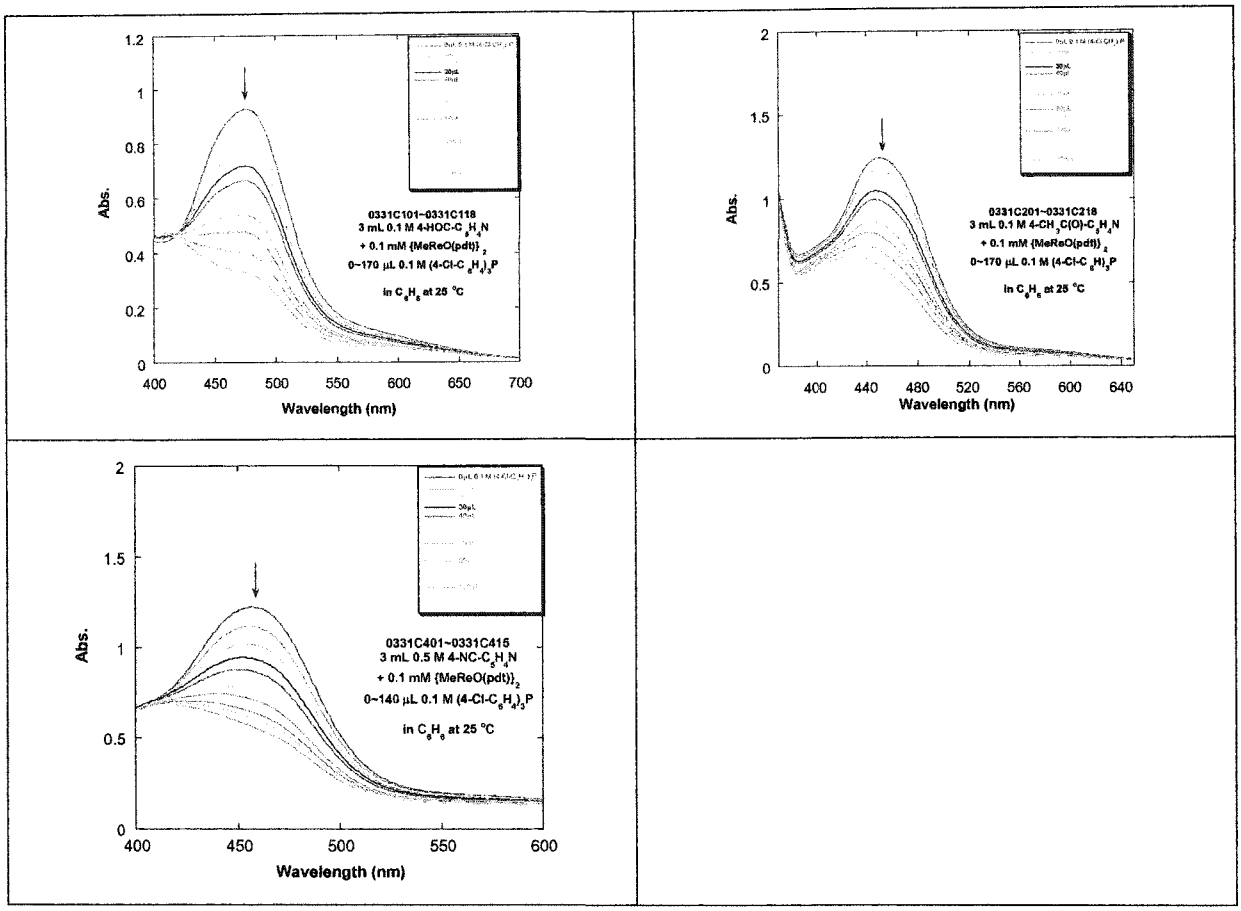


Table S-1. Rate constants of reaction between MeReO(edt)($C_5H_5N$) and $Ph_3P$ in $C_6H_6$ at 283~323 K.

| T (K) | k (L $mol^{-1}$ $s^{-1}$) |
|---|---|
| 283 | 72 |
| 288 | 87 |
| 293 | 106 |
| 298 | 126 |
| 303 | 151 |
| 308 | 178 |
| 313 | 211 |
| 318 | 249 |
| 323 | 286 |

**Table S-2**. Pseudo-first-order rate constants of reaction between MeReO(dt)(4-X-$C_5H_4N$) (0.05 mM) and $P(C_6H_4\text{-}4\text{-}Y)_3$ in $C_6H_6$ at 25 °C.

| dt | X | [4-X- $C_5H_4N$] /M | Y | [$P(C_6H_4\text{-}4\text{-}Y)_3$] /M | $k_{obs.}$ /$s^{-1}$ |
|---|---|---|---|---|---|
| edt | OMe | 0.01 | OMe | 0.005 | 1.23 |
| edt | OMe | 0.01 | OMe | 0.010 | 2.09 |
| edt | OMe | 0.01 | OMe | 0.015 | 3.36 |
| edt | OMe | 0.01 | OMe | 0.020 | 4.64 |
| edt | OMe | 0.01 | Me | 0.005 | 0.563 |
| edt | OMe | 0.01 | Me | 0.010 | 1.18 |
| edt | OMe | 0.01 | Me | 0.015 | 1.79 |
| edt | OMe | 0.01 | Me | 0.020 | 2.41 |
| edt | OMe | 0.01 | H | 0.010 | 1.037 |
| edt | OMe | 0.01 | H | 0.030 | 3.083 |
| edt | OMe | 0.01 | H | 0.050 | 4.99 |
| edt | OMe | 0.01 | H | 0.070 | 6.78 |
| edt | OMe | 0.01 | F | 0.005 | 0.784 |
| edt | OMe | 0.01 | F | 0.00865 | 1.314 |
| edt | OMe | 0.01 | F | 0.015 | 2.24 |
| edt | OMe | 0.01 | F | 0.020 | 2.92 |
| edt | OMe | 0.01 | Cl | 0.005 | 0.923 |
| edt | OMe | 0.01 | Cl | 0.010 | 1.83 |
| edt | OMe | 0.01 | Cl | 0.0088 | 1.67 |
| edt | OMe | 0.01 | Cl | 0.0118 | 2.19 |
| edt | Me | 0.01 | OMe | 0.005 | 1.237 |
| edt | Me | 0.01 | OMe | 0.010 | 1.85 |
| edt | Me | 0.01 | OMe | 0.015 | 3.04 |

| | | | | | |
|---|---|---|---|---|---|
| edt | Me | 0.01 | OMe | 0.020 | 4.18 |
| edt | Me | 0.01 | Me | 0.005 | 0.589 |
| edt | Me | 0.01 | Me | 0.010 | 1.082 |
| edt | Me | 0.01 | Me | 0.015 | 1.67 |
| edt | Me | 0.01 | Me | 0.020 | 2.21 |
| edt | Me | 0.01 | H | 0.010 | 0.933 |
| edt | Me | 0.01 | H | 0.030 | 2.76 |
| edt | Me | 0.01 | H | 0.050 | 4.54 |
| edt | Me | 0.01 | H | 0.070 | 6.39 |
| edt | Me | 0.01 | F | 0.005 | 0.698 |
| edt | Me | 0.01 | F | 0.00865 | 1.193 |
| edt | Me | 0.01 | F | 0.015 | 2.02 |
| edt | Me | 0.01 | F | 0.020 | 2.70 |
| edt | Me | 0.01 | Cl | 0.005 | 0.881 |
| edt | Me | 0.01 | Cl | 0.010 | 1.628 |
| edt | Me | 0.01 | Cl | 0.0088 | 1.41 |
| edt | Me | 0.01 | Cl | 0.0118 | 1.88 |
| edt | H | 0.01 | OMe | 0.005 | 1.96 |
| edt | H | 0.01 | OMe | 0.010 | 2.57 |
| edt | H | 0.01 | OMe | 0.015 | 4.26 |
| edt | H | 0.01 | OMe | 0.020 | 6.24 |
| edt | H | 0.01 | Me | 0.005 | 0.801 |
| edt | H | 0.01 | Me | 0.010 | 1.478 |
| edt | H | 0.01 | Me | 0.015 | 2.27 |
| edt | H | 0.01 | Me | 0.020 | 3.04 |
| edt | H | 0.01 | H | 0.010 | 1.282 |
| edt | H | 0.01 | H | 0.020 | 2.56 |
| edt | H | 0.01 | H | 0.030 | 3.84 |
| edt | H | 0.01 | H | 0.040 | 5.14 |

| | | | | | |
|---|---|---|---|---|---|
| edt | H | 0.01 | H | 0.050 | 6.39 |
| edt | H | 0.01 | H | 0.060 | 7.65 |
| edt | H | 0.01 | H | 0.070 | 8.88 |
| edt | H | 0.01 | H | 0.080 | 10.22 |
| edt | H | 0.01 | F | 0.005 | 0.875 |
| edt | H | 0.01 | F | 0.00865 | 1.521 |
| edt | H | 0.01 | F | 0.015 | 2.65 |
| edt | H | 0.01 | F | 0.020 | 3.64 |
| edt | H | 0.01 | Cl | 0.005 | 1.033 |
| edt | H | 0.01 | Cl | 0.010 | 1.88 |
| edt | H | 0.01 | Cl | 0.0088 | 1.595 |
| edt | H | 0.01 | Cl | 0.0118 | 2.12 |
| edt | HOC | 0.1 | OMe | 0.005 | 2.274 |
| edt | HOC | 0.1 | OMe | 0.010 | 4.87 |
| edt | HOC | 0.1 | OMe | 0.015 | 7.63 |
| edt | HOC | 0.1 | OMe | 0.020 | 10.98 |
| edt | HOC | 0.1 | Me | 0.005 | 1.50 |
| edt | HOC | 0.1 | Me | 0.010 | 2.94 |
| edt | HOC | 0.1 | Me | 0.015 | 4.23 |
| edt | HOC | 0.1 | Me | 0.020 | 5.64 |
| edt | HOC | 0.1 | H | 0.010 | 2.17 |
| edt | HOC | 0.1 | H | 0.030 | 6.53 |
| edt | HOC | 0.1 | H | 0.050 | 10.58 |
| edt | HOC | 0.1 | H | 0.070 | 14.3 |
| edt | HOC | 0.1 | F | 0.005 | 0.875 |
| edt | HOC | 0.1 | F | 0.00865 | 1.516 |
| edt | HOC | 0.1 | F | 0.015 | 2.46 |
| edt | HOC | 0.1 | F | 0.020 | 3.36 |
| edt | HOC | 0.1 | Cl | 0.005 | 1.022 |

| | | | | | |
|---|---|---|---|---|---|
| edt | HOC | 0.1 | Cl | 0.010 | 1.972 |
| edt | HOC | 0.1 | Cl | 0.0088 | 1.62 |
| edt | HOC | 0.1 | Cl | 0.0118 | 2.16 |
| edt | Ac | 0.1 | OMe | 0.005 | 2.18 |
| edt | Ac | 0.1 | OMe | 0.010 | 4.57 |
| edt | Ac | 0.1 | OMe | 0.015 | 7.05 |
| edt | Ac | 0.1 | OMe | 0.020 | 9.83 |
| edt | Ac | 0.1 | Me | 0.005 | 1.458 |
| edt | Ac | 0.1 | Me | 0.010 | 2.75 |
| edt | Ac | 0.1 | Me | 0.015 | 3.76 |
| edt | Ac | 0.1 | Me | 0.020 | 5.10 |
| edt | Ac | 0.1 | H | 0.010 | 1.95 |
| edt | Ac | 0.1 | H | 0.030 | 5.86 |
| edt | Ac | 0.1 | H | 0.050 | 9.84 |
| edt | Ac | 0.1 | H | 0.070 | 13.6 |
| edt | Ac | 0.1 | F | 0.005 | 0.875 |
| edt | Ac | 0.1 | F | 0.00865 | 1.516 |
| edt | Ac | 0.1 | F | 0.015 | 2.46 |
| edt | Ac | 0.1 | F | 0.020 | 3.36 |
| edt | Ac | 0.1 | Cl | 0.005 | 1.022 |
| edt | Ac | 0.1 | Cl | 0.010 | 1.972 |
| edt | Ac | 0.1 | Cl | 0.0088 | 1.62 |
| edt | Ac | 0.1 | Cl | 0.0118 | 2.16 |
| edt | CN | 0.1 | OMe | 0.005 | 5.02 |
| edt | CN | 0.1 | OMe | 0.010 | 10.6 |
| edt | CN | 0.1 | OMe | 0.015 | 18.0 |
| edt | CN | 0.1 | OMe | 0.020 | 24.7 |
| edt | CN | 0.1 | Me | 0.005 | 2.86 |
| edt | CN | 0.1 | Me | 0.010 | 5.70 |

| | | | | | |
|---|---|---|---|---|---|
| edt | CN | 0.1 | Me | 0.015 | 8.80 |
| edt | CN | 0.1 | Me | 0.020 | 12.0 |
| edt | CN | 0.1 | H | 0.010 | 4.84 |
| edt | CN | 0.1 | H | 0.030 | 15.5 |
| edt | CN | 0.1 | H | 0.050 | 24.7 |
| edt | CN | 0.1 | H | 0.070 | 32.6 |
| edt | CN | 0.1 | F | 0.005 | 1.226 |
| edt | CN | 0.1 | F | 0.00865 | 2.48 |
| edt | CN | 0.1 | F | 0.015 | 3.93 |
| edt | CN | 0.1 | F | 0.020 | 5.80 |
| edt | CN | 0.1 | Cl | 0.00295 | 0.73 |
| edt | CN | 0.1 | Cl | 0.00589 | 1.46 |
| edt | CN | 0.1 | Cl | 0.00884 | 2.21 |
| edt | CN | 0.1 | Cl | 0.0118 | 2.98 |
| edt | $NMe_2$ | 0.01 | OMe | 0.005 | 0.490 |
| edt | $NMe_2$ | 0.01 | OMe | 0.010 | 0.868 |
| edt | $NMe_2$ | 0.01 | OMe | 0.015 | 1.351 |
| edt | $NMe_2$ | 0.01 | OMe | 0.020 | 1.832 |
| edt | $NMe_2$ | 0.01 | Me | 0.005 | 0.278 |
| edt | $NMe_2$ | 0.01 | Me | 0.010 | 0.485 |
| edt | $NMe_2$ | 0.01 | Me | 0.015 | 0.760 |
| edt | $NMe_2$ | 0.01 | Me | 0.020 | 1.01 |
| edt | $NMe_2$ | 0.01 | H | 0.010 | 0.559 |
| edt | $NMe_2$ | 0.01 | H | 0.030 | 1.363 |
| edt | $NMe_2$ | 0.01 | H | 0.050 | 2.14 |
| edt | $NMe_2$ | 0.01 | H | 0.070 | 2.96 |
| edt | $NMe_2$ | 0.01 | F | 0.005 | 1.31 |
| edt | $NMe_2$ | 0.01 | F | 0.00865 | 1.61 |
| edt | $NMe_2$ | 0.01 | F | 0.015 | 2.94 |

| edt | $NMe_2$ | 0.01 | F | 0.020 | 3.40 |
|---|---|---|---|---|---|
| | | | | | |
| pdt | $NMe_2$ | 0.01 | H | 0.010 | 1.035 |
| pdt | $NMe_2$ | 0.01 | H | 0.020 | 1.30 |
| pdt | $NMe_2$ | 0.01 | H | 0.030 | 1.59 |
| pdt | $NMe_2$ | 0.01 | H | 0.040 | 1.85 |
| pdt | OMe | 0.01 | OMe | 0.005 | 0.773 |
| pdt | OMe | 0.01 | OMe | 0.010 | 1.60 |
| pdt | OMe | 0.01 | OMe | 0.015 | 2.31 |
| pdt | OMe | 0.01 | OMe | 0.020 | 3.16 |
| pdt | OMe | 0.01 | Me | 0.005 | 0.460 |
| pdt | OMe | 0.01 | Me | 0.010 | 0.917 |
| pdt | OMe | 0.01 | Me | 0.015 | 1.373 |
| pdt | OMe | 0.01 | Me | 0.020 | 1.821 |
| pdt | OMe | 0.01 | H | 0.010 | 0.840 |
| pdt | OMe | 0.01 | H | 0.020 | 1.628 |
| pdt | OMe | 0.01 | H | 0.030 | 2.406 |
| pdt | OMe | 0.01 | H | 0.040 | 3.15 |
| pdt | OMe | 0.01 | F | 0.005 | 0.972 |
| pdt | OMe | 0.01 | F | 0.00865 | 1.505 |
| pdt | OMe | 0.01 | F | 0.015 | 2.30 |
| pdt | OMe | 0.01 | F | 0.020 | 3.01 |
| pdt | OMe | 0.01 | Cl | 0.005 | 1.695 |
| pdt | OMe | 0.01 | Cl | 0.010 | 2.57 |
| pdt | OMe | 0.01 | Cl | 0.0088 | 2.23 |
| pdt | OMe | 0.01 | Cl | 0.0118 | 2.72 |
| pdt | Me | 0.01 | OMe | 0.005 | 0.680 |
| pdt | Me | 0.01 | OMe | 0.010 | 1.373 |
| pdt | Me | 0.01 | OMe | 0.015 | 2.03 |

| | | | | | |
|---|---|---|---|---|---|
| pdt | Me | 0.01 | OMe | 0.020 | 2.76 |
| pdt | Me | 0.01 | Me | 0.005 | 0.414 |
| pdt | Me | 0.01 | Me | 0.010 | 0.832 |
| pdt | Me | 0.01 | Me | 0.015 | 1.233 |
| pdt | Me | 0.01 | Me | 0.020 | 1.637 |
| pdt | Me | 0.01 | H | 0.010 | 0.745 |
| pdt | Me | 0.01 | H | 0.020 | 1.46 |
| pdt | Me | 0.01 | H | 0.030 | 2.17 |
| pdt | Me | 0.01 | H | 0.040 | 2.87 |
| pdt | Me | 0.01 | F | 0.005 | 0.815 |
| pdt | Me | 0.01 | F | 0.00865 | 1.283 |
| pdt | Me | 0.01 | F | 0.015 | 1.997 |
| pdt | Me | 0.01 | F | 0.020 | 2.64 |
| pdt | Me | 0.01 | Cl | 0.005 | 1.34 |
| pdt | Me | 0.01 | Cl | 0.010 | 2.15 |
| pdt | Me | 0.01 | Cl | 0.0088 | 1.85 |
| pdt | Me | 0.01 | Cl | 0.0118 | 2.30 |
| pdt | H | 0.01 | OMe | 0.005 | 0.929 |
| pdt | H | 0.01 | OMe | 0.010 | 1.91 |
| pdt | H | 0.01 | OMe | 0.015 | 2.79 |
| pdt | H | 0.01 | OMe | 0.020 | 3.86 |
| pdt | H | 0.01 | Me | 0.005 | 0.568 |
| pdt | H | 0.01 | Me | 0.010 | 1.148 |
| pdt | H | 0.01 | Me | 0.015 | 1.70 |
| pdt | H | 0.01 | Me | 0.020 | 2.28 |
| pdt | H | 0.01 | H | 0.010 | 1.049 |
| pdt | H | 0.01 | H | 0.020 | 2.09 |
| pdt | H | 0.01 | H | 0.030 | 3.13 |
| pdt | H | 0.01 | H | 0.040 | 4.10 |

| | | | | | |
|---|---|---|---|---|---|
| pdt | H | 0.01 | F | 0.005 | 0.931 |
| pdt | H | 0.01 | F | 0.00865 | 1.563 |
| pdt | H | 0.01 | F | 0.015 | 2.51 |
| pdt | H | 0.01 | F | 0.020 | 3.39 |
| pdt | H | 0.01 | Cl | 0.005 | 1.17 |
| pdt | H | 0.01 | Cl | 0.010 | 2.15 |
| pdt | H | 0.01 | Cl | 0.0088 | 1.80 |
| pdt | H | 0.01 | Cl | 0.0118 | 2.36 |
| pdt | HOC | 0.1 | OMe | 0.005 | 1.84 |
| pdt | HOC | 0.1 | OMe | 0.010 | 3.91 |
| pdt | HOC | 0.1 | OMe | 0.015 | 5.42 |
| pdt | HOC | 0.1 | OMe | 0.020 | 7.33 |
| pdt | HOC | 0.1 | Me | 0.005 | 1.14 |
| pdt | HOC | 0.1 | Me | 0.010 | 2.29 |
| pdt | HOC | 0.1 | Me | 0.015 | 3.57 |
| pdt | HOC | 0.1 | Me | 0.020 | 4.75 |
| pdt | HOC | 0.1 | H | 0.010 | 1.72 |
| pdt | HOC | 0.1 | H | 0.020 | 3.46 |
| pdt | HOC | 0.1 | H | 0.030 | 5.25 |
| pdt | HOC | 0.1 | H | 0.040 | 6.92 |
| pdt | HOC | 0.1 | F | 0.005 | 0.901 |
| pdt | HOC | 0.1 | F | 0.00865 | 1.55 |
| pdt | HOC | 0.1 | F | 0.015 | 2.64 |
| pdt | HOC | 0.1 | F | 0.020 | 3.50 |
| pdt | HOC | 0.1 | Cl | 0.00295 | 1.046 |
| pdt | HOC | 0.1 | Cl | 0.00589 | 1.65 |
| pdt | HOC | 0.1 | Cl | 0.0088 | 2.26 |
| pdt | HOC | 0.1 | Cl | 0.0118 | 2.87 |
| pdt | Ac | 0.1 | OMe | 0.005 | 1.82 |

| | | | | | |
|---|---|---|---|---|---|
| pdt | Ac | 0.1 | OMe | 0.010 | 3.70 |
| pdt | Ac | 0.1 | OMe | 0.015 | 4.97 |
| pdt | Ac | 0.1 | OMe | 0.020 | 6.73 |
| pdt | Ac | 0.1 | Me | 0.005 | 1.035 |
| pdt | Ac | 0.1 | Me | 0.010 | 2.09 |
| pdt | Ac | 0.1 | Me | 0.015 | 3.02 |
| pdt | Ac | 0.1 | Me | 0.020 | 4.01 |
| pdt | Ac | 0.1 | H | 0.010 | 1.565 |
| pdt | Ac | 0.1 | H | 0.020 | 3.16 |
| pdt | Ac | 0.1 | H | 0.030 | 4.78 |
| pdt | Ac | 0.1 | H | 0.040 | 6.24 |
| pdt | Ac | 0.1 | F | 0.005 | 0.924 |
| pdt | Ac | 0.1 | F | 0.00865 | 1.579 |
| pdt | Ac | 0.1 | F | 0.015 | 2.78 |
| pdt | Ac | 0.1 | F | 0.020 | 3.68 |
| pdt | Ac | 0.1 | Cl | 0.00295 | 1.422 |
| pdt | Ac | 0.1 | Cl | 0.00589 | 2.06 |
| pdt | Ac | 0.1 | Cl | 0.0088 | 2.69 |
| pdt | Ac | 0.1 | Cl | 0.0118 | 3.33 |
| pdt | CN | 0.1 | OMe | 0.005 | 3.35 |
| pdt | CN | 0.1 | OMe | 0.010 | 7.07 |
| pdt | CN | 0.1 | OMe | 0.015 | 11.1 |
| pdt | CN | 0.1 | OMe | 0.020 | 15.9 |
| pdt | CN | 0.1 | Me | 0.005 | 2.32 |
| pdt | CN | 0.1 | Me | 0.010 | 4.67 |
| pdt | CN | 0.1 | Me | 0.015 | 7.10 |
| pdt | CN | 0.1 | Me | 0.020 | 9.67 |
| pdt | CN | 0.1 | H | 0.010 | 4.09 |
| pdt | CN | 0.1 | H | 0.020 | 8.30 |

| | | | | | |
|---|---|---|---|---|---|
| pdt | CN | 0.1 | H | 0.030 | 12.4 |
| pdt | CN | 0.1 | H | 0.040 | 15.7 |
| pdt | CN | 0.1 | F | 0.005 | 1.24 |
| pdt | CN | 0.1 | F | 0.00865 | 2.18 |
| pdt | CN | 0.1 | F | 0.015 | 3.72 |
| pdt | CN | 0.1 | F | 0.020 | 5.16 |
| pdt | CN | 0.1 | Cl | 0.00295 | 0.926 |
| pdt | CN | 0.1 | Cl | 0.00589 | 1.767 |
| pdt | CN | 0.1 | Cl | 0.00884 | 2.64 |
| pdt | CN | 0.1 | Cl | 0.0118 | 3.51 |

# CHAPTER V. KINETICS AND MECHANISMS OF REACTIONS OF ReO($\kappa^2$-edt)($\kappa^2$-edtMe): PHOSPHANE DISPLACEMENT OF THE THIOETHER GROUP AND INVERSION OF THE THIOETHER SULFUR

A manuscript published in *Organometallics*

Xiaopeng Shan, James H. Espenson

**Abstract**

Phosphanes ($PZ_3$) convert ReO($\kappa^2$-edt)($\kappa^2$-edtMe) (**1**) into ReO($\kappa^2$-edt)($\kappa^1$-edtMe)($PZ_3$) (**2**) in equilibrium reactions that have been studied in benzene at 25.0 °C. The equilibrium constants and rate constants were evaluated by NMR spectroscopy and stopped-flow studies. The equilibrium constants were correlated by the Hammett equation. A negative correlation constant resulted, $\rho_K = -1.75$, which indicates an electronic effect on the equilibrium that is in agreement with reaction constants for the kinetics, $\rho_{for} = -0.19$ and $\rho_{rev} = 1.46$, for forward and reverse reactions, respectively. The small reaction constant for the forward reaction and large value for the reverse reaction can be explained by proposing an early transition state of the substitution reaction. In other words, the Re–P bond is not substantially made at the point where the Re–SMe bond is broken to a considerable extent. The kinetics of inversion of the thioether sulfur was investigated by determining the temperature profile of the NMR spectra, from which $\Delta H^{\ddagger} = 24 \pm 1$ kJ mol$^{-1}$. From the combination of results from above two reactions, a planar intermediate mechanism is being proposed for the sulfur inversion.

## Introduction

Recent series of $Re^{V}$ or $Re^{VII}$ complexes catalyze oxygen atom transfer reactions that are analogous, stoichiometrically and to a great extent mechanistically, to those catalyzed by molybdenum enzymes.[1-7] Many of the rhenium compounds are prepared from reactions between methyltrioxorhenium(VII), MTO, and alkyl or aryl dithiols.[8-10] Usually the Re(VII) of MTO is reduced to lower valent Re(V) by oxidation of a dithiol to a disulfide. Recently we prepared an entirely new type of product from the reaction between MTO and 1,2-ethanedithiol ($edtH_2$). This gave rise to $Re^{V}$ compound **1**.[11]

$$MeReO_3 + 2\ HS(CH_2)_2SH \rightarrow \text{ReO}(\kappa^2\text{-edt})(\kappa^2\text{-edtMe})\ (\mathbf{1}) + 2\ H_2O \qquad (1)$$

Compound **1** contains chelated 1,2-ethanedithiolate (edt) and 2-(mercaptomethyl) methylthioether (edtMe) ligands. Although numerous transition metal complexes with thiolate or thioether ligands have been synthesized and characterized,[12-17] only less commonly have mixed thiolate-thioether complexes been obtained.[18-20]

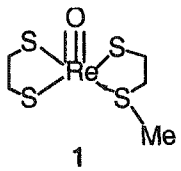


**1**

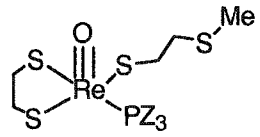


**2**

Inversion of sulfur atoms of a coordinated thioether ligand has been widely discussed, but the mechanism remains uncertain.[21-26] In this paper, we report the kinetics and mechanism of ligand (phosphane) insertion (eq 2) into the rhenium-thioether bond to generate a phosphane-rhenium(V) compound **2**. Also, sulfur inversion of the thioether ligand has been studied, and a mechanism proposed for it.

$$ReO(\kappa^2\text{-edt})(\kappa^2\text{-edtMe})\ (\mathbf{1}) + PZ_3 = ReO(\kappa^2\text{-edt})(\kappa^1\text{-edtMe})(PZ_3)\ (\mathbf{2}) \qquad (2)$$

**Experimental Section**

**Materials and Instrumentation.** Compound **1** was synthesized from MTO and 1,2-ethanedithiol as reported previously.[11] The phosphanes were purchased from Aldrich or Strem and were used as received. Spectranalyzed benzene (Aldrich) was used as the solvent for UV-visible studies. $D_8$-Toluene and $D_6$-benzene were employed as solvents for NMR spectroscopy. An OLIS rapid-scan stopped flow instrument was used to monitor reaction 2. A Bruker DRX-400 MHz spectrometer was used to recorded $^1H$ NMR spectra.

**Kinetic Studies.** An absorbance increase around 390 nm accompanies reaction 2. A typical repetitive scan is shown in Figure 1 for $P(C_6H_4\text{-}4\text{-}OMe)_3$.

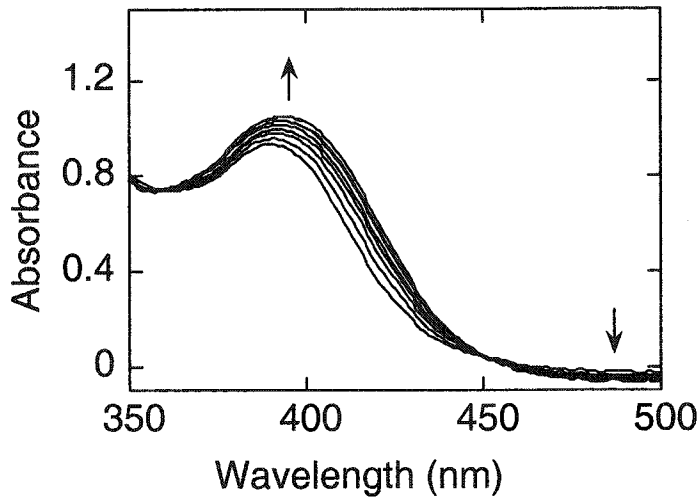


**Figure** 1. Repetitive scan data for the reaction between 0.1 mM ReO($\kappa^2$-edt)( $\kappa^2$-edtMe) and 10 mM P($p$-MeOC$_6$H$_4$)$_3$ , showing spectra at 0.2 s intervals in benzene at 25.0 °C.

An isosbestic point was found for this particular phosphane at 450 nm. The absorbance-time data at 415 nm were extracted from the repetitive scans. Because an excess of the phosphanes was used for the kinetic studies, the data could be fitted to eq 3, from which values of $k_\Psi$ were obtained. Figure 2 shows the plot of $k_\Psi$ against the concentration of this phosphane. Such plots for this and other phosphanes are linear, with slopes representing the second-order rate constants for the forward direction, $k_{for}$, and intercepts the first-order rate constant for the reverse direction, $k_{rev}$, as in eq 4.

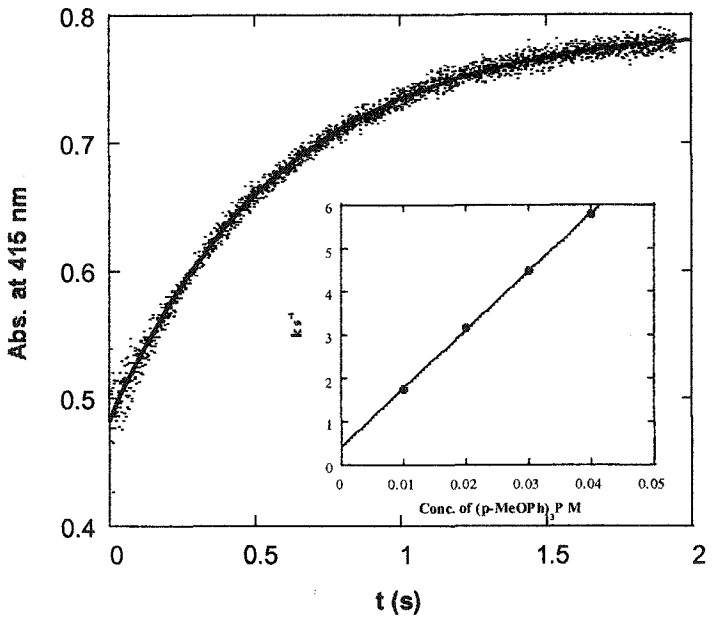


**Figure 2.** A plot of $k_\psi$ against the concentration of $P(p\text{-}MeOC_6H_4)_3$, for reaction 2 in benzene at 25.0 °C, according to eq 4.

$$Abs_t = Abs_e + (Abs_0 - Abs_e)\exp(-k_\psi \times t) \quad (3)$$

$$k_\psi = k_{for}[PZ_3] + k_{rev} \quad (4)$$

The kinetics of sulfur inversion was investigated by the line-shape change in NMR spectra from –40 °C to room temperature. The width at half-height ($W_{1/2}$) of the resonance peak at 1.94 ppm and 7.00 ppm was measured by XPLOTED software from Bruker. The peak at 1.94 ppm is from the thioether methyl group of **1**, and that at 7.00 ppm from the solvent. Compared with the solvent peak, the methyl resonance at 1.94 ppm shows obvious line-broadening effect when the temperature decreases. The values of $W_{1/2}$ are given in Table S-1 in the Supporting Information. Values of $W_{1/2}$ varied with the rate constant of inversion, $k_{inv}$, according to the eq 5, where $\delta\nu$ is the difference between the chemical shift for the methyl group and $W_0$ is the half-width of the peak without inversion.

$$k_{inv} = \frac{\pi \times (\delta\nu)^2}{2(W_{1/2} - W_0)} \quad (5)$$

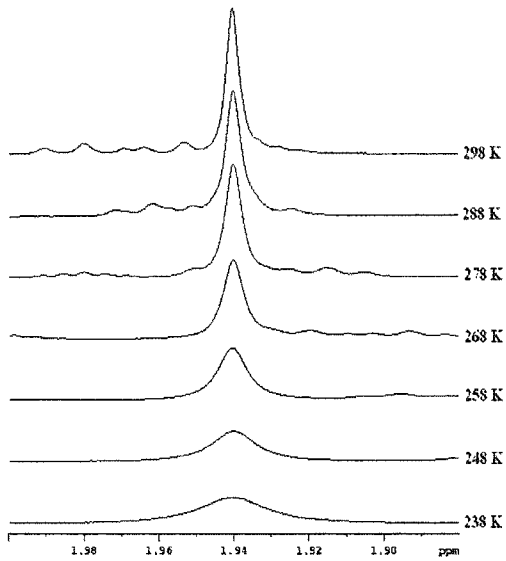


**Figure 3**. Line broadening effects in the $^1$H-NMR spectrum of ReO($\kappa^2$-edt)($\kappa^2$-edtMe), **1**, in $D_8$-toluene, which arises from inversion at sulfur.

**Equilibrium Study.** The equilibrium constants for reaction 2 were measured by NMR spectra of mixtures of **1** and phosphanes in $D_6$-benzene at 25 °C. Some of the equilibrium constants were calculated from kinetic data by $K = k_{for}/k_{rerv}$.

**Temperature Profiles.** The temperature profile of reaction 2 was investigated by using a temperature-controlled water bath in conjunction with the OLIS rapid-scan instrument. Temperatures were varied from 15 to 40 °C and were controlled to within ±0.2 °C. An Eyring plot is depicted in Figure 4 and the rate constants were fitted by eq 6 to obtain values of the activation parameters.

$$\ln\left(\frac{k}{T}\right) = \ln\left(\frac{k_B}{h}\right) + \frac{\Delta S^{\ddagger}}{R} - \frac{\Delta H^{\ddagger}}{RT} \qquad (6)$$

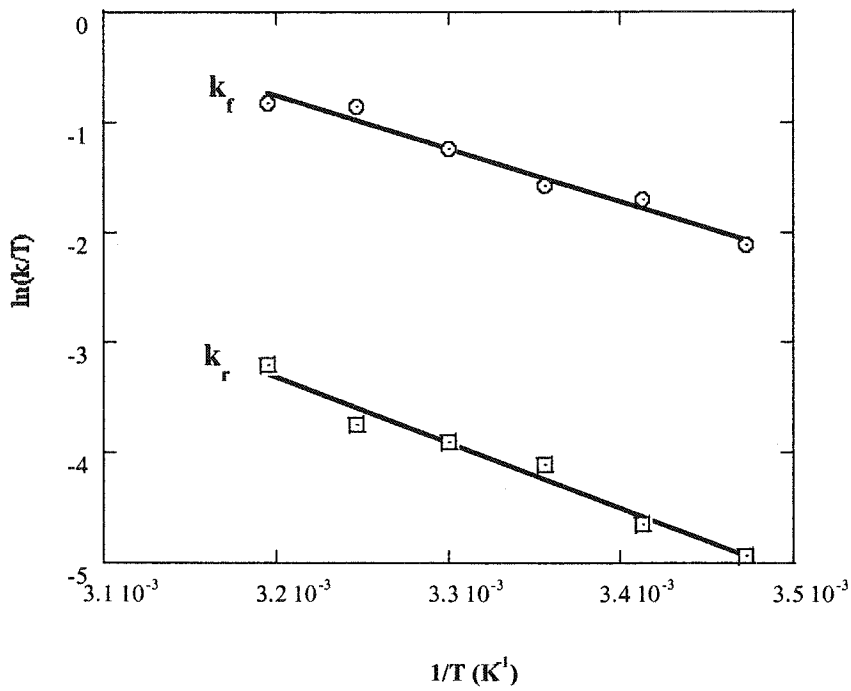


**Figure 4.** Analysis of kinetic data for the rate constants $k_{for}$ (top) and $k_{rev}$ for the reaction $ReO(\kappa^2\text{-edt})(\kappa^2\text{-edtMe}) + PPh_3 \rightleftharpoons ReO(\kappa^2\text{-edt})(\kappa^1\text{-edtMe})(PPh_3)$ by the Eyring equation. Forward direction: $\Delta H^{\ddagger} = 40(4)$ kJ mol$^{-1}$; $\Delta S^{\ddagger} = -76(7)$ J K$^{-1}$ mol$^{-1}$; Reverse direction: $\Delta H^{\ddagger} = 50(4)$ kJ mol$^{-1}$; $\Delta S^{\ddagger} = -66(7)$ J K$^{-1}$ mol$^{-1}$.

The sulfur inversion process was studied by taking $^1$H NMR spectra at temperatures between 233.7 and 298 K. An Eyring plot is given in figure 5 and fitted by equation (7). Activation enthalpy was obtained from the slope. The activation entropy is not available because $\delta\nu$ is not known.

$$\ln[(W_{1/2} - W_0)T] = \ln\left(\frac{\pi \times (\delta\nu)^2}{2}\right) - \ln\left(\frac{k_B}{h}\right) - \frac{\Delta S^{\ddagger}}{R} + \frac{\Delta H^{\ddagger}}{RT} \qquad (7)$$

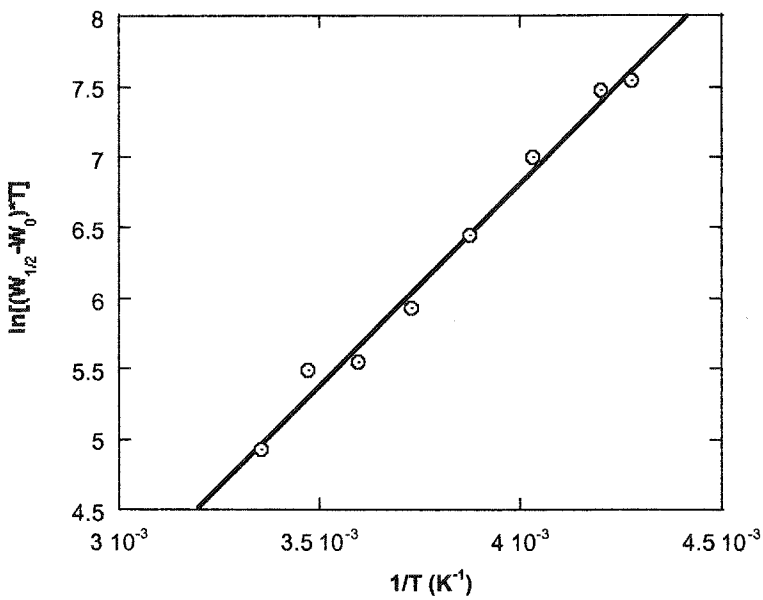


**Figure 5.** $\ln[(W_{1/2} - W_0) \times T]$ against 1/T for compound **1** in $D_8$-toluene from 233.7 to 298 K.

## Results

**Equilibrium of Thioether-Phosphane Substitution Reactions.** A series of such reactions as in eq 2 with $PZ_3$ reagents have been explored. The equilibrium constants are given in Table 1. For the series with $P(p\text{-}XC_6H_4)_3$, K increases as electron-donating groups are placed on the aryl group.

Table 1. Equilibrium and Rate Constants for Phosphine Coordination to Re($\kappa^2$-edt)($\kappa^2$-edtMe)[a]

| Phosphine | $k_f$/L mol$^{-1}$ s$^{-1}$ [b] | $k_r$/s$^{-1}$ [b] | K | |
|---|---|---|---|---|
| | | | kin.[c] | direct |
| P(4-MeOC-$_6$H$_4$)$_3$ | $(1.35 \pm 0.02) \times 10^2$ | $(4.3 \pm 0.5) \times 10^{-1}$ | $(3.1 \pm 0.4) \times 10^2$ | $(3.2 \pm 0.3) \times 10^2$ [d] |
| P(4-MeC$_6$H$_4$)$_3$ | $(7.61 \pm 0.07) \times 10^1$ | $1.30 \pm 0.07$ | $(5.9 \pm 0.3) \times 10^1$ | $(6.7 \pm 0.7) \times 10^1$ [d] |
| P(3-MeC$_6$H$_4$)$_3$ | $(4.91 \pm 0.09) \times 10^1$ | $2.42 \pm 0.03$ | $(2.03 \pm 0.04) \times 10^1$ | $(3.2 \pm 0.5) \times 10^1$ [e] |
| PPh$_3$ | $(6.20 \pm 0.09) \times 10^1$ | $4.86 \pm 0.09$ | $(1.28 \pm 0.02) \times 10^1$ | $8.0 \pm 0.8$ [d] |
| P(4-FC$_6$H$_4$)$_3$ | $(9.2 \pm 1.6) \times 10^1$ | $(1.52 \pm 0.06) \times 10^1$ | $6 \pm 1$ | $3.5 \pm 0.4$ [d] |
| P(3-MeOC-$_6$H$_4$)$_3$ | $(1.06 \pm 0.03) \times 10^2$ | $7.54 \pm 0.08$ | $(1.41 \pm 0.04) \times 10^1$ | $(1.12 \pm 0.05) \times 10^1$ [e] |
| P(4-ClC$_6$H$_4$)$_3$ | – | – | – | $(7.8 \pm 0.8) \times 10^{-1}$ [d] |
| PMePh$_2$ | $(8.1 \pm 0.3) \times 10^2$ | – | – | $(2.58 \pm 0.09) \times 10^3$ [e] |
| P(c-C$_6$H$_{13}$)Ph$_2$ | $(8.1 \pm 0.3) \times 10^1$ | $(4.3 \pm 0.7) \times 10^{-1}$ | $(1.9 \pm 0.3) \times 10^2$ | – |
| P(c-C$_6$H$_{13}$)$_2$Ph | $(1.10 \pm 0.02) \times 10^1$ | $(5.4 \pm 0.4) \times 10^{-2}$ | $(2.0 \pm 0.2) \times 10^2$ | – |

[a] In benzene at 25.0 °C; [b] From eq (3) $k_{obs.} = k_f[PZ_3] + k_r$; [c] From $k_f/k_r$; [d] From NMR integration; [e] From UV/Vis titration.

The equilibrium constants were correlated by the Hammett equation against the substituent constants $3\sigma$, affording $\rho_K = -1.75$, as shown in Figure 6. This indicates a

substantial electronic effect on the equilibrium position of these reactions. The small increase of $K_e$ from $Cy_2PhP$ to $CyPh_2P$, compared with the 20-fold increase from $Ph_3P$ to $CyPh_2P$, shows evidence of the different steric demands of this group of ligands. The reaction with the smallest and most electronic dense phosphane, $PMe_2Ph$, has the largest equilibrium constant, $K = 2580$.

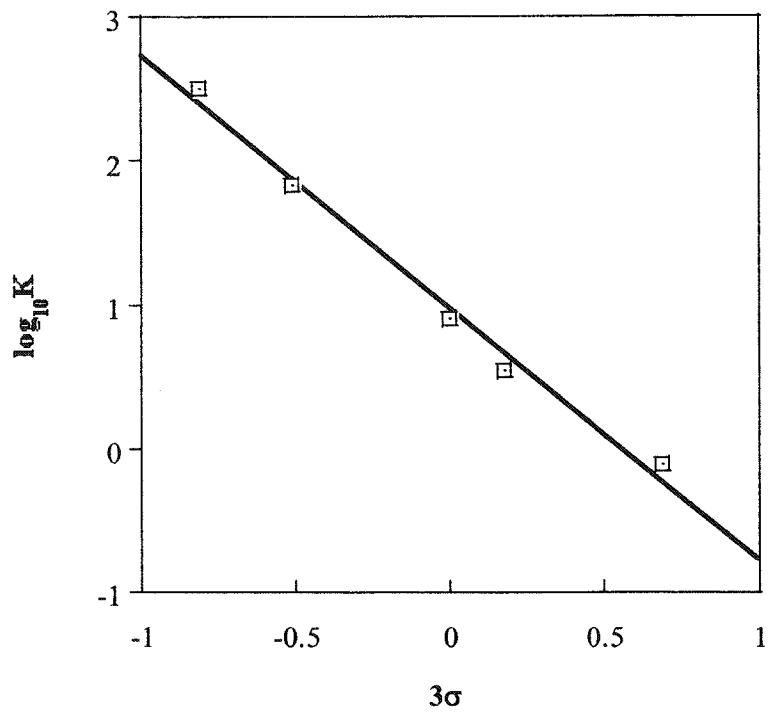


**Figure 6.** Hammett correlation of the equilibrium constants for reaction 2 with $PAr_3$ reagents against the substituent constants.

**Kinetics of Ligand Substitution.** Values of $k_{for}$ and $k_{rev}$ are presented in Table 1. For the series with $P(p\text{-}XC_6H_4)_3$, values of $k_{for}$ increase slightly as electron-donating substituents are placed on the aryl group. To the contrary, the values of $k_{rev}$ decrease dramatically in the same series. Both series of rate constants could be correlated by the Hammett equation with the substituent constants $3\sigma$, affording $\rho_{for} = -0.19$ and $\rho_{rev} = 1.46$, as shown in Figure 7. We conclude from this analysis that ligand substitution goes through an early transition state.

That is, the Re–P bond is not substantially made at the point where the Re–SMe bond is broken to a considerable extent.

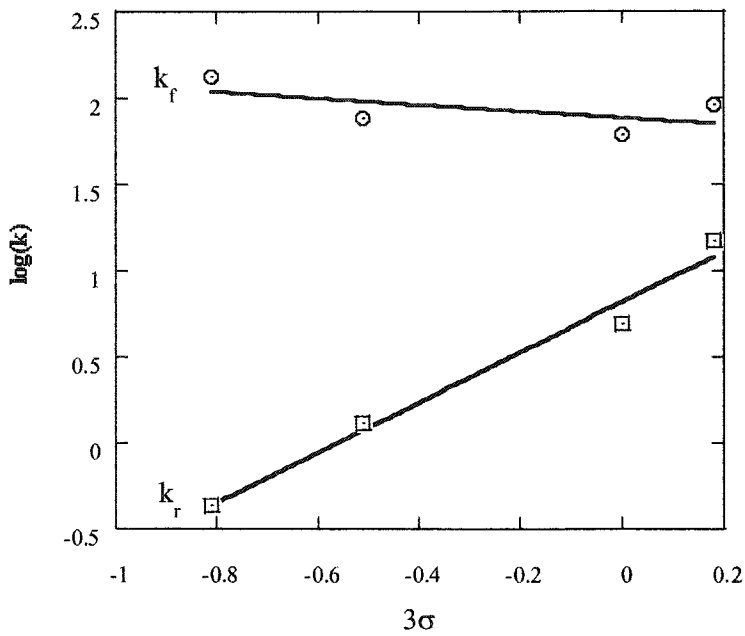


**Figure 7.** Hammett analysis of the rate constants $k_{for}$ and $k_{rev}$ for the reaction $ReO(\kappa^2\text{-edt})(\kappa^2\text{-edtMe}) + PAr_3 \rightleftharpoons ReO(\kappa^2\text{-edt})(\kappa^1\text{-edtMe})(PAr_3)$.

Temperature profiles of the forward and reverse rate constants were derived from the plots presented in Figure 4. Activation parameters for $k_{for}$ and $k_{rev}$ are summarized in Table 2 for the case of $PPh_3$. The activation enthalpy for the reverse direction is 10 kJ $mol^{-1}$ bigger than that of forward direction, because of the stronger Re–P bond. Both directions have similar negative activation entropies indicative of an associative transition state.

**Table 2.** Activation Energy Parameters for Ligand Substitution and Sulfur Inversion Reactions of **1** in Benzene.

| | $\Delta H^{\ddagger}$/kJ mol$^{-1}$ | $\Delta S^{\ddagger}$/J K$^{-1}$ mol$^{-1}$ |
|---|---|---|
| $k_{for}$ | 40(4) | –76(7) |
| $k_{rev}$ | 50(40 | –66(7) |
| $k_{inv}$ | 24(1) | |

**Sulfur Inversion.** Obvious line-broadening effect of the $^1$H resonance peak of methyl group in **1** has been observed as the temperature was decreased from 298 to 233.7 K. This kind of line-shape change is caused from the rapid inversion of the thioether sulfur.[26-31] The activation enthalpy has been obtained from Figure 5 fitted by eq 7 and listed in Table 2. It is smaller than the activation enthalpy of Re–S ligand substitution. Because $\delta\nu$ is not known, the rate constant and activation entropy for sulfur inversion cannot be determined.

## Discussion

**Mechanism of Ligand Substitution.** Reaction 2 does not occur in a single step. Indeed it cannot, because of restrictions imposed by the principle of microscopic reversibility that require a mechanism that is symmetric in the forward and reverse directions. The new donor atoms, P in one direction and thioether S in the other, enter axially and each must leave from that same site. Building on our earlier work,[32,33] we propose the mechanism given in Scheme 1.

**Scheme 1.** Competitive and reversible coordination of phosphane and thioether

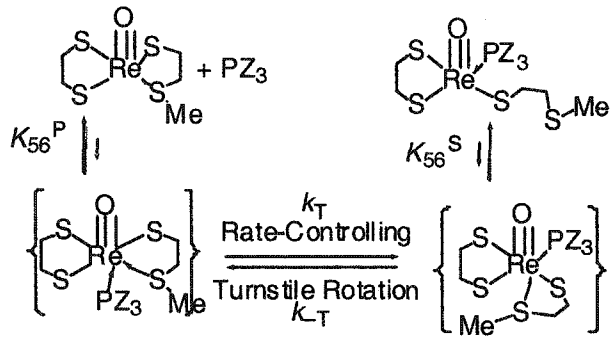

According to Scheme 1, $k_{for} = K_{56}^{P} \times k_T$ and $k_{rev} = K_{56}^{S} \times k_{-T}$. Both values of $K_{56}$ are << 1, and no six-coordinate intermediate attains a concentration that would permit its detection. Values of $k_{for}$ in the series of $P(p\text{-}XC_6H_4)_3$ reactants show relatively little variation, because $k_{for}$ includes the contribution of $K_{56}^{P}$, such that little discrimination among the $PZ_3$ reagents will be seen owning to the labile attachment of $PZ_3$ on Re. Furthermore, with $k_T$ attributed to a reaction with an early transition state, the influence of $PZ_3$ will not be great. On the contrary, significant changes in $k_{rev}$ were recorded. They simply reflect the significant extent of Re–P bond cleavage at the same transition state. As with $k_{for}$, little variation of $k_{rev}$ arises from variations in $K_{56}^{S}$

**Mechanism of Sulfur Inversion.** Two mechanisms have proposed in the literature for sulfur inversion in thioether coordinated transition metal complexes. The alternative pathways are presented in Scheme 2.[17,24-26,29,34-36] They consist of pathway **a** involving a planar intermediate or pathway **b** with a dissociation-recombination step. To date, no solid evidence determines which pathway such reactions utilize. In our study, the activation enthalpy is only 24(1) kJ $mol^{-1}$, which is much smaller than values previously reported.[36,37] Indeed, the value of $k_{rev}$ for the cleavage of Re–S bond showed an activation enthalpy that is much larger than that of sulfur inversion. Thus pathway **a** with the planar intermediate appears more likely in this case than the dissociation-recombination pathway **b**.

**Scheme 2**. Pyramidal sulfur inversion of **1**.

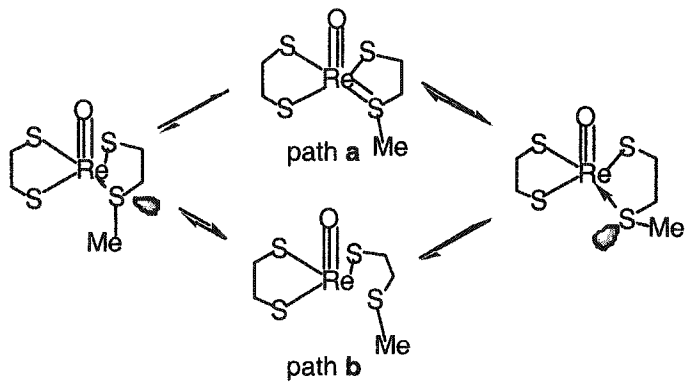

**References**

(1) Wang, Y.; Espenson, J. H. *Inorg. Chem.* **2002**, *41*, 2266-2274.

(2) Gangopadhyay, J.; Sengupta, S.; Bhattacharyya, S.; Chakraborty, I.; Chakravorty, A. *Inorg. Chem.* **2002**, *41*, 2616-2622.

(3) Arias, J.; Newlands, C. R.; Abu-Omar, M. M. *Inorg. Chem.* **2001**, *40*, 2185-2192.

(4) Bhattacharyya, S.; Chakraborty, I.; Dirghangi, B. K.; Chakravorty, A. *Inorg. Chem.* **2001**, *40*, 286-293.

(5) Bhattacharyya, S.; Chakraborty, I.; Dirghangi, B. K.; Chakravorty, A. *Chem. Commun.* **2000**, 1813-1814.

(6) Gable, K. P.; Brown, E. C. *Organometallics* **2000**, *19*, 944-946.

(7) Seymore, S. B.; Brown, S. N. *Inorg. Chem.* **2000**, *39*, 325-332.

(8) Espenson, J. H.; Shan, X.; Wang, Y.; Huang, R.; Lahti, D. W.; Dixon, J.; Lente, G.; Ellern, A.; Guzei, I. A. *Inorg. Chem.* **2002**, *41*, 2583-2591.

(9) Jacob, J.; Guzei, I. A.; Espenson, J. H. *Inorg. Chem.* **1999**, *38*, 1040-1041.

(10) Takacs, J.; Cook, M. R.; Kiprof, P.; Kuchler, J. G.; Herrmann, W. A. *Organometallics* **1991**, *10*, 316-320.

(11) Shan, X.-P.; Espenson, J. H. *Angew. Chem. Int. Ed.* **2002**, *41*, 3870-3809.

(12) Stephan, D. W.; Nadasdi, T. T. *Coord. Chem. Rev.* **1996**, *147*, 147-208.

(13) Krebs, B.; Henkel, G. *Angew. Chem.* **1991**, *103*, 785-804 (See also Angew. Chem., Int. Ed.Engl., 1991, 1930(1997), 1769-1988).

(14) Blower, P. J.; Dilworth, J. R. *Coord. Chem. Rev.* **1987**, *76*, 121-185.

(15) Sellmann, D.; Geipel, F.; Heinemann, F. W. *European Journal of Inorganic Chemistry* **2000**, 59-63.

(16) Zeltner, S.; Olk, R.-M.; Joerchel, P.; Sieler, J. *Zeitschr. Anorgan, Allgem. Chem.* **1999**, *625*, 368-373.

(17) Benson, I. B.; Knox, S. A. R.; Naish, P. J.; Welch, A. J. *J. Chem. Soc., Dalton Trans.* **1981**, 2235-2244.

(18) Mullen, G. E. D.; Blower, P. J.; Price, D. J.; Powell, A. K.; Howard, M. J.; Went, M. J. *Inorg. Chem.* **2000**, *39*, 4093-4098.

(19) Al-Jeboori, M. J.; Dilworth, J. R.; Hiller, W. *Inorg. Chim. Acta* **1999**, *285*, 76-80.

(20) Zhuang, W.-W.; Hoffman, D. M.; Lappas, D.; Cohen, J. *Polyhedron* **1998**, *17*, 2583-2586.

(21) Abel, E. W.; Kite, K.; Williams, B. L. *J. Chem. Soc., Dalton Trans.* **1983**, 1017-1018.

(22) Abel, E. W.; Moss, I.; Orrell, K. G.; Sik, V. *J. Organomet. Chem.* **1987**, *326*, 187-200.

(23) Abel, E. W.; Budgen, D. E.; Moss, I.; Orrell, K. G.; Sik, V. *J. Organomet. Chem.* **1989**, *362*, 105-115.

(24) Albeniz, A. C.; Espinet, P.; Lin, Y.-S. *Organometallics* **1996**, *15*, 5010-5017.

(25) Ascenso, J. R.; Carvalho, M. d. D.; Dias, A. R.; Romao, C. C.; Calhorda, M. J.; Veiros, L. F. *J. Organomet. Chem.* **1994**, *470*, 147-152.

(26) Evans, D. R.; Huang, M.; Seganish, W. M.; Chege, E. W.; Lam, Y.-F.; Fettinger, J. C.; Williams, T. L. *Inorg. Chem.* **2002**, *41*, 2633-2641.

(27) Abel, E. W.; Farrow, G. W.; Orrell, K. G.; Sik, V. *J. Chem. Soc., Dalton Trans.* **1977**, 42-46.

(28) Abel, E. W.; Booth, M.; Orrell, K. G. *J. Chem. Soc., Dalton Trans.* **1980**, 1582-1592.

(29) Abel, E. W.; Bhargava, S. K.; Orrell, K. G.; Sik, V. *Inorg. Chim. Acta* **1981**, *49*, 25-30.

(30) Abel, E. W.; Bhargava, S. K.; Orrell, K. G.; Platt, A. W. G.; Sik, V.; Cameron, T. S. *J. Chem. Soc., Dalton Trans.* **1985**, 345-353.

(31) Abel, E. W.; Long, N. J.; Orrell, K. G.; Osborne, A. G.; Sik, V.; Bates, P. A.; Hursthouse, M. B. *J. Organomet. Chem.* **1990**, *394*, 455-468.

(32) Espenson, J. H.; Shan, X.; Lahti, D. W.; Rockey, T. M.; Saha, B.; Ellern, A. *Inorg. Chem.* **2001**, *40*, 6717-6724.

(33) Lahti, D. W.; Espenson, J. H. *J. Amer. Chem. Soc.* **2001**, *123*, 6014-6024.

(34) Abel, E. W.; Farrow, G. W.; Orrell, K. G. *J. Chem. Soc., Dalton Trans.* **1976**, 1160-1163.

(35) Abel, E. W.; Orrell, K. G.; Poole, M. C.; Sik, V. *Polyhedron* **1999**, *18*, 1345-1353.

(36) Rivera, G.; Bernes, S.; Rodriguez de Barbarin, C.; Torrens, H. *Inorg. Chem.* **2001**, *40*, 5575-5580.

(37) Abel, E. W.; Booth, M.; Orrell, K. G.; Pring, G. M. *J. Chem. Soc., Dalton Trans.* **1981**, 1944-1950.

**Supporting Information**

Table S-1. $W_{1/2}$ of the resonance peak at 1.94 ppm for $CH_3$ of **1** and 7.00 ppm for $CH_3$ of toluene.

Figure S-1. Plot of $k_{□}$ vs [$PPh_3$] at 15-40 °C.

Figure S-2. Plot of $k_{□}$ vs [$CyPh_2P$] and [$Cy_2PhP$] at 25 °C.

Figure S-3. Plot of $k_{□}$ vs [$MePh_2P$] at 25 °C.

Figure S-2. Plot of $k_{□}$ vs [(4-X-$C_6H_4$)$_3$P] at 25 °C. X = F, H, Me, MeO.

Table S-1. $W_{1/2}$ of the resonance peak at 1.94 ppm for $CH_3$ of **1** and 7.00 ppm for $CH_3$ of toluene.

| T (K) | $W_{1/2}$ (Hz) at 1.94 ppm | $W_{1/2}$ (Hz) at 7.00 ppm |
|---|---|---|
| 298 | 1.57 | 3.34 |
| 288 | 1.95 | 3.32 |
| 278 | 2.03 | 3.33 |
| 268 | 2.51 | 3.29 |
| 258 | 3.54 | 3.28 |
| 248 | 5.50 | 3.27 |
| 238 | 8.48 | 3.35 |
| 233.7 | 9.20 | 3.93 |

Figure S-1. Plot of $k_e$ vs [$PPh_3$] at 15-40 °C

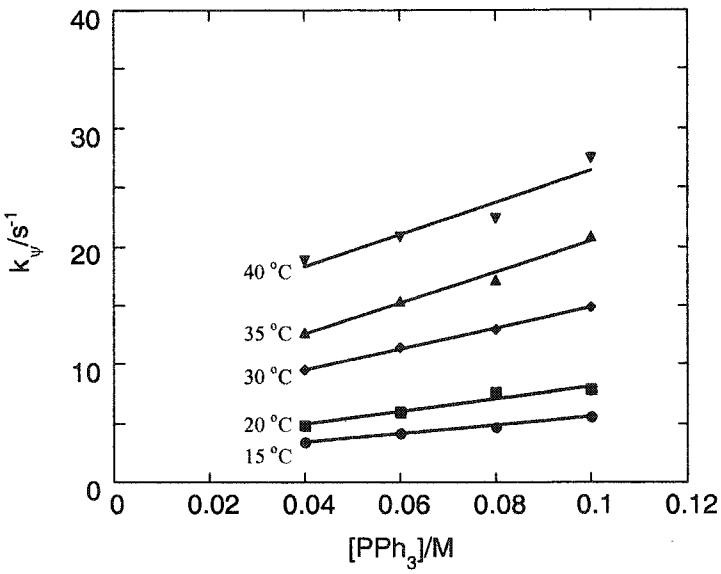


Figure S-2. Plot of $k_{obs.}$ vs [$CyPh_2P$] and [$Cy_2PhP$] at 25 °C.

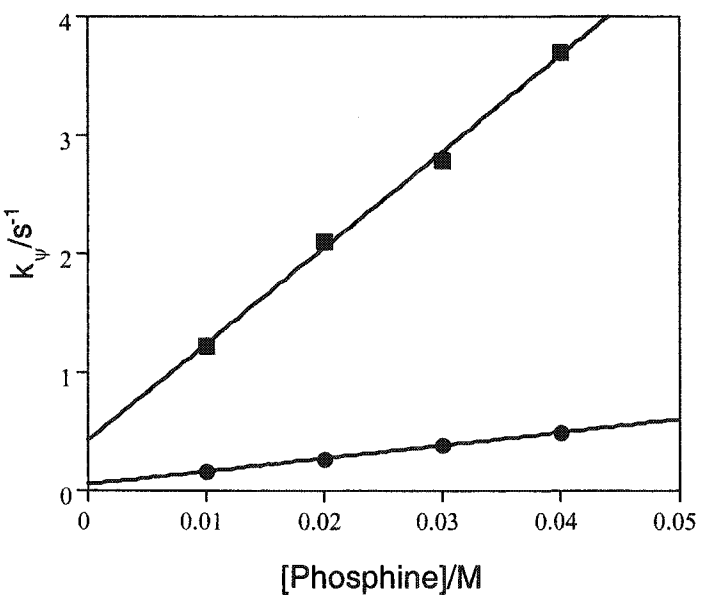

Figure S-3. Plot of $k_{obs.}$ vs [$MePh_2P$] at 25 °C.

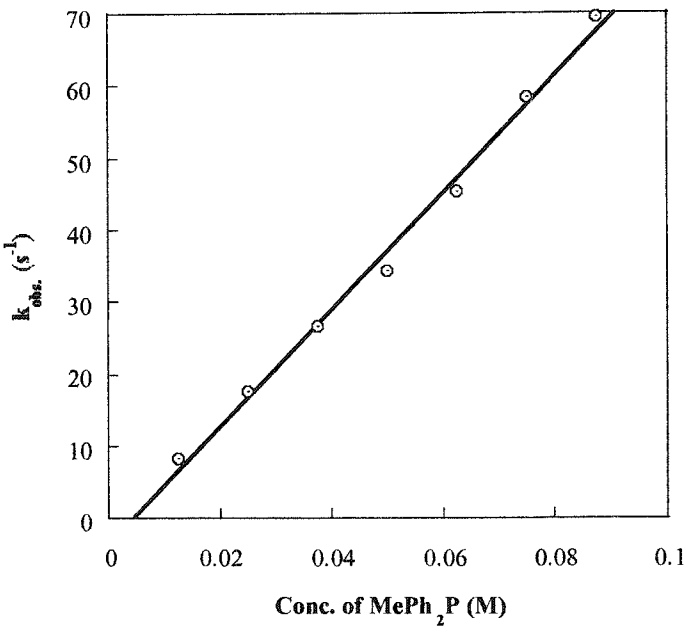


Figure S-4. Plot of $k_{obs.}$ vs [$(4\text{-X-}C_6H_4)_3P$] at 25 °C. X = F, H, Me, MeO.

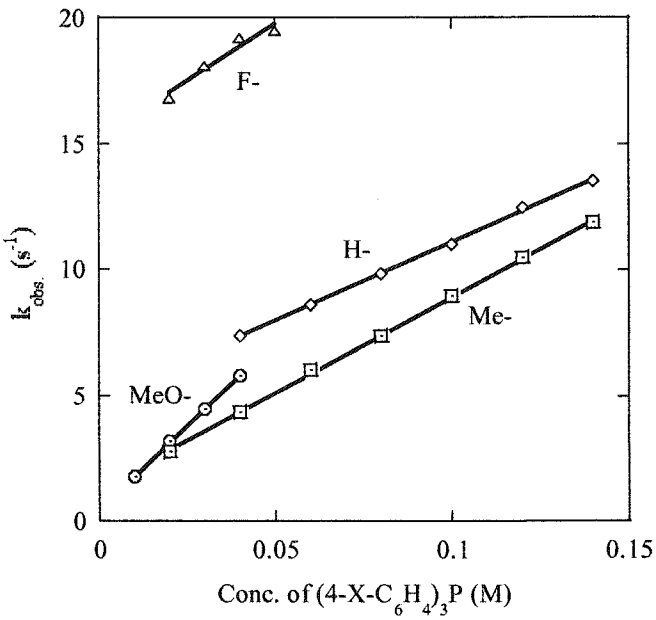

# CHAPTER VI. SYNTHESES AND OXIDATION OF METHYLOXORHENIUM(V) COMPLEXES WITH TRIDENTATE LIGANDS

A manuscript submitted to *Inorganic Chemistry*

Xiaopeng Shan, Arkady Ellern, Ilia A. Guzei, James H. Espenson

**Abstract**

Four new methyloxorhenium(V) compounds were synthesized with these tridentate chelating ligands: 2-mercaptoethyl sulfide (abbreviated HSSSH), 2-mercaptoethyl ether (HSOSH), thioldiglycolic acid (HOSOH) and 2-(salicylideneamino)benzoic acid (HONOH). Their reactions with $MeReO_3$ under suitable conditions led to these products: MeReO(SSS), **1**, MeReO(SOS), **2**, MeReO(OSO)($PAr_3$), **3** and MeReO(ONO)($PPh_3$), **4**. These compounds were characterized spectroscopically and crystallographically. Compounds **1** and **2** have a five-coordinate distorted square pyramidal geometry about rhenium, whereas **3** and **4** are six-coordinate compounds with distorted octahedral structures. The kinetics of oxidation of **2** and **3** in chloroform with pyridine N-oxides follow different patterns. The oxidation of **2** shows first-order dependences on the concentrations of **2** and the ring-substituted pyridine N-oxide. The Hammett analysis of the rate constants gives a remarkably large and negative reaction constant, $\rho = -4.6$. The rate of oxidation of **3** does not depend on the concentration or the identity of the pyridine N-oxide, but it is directly proportional to the concentration of water, both an accidental and then a deliberate co-solvent. The mechanistic differences have been interpreted as reflecting the different steric demands of five and six coordinate rhenium compounds.

## Introduction

The oxidation of rhenium(V) complexes to rhenium(VII)[1] is an essential step in the catalytic cycle by which such a pair catalyzes oxygen atom transfer reactions.[2-10] Steric demand is always an important issue for such catalysts.[11-13] Different ligands for rhenium(V) complexes have been employed, especially those with "3+1" [14-16], "3+2"[17,18] and "3+1+1"[19,20] coordination shells. They differ in geometry as well as coordination number.

In this paper, we describe the syntheses of four new rhenium(V) compounds with tridentate ligands, the molecular structures of which are displayed in Chart 1. The oxidation of three of these compounds was investigated. Compound **4** was not studied because of its insolubility.

**Chart 1**

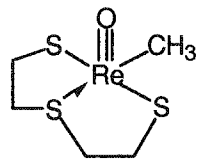


MeReO(SSS) **1**

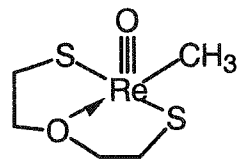


MeReO(SOS) **2**

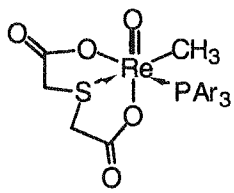


MeReO(OSO)PAr$_3$ **3**

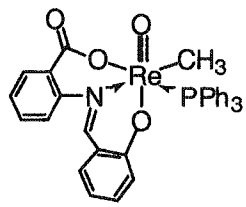


MeReO(ONO)PPh$_3$ **4**

**Experimental Section**

**Materials and Instrumentation.** Methyltrioxorhenium(VII), $CH_3ReO_3$ or MTO, was prepared from sodium perrhenate, tetramethyl tin and chlorotrimethylsilane.[21] The di(benzenethiolato)-methyl-oxorhenium(V) dimer, $\{MeReO(bt)_2\}_2$, was synthesized from MTO and benzenethiol, btH.[22] The tridentate ligand, 2-(salicylideneamino)benzoic acid (abbreviated HONOH) was synthesized from salicylaldehyde and 2-aminobenzoic acid.[23] Other ligands, the abbreviations of which follow from their chemical names: 2-mercaptoethyl sulfide (HSSSH), 2-mercaptoethyl ether (HSOSH), thioldiglycolic acid (HOSOH) and chemicals were purchased from Aldrich and used as received. $D_6$-benzene and $D_1$-chloroform were employed as solvents for NMR spectroscopy. ACS grade chloroform was used as the solvent for UV-visible measurements.

A Bruker DRX-400 spectrometer was used to record the $^1H$, $^{13}C$ and $^{31}P$ spectra. The chemical shift for $^1H$ was defined relative to that of the residual proton of the solvent, $\delta$ 7.16 for benzene and $\delta$ 7.27 for chloroform. Shimadzu UV 3101PC and 2502PC

spectrophotometers were used to record UV-visible spectra and monitor the reaction kinetics. Infrared spectra were determined with a Nicolet-500 spectrometer. Elemental analyses were performed by Desert Analytics Laboratory.

**Syntheses of 1** and **2**. These compounds were prepared from $\{MeReO(bt)_2\}_2$ (87 mg, 0.1 mmol) and the tridentate ligand (0.2 mmol) in 20 mL of toluene. After stirring the mixture for 4 hours, 20 mL of hexanes was layered on the top of the solution and the mixture placed in a freezer at ca. –12 °C. After 24 h a dark red powder had deposited; it was filtered and rinsed with hexanes. A crystal suitable for x-ray diffraction analysis was obtained by recrystallization from methylene chloride-hexanes. The acidic form of tridentate ligand can be abbreviated as HXYXH, thus the general chemical equation for these syntheses is

$$\{MeReO(bt)_2\}_2 + 2\ HXYXH \rightarrow 2\ MeReO(XYX) + 4\ btH \qquad (1)$$

**1** was obtained in 84% yield. NMR ($D_6$-benzene) $^1H$: δ 3.55 (s, 3H), 3.28 (m, 2H), 2.42 (m, 2H), 2.25 (m, 2H), 0.56 (m, 2H); $^{13}C$: 48.0, 43.5, 5.1. IR ($CHCl_3$): 984 $cm^{-1}$. UV-Vis ($CHCl_3$), $\lambda_{max}$/nm (log ε/L $mol^{-1}$ $cm^{-1}$): 252 (4.04) and 360 (sh). Elemental Analysis: $C_5H_{11}OReS_3$, Found (Calcd.) C: 16.36 (16.25), H: 2.82 (3.00), S: 26.15 (26.03).

**2** was obtained in 66% yield. NMR ($D_6$-benzene) $^1H$: δ 4.42 (s, 3H), 3.00 (m, 2H), 2.57 (m, 2H), 2.49 (m, 2H), 2.20 (m, 2H); $^{13}C$: 85.1, 40.2, 4.0. IR ($CHCl_3$): 997 $cm^{-1}$. UV-Vis ($CHCl_3$), $\lambda_{max}$/nm: 290 (sh). Elemental Analysis: $C_5H_{11}O_2ReS_2$, Found (Calcd.) C: 18.25 (16.99), H: 2.96 (3.14), S: 17.94 (18.14).

**Syntheses of 3** and **4.** These compounds were prepared from MTO (250 mg, 1 mmol), the tridentate ligand (1 mmol) and 2 mmol of triphenylphosphane for **4** or the desired triarylphosphane for **3** in 20 mL of $CH_2Cl_2$. After stirring the mixture for 10 h, 20 mL of hexanes was layered on the top of the solution and the mixture placed in a freezer at ca. –12 °C. After 24 h a blue (**3**) powder or dark red (**4**) crystal had deposited. Each substance was filtered and rinsed by hexanes. The crystal of **4** directly from the synthesis was suitable for x-ray diffraction analysis. Recrystallization of **3** from methylene chloride-hexanes was needed to obtain diffraction-quality crystals. When the acidic form of the ligand is abbreviated HXYXH, the general chemical equation for the syntheses is

$$MeReO_3 + HXYXH + PAr_3 \rightarrow MeReO(XYX) + H_2O + OPAr_3 \qquad (2)$$

**3**–$PPh_3$ was obtained in 93% yield. NMR ($D_1$-chloroform) $^1H$: δ 7.47~7.70 (m, 15H), 4.58 (d, 3H), 3.61 (d, 1H), 3.36 (d, 1H), 2.89 (d, 1H), 1.38 (d, 1H); $^{13}C$: 185.7, 177.8, 134.1 (d), 132.1 (d), 131.5 (d), 129.2 (d), 128.6 (d), 37.9, 36.6, 15.4; $^{31}P$: 0.45. IR ($CHCl_3$): 1007 $cm^{-1}$. UV-Vis ($CHCl_3$), $\lambda_{max}$/nm: 265 (sh) and 300 (sh). Elemental Analysis: $C_{23}H_{22}O_5PReS$: Found (Calcd.) C: 43.97 (44.01), H: 3.51 (3.53), S: 4.66 (5.11), P: 4.30 (4.93). **3**–OMe was synthesized from tris(4-methoxyphenyl)phosphane in 87% yield. NMR ($D_1$-chloroform) $^1H$: δ 7.42~7.47 (m, 6H), 7.00~7.03 (m, 6H), 4.58 (d, 3H), 3.87 (s, 9H), 3.62 (d, 1H), 3.37 (d, 1H), 2.94 (d, 1H), 1.54 (d, 1H); $^{13}C$: 185.8, 178.0, 135.6 (d), 134.0 (d), 123.0 (d), 114.7 (d), 114.2 (d), 55.5, 38.2, 36.7, 15.4; $^{31}P$: –2.75. IR ($CHCl_3$): 1007 $cm^{-1}$. UV-Vis ($CHCl_3$), $\lambda_{max}$/nm: 350 (sh). **3**–F was synthesized from tris(4-fluorophenyl)phosphane in 88% yield. NMR ($D_1$-chloroform) $^1H$: δ 7.50~7.57 (m, 6H), 7.18~7.28 (m, 6H), 4.51 (d, 3H), 3.64 (d, 1H), 3.43 (d, 1H), 3.02 (d, 1H), 1.63 (d, 1H); $^{13}C$: 185.4, 177.9, 164.2 (q), 136.4 (q), 117.0 (m), 378.0, 36.4, 15.7; $^{31}P$: δ –0.86. IR ($CHCl_3$): 1007 $cm^{-1}$. UV-Vis ($CHCl_3$), $\lambda_{max}$/nm: 300 (sh).

**4** was obtained in 93% yield. NMR ($D_2$-methylene chloride) $^1H$: δ 8.01 (m, 1H), 7.65 (s, 1H), 7.57 (m, 1H), 7.48 (m, 1H), 7.29 (d, 1H), 7.03 (m, 1H), 6.78 (m, 2H), 6.56 (d, 1H) 4.40 (d, 3H); $^{13}C$:too insoluble; $^{31}P$: –7.18. IR ($CHCl_3$): 984 $cm^{-1}$. UV-Vis ($CHCl_3$), $\lambda_{max}$/nm: 300 (sh), 360 (sh) and 420 (sh). Elemental Analysis: $C_{33}H_{27}NO_4PRe$: Found (Calcd.) C: 53.83 (55.15), H: 3.59 (3.79), N: 1.85 (1.95), P: 4.02 (4.31).

**X-ray Structure Determination.** The crystal evaluation and data collection were performed on a Bruker CCD-1000 diffractometer with Mo $K_\alpha$ ($\lambda$ = 0.71073 Å) radiation, graphite monochromator and a detector-to-crystal distance of 5.04 cm. All crystals were stable at ambient conditions, therefore routine procedures were used for mounting and centering of the samples. The data were collected by using the hemisphere (**1**, **2**) and full sphere (**3**, **4**) routines for better redundancy. Data sets were corrected for Lorentz and polarization effects. The multi-scan absorption correction was based on fitting a function to the empirical transmission surface as sampled by multiple equivalent measurements using SADABS[24] software.

The positions of the most of atoms were found by direct (**1**, **2**) or Patterson (**3**, **4**) methods. The remaining non-hydrogen atoms were located in an alternating series of least-squares

cycles on difference Fourier maps and were refined in full-matrix anisotropic approximation. All hydrogen atoms were placed in the structure factor calculation at idealized positions and were allowed to ride on the neighboring atoms with relative isotropic displacement coefficients. The calculations were performed with SHELXTL software package.[24]

**Kinetics.** Reactions of compound **2** with pyridine N-oxides were monitored by the decrease in absorbance of **2** at 525 nm. Concentrations of pyridine N-oxides were at least ten times higher than that of **2**, allowing the absorbance–time data to be fitted to pseudo-first-order kinetics,

$$Abs_t = Abs_\infty + (Abs_0 - Abs_\infty) \times \exp(-k_\psi t) \quad (3)$$

Reactions of compounds **3**–$PPh_3$, **3**–OMe and **3**–F with pyridine N-oxides was carried out in the presence of the nucleophiles water, $Cl^-$ or methanol. Reactions were monitored by the changes in absorbance at 604, 367 and 350 nm according to the reagent used. The concentrations of the nucleophiles were at least 10-fold higher than that of **3**–L, allowing the absorbance-time data to be fitted to pseudo-first-order kinetics, according to eq 3. The stoichiometric reaction is

$$MeReO(OSO)(PAr_3) + 2PyO + H_2O \rightarrow MTO + Ar_3PO + HOSOH + 2Py \quad (4)$$

## Results

**Structures.** Table 1 shows the crystallographic parameters for the four new oxorhenium(V) compounds and Figure 1 depicts their molecular structures.

**Table 1**. Crystallographic data for compounds **1**, **2**, **3** and **4**.

| | **1** | **2** | **3**–$PPh_3$ | **4** |
|---|---|---|---|---|
| Color | Dark red | Dark red | Blue | Dark red |
| chemical formula | $C_5H_{11}ORES_3$ | $C_5H_{11}O_2ReS_2$ | $C_{23}H_{22}O_5PReS$ | $C_{33}H_{27}NO_4PRe$ |
| unit cell dimensions | | | | |
| a, Å | 8.9289(6) | 7.8318(5) | 21.682(8) | 11.7111(15) |
| b, Å | 8.9178(6) | 10.4827(6) | 10.833(4) | 13.6521(16) |
| c, Å | 11.8518(7) | 10.9106(6) | 19.248(7) | 17.873(2) |
| β, deg | 90 | 90.2451(10) | 94.396(6) | 100.867(2) |
| volume, Å | 943.71(11) | 895.73(9) | 4508(3) | 2806.3(6) |
| Z | 4 | 4 | 8 | 4 |
| formula wt | 369.52 | 353.46 | 627.64 | 718.73 |
| space group | $Cmc2_1$ | $P2_1/n$ | C2/c | $P2_1/n$ |
| temp, K | 173(2) | 173(2) | 173(2) | 298(2) |
| wavelength, Å | 0.71073 | 0.71073 | 0.71073 | 0.71073 |
| density (calcd), $Mg/m^3$ | 2.601 | 2.621 | 1.850 | 1.701 |
| abs coeff, $mm^{-1}$ | 13.476 | 13.974 | 5.587 | 4.427 |
| R indices (all data)[a] | R1 = 0.0219 wR2 = 0.0573 | R1 = 0.0325 wR2 = 0.0799 | R1 = 0.0499 wR2 = 0.0881 | R1 = 0.0349 wR2 = 0.0814 |
| final R indices [$I > 2\sigma(I)$][a] | R1 = 0.0215 wR2 = 0.0570 | R1 = 0.0304 wR2 = 0.0788 | R1 = 0.0408 wR2 = 0.0861 | R1 = 0.0279 wR2 = 0.0757 |

[a] $R1 = \Sigma \mid |F_0|-|F_c| \mid / \Sigma |F_0|$; $wR2 = \{ \Sigma [ w(F_o^2-F_c^2)^2 ] / \Sigma [ w(F_0^2)^2 ] \}^{1/2}$.

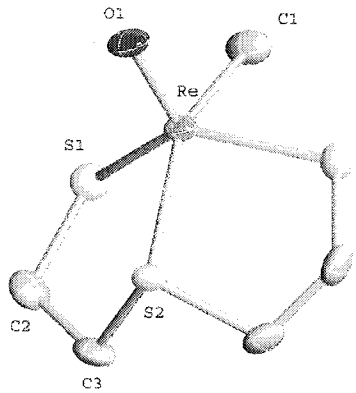


**1**

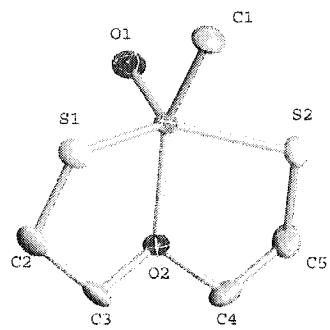


**2**

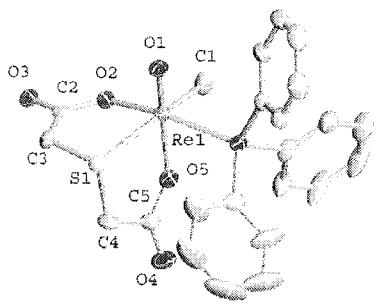


**3**

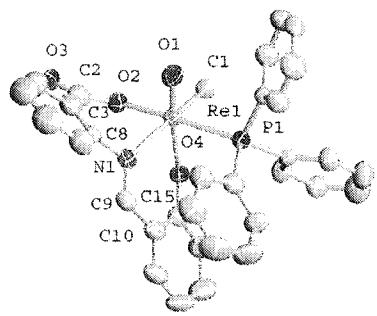


**4**

**Figure 1**. Crystallographically-determined structures of **1-4**.

Table 2 lists the important bond distances and angles of **1** and **2**. In both compounds, the rhenium atom lies at the center of a distorted square-pyramid defined by its axial ligand, the terminal oxo group, and the equatorial plane occupied by the methyl group and three donor atoms of the tridentate ligand. The Re≡O distances are almost identical at 168 pm and the Re–C bond distances are in the range 212–216 pm. The only difference between the two is that **1** has a thioether sulfur donor and **2** an ether oxygen. It is notable that the C–O–Re angle is 122° around the ether oxygen atom of **2** is closer to 120° than the 108° C–S–Re angle around the thioether sulfur of **1**. It seems that the longer d(Re–S) of 234 pm, versus d(Re–O) 209 pm, allows greater flexibility in the five-membered rings of **1**.

**Table 2**. Selected Bond Lengths (pm) and Angles (°) of **1** and **2**.

| | **1** | **2** |
|---|---|---|
| Re-O(1) | 168.9(4) | 167.4(5) |
| Re-C(1) | 216.3(6) | 211.8(7) |
| Re-S(1) | 228.46(10) | 227.69(18) |
| Re-S(2) or Re-O(2) | 233.86(19) | 209.4(4) |
| Re-S(1a) or Re-S(2) | 228.46(10) | 227.55(17) |

| | **1** | **2** |
|---|---|---|
| O(1)-Re-C(1) | 103.6(2) | 101.3(3) |
| O(1)-Re-S(1) | 115.45(4) | 112.33(19) |
| O(1)–Re–S(2) | NA | 112.00(19) |
| O(1)-Re-S(2) or O(1)-Re-O(2) | 109.34(14) | 116.1(2) |
| C(3)-S(2)-C(3a) or C(3)-O(2)-C(4) | 101.9(3) | 109.6(5) |
| C(3)-S(2)-Re or C(3)-O(2)-Re | 108.02(4) | 122.3(4) |
| S(1)-Re-S(1a) or S(1)-Re-S(2) | 128.75(7) | 135.67(7) |
| C(1)-Re-S(2) or C(1)-Re-O(2) | 147.10(18) | 142.6(2) |

Table 3 summarizes the important bond distances and angles of **3** and **4**. In both compounds, the rhenium atom lies the center of a distorted octahedron defined by its axial

ligands, the terminal oxo group and one oxygen donor atom of the tridentate ligands, OSO and ONO. The Re≡O and Re–C distances are virtually identical in the two at 168 and 213 pm. The thioether Re–S distance in **3** is 19 pm longer than that in **1**, whereas the Re–N bond distance in **4**, 216 pm, lies in the normal range of Re–N single bonds, 211-220 pm.[25-27] The donor atoms trans to the terminal oxo groups in **3** and **4** do not lie notably closer or farther away from rhenium than do their counterparts in the equatorial plane. This is surprising because in other six-coordinate oxorhenium(V) compounds, the group trans to Re≡O lies at a longer distance.[25,28] Perhaps the structures of **3** and **4** reflect P–Re π back-bonding. In support of that we note that the $^{31}P$ chemical shifts of **3**–$PPh_3$ (δ 0.45) and **4** (–7.2) lie near that of free $PPh_3$ (–4.4 ppm) whereas in other cases they are usually well downfield, MeReO(ethanedithiolate)$PPh_3$ (δ –31.6 ppm) being typical.

**Table 3**. Selected Bond Lengths (pm) and Angles (°) of **3** and **4**.

| | **3** | **4** |
|---|---|---|
| Re-O(1) | 167.4(4) | 168.1(3) |
| Re-C(1) | 212.9(6) | 213.8(4) |
| Re-P | 244.69(15) | 247.25(14) |
| Re-S or Re-N | 253.37(16) | 216.5(4) |
| Re-O(2) | 203.3(4) | 205.7(4) |
| Re-O(4) | 203.9(4) | 201.9(3) |

| | 3 | 4 |
|---|---|---|
| O(1)-Re-C(1) | 103.1(2) | 98.98(16) |
| O(1)-Re-S or N | 93.92(15) | 98.78(14) |
| O(1)-Re-P | 92.18(14) | 86.58(11) |
| O(1)-Re-O(2) | 102.32(18) | 98.38(13) |
| O(1)-Re-O(4) | 165.76(18) | 169.17(15) |
| C(3)-S-Re or C(8)-N-Re | 95.66(19) | 112.2(3) |
| C(4)-S-Re or C(9)-N-Re | 100.5(2) | 129.7(3) |
| C(3)-S-C(4) or C(8)-N-C(9) | 103.0(3) | 118.1(4) |
| P-Re-O(2) | 164.43(11) | 174.56(8) |

**Oxidation of 1**. Compound **1** is least reactive rhenium(V) compound that we have dealt with. For example, **1** is not oxidized by sulfoxides, pyridine N-oxides or alkyl hydroperoxides. The decomposition of **1** with $H_2O_2$ is self-catalyzed owing to the generation of MTO, a well-known catalyst for the oxidation of organic or inorganic substrates by hydrogen peroxide.[29-32] The oxidation products are MTO and the cyclic disulfide, which were identified by NMR spectroscopy,

$$1 + 2H_2O_2 \xrightarrow{MTO} MTO + S(CH_2CH_2S)_2 + 2H_2O \quad (5)$$

**Oxidation of 2**. Compound **2** is readily oxidized by sulfoxides and pyridine N-oxides to MTO and the cyclic disulfide, eq 6.

$$MeReO(SOS) + 2PyO / R_2SO \rightarrow MTO + O(CH_2CH_2S)_2 + 2Py / R_2S \quad (6)$$

Kinetic studies of the oxidation of **2** with pyridine N-oxides were carried out at 25 °C in chloroform. Figure 2 depicts the pseudo-first-order rate constants against the concentration of pyridine N-oxide and its aromatic ring-substituted derivatives. The data form straight lines that pass through the origin. Thus the rate equation is

$$-\frac{d[\mathbf{2}]}{dt} = k[\mathbf{2}] \cdot [X - C_5H_4NO] \quad (7)$$

The second-order rate constants are listed in Table 4. 4-Methoxypyridine N-oxide, with the most electron-donating substituent, is the most reactive, with $k = (4.82 \pm 0.07) \times 10^{-2}$ L mol$^{-1}$

$s^{-1}$. An analysis of the rate constants by the Hammett equation is presented in Figure 3; it gives a remarkably large and negative reaction constant, $\rho = -4.6$. This suggests a multi-step reaction sequence.[9] The reaction rate was not changed by the deliberate addition of water or methanol.

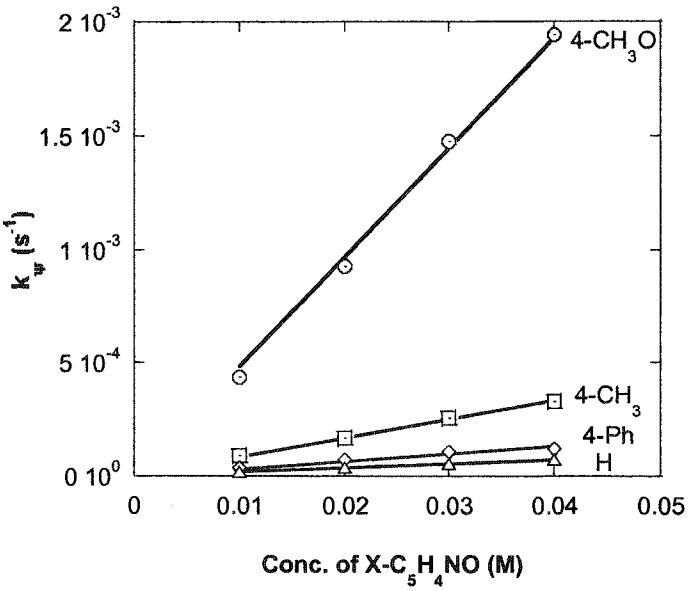


**Figure 2.** Plots of the pseudo-first-order rate constants for the reactions of **2** against the concentrations of pyridine N-oxides. The reaction was studied in $CHCl_3$ at 25 °C.

**Table 4**. Rate Constants for the Oxidation of **2** by Ring-Substituted Pyridine N-Oxides.

| $X\text{-}C_5H_4N$ | $k_{PyO}/10^{-3}$ L $mol^{-1}$ $s^{-1}$ |
|---|---|
| 4-MeO | 48.2(7) |
| 4-Me | 8.4(1) |
| 3-Me | 4.8(1) |
| 4-Ph | 3.3(2) |
| H | 1.84(3) |

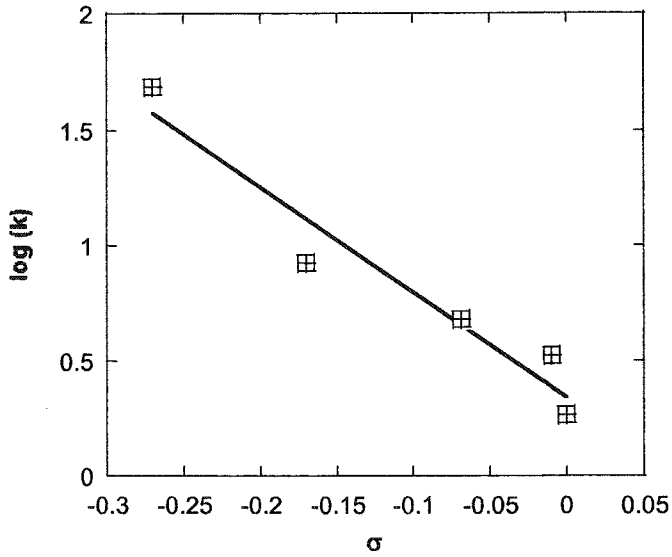


**Figure 3**. Analysis of the rate constants for the oxidation of **2** by Pyridine N-oxide by the Hammett equation.

**Oxidation of 3**. Compound **3**–$PPh_3$ and its $PAr_3$ ring-substituted derivatives are oxidized to MTO, phosphane oxide and thioldiglycolic acid, as in eq 4, by pyridine N-oxides in chloroform in the presence of water.

These reactions show first-order dependences on [$H_2O$] and [**3**]. Figure 4 depicts the pseudo-first-order rate constants for the three derivatives of **3** against the concentration of water and the second-order rate constants are listed in Table 5.

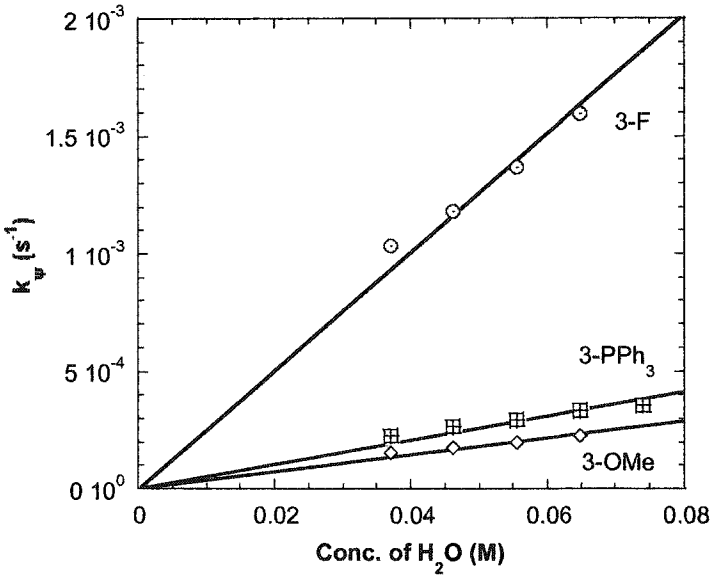


**Figure 4.** Plots of the pseudo-first-order rate constants for the reactions of the three derivatives of **3** against the concentration of water. The reaction was studied in $CHCl_3$ at 25.0 °C.

**Table 5.** Rate constants for the oxidation of **3** and its derivatives with ring-substituted triphenylphosphanes by 4-picoline N-oxide at presence of nucleophiles.

| Reactant | Lewis Base | $k/10^{-3}$ L $mol^{-1}$ $s^{-1}$ |
|---|---|---|
| **3**–$PPh_3$ | $H_2O$ | 3.9(1) |
| **3**–$PPh_3$ | $D_2O$ | 3.6(2) |
| **3**–$PPh_3$ | $CH_3OH$ | 0.88(5) |
| **3**–$PPh_3$ | $Bu_4N^+Cl^-$ | 0.75(1) |
| **3**–OMe | $H_2O$ | 2.59(9) |
| **3**–F | $H_2O$ | 20(1) |

Varying the concentration of 4-picoline N-oxide from 20 mM to 40 mM gave the same rate constant, $(3.9 \pm 0.1) \times 10^{-3}$ (20 mM 4-PicO) and $(4.0 \pm 0.1) \times 10^{-3}$ L $mol^{-1}$ $s^{-1}$ (40 mM

4-PicO). Different pyridine N-oxides also gave the same value of rate constant: $(3.9 \pm 0.1) \times 10^{-3}$ (20 mM 4-PicO) and $(4.0 \pm 0.1) \times 10^{-3}$ L mol$^{-1}$ s$^{-1}$ (20 mM 4-Ph-$C_5H_4NO$).

The substituents on the aromatic ring of $PAr_3$ coordinated to rhenium in compound **3** show considerable effect. Second-order rate constant of **3**–F, with the most electron withdrawing substituent, is almost 10 fold bigger than that of **3**–OMe, containing the most electron-donating substituent.

Deuterated water was employed to check for a kinetic isotope effect. It gave the same value of rate constant: $(3.9 \pm 0.1) \times 10^{-3}$ ($H_2O$) and $(3.6 \pm 0.2) \times 10^{-3}$ L mol$^{-1}$ s$^{-1}$ ($D_2O$). Also other nucleophiles, $Cl^-$ and methanol, were found to accelerate the oxidation of **3** with 4-picoline N-oxides. The reactions show first-order dependences on the concentrations of the nucleophile and **3**. Figure 5 depicts the pseudo-first-order rate constants against the concentration of nucleophiles; the rate constants are listed in Table 5.

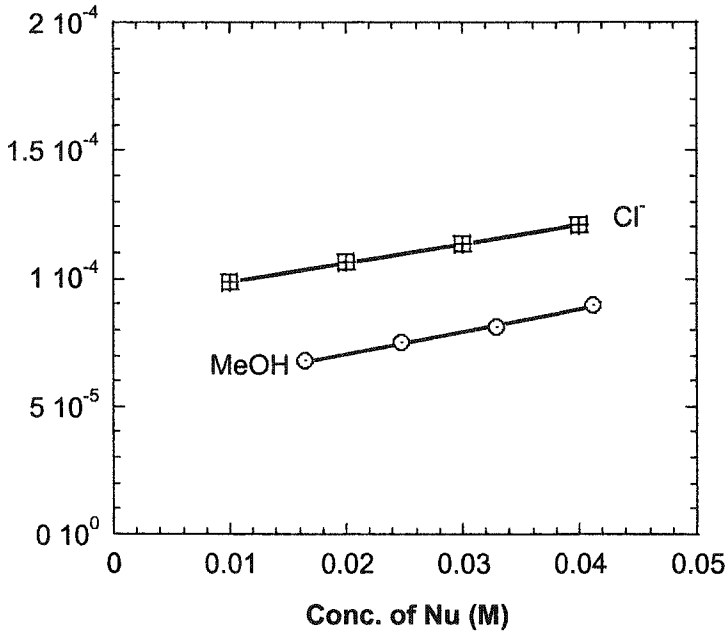


**Figure 5.** The effect of other nucleophiles, $Cl^-$ and MeOH, on the oxidation of **3** is proportional to [Nu] in $CHCl_3$ at 25 °C. The intercepts reflect the effect of the residual water in the solutions.

## Discussion

**Mechanism of the Oxidation of 2.** Scheme 1 shows the proposed mechanism for oxidation of **2**. No doubt, coordination of pyridine N-oxides to rhenium is the first step of oxidation of **2**, since there is an empty position trans to terminal oxo group.

**Scheme 1**. Direct Oxidation of **2** by Pyridine N-Oxide

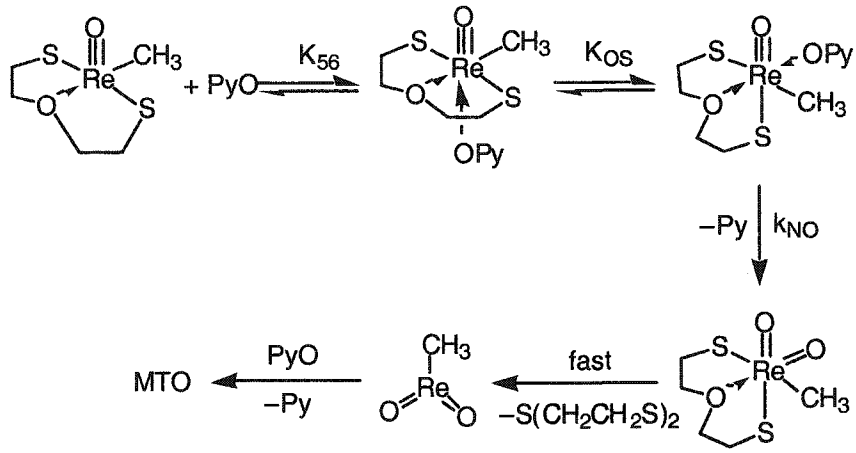


The reaction begins with the coordination of PyO at the vacant coordination site on **2**. This particular reaction cannot be evaluated, owing to the subsequent reactions that ensue. But with different ligands that do not react further, some definite statements can be made. With monodentate ligands, even those that might be anticipated to have large values of $K_{56}$, a six-coordinate complex never builds up to a detectable level. Only with a bidentate ligand such as 2,2'-bipyridine, where the chelate effect dominates, does a six-coordinate species form to a measurable extent. On that basis, it appears that the equilibrium constant in Scheme 1 is $K_{56} << 1$. In other words, the enthalpy gain from the formation of a Re–O bond is minimal. According to our earlier work, the PyO enters the equatorial plane by way of a turnstile rotation mechanism.[33] The driving force for the isomerization is to avoid, after the Py–O bond cleavage, formation of a *trans*-dioxorhenium(VII) intermediate, which would lie at a much higher energy for a $d^0$ species than would the *cis* isomer.[34,35] Unlike previous work on oxidation of rhenium compounds containing a dithiolate ligand,[9] all of intermediates are six-coordinate without further addition of another molecule of pyridine N-oxide because of the chelating tridentate ligands.

Because a thiolate sulfur is more strongly bound to rhenium than an oxygen atom donor, $K_{OS} << 1$. Clearly the cleavage of the N–O bond is the rate-controlling step. The dramatic electronic effect of the substituents on the pyridine N-oxides comes from the combined term represented by the experimental $k = K_{56}K_{OS}k_{NO}$. Each of the three components of k can be expected on the basis of the chemistry at that step to contribute a negative value to the overall value of the reaction constant: $\rho_k = \rho_{56} + \rho_{OS} + \rho_{NO}$. The steps following the rate-controlling step were proposed without further experimental evidence explicit to this case; they are, however, consistent with the known chemistry of these compounds which, at the Re(VII) stage, oxidize dithiolates to disulfides.[1,36]

Scheme 1 is also suitable for the oxidation of **1**, and its lower reactivity with pyridine N-oxides must come from smaller values of $K_{OS}$ and $k_{NO}$ caused by the trans effect from thioether sulfur, a better electron donor than the ether oxygen of **2**.

**Mechanism of the Oxidation of 3.** The kinetics of oxidation of **3** shows first-order dependences on [**3**] and [$H_2O$], but the rate is independent of [PyO]. Pyridine N-oxide is, however, required to complete the stoichiometric transformation. Once the involvement of water was suspected, this was checked by its deliberate addition at known levels. Because there is no H-D kinetic isotope effect, it is not likely that $H_2O$ or $D_2O$ attacks directly at a carboxylato oxygen. We propose that attack is instead at rhenium, accompanying which the Re–S bond to the thioether is broken. Formation of an initial Re–$OH_2$ bond not only assists in ligand hydrolysis, but also advances the formation of one of the new Re=O bonds that must appear in the product. The rate constants for $H_2O$ attack lie in the order **3**-F > **3**-$PPh_3$ > **3**-OMe, as one would expect for a mechanism involving initial nucleophilic attack at rhenium.

This formulation suggests that nucleophiles other than $H_2O$ should be able to carry out the first, non-hydrolytic step. That indeed proved so, and both $Cl^-$ and MeOH reacted in a catalytic fashion and were not transformed during the reaction. The rate law in these cases was k[**3**][Nu]. With these nucleophiles as well, the rate is not dependent on [PyO].

Scheme 2 shows the sequence of proposed reactions. Because the rates are independent of [$H_2O$], it must enter later, and so it is reasonable to interpret the data in terms of nucleophilic attack as being rate-controlling.

**Scheme 2.** Nucleophile-Induced Pathway for the Oxidation of **3** by PyO

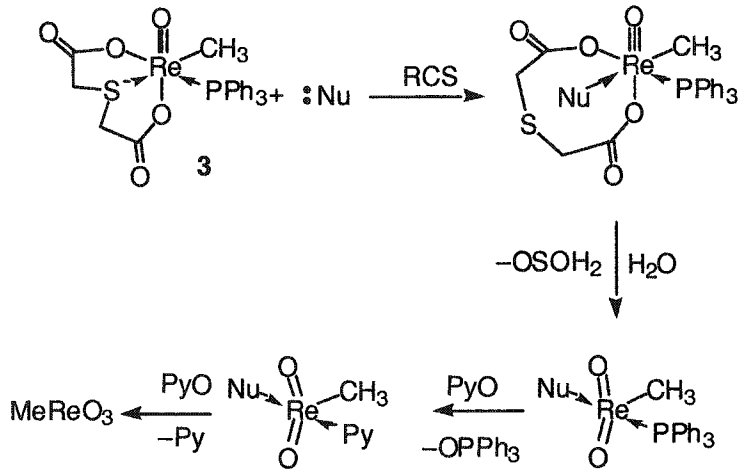


**Steric Influences.** The different pathways adopted for the oxidation of **2** and **3** can be traced to their different coordination numbers, which creates a higher steric demand for **3**. This can be seen from second-order rate constants (L $mol^{-1}$ $s^{-1}$) of oxidation of **3** with presence of different nucleophiles, $(3.9 \pm 0.1) \times 10^{-3}$ ($H_2O$), $(0.88 \pm 0.05) \times 10^{-3}$ (MeOH) and $(0.75 \pm 0.01) \times 10^{-3}$ ($Cl^-$). Both MeOH and $Cl^-$ are stronger nucleophiles than water, but the reaction with water is 4-5 times faster. The steric demands of MeOH (195 pm van der Waals radius)[37] and $Cl^-$ (180 pm ionic radius) exceed that of water (140 pm van der Waals radius).[38]

**References**

(1) Lente, G.; Espenson, J. H. *Inorg. Chem.* **2000**, *39*, 4809-4814.

(2) Arias, J.; Newlands, C. R.; Abu-Omar, M. M. *Inorg. Chem.* **2001**, *40*, 2185-2192.

(3) Arterburn, J. B.; Nelson, S. L. *J. Org. Chem.* **1996**, *61*, 2260-2261.

(4) Arterburn, J. B.; Perry, M. C. *Organic Letters* **1999**, *1*, 769-771.

(5) Gable, K. P.; Brown, E. C. *Organometallics* **2000**, *19*, 944-946.

(6) Gunaratne, H. Q. N.; McKervey, M. A.; Feutren, S.; Finlay, J.; Boyd, J. *Tetrahedron Lett.* **1998**, *39*, 5655-5658.

(7) Huang, R.; Espenson, J. H. *J. Mol. Catal. A:* **2001**, *168*, 39-46.

(8) Wang, Y.; Espenson, J. H. *Organic Letters* **2000**, *2*, 3525-3526.

(9) Wang, Y.; Espenson, J. H. *Inorg. Chem.* **2002**, *41*, 2266-2274.

(10) Wang, Y.; Lente, G.; Espenson, J. H. *Inorg. Chem.* **2002**, *41*, 1272-1280.

(11) Zapf, A.; Beller, M. *Chemistry--A European Journal* **2001**, *7*, 2908-2915.

(12) Panin, A. N.; Dzhabieva, Z. M.; Nedorezova, P. M.; Tsvetkova, V. I.; Saratovskikh, S. L.; Babkina, O. N.; Bravaya, N. M. *J. Polymer Sci., A* **2001**, *39*, 1915-1930.

(13) Cantrell, G. K.; Meyer, T. Y. *J. Amer. Chem. Soc.* **1998**, *120*, 8035-8042.

(14) Babich, J. W.; Graham, W.; Femia, F. J.; Dong, Q.; Barzana, M.; Ferrill, K.; Fischman, A. J.; Zubieta, J. *Inorg. Chim. Acta* **2001**, *323*, 23-36.

(15) Papadopoulos, M.; Tsoukalas, C.; Pirmettis, I.; Nock, B.; Maina, T.; Abedin, Z.; Raptopoulou, C. P.; Terzis, A.; Chiotellis, E. *Inorg. Chim. Acta* **1999**, *285*, 97-106.

(16) Heimbold, I.; Drews, A.; Kretzschmar, M.; Varnas, K.; Hall, H.; Halldin, C.; Syhre, R.; Kraus, W.; Pietzsch, H. J.; Seifert, S.; Brust, P.; Johannsen, B. *Nucl. Med. Biol.* **2002**, *29*, 375-387.

(17) Mevellec, F.; Roucoux, A.; Noiret, N.; Patin, H. *Inorg. Chim. Acta* **2002**, *332*, 30-36.

(18) Nock, B.; Maina, T.; Tisato, F.; Papadopoulos, M.; Raptopoulou, C. P.; Terzis, A.; Chiotellis, E. *Inorg. Chem.* **2000**, *39*, 2178-2184.

(19) Mevellec, F.; Roucoux, A.; Noiret, N.; Patin, H. *Journal of the Chemical Society, Dalton Transactions* **2001**, 3603-3610.

(20) Nock, B.; Pietzsch, H. J.; Tisato, F.; Maina, T.; Leibnitz, P.; Spies, H.; Chiotellis, E. *Inorg. Chim. Acta* **2000**, *304*, 26-32.

(21) Herrmann, W. A.; Kratzer, R. M.; Fischer, R. W. *Angew. Chem., Int. Ed.* **1997**, *36*, 2652-2654.

(22) Takacs, J.; Cook, M. R.; Kiprof, P.; Kuchler, J. G.; Herrmann, W. A. *Organometallics* **1991**, *10*, 316-320.

(23) Westland, A. D.; Tarafder, M. T. H. *Inorg. Chem.* **1981**, *20*, 3992-3995.

(24) Blessing, R. H. *Acta Cryst. Sect. A* **1995**, *51*, 33-38.

(25) Espenson, J. H.; Shan, X.; Lahti, D. W.; Rockey, T. M.; Saha, B.; Ellern, A. *Inorg. Chem.* **2001**, *40*, 6717-6724.

(26) Lente, G.; Guzei, I. A.; Espenson, J. H. *Inorg. Chem.* **2000**, *39*, 1311-1319.

(27) Lente, G.; Jacob, J.; Guzei, I. A.; Espenson, J. H. *Inorg. React. Mechs.* **2000**, *2*, 169-177.

(28) Shan, X.; Ellern, A.; Espenson, J. H. *Inorg. Chem.* **2002**, *in press*.

(29) Abu-Omar, M. M.; Espenson, J. H. *J. Am. Chem. Soc.* **1995**, *117*, 272-280.

(30) Al-Ajlouni, A. M.; Espenson, J. H. *J. Am. Chem. Soc.* **1995**, *117*, 9243-9250.

(31) Espenson, J. H. *Chem. Commun.* **1999**, 479-488.

(32) Espenson, J. H.; Abu-Omar, M. M. *Adv. Chem. Series* **1997**, *253*, 99-134.

(33) Lahti, D. W.; Espenson, J. H. *J. Amer. Chem. Soc.* **2001**, *123*, 6014-6024.

(34) Barea, G.; Lledos, A.; Maseras, F.; Jean, Y. *Inorg. Chem.* **1998**, *37*, 3321-3325.

(35) Mingos, D. M. P. *J. Organomet. Chem.* **1979**, *179*, C29-C33.

(36) Jacob, J.; Guzei, I. A.; Espenson, J. H. *Inorg. Chem.* **1999**, *38*, 3266-3267.

(37) Khimenko, M. T. *Zh. Fiz. Khim.* **1969**, *43*, 1861-1864.

(38) Goede, A.; Preissner, R.; Froemmel, C. *Journal of Computational Chemistry* **1997**, *18*, 1113-1123.

**Supporting Information**

Table of contents:

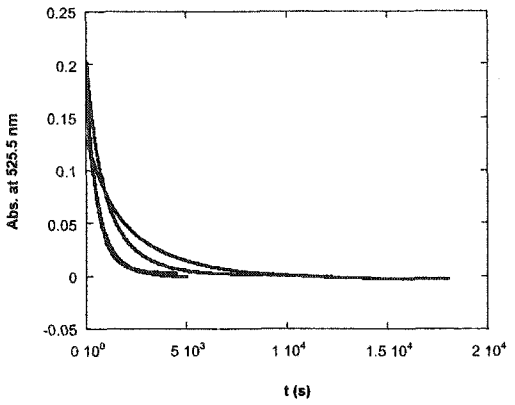


Figure S-1. Kinetic traces for reaction of **2** with 10~40 mM 4-MeO-Pyridine N-oxide in $CHCl_3$ at 25 °C.

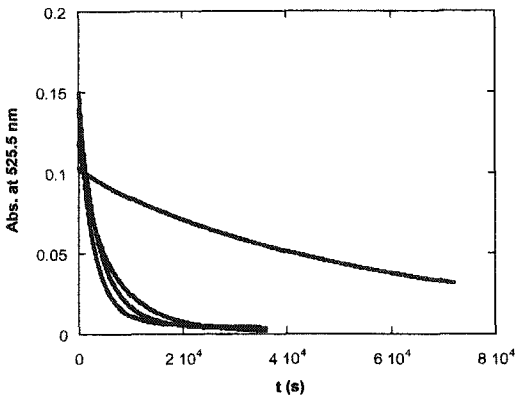


Figure S-2. Kinetic traces for reaction of **2** with 10~40 mM 4-picoline N-oxide in $CHCl_3$ at 25 °C.

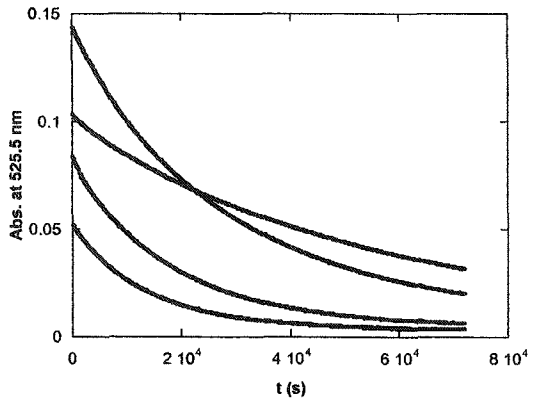


Figure S-3. Kinetic traces for reaction of **2** with 10~40 mM 4-pyridine N-oxide in $CHCl_3$ at 25 °C.

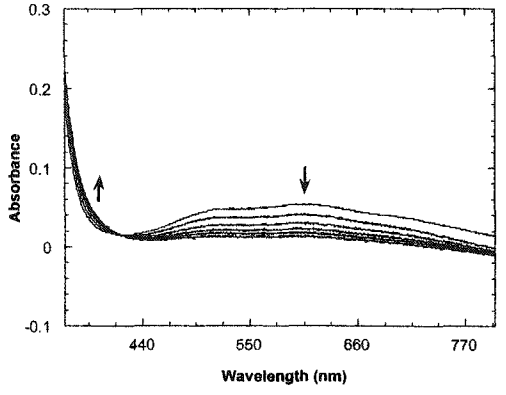


Figure S-4. Repetitive scans for reaction of 1 mM **3** with 20 mM 4-picoline N-oxide and 2 μL water in $CHCl_3$ at 25 °C.

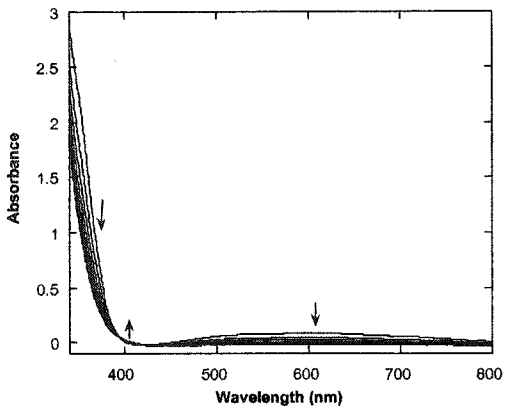


Figure S-5. Repetitive scans for reaction of 2 mM MeReO(OSO)[(4-MeO-$C_6H_4$)$_3$P] with 20 mM 4-picoline N-oxide and 2 μL water in $CHCl_3$ at 25 °C.

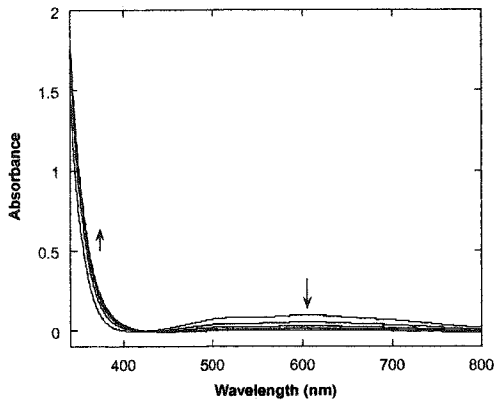


Figure S-6. Repetitive scans for reaction of 2 mM MeReO(OSO)[(4-F-$C_6H_4$)$_3$P] with 20 mM 4-picoline N-oxide and 2 μL water in $CHCl_3$ at 25 °C.

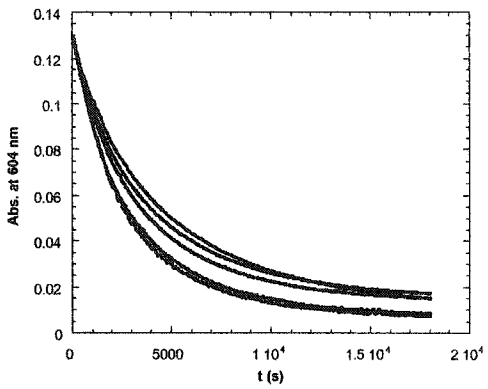


Figure S-7. Kinetic traces for reaction of 2 mM **3** with 20 mM 4-picoline N-oxide and 0~4 μL water in $CHCl_3$ at 25 °C.

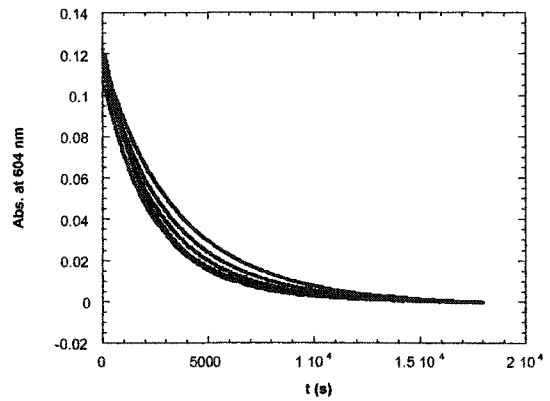


Figure S-8. Kinetic traces for reaction of 2 mM **3** with 40 mM 4-picoline N-oxide and 2~4 μL water in $CHCl_3$ at 25 °C.

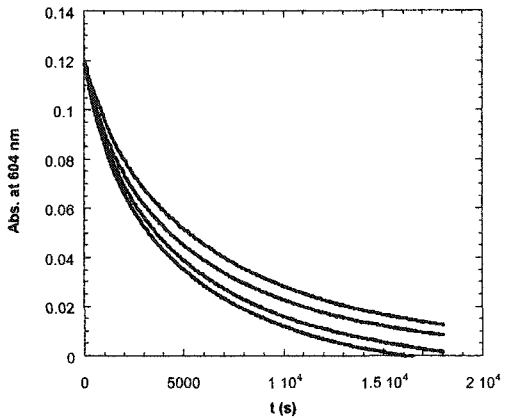


Figure S-9. Kinetic traces for reaction of 2 mM **3** with 20 mM 4-phenylpyridine N-oxide and 2~3.5 μL water in $CHCl_3$ at 25 °C.

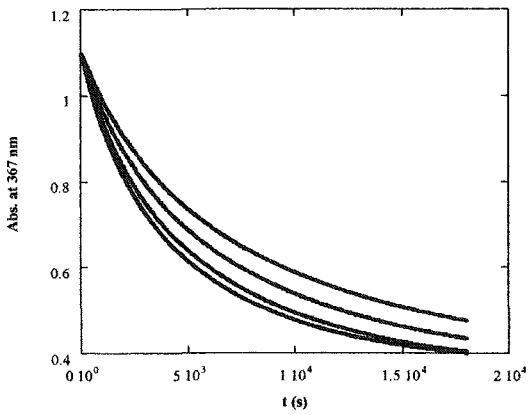


Figure S-10. Kinetic traces for reaction of 2 mM MeReO(OSO)[(4-MeO-$C_6H_4$)$_3$P] with 20 mM 4-picoline N-oxide and 2~3.5 μL water in $CHCl_3$ at 25 °C.

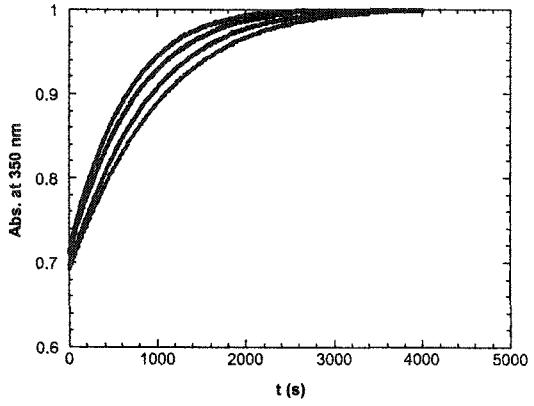


Figure S-11. Kinetic traces for reaction of 2 mM MeReO(OSO)[(4-F-$C_6H_4$)$_3$P] with 20 mM 4-picoline N-oxide and 2~3.5 μL water in $CHCl_3$ at 25 °C.

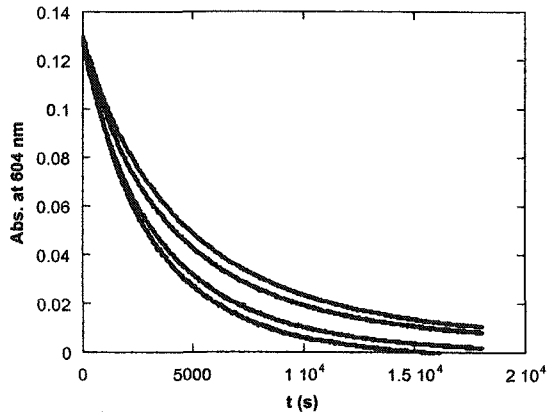


Figure S-12. Kinetic traces for reaction of 2 mM **3** with 20 mM 4-picoline N-oxide and 2~3.5 μL $D_2O$ in $CHCl_3$ at 25 °C.

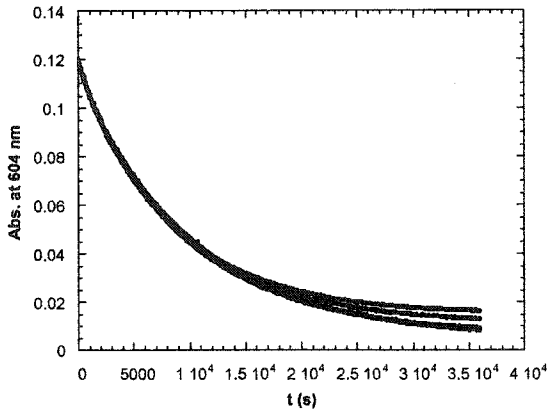


Figure S-13. Kinetic traces for reaction of 2 mM **3** with 20 mM 4-picoline N-oxide and 2~3.5 μL methanol in $CHCl_3$ at 25 °C.

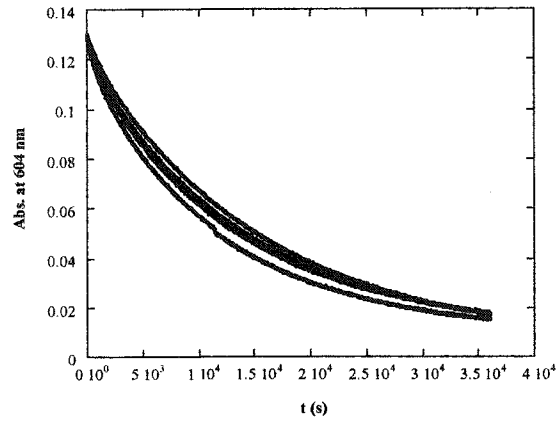


Figure S-14. Kinetic traces for reaction of 2 mM **3** with 20 mM 4-picoline N-oxide and 10~40 mM $Bu_4N^+ Cl^-$ in $CHCl_3$ at 25 °C.

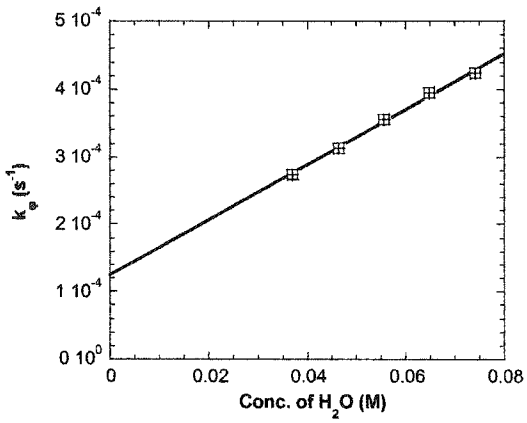


Figure S-15. Plot of $k_\Psi$ against $[H_2O]$ for reaction of 2 mM **3** with 40 mM 4-picoline N-oxide and 2~4 μL water in $CHCl_3$ at 25 °C.

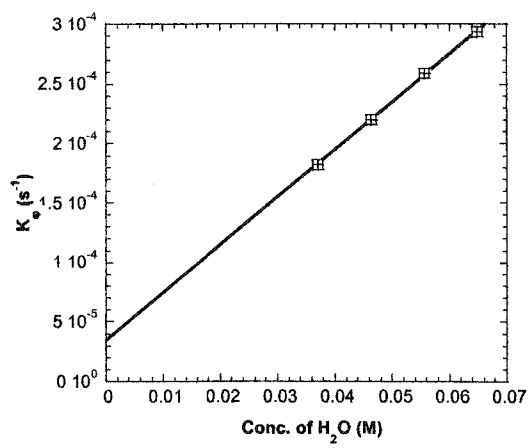


Figure S-16. Plot of $k_\Psi$ against $[H_2O]$ for reaction of 2 mM **3** with 20 mM 4-phenylpyridine N-oxide and 2~4 μL water in $CHCl_3$ at 25 °C.

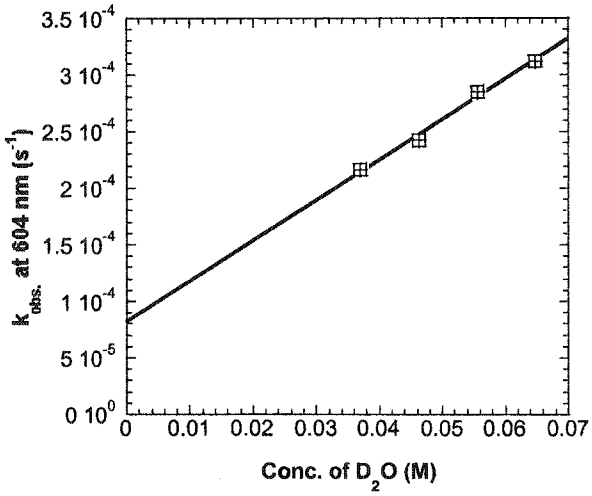


Figure S-17. Plot of $k_{\Psi}$ against $[D_2O]$ for reaction of 2 mM **3** with 20 mM 4-picoline N-oxide and 2~4 μL $D_2O$ in $CHCl_3$ at 25 °C.

S-18. Crystal data of compound **1**.

Table A. Crystal data and structure refinement for **1**.

| Identification code | 1 | |
|---|---|---|
| Empirical formula | $C_5H_{11}OReS_3$ | |
| Formula weight | 369.52 | |
| Temperature | 173(2) K | |
| Wavelength | 0.71073 Å | |
| Crystal system | Orthorhombic | |
| Space group | $Cmc2_1$ | |
| Unit cell dimensions | a = 8.9289(6) Å | $\alpha$= 90°. |
| | b = 8.9178(6) Å | $\beta$= 90°. |
| | c = 11.8518(7) Å | $\gamma$ = 90°. |
| Volume | 943.71(11) $Å^3$ | |
| Z | 4 | |
| Density (calculated) | 2.601 $Mg/m^3$ | |
| Absorption coefficient | 13.476 $mm^{-1}$ | |
| F(000) | 688 | |
| Crystal size | 0.40 × 0.30 × 0.20 $mm^3$ | |
| Theta range for data collection | 3.23 to 28.24°. | |
| Index ranges | $-11 \le h \le 11$, $-11 \le k \le 11$, $-15 \le l \le 15$ | |
| Reflections collected | 3831 | |
| Independent reflections | 1186 [R(int) = 0.0262] | |
| Completeness to theta = 28.24° | 98.3 % | |
| Absorption correction | Empirical with SADABS | |
| Refinement method | Full-matrix least-squares on $F^2$ | |

| | |
|---|---|
| Data / restraints / parameters | 1186 / 2 / 53 |
| Goodness-of-fit on $F^2$ | 1.084 |
| Final R indices [I>2sigma(I)] | R1 = 0.0215, wR2 = 0.0570 |
| R indices (all data) | R1 = 0.0219, wR2 = 0.0573 |
| Largest diff. peak and hole | 1.181 and -1.660 e.Å$^{-3}$ |

Table B. Atomic coordinates ( $\times 10^4$) and equivalent isotropic displacement parameters (Å$^2$ $\times 10^3$) for **1**. U(eq) is defined as one third of the trace of the orthogonalized $U_{ij}$ tensor.

| | x | y | z | U(eq) |
|---|---|---|---|---|
| Re | 0 | 2467(1) | 148(1) | 17(1) |
| S(2) | 0 | 1109(1) | 1836(1) | 20(1) |
| S(1) | 2307(1) | 3264(1) | 727(1) | 26(1) |
| O(1) | 0 | 1264(5) | -953(3) | 26(1) |
| C(1) | 0 | 4649(7) | -650(5) | 31(1) |
| C(2) | 2889(5) | 2059(7) | 1900(4) | 29(1) |
| C(3) | 1584(5) | 1741(5) | 2680(3) | 29(1) |

Table C. Bond lengths [Å] and angles [°] for **1**.

| | | | |
|---|---|---|---|
| Re-O(1) | 1.689(4) | S(2)-C(3) | 1.822(4) |
| Re-C(1) | 2.163(6) | S(2)-C(3)#1 | 1.822(4) |
| Re-S(1) | 2.2846(10) | S(1)-C(2) | 1.833(6) |
| Re-S(1)#1 | 2.2846(10) | S(1)-C(2) | 1.513(7) |
| Re-S(2) | 2.3386(19) | | |

| | | | |
|---|---|---|---|
| O(1)-Re-C(1) | 103.6(2) | S(1)-Re-S(2) | 84.50(5) |
| O(1)-Re-S(1) | 115.45(4) | S(1)#1-Re-S(2) | 84.50(5) |
| C(1)-Re-S(1) | 81.46(7) | C(3)-S(2)-C(3)#1 | 101.9(3) |
| O(1)-Re-S(1)#1 | 115.45(4) | C(3)-S(2)-Re | 108.02(14) |
| C(1)-Re-S(1)#1 | 81.46(7) | C(3)#1-S(2)-Re | 108.02(14) |

| | |
|---|---|
| S(1)-Re-S(1)#1 128.75(7) | C(2)-S(1)-Re 107.53(16) |
| O(1)-Re-S(2) 109.34(14) | C(3)-C(2)-S(1) 110.8(3) |
| C(1)-Re-S(2) 147.10(18) | C(2)-C(3)-S(2) 108.7(3) |

Symmetry transformations used to generate equivalent atoms:

#1 –x,y,z

Table D. Anisotropic displacement parameters ($Å^2 \times 10^3$) for **1**. The anisotropic displacement factor exponent takes the form: $-2\pi^2[ h^2 a^{*2}U_{11} + ... + 2 h k a^* b^* U_{12} ]$

| | $U_{11}$ | $U_{22}$ | $U_{33}$ | $U_{23}$ | $U_{13}$ | $U_{12}$ |
|---|---|---|---|---|---|---|
| Re | 23(1) | 16(1) | 12(1) | -1(1) | 0 | 0 |
| S(2) | 24(1) | 21(1) | 13(1) | 1(1) | 0 | 0 |
| S(1) | 26(1) | 27(1) | 26(1) | 0(1) | 0(1) | -7(1) |
| O(1) | 41(2) | 24(2) | 14(2) | -6(2) | 0 | 0 |
| C(1) | 50(4) | 20(3) | 22(3) | 1(2) | 0 | 0 |
| C(2) | 23(2) | 32(2) | 31(2) | -3(2) | -12(2) | -5(2) |
| C(3) | 35(2) | 35(2) | 17(2) | 1(2) | -10(2) | 1(2) |

Table E. Hydrogen coordinates ( $\times 10^4$) and isotropic displacement parameters ($Å^2 \times 10^3$) for **1**.

| | x | y | z | U(eq) |
|---|---|---|---|---|
| H(1A) | -4 | 5431 | -69 | 46 |
| H(1B) | -894 | 4750 | -1123 | 46 |
| H(1C) | 898 | 4753 | -1118 | 46 |
| H(2A) | 3285 | 1102 | 1600 | 34 |
| H(2B) | 3700 | 2557 | 2329 | 34 |
| H(3A) | 1311 | 2661 | 3099 | 35 |
| H(3B) | 1865 | 958 | 3232 | 35 |

S-19. Crystal data of compound **2**.

Table A. Crystal data and structure refinement for **2**.

| Identification code | **2** | |
|---|---|---|
| Empirical formula | $C_5H_{11}O_2ReS_2$ | |
| Formula weight | 353.46 | |
| Temperature | 173(2) K | |
| Wavelength | 0.71073 Å | |
| Crystal system | Monoclinic | |
| Space group | $P2_1/n$ | |
| Unit cell dimensions | a = 7.8318(5) Å | α= 90°. |
| | b = 10.4827(6) Å | β= 90.2451(10)°. |
| | c = 10.9106(6) Å | γ = 90°. |
| Volume | 895.73(9) $Å^3$ | |
| Z | 4 | |
| Density (calculated) | 2.621 $Mg/m^3$ | |
| Absorption coefficient | 13.974 $mm^{-1}$ | |
| F(000) | 656 | |
| Crystal size | 0.30 × 0.20 × 0.20 $mm^3$ | |
| Theta range for data collection | 3.20 to 26.36°. | |
| Index ranges | $-9 \le h \le 9, 0 \le k \le 13, 0 \le l \le 13$ | |
| Reflections collected | 5255 | |
| Independent reflections | 1735 [R(int) = 0.0265] | |
| Completeness to theta = 26.36° | 95.2 % | |
| Absorption correction | Empirical with SADABS | |
| Refinement method | Full-matrix least-squares on $F^2$ | |

| | |
|---|---|
| Data / restraints / parameters | 1735 / 0 / 92 |
| Goodness-of-fit on $F^2$ | 1.083 |
| Final R indices [I>2sigma(I)] | R1 = 0.0304, wR2 = 0.0788 |
| R indices (all data) | R1 = 0.0325, wR2 = 0.0799 |
| Largest diff. peak and hole | 1.535 and -2.704 e.Å$^{-3}$ |

Table B. Atomic coordinates ( × $10^4$) and equivalent isotropic displacement parameters (Å$^2$ × $10^3$) for **2**. U(eq) is defined as one third of the trace of the orthogonalized $U_{ij}$ tensor.

| | X | y | z | U(eq) |
|---|---|---|---|---|
| Re | 358(1) | 1228(1) | 2296(1) | 14(1) |
| S(1) | 2321(2) | -353(2) | 2056(2) | 27(1) |
| S(2) | -1745(2) | 1672(2) | 3663(2) | 23(1) |
| O(1) | 464(6) | 2323(5) | 1181(4) | 27(1) |
| O(2) | 1868(6) | 1574(4) | 3849(4) | 16(1) |
| C(1) | -1393(9) | -95(7) | 1531(7) | 27(2) |
| C(2) | 4105(9) | 383(8) | 2879(7) | 26(2) |
| C(3) | 3475(8) | 886(8) | 4081(7) | 24(2) |
| C(4) | 1124(10) | 1983(7) | 5019(6) | 25(2) |
| C(5) | -553(9) | 2626(8) | 4767(7) | 30(2) |

Table C. Bond lengths [Å] and angles [°] for **2**.

| | | | |
|---|---|---|---|
| Re-O(1) | 1.674(5) | S(2)-C(5) | 1.820(7) |
| Re-O(2) | 2.094(4) | O(2)-C(4) | 1.470(7) |
| Re-C(1) | 2.118(7) | O(2)-C(3) | 1.471(8) |
| Re-S(2) | 2.2755(17) | C(2)-C(3) | 1.499(10) |
| Re-S(1) | 2.2769(18) | C(4)-C(5) | 1.501(10) |
| S(1)-C(2) | 1.828(7) | | |

| | | | |
|---|---|---|---|
| O(1)-Re-O(2) | 116.1(2) | C(2)-S(1)-Re | 98.7(2) |

| | |
|---|---|
| O(1)-Re-C(1) 101.3(3) | C(5)-S(2)-Re 100.1(2) |
| O(2)-Re-C(1) 142.6(2) | C(4)-O(2)-C(3) 109.6(5) |
| O(1)-Re-S(2) 112.00(19) | C(4)-O(2)-Re 121.9(4) |
| O(2)-Re-S(2) 80.90(13) | C(3)-O(2)-Re 122.3(4) |
| C(1)-Re-S(2) 85.6(2) | C(3)-C(2)-S(1) 108.9(5) |
| O(1)-Re-S(1) 112.33(19) | O(2)-C(3)-C(2) 107.8(5) |
| O(2)-Re-S(1) 80.76(13) | O(2)-C(4)-C(5) 108.8(5) |
| C(1)-Re-S(1) 85.1(2) | C(4)-C(5)-S(2) 108.7(5) |
| S(2)-Re-S(1) 135.67(7) | |

Table D. Anisotropic displacement parameters ($Å^2 \times 10^3$) for **2**. The anisotropic displacement factor exponent takes the form: $-2\pi^2[ h^2 a^{*2}U_{11} + ... + 2 h k a^* b^* U_{12} ]$

| | $U_{11}$ | $U_{22}$ | $U_{33}$ | $U_{23}$ | $U_{13}$ | $U_{12}$ |
|---|---|---|---|---|---|---|
| Re | 14(1) | 15(1) | 13(1) | 1(1) | -2(1) | 1(1) |
| S(1) | 25(1) | 26(1) | 30(1) | -10(1) | -5(1) | 9(1) |
| S(2) | 15(1) | 28(1) | 27(1) | -7(1) | 3(1) | -3(1) |
| O(1) | 28(3) | 30(3) | 23(2) | 8(2) | -5(2) | -7(2) |
| O(2) | 18(2) | 16(2) | 14(2) | -1(2) | -3(2) | -1(2) |
| C(1) | 24(4) | 29(4) | 27(4) | -8(3) | -7(3) | -7(3) |
| C(2) | 18(3) | 28(4) | 33(4) | 1(3) | -6(3) | 11(3) |
| C(3) | 12(3) | 32(4) | 28(4) | 4(3) | -8(3) | 2(3) |
| C(4) | 33(4) | 29(4) | 14(3) | -6(3) | 0(3) | 0(3) |
| C(5) | 25(4) | 35(4) | 29(4) | -14(3) | 4(3) | -2(3) |

Table E. Hydrogen coordinates ( $\times 10^4$) and isotropic displacement parameters ($Å^2 \times 10^3$) for **2**.

| | x | y | z | U(eq) |
|---|---|---|---|---|
| H(1A) | -2448 | 349 | 1303 | 40 |
| H(1B) | -1648 | -758 | 2136 | 40 |

| | | | | |
|---|---|---|---|---|
| H(1C) | -891 | -487 | 801 | 40 |
| H(2A) | 5017 | -255 | 3021 | 31 |
| H(2B) | 4587 | 1088 | 2386 | 31 |
| H(3A) | 3277 | 173 | 4658 | 28 |
| H(3B) | 4331 | 1468 | 4447 | 28 |
| H(4A) | 1908 | 2583 | 5440 | 30 |
| H(4B) | 950 | 1235 | 5558 | 30 |
| H(5A) | -357 | 3491 | 4434 | 36 |
| H(5B) | -1211 | 2707 | 5536 | 36 |

S-20. Crystal data of compound **3**.

Table A. Crystal data and structure refinement for **3**.

| Identification code | **3** | |
|---|---|---|
| Empirical formula | $C_{23}H_{22}O_5PReS$ | |
| Formula weight | 627.64 | |
| Temperature | 173(2) K | |
| Wavelength | 0.71073 Å | |
| Crystal system | Monoclinic | |
| Space group | C2/c | |
| Unit cell dimensions | a = 21.682(8) Å | α= 90°. |
| | b = 10.833(4) Å | β= 94.396(6)°. |
| | c = 19.248(7) Å | γ = 90°. |
| Volume | 4508(3) $Å^3$ | |
| Z | 8 | |
| Density (calculated) | 1.850 $Mg/m^3$ | |
| Absorption coefficient | 5.587 $mm^{-1}$ | |
| F(000) | 2448 | |
| Crystal size | 0.2 × 0.2 × 0.1 $mm^3$ | |

| | |
|---|---|
| Theta range for data collection | 1.88 to 28.28°. |
| Index ranges | $-25 \leq h \leq 28$, $-14 \leq k \leq 14$, $-25 \leq l \leq 22$ |
| Reflections collected | 13523 |
| Independent reflections | 5106 [R(int) = 0.0472] |
| Completeness to theta = 28.28° | 91.2 % |
| Absorption correction | None |
| Refinement method | Full-matrix least-squares on $F^2$ |
| Data / restraints / parameters | 5106 / 0 / 280 |
| Goodness-of-fit on $F^2$ | 1.152 |
| Final R indices [I>2sigma(I)] | R1 = 0.0408, wR2 = 0.0861 |
| R indices (all data) | R1 = 0.0499, wR2 = 0.0881 |
| Largest diff. peak and hole | 2.052 and -2.467 e.Å$^{-3}$ |

Table B. Atomic coordinates ( $\times 10^4$) and equivalent isotropic displacement parameters (Å$^2$ $\times 10^3$) for **3**. U(eq) is defined as one third of the trace of the orthogonalized $U_{ij}$ tensor.

| | x | y | z | U(eq) |
|---|---|---|---|---|
| Re | 936(1) | 8518(1) | 1589(1) | 16(1) |
| S | -132(1) | 7634(1) | 1283(1) | 19(1) |
| P | 1543(1) | 6723(1) | 2002(1) | 18(1) |
| C(1) | 1781(3) | 9457(6) | 1455(3) | 29(1) |
| C(2) | -6(3) | 10074(5) | 796(3) | 18(1) |
| C(3) | -469(3) | 9060(5) | 936(3) | 21(1) |
| C(4) | 5(3) | 6773(5) | 512(3) | 24(1) |
| C(5) | 677(3) | 6846(5) | 312(3) | 22(1) |
| C(6) | 1204(3) | 5224(6) | 1762(3) | 29(1) |

| | | | | |
|---|---|---|---|---|
| C(7) | 586(4) | 5047(7) | 1856(4) | 46(2) |
| C(8) | 309(5) | 3914(8) | 1663(5) | 68(3) |
| C(9) | 660(6) | 2994(9) | 1395(5) | 76(4) |
| C(10) | 1271(7) | 3178(8) | 1314(4) | 72(3) |
| C(11) | 1534(5) | 4268(6) | 1493(4) | 51(2) |
| C(12) | 2320(3) | 6691(6) | 1690(3) | 27(1) |
| C(13) | 2382(3) | 6578(7) | 970(3) | 37(2) |
| C(14) | 2968(4) | 6611(8) | 737(4) | 51(2) |
| C(15) | 3483(4) | 6726(7) | 1180(5) | 54(2) |
| C(16) | 3416(4) | 6823(7) | 1880(4) | 46(2) |
| C(17) | 2842(3) | 6793(6) | 2139(4) | 32(2) |
| C(18) | 1669(3) | 6688(5) | 2947(3) | 20(1) |
| C(19) | 1605(3) | 5602(6) | 3319(3) | 25(1) |
| C(20) | 1697(3) | 5606(7) | 4042(3) | 36(2) |
| C(21) | 1854(3) | 6687(7) | 4385(3) | 38(2) |
| C(22) | 1932(3) | 7769(7) | 4027(3) | 34(2) |
| C(23) | 1828(3) | 7767(6) | 3305(3) | 25(1) |
| O(1) | 783(2) | 8907(4) | 2399(2) | 24(1) |
| O(2) | 567(2) | 9954(3) | 1018(2) | 21(1) |
| O(3) | -208(2) | 11010(4) | 500(2) | 23(1) |
| O(4) | 1039(2) | 7630(4) | 671(2) | 21(1) |
| O(5) | 830(2) | 6201(4) | -155(2) | 37(1) |

Table C. Bond lengths [Å] and angles [°] for **3**.

| | | | |
|---|---|---|---|
| Re-O(1) | 1.674(4) | C(6)-C(7) | 1.380(10) |
| Re-O(2) | 2.033(4) | C(7)-C(8) | 1.404(11) |
| Re-O(4) | 2.039(4) | C(8)-C(9) | 1.378(16) |
| Re-C(1) | 2.129(6) | C(9)-C(10) | 1.360(16) |
| Re-P | 2.4469(15) | C(10)-C(11) | 1.345(12) |

| | | | |
|---|---|---|---|
| Re-S | 2.5337(16) | C(12)-C(17) | 1.376(9) |
| S-C(4) | 1.797(6) | C(12)-C(13) | 1.408(8) |
| S-C(3) | 1.815(6) | C(13)-C(14) | 1.381(10) |
| P-C(18) | 1.819(6) | C(14)-C(15) | 1.358(13) |
| P-C(6) | 1.827(7) | C(15)-C(16) | 1.369(11) |
| P-C(12) | 1.830(6) | C(16)-C(17) | 1.376(9) |
| C(2)-O(3) | 1.228(7) | C(18)-C(23) | 1.387(8) |
| C(2)-O(2) | 1.288(7) | C(18)-C(19) | 1.390(8) |
| C(2)-C(3) | 1.527(8) | C(19)-C(20) | 1.390(8) |
| C(4)-C(5) | 1.538(8) | C(20)-C(21) | 1.373(11) |
| C(5)-O(5) | 1.205(7) | C(21)-C(22) | 1.376(10) |
| C(5)-O(4) | 1.315(7) | C(22)-C(23) | 1.391(8) |
| C(6)-C(11) | 1.381(9) | | |

| | | | |
|---|---|---|---|
| O(1)-Re-O(2) | 102.32(18) | O(4)-C(5)-O(5) | 125.4(6) |
| O(1)-Re-O(4) | 165.76(18) | O(5)-C(5)-C(4) | 118.4(5) |
| O(2)-Re-O(4) | 87.52(15) | O(4)-C(5)-C(4) | 116.2(5) |
| O(1)-Re-C(1) | 103.1(2) | C(11)-C(6)-C(7) | 118.8(7) |
| O(2)-Re-C(1) | 82.9(2) | C(11)-C(6)-P | 123.4(6) |
| O(4)-Re-C(1) | 88.2(2) | C(7)-C(6)-P | 117.8(5) |
| O(1)-Re-P | 92.18(14) | C(6)-C(7)-C(8) | 119.1(9) |
| O(2)-Re-P | 164.43(11) | C(9)-C(8)-C(7) | 119.6(10) |
| O(4)-Re-P | 79.32(11) | C(10)-C(9)-C(8) | 120.5(8) |
| C(1)-Re-P | 88.39(18) | C(11)-C(10)-C(9) | 119.8(10) |
| O(1)-Re-S | 93.92(15) | C(10)-C(11)-C(6) | 122.2(10) |
| O(2)-Re-S | 81.30(12) | C(17)-C(12)-C(13) | 119.3(6) |
| O(4)-Re-S | 77.24(12) | C(17)-C(12)-P | 121.8(5) |
| C(1)-Re-S | 158.86(18) | C(13)-C(12)-P | 118.9(5) |
| P-Re-S | 103.58(5) | C(14)-C(13)-C(12) | 118.5(7) |
| C(4)-S-C(3) | 103.0(3) | C(15)-C(14)-C(13) | 122.2(7) |

| | | | |
|---|---|---|---|
| C(4)-S-Re | 100.5(2) | C(14)-C(15)-C(16) | 118.7(7) |
| C(3)-S-Re | 95.66(19) | C(15)-C(16)-C(17) | 121.5(8) |
| C(18)-P-C(6) | 105.1(3) | C(12)-C(17)-C(16) | 119.9(7) |
| C(18)-P-C(12) | 104.8(3) | C(23)-C(18)-C(19) | 119.1(5) |
| C(6)-P-C(12) | 105.2(3) | C(23)-C(18)-P | 119.5(4) |
| C(18)-P-Re | 112.14(18) | C(19)-C(18)-P | 121.4(5) |
| C(6)-P-Re | 115.3(2) | C(18)-C(19)-C(20) | 120.1(6) |
| C(12)-P-Re | 113.23(19) | C(21)-C(20)-C(19) | 119.6(6) |
| O(3)-C(2)-O(2) | 122.6(5) | C(20)-C(21)-C(22) | 121.4(6) |
| O(3)-C(2)-C(3) | 117.4(5) | C(21)-C(22)-C(23) | 118.8(6) |
| O(2)-C(2)-C(3) | 120.0(5) | C(18)-C(23)-C(22) | 120.9(6) |
| C(2)-C(3)-S | 115.2(4) | C(2)-O(2)-Re | 125.9(3) |
| C(5)-C(4)-S | 113.5(4) | C(5)-O(4)-Re | 131.2(3) |

Table D. Anisotropic displacement parameters ($Å^2 \times 10^3$) for **3**. The anisotropic displacement factor exponent takes the form: $-2\pi^2[ h^2 a^{*2}U_{11} + ... + 2 h k a^* b^* U_{12} ]$

| | $U_{11}$ | $U_{22}$ | $U_{33}$ | $U_{23}$ | $U_{13}$ | $U_{12}$ |
|---|---|---|---|---|---|---|
| Re | 20(1) | 14(1) | 14(1) | -1(1) | 1(1) | 1(1) |
| S | 22(1) | 18(1) | 18(1) | -1(1) | 4(1) | -2(1) |
| P | 23(1) | 16(1) | 15(1) | 0(1) | 2(1) | 3(1) |
| C(1) | 22(3) | 24(3) | 42(4) | 7(3) | 3(3) | 0(2) |
| C(2) | 28(3) | 19(3) | 7(2) | -5(2) | 3(2) | 1(2) |
| C(3) | 21(3) | 18(3) | 25(3) | 1(2) | 4(2) | 3(2) |
| C(4) | 32(3) | 25(3) | 16(3) | -5(2) | 0(2) | -4(2) |
| C(5) | 30(3) | 19(3) | 16(3) | -1(2) | 0(2) | -1(2) |
| C(6) | 51(4) | 19(3) | 16(3) | 4(2) | -9(3) | 7(3) |
| C(7) | 46(4) | 30(4) | 59(5) | 12(3) | -17(4) | -14(3) |
| C(8) | 75(7) | 37(5) | 86(7) | 25(5) | -42(5) | -26(5) |
| C(9) | 142(11) | 35(5) | 46(5) | 2(4) | -29(6) | -45(6) |

| | | | | | | |
|---|---|---|---|---|---|---|
| C(10) | 154(12) | 21(4) | 41(5) | -7(3) | 5(6) | 0(5) |
| C(11) | 106(7) | 18(3) | 30(4) | 0(3) | 7(4) | 11(4) |
| C(12) | 31(3) | 27(3) | 26(3) | 9(2) | 12(3) | 11(3) |
| C(13) | 37(4) | 55(5) | 21(3) | 5(3) | 5(3) | 23(3) |
| C(14) | 55(5) | 67(6) | 35(4) | 22(4) | 29(4) | 41(4) |
| C(15) | 45(5) | 51(5) | 71(6) | 26(4) | 38(4) | 26(4) |
| C(16) | 36(4) | 51(5) | 53(5) | 12(4) | 18(4) | 13(3) |
| C(17) | 32(3) | 31(4) | 35(4) | 3(3) | 5(3) | 8(3) |
| C(18) | 20(3) | 25(3) | 15(3) | 2(2) | 1(2) | 4(2) |
| C(19) | 28(3) | 25(3) | 21(3) | 6(2) | 5(2) | 2(3) |
| C(20) | 33(3) | 44(4) | 30(3) | 18(3) | 3(3) | 0(3) |
| C(21) | 36(4) | 61(5) | 19(3) | 7(3) | 4(3) | 10(3) |
| C(22) | 29(3) | 48(4) | 22(3) | -11(3) | -4(3) | 4(3) |
| C(23) | 23(3) | 29(3) | 21(3) | 2(2) | -2(2) | -1(2) |
| O(1) | 33(2) | 25(2) | 15(2) | -2(2) | 0(2) | 6(2) |
| O(2) | 24(2) | 15(2) | 24(2) | 4(2) | 1(2) | 0(2) |
| O(3) | 30(2) | 18(2) | 20(2) | 3(2) | 3(2) | 5(2) |
| O(4) | 28(2) | 21(2) | 14(2) | 2(2) | 5(2) | 3(2) |
| O(5) | 43(3) | 36(3) | 33(3) | -15(2) | 10(2) | 3(2) |

Table E. Hydrogen coordinates ( $\times 10^4$) and isotropic displacement parameters ($Å^2 \times 10^3$) for **3**.

| | x | y | z | U(eq) |
|---|---|---|---|---|
| H(1A) | 2042 | 9440 | 1894 | 44 |
| H(1B) | 1693 | 10315 | 1321 | 44 |
| H(1C) | 1997 | 9048 | 1090 | 44 |
| H(3A) | -716 | 8872 | 494 | 26 |
| H(3B) | -757 | 9381 | 1268 | 26 |
| H(4A) | -103 | 5896 | 586 | 29 |

| | | | | |
|---|---|---|---|---|
| H(4B) | -273 | 7087 | 119 | 29 |
| H(7) | 351 | 5684 | 2048 | 55 |
| H(8) | -117 | 3781 | 1718 | 82 |
| H(9) | 474 | 2225 | 1265 | 91 |
| H(10) | 1511 | 2538 | 1132 | 87 |
| H(11) | 1961 | 4385 | 1433 | 62 |
| H(13) | 2028 | 6481 | 652 | 45 |
| H(14) | 3013 | 6552 | 251 | 61 |
| H(15) | 3882 | 6739 | 1008 | 65 |
| H(16) | 3774 | 6913 | 2193 | 55 |
| H(17) | 2807 | 6843 | 2627 | 39 |
| H(19) | 1499 | 4856 | 3080 | 30 |
| H(20) | 1653 | 4866 | 4298 | 43 |
| H(21) | 1908 | 6688 | 4879 | 46 |
| H(22) | 2055 | 8503 | 4269 | 40 |
| H(23) | 1865 | 8515 | 3054 | 29 |

S-21. Crystal data of compound **4**.

Table A. Crystal data and structure refinement for **4**.

| Identification code | **4** | |
|---|---|---|
| Empirical formula | $C_{33}H_{27}NO_4PRe$ | |
| Formula weight | 718.73 | |
| Temperature | 298(2) K | |
| Wavelength | 0.71073 Å | |
| Crystal system | Monoclinic | |
| Space group | P2(1)/n | |
| Unit cell dimensions | a = 11.7111(15) Å | $\alpha$= 90°. |
| | b = 13.6521(16) Å | $\beta$= 100.867(2)°. |
| | c = 17.873(2) Å | $\gamma$ = 90°. |

| | |
|---|---|
| Volume | 2806.3(6) $Å^3$ |
| Z | 4 |
| Density (calculated) | 1.701 $Mg/m^3$ |
| Absorption coefficient | 4.427 $mm^{-1}$ |
| F(000) | 1416 |
| Crystal size | 0.42 × 0.25 × 0.10 $mm^3$ |
| Theta range for data collection | 2.29 to 24.00°. |
| Index ranges | $-10 \le h \le 13$, $-15 \le k \le 5$, $-17 \le l \le 20$ |
| Reflections collected | 6566 |
| Independent reflections | 4113 [R(int) = 0.0184] |
| Completeness to theta = 24.00° | 93.2 % |
| Absorption correction | Empirical |
| Max. and min. transmission | 0.64 and 0.30 |
| Refinement method | Full-matrix least-squares on $F^2$ |
| Data / restraints / parameters | 4113 / 0 / 361 |
| Goodness-of-fit on $F^2$ | 1.008 |
| Final R indices [I>2sigma(I)] | R1 = 0.0279, wR2 = 0.0757 |
| R indices (all data) | R1 = 0.0349, wR2 = 0.0814 |
| Largest diff. peak and hole | 2.494 and -1.441 $e.Å^{-3}$ |

$R1 = \Sigma \, | \, |Fo| - |F_c| \, | \, / \, \Sigma \, |F_o|$ and $wR2 = \{ \, \Sigma \, [ \, w(F_o^2 - F_c^2)^2 \, ] \, / \, \Sigma \, [ \, w(F_o^2)^2 \, ] \, \}^{1/2}$

Table B. Atomic coordinates ( × $10^4$) and equivalent isotropic displacement parameters ($Å^2$ × $10^3$) for **4**. U(eq) is defined as one third of the trace of the orthogonalized $U_{ij}$ tensor.

| | x | y | z | U(eq) |
|---|---|---|---|---|
| Re | 1646(1) | 7550(1) | 1560(1) | 28(1) |

| | | | | |
|---|---|---|---|---|
| C(1) | 2219(4) | 7820(3) | 2750(3) | 41(1) |
| C(2) | -925(4) | 7221(3) | 1453(3) | 36(1) |
| C(3) | -915(4) | 6727(3) | 698(3) | 37(1) |
| C(4) | -1778(4) | 6020(4) | 457(3) | 49(1) |
| C(5) | -1863(5) | 5554(4) | -226(3) | 58(2) |
| C(6) | -1095(5) | 5778(4) | -692(3) | 56(2) |
| C(7) | -260(4) | 6490(3) | -490(3) | 46(1) |
| C(8) | -166(4) | 6965(3) | 205(3) | 33(1) |
| C(9) | 694(4) | 8437(3) | -68(3) | 37(1) |
| C(10) | 1369(4) | 9308(3) | 84(3) | 37(1) |
| C(11) | 1493(4) | 9945(3) | -509(3) | 51(1) |
| C(12) | 2047(5) | 10816(4) | -369(4) | 56(2) |
| C(13) | 2442(5) | 11125(4) | 381(4) | 59(2) |
| C(14) | 2303(4) | 10525(3) | 975(3) | 47(1) |
| C(15) | 1809(4) | 9600(3) | 841(3) | 36(1) |
| C(16) | 3676(4) | 7822(3) | 296(3) | 31(1) |
| C(17) | 2974(4) | 7222(3) | -243(3) | 38(1) |
| C(18) | 2931(5) | 7369(4) | -1011(3) | 50(2) |
| C(19) | 3565(5) | 8100(4) | -1265(3) | 59(2) |
| C(20) | 4262(5) | 8690(4) | -739(3) | 61(2) |
| C(21) | 4313(4) | 8552(3) | 29(3) | 43(1) |
| C(22) | 4700(4) | 8444(3) | 1824(2) | 31(1) |
| C(23) | 4360(4) | 9247(3) | 2195(3) | 39(1) |
| C(24) | 5191(5) | 9914(3) | 2551(3) | 49(1) |
| C(25) | 6338(4) | 9781(3) | 2542(3) | 44(1) |
| C(26) | 6684(4) | 8969(3) | 2183(3) | 43(1) |
| C(27) | 5882(4) | 8303(3) | 1826(3) | 39(1) |
| C(28) | 4341(4) | 6394(3) | 1477(2) | 31(1) |
| C(29) | 4296(4) | 5924(3) | 2162(3) | 40(1) |

| | | | | |
|---|---|---|---|---|
| C(30) | 4775(4) | 4998(3) | 2314(3) | 47(1) |
| C(31) | 5313(4) | 4544(3) | 1791(3) | 49(1) |
| C(32) | 5399(4) | 5006(3) | 1131(3) | 45(1) |
| C(33) | 4922(4) | 5943(3) | 975(3) | 39(1) |
| N | 658(3) | 7736(3) | 417(2) | 32(1) |
| O(1) | 1769(2) | 6323(2) | 1565(2) | 41(1) |
| O(2) | 14(3) | 7647(2) | 1823(2) | 36(1) |
| O(3) | -1804(3) | 7184(3) | 1723(2) | 52(1) |
| O(4) | 1728(2) | 9015(2) | 1429(2) | 34(1) |
| P | 3642(1) | 7591(1) | 1294(1) | 27(1) |

Table C. Bond lengths [Å] and angles [°] for **4**.

| | | | |
|---|---|---|---|
| Re-O(1) | 1.681(3) | C(14)-C(15) | 1.392(6) |
| Re-O(4) | 2.019(3) | C(15)-O(4) | 1.337(5) |
| Re-O(2) | 2.057(4) | C(16)-C(21) | 1.382(6) |
| Re-C(1) | 2.138(4) | C(16)-C(17) | 1.406(6) |
| Re-N | 2.165(4) | C(16)-P | 1.819(5) |
| Re-P | 2.4725(14) | C(17)-C(18) | 1.379(8) |
| C(2)-O(3) | 1.217(6) | C(18)-C(19) | 1.371(8) |
| C(2)-O(2) | 1.307(6) | C(19)-C(20) | 1.382(7) |
| C(2)-C(3) | 1.511(7) | C(20)-C(21) | 1.375(7) |
| C(3)-C(8) | 1.394(6) | C(22)-C(23) | 1.379(6) |
| C(3)-C(4) | 1.405(6) | C(22)-C(27) | 1.396(6) |
| C(4)-C(5) | 1.363(7) | C(22)-P | 1.829(4) |
| C(5)-C(6) | 1.370(8) | C(23)-C(24) | 1.395(6) |
| C(6)-C(7) | 1.378(7) | C(24)-C(25) | 1.359(7) |
| C(7)-C(8) | 1.386(6) | C(25)-C(26) | 1.378(6) |
| C(8)-N | 1.431(6) | C(26)-C(27) | 1.375(6) |
| C(9)-N | 1.297(5) | C(28)-C(33) | 1.370(6) |
| C(9)-C(10) | 1.425(6) | C(28)-C(29) | 1.392(6) |
| C(10)-C(11) | 1.398(6) | C(28)-P | 1.829(4) |

| | | | |
|---|---|---|---|
| C(10)-C(15) | 1.412(6) | C(29)-C(30) | 1.389(6) |
| C(11)-C(12) | 1.355(7) | C(30)-C(31) | 1.371(7) |
| C(12)-C(13) | 1.399(8) | C(31)-C(32) | 1.357(6) |
| C(13)-C(14) | 1.375(7) | C(32)-C(33) | 1.403(6) |

| | | | |
|---|---|---|---|
| O(1)-Re-O(4) | 169.17(15) | O(4)-C(15)-C(10) | 121.2(4) |
| O(1)-Re-O(2) | 98.38(13) | C(14)-C(15)-C(10) | 119.1(4) |
| O(4)-Re-O(2) | 91.65(11) | C(21)-C(16)-C(17) | 117.8(4) |
| O(1)-Re-C(1) | 98.98(16) | C(21)-C(16)-P | 125.2(3) |
| O(4)-Re-C(1) | 86.09(15) | C(17)-C(16)-P | 116.9(4) |
| O(2)-Re-C(1) | 83.82(17) | C(18)-C(17)-C(16) | 120.3(5) |
| O(1)-Re-N | 98.78(14) | C(19)-C(18)-C(17) | 121.0(5) |
| O(4)-Re-N | 78.57(13) | C(18)-C(19)-C(20) | 119.1(5) |
| O(2)-Re-N | 81.60(15) | C(21)-C(20)-C(19) | 120.5(5) |
| C(1)-Re-N | 158.45(17) | C(20)-C(21)-C(16) | 121.3(4) |
| O(1)-Re-P | 86.58(11) | C(23)-C(22)-C(27) | 119.0(4) |
| O(4)-Re-P | 83.56(9) | C(23)-C(22)-P | 121.8(3) |
| O(2)-Re-P | 174.56(8) | C(27)-C(22)-P | 119.2(3) |
| C(1)-Re-P | 93.24(14) | C(22)-C(23)-C(24) | 119.9(5) |
| N-Re-P | 99.91(11) | C(25)-C(24)-C(23) | 120.9(5) |
| O(3)-C(2)-O(2) | 120.8(5) | C(24)-C(25)-C(26) | 119.4(4) |
| O(3)-C(2)-C(3) | 118.9(4) | C(27)-C(26)-C(25) | 120.8(5) |
| O(2)-C(2)-C(3) | 120.2(4) | C(26)-C(27)-C(22) | 120.0(4) |
| C(8)-C(3)-C(4) | 117.9(5) | C(33)-C(28)-C(29) | 118.4(4) |
| C(8)-C(3)-C(2) | 124.9(4) | C(33)-C(28)-P | 123.0(3) |
| C(4)-C(3)-C(2) | 117.0(5) | C(29)-C(28)-P | 118.6(3) |
| C(5)-C(4)-C(3) | 121.4(5) | C(30)-C(29)-C(28) | 120.7(5) |
| C(4)-C(5)-C(6) | 119.7(5) | C(31)-C(30)-C(29) | 119.9(5) |
| C(5)-C(6)-C(7) | 120.8(5) | C(32)-C(31)-C(30) | 120.1(4) |
| C(6)-C(7)-C(8) | 119.9(5) | C(31)-C(32)-C(33) | 120.3(5) |

| | |
|---|---|
| C(7)-C(8)-C(3) 120.2(4) | C(28)-C(33)-C(32) 120.5(4) |
| C(7)-C(8)-N 121.2(4) | C(9)-N-C(8) 118.1(4) |
| C(3)-C(8)-N 118.5(4) | C(9)-N-Re 129.7(3) |
| N-C(9)-C(10) 125.1(4) | C(8)-N-Re 112.2(3) |
| C(11)-C(10)-C(15) 118.7(4) | C(2)-O(2)-Re 125.8(3) |
| C(11)-C(10)-C(9) 120.5(4) | C(15)-O(4)-Re134.0(3) |
| C(15)-C(10)-C(9) 120.4(4) | C(16)-P-C(28) 103.8(2) |
| C(12)-C(11)-C(10) 121.4(5) | C(16)-P-C(22) 105.0(2) |
| C(11)-C(12)-C(13) 120.1(5) | C(28)-P-C(22) 103.85(18) |
| C(14)-C(13)-C(12) 119.6(5) | C(16)-P-Re 112.89(15) |
| C(13)-C(14)-C(15) 120.9(5) | C(28)-P-Re 110.65(15) |
| O(4)-C(15)-C(14) 119.7(4) | C(22)-P-Re 119.19(15) |

Table D. Anisotropic displacement parameters ($Å^2 \times 10^3$) for **4**. The anisotropic displacement factor exponent takes the form: $-2\pi^2[\, h^2 a^{*2} U_{11} + \ldots + 2\, h\, k\, a^* b^* U_{12}\,]$

| | $U_{11}$ | $U_{22}$ | $U_{33}$ | $U_{23}$ | $U_{13}$ | $U_{12}$ |
|---|---|---|---|---|---|---|
| Re | 30(1) | 30(1) | 24(1) | 0(1) | 5(1) | 0(1) |
| C(1) | 46(3) | 45(2) | 30(3) | -3(2) | 5(2) | -4(2) |
| C(2) | 31(3) | 34(2) | 43(3) | 11(2) | 6(2) | 8(2) |
| C(3) | 34(3) | 34(2) | 41(3) | 6(2) | -1(2) | 4(2) |
| C(4) | 44(3) | 51(3) | 50(3) | 13(2) | -1(3) | -9(2) |
| C(5) | 59(4) | 49(3) | 56(4) | 2(3) | -10(3) | -16(3) |
| C(6) | 69(4) | 49(3) | 43(3) | -11(2) | -6(3) | -4(3) |
| C(7) | 49(3) | 52(3) | 35(3) | 0(2) | 0(2) | 3(2) |
| C(8) | 29(3) | 37(2) | 33(3) | 3(2) | 3(2) | 4(2) |
| C(9) | 38(3) | 47(2) | 27(3) | 4(2) | 4(2) | 7(2) |
| C(10) | 35(3) | 37(2) | 39(3) | 9(2) | 10(2) | 7(2) |
| C(11) | 54(3) | 54(3) | 45(3) | 17(2) | 12(3) | 14(2) |
| C(12) | 62(4) | 44(3) | 69(4) | 31(3) | 26(3) | 9(2) |

| | | | | | | |
|---|---|---|---|---|---|---|
| C(13) | 58(4) | 38(3) | 83(5) | 14(3) | 22(3) | 1(2) |
| C(14) | 51(3) | 34(2) | 58(3) | 6(2) | 12(3) | 1(2) |
| C(15) | 34(3) | 32(2) | 45(3) | 7(2) | 13(2) | 7(2) |
| C(16) | 35(3) | 32(2) | 27(3) | -2(2) | 7(2) | 6(2) |
| C(17) | 41(3) | 42(2) | 30(3) | -3(2) | 3(2) | 4(2) |
| C(18) | 61(4) | 57(3) | 31(3) | -13(2) | 5(3) | 9(2) |
| C(19) | 85(4) | 64(3) | 32(3) | 9(3) | 19(3) | 6(3) |
| C(20) | 76(4) | 64(3) | 46(3) | 17(3) | 20(3) | -9(3) |
| C(21) | 53(3) | 45(3) | 32(3) | 2(2) | 9(2) | -7(2) |
| C(22) | 33(3) | 33(2) | 27(3) | -1(2) | 3(2) | -3(2) |
| C(23) | 34(3) | 40(2) | 41(3) | -10(2) | 5(2) | -2(2) |
| C(24) | 61(4) | 41(3) | 45(3) | -17(2) | 9(3) | -3(2) |
| C(25) | 43(3) | 49(3) | 37(3) | -7(2) | 1(2) | -10(2) |
| C(26) | 31(3) | 57(3) | 40(3) | -4(2) | 1(2) | -5(2) |
| C(27) | 34(3) | 43(2) | 38(3) | -7(2) | 4(2) | 2(2) |
| C(28) | 31(2) | 26(2) | 33(3) | -1(2) | 2(2) | 1(2) |
| C(29) | 40(3) | 45(3) | 36(3) | 4(2) | 10(2) | 7(2) |
| C(30) | 45(3) | 48(3) | 45(3) | 18(2) | 1(3) | 1(2) |
| C(31) | 44(3) | 33(2) | 66(4) | 5(2) | 4(3) | 8(2) |
| C(32) | 46(3) | 43(2) | 48(3) | -8(2) | 13(3) | 15(2) |
| C(33) | 39(3) | 43(2) | 35(3) | 0(2) | 9(2) | 6(2) |
| N | 31(2) | 42(2) | 23(2) | 0(2) | 9(2) | 6(2) |
| O(1) | 38(2) | 33(2) | 52(2) | -3(1) | 8(2) | -4(1) |
| O(2) | 34(2) | 45(2) | 32(2) | -1(1) | 12(2) | 1(1) |
| O(3) | 34(2) | 69(2) | 59(3) | 5(2) | 22(2) | 3(2) |
| O(4) | 42(2) | 27(2) | 34(2) | 0(1) | 10(2) | 0(1) |
| P | 30(1) | 28(1) | 23(1) | -3(1) | 4(1) | 0(1) |

Table E. Hydrogen coordinates ( $\times 10^4$) and isotropic displacement parameters ($Å^2 \times 10^3$) for **4**.

| | x | y | z | U(eq) |
|---|---|---|---|---|
| H(1A) | 1988 | 8467 | 2871 | 61 |
| H(1B) | 3051 | 7767 | 2875 | 61 |
| H(1C) | 1876 | 7347 | 3038 | 61 |
| H(4) | -2304 | 5867 | 770 | 59 |
| H(5) | -2439 | 5087 | -375 | 69 |
| H(6) | -1138 | 5444 | -1150 | 67 |
| H(7) | 239 | 6651 | -818 | 56 |
| H(9) | 244 | 8366 | -553 | 45 |
| H(11) | 1188 | 9767 | -1009 | 61 |
| H(12) | 2164 | 11209 | -773 | 68 |
| H(13) | 2798 | 11734 | 477 | 70 |
| H(14) | 2542 | 10741 | 1474 | 56 |
| H(17) | 2537 | 6723 | -81 | 46 |
| H(18) | 2465 | 6967 | -1363 | 60 |
| H(19) | 3526 | 8198 | -1784 | 71 |
| H(20) | 4701 | 9184 | -905 | 73 |
| H(21) | 4784 | 8957 | 375 | 52 |
| H(23) | 3578 | 9344 | 2208 | 47 |
| H(24) | 4956 | 10457 | 2797 | 59 |
| H(25) | 6885 | 10233 | 2776 | 53 |
| H(26) | 7470 | 8871 | 2183 | 52 |
| H(27) | 6126 | 7759 | 1585 | 46 |
| H(29) | 3942 | 6234 | 2522 | 48 |
| H(30) | 4731 | 4686 | 2770 | 56 |
| H(31) | 5620 | 3919 | 1888 | 58 |
| H(32) | 5775 | 4699 | 781 | 55 |
| H(33) | 5001 | 6261 | 527 | 47 |

# CHAPTER VII. METHYL(OXO)RHENIUM(V) COMPLEXES WITH CHELATING LIGANDS

A manuscript submitted to *Inorganic Syntheses*

Xiaopeng Shan AND James H. Espenson

## Introduction

During the period 1998-2003, members of a new class of rhenium(V) compounds were synthesized and characterized. Many of them are useful catalysts for oxygen atom transfer reactions, such as

$$C_5H_5NO + PPh_3 \rightarrow C_5H_5N + Ph_3PO$$

which do not occur at all, despite a considerable driving force. In the case shown, $\Delta G°$ is ca. –300 kJ $mol^{-1}$. The further importance of these compounds is their relation to the more extensively studied molybdenum and tungsten oxotransferase enzymes and their mimics.

Most of the compounds are five-coordinate, with a square pyramidal geometry about rhenium. The equatorial positions are occupied by the $CH_3$ group, a heteroatom (usually S, P, N or O) and by the two donor atoms of bidentate chelate, which in many instances is a dithiolate. The second set of compounds is six-coordinate, with the lower axial position trans to the terminal oxo group occupied by one arm of a chelate ligand that is also connected to an equatorial position. In this general sense, then, with E representing one or another of the heteroatoms, the structural formulas are:

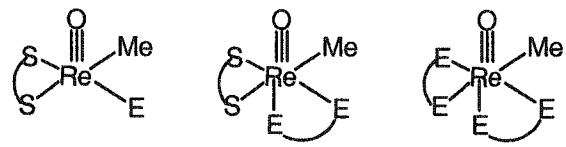


All of these compounds have been prepared from methyltrioxorhenium(VII), abbreviated as MTO. Reduction to rhenium(V) is accomplished in these procedures with thiols, phosphanes and sulfanes. Suitable stabilizing ligands must be present to intercept $MeReO_2 \cdot L_2$, which is quite reactive: even perchlorate ions are reduced by it. With neither a stabilizing ligand nor an oxidant, a black precipitate is formed from the polymerization of methyldioxorhenium(V).

**Methyl(oxo)rhenium(V) dithiolate dimers: {MeReO($\kappa^2$-dithiolate)}$_2$**

The dimeric compounds were prepared from MTO and a dithiol that will form a five- or six-membered chelate with rhenium. Three procedures were used, in one of which {MeReO(SPh)$_2$}$_2$ was first prepared. The structural formulas of the products are these:

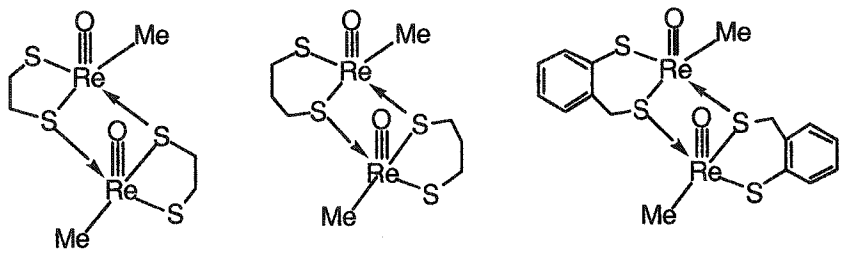


*Procedure 1*

$$2\ \text{MTO} + 4\ \text{mtpH}_2 \rightarrow \{\text{MeReO(mtp)}\}_2 + \text{S,S'-mtp} + 4\ \text{H}_2\text{O}$$

To a stirred solution containing MTO (200 mg, 0.8 mmol) in toluene (10 mL) cooled in an ice-water bath, mtpH$_2$ (0.5 mL, 3.2 mmol) was added dropwise. After 15 min, hexane (5 mL) was added and the reaction mixture kept in a freezer overnight. Fine needle-like crystals precipitated and were filtered, washed with cold hexane and dried. Yield: 259 mg (88%).

*Anal.* Calc. for $C_{16}H_{18}O_2Re_2S_4$: C 25.85, H 2.44, S 17.27; Found: C 26.58, H 2.53, S 17.33. $^1$H NMR ($C_6D_6$): δ 7.52 (d, 2H, J = 8 Hz), 7.03 (m, 2H), 6.91 (m, 4H), 4.05 (d, 2H, J = 10.8 Hz), 3.53 (d, 2H, J = 10.8 Hz), 2.91 (s, 6H). $^{13}$C NMR ($C_6D_6$): 141.95, 135.81, 10.62, 130.56, 127.87, 36.91, 17.10.

*Procedure 2*

$$\{\text{MeReO(SPh)}_2\}_2 + 2\ \text{HS(CH}_2)_n\text{SH}\ \ (n=2, 3) \rightarrow \{\text{MeReO[S(CH}_2)_n\text{S]}\}_2 + 4\ \text{PhSH}$$

A solution containing {MeReO(SPh)$_2$}$_2$ (87 mg, 0.1 mmol) in toluene (10 mL) was treated with 1,3-propanedithiol, 0.25 mmol) and then stirred for 4 h. The solution was concentrated to 1 mL by vacuum and hexane (5 mL) was layered on it. This produced a brown {MeReO(pdt)}$_2$, which was filtered and washed with hexanes. Yield 55 mg (85%).

*Anal.* Calc. for $C_8H_{16}O_2Re_2S_4$: C 14.85, H 2.80, S 19.83; Found: C 15.17, H 2.65, S 19.89. $^1$H NMR ($C_6D_6$): δ 32.84 (s, 6H), 2.65 (m, 4H), 2.43 (m, 2H), 2.18 (m, 4H), 2.08 (m, 2H). $^{13}$C NMR ($C_6D_6$): 34.0, 33.1, 29.5, 19.6.

The same procedure was used for {MeReO(edt)}$_2$, except that $Me_2S$ (2 mmol) was added to catalyze the reaction. Yield 45 mg (73%).

*Anal.* Calc. for $C_6H_{14}O_2Re_2S_4$: C 11.82, H 2.39, S 20.93; Found: C 11.73, H 2.27, S 20.82. $^1$H NMR ($C_6D_6$): δ 3.65 (m, 2H), 2.62 (s, 6H), 2.37 (m, 2H), 2.24 (m, 2H), 1.92 (m, 2H). $^{13}$C NMR ($C_6D_6$): 47.1, 36.6, 13.2.

*Procedure 3*

$$MTO + diphenylacetylene + PPh_3 \rightarrow MeReO_2(\eta^2\text{-diphenylacetylene}) + OPPh_3$$

$$2\ MeReO_2(\eta^2\text{-diphenylacetylene}) + 2\ edtH_2 \rightarrow \{MeReO(edt)\}_2 + 2\ diphenylacetylene$$

To a stirred solution containing MTO (250 mg, 1.0 mmol) and diphenylacetylene (178 mg, 1.0 mmol), $PPh_3$ (262 mg, 1.0 mmol) was added. After 10 min. the color of the resulting solution changed from colorless to yellow. Then 1,2-ethanedithiol (94 mg, 84 μL, 1.0 mmol) was added dropwise. The mixture was stirred at room temperature for 6 h and layered with hexane (20 mL). After 2 days, a brown-black solid deposited out and was collected by filtration and washed with hexane. Yield: 370 mg (60%).

**Methyl(oxo)rhenium(V) dithiolate monomers: [MeReO(κ$^2$-dithiolate)L]**

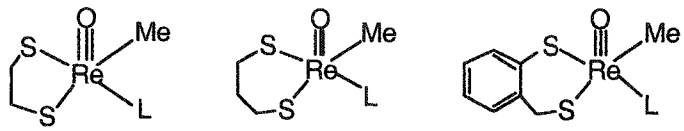


One method is treatment of the dimer from Part A with a Lewis base such as a pyridine, phosphane or thiourea. Alternatively, MeReO(SPh)$_2$L' (L' is often 4-*tert*-butylpyridine) can first be prepared and then converted to the product with a dithiol. The second procedure is required if L is a bidentate chelate.

*Procedure 1*

$$\{MeReO(dithiolato)\}_2 + 2\ L \rightarrow 2\ MeReO(dithiolato)L$$

To a solution of methyloxorhenium(V) dithiolato dimeric compounds in benzene, a Lewis base was added in excess. This reaction comes to equilibrium, and excess ligand is

needed, especially for pyridines. The resulting mixture was stirred until the reaction was complete, as determined by the color change. It was layered with the same volume of hexane and kept in a freezer overnight. A solid precipitated out and was collected by filtration and washing with hexane.

L = pyridine: MeReO(mtp)(Py) was synthesized from $\{MeReO(mtp)\}_2$ and pyridine. The color change during the reaction is from yellow to green. The analogous procedure is used for ring-substituted pyridines.

*Anal.* $^1H$ NMR($C_6D_6$): δ 7.72 (m, 3H), 7.14 (m, 2H), 6.35 (m, 1H), 6.24 (m, 2H), 4.67 (d, 1H, J = 12.0 Hz), 3.65 (d, 1H, J = 12.0 Hz), 2.76 (s, 3H). UV(benzene): 608 nm(255 $M^{-1}cm^{-1}$), 368 nm (7540 $M^{-1}cm^{-1}$).

L = 1,1,3,3-tetramethylthiourea (tmtu): MeReO(mtp)(tmtu) was synthesized from $\{MeReO(mtp)\}_2$ and 1,1,3,3-tetramethylthiourea (tmtu). The color change during the reaction is from yellow to pink.

*Anal.* $^1H$ NMR ($C_6D_6$): δ 7.44 (d, 1H, j =7.6 Hz), 7.25 (m, 2H), 7.13 (m, 1H), 4.73 (d, 1H, j =11.6 Hz), 3.21 (s, 12H), 2.96 (d, 1H, J = 11.6 Hz), 2.31 (s, 3H). $^{13}C$ NMR ($C_6D_6$): 193.94, 143.44, 141.40, 128.61, 128.00, 127.15, 125.91, 44.30, 39.44, 11.58. UV(benzene): 608 nm (255 $M^{-1}cm^{-1}$).

MeReO(edt)(tmtu) was synthesized from $\{MeReO(edt)\}_2$ and 1,1,3,3-tetramethylthiourea. The color changed during the reaction from brown to violet. Yield: 76%.

*Anal.* $^1H$ NMR ($C_6D_6$): δ 3.58 (m, 1H), 3.25 (s, 3H), 3.13 (m, 1H), 3.04 (m, 1H), 2.69 (m, 1H), 2.38 (sb, 12H); $^{13}C$ ($C_6D_6$): δ 46.2, 43.2, 6.80.

L = triphenylphosphane: MeReO(mtp)($PPh_3$) was synthesized from $\{MeReO(mtp)\}_2$ and $PPh_3$. The color change during the reaction is from yellow to green. Yield: 90%

*Anal.* Calc. for $C_{26}H_{24}OPReS_2$: C 49.25, H 3.82, S 10.12; Found: C 49.25, H 3.60, S 9.78. $^1H$ NMR ($C_6D_6$): δ 7.84 (d, 1H, J = 7.6 Hz), 7.67 (m, 6H), 7.11 (t, 1H, J = 7.6 Hz), 7.04 (d, 1H), 6.90 (m, 10 H), 4.80 (d, 1H, J = 10.6 Hz), 3.25 (d, 1H, J = 10.6 Hz), 2.97 (d, 3H, J = 8.4 Hz). $^{13}C$ NMR($C_6D_6$): 142.66, 140.37, 137.84 (d, J = 9.2 Hz), 134.62 (d, J = 7.7 Hz), 133.99 (d, J = 14.7 Hz), 131.14 (d, J = 1.7 Hz), 130.98, 130.47, 129.29, 126.29, 42.54 (d, J = 7.1 Hz), 15.45 9d, J = 3Hz). $^{31}P$ NMR ($C_6D_6$): 27.82. UV(benzene): 606 nm (190 $M^{-1}cm^{-1}$).

The same procedure works for alkyl and aryl phosphanes in general. MeReO(mtp)PMePh$_2$ was synthesized from {MeReO(mtp)}$_2$ and PMePh$_2$. Yield; 80%.

*Anal.* Calc. for $C_{21}H_{22}OPReS_2$: C 44.12, H 3.88, S 11.2; Found: C 44.72, H 3.87, S 10.2.

*Procedure 2*

$$\{MeReO(SPh)_2\}_2 + 2\ PPh_3 \rightarrow 2\ MeReO(SPh)_2(PPh_3)$$

$$MeReO(SPh)_2(PPh_3) + edtH_2 \rightarrow MeReO(edt)(PPh_3) + 2\ PhSH$$

A stirred solution of {MeReO(SPh)$_2$}$_2$ (87.0 mg, 0.1 mmol) in toluene (10 mL) was treated with PPh$_3$ (65.6 mg, 0.25 mmol) at room temperature. After 1 h, the mixture was concentrated to 1 mL by vacuum, and hexane (10 mL) was layered on top. The resulting mixture was kept in a freezer overnight. A green powder, MeReO(SPh)$_2$(PPh$_3$), deposited. It was collected by filtration and washed with hexane. Yield, 81%. 1,2-Ethanedithiol (14.2 mg, 0.01 mL, 0.125 mmol) was added to a stirred solution of MeReO(SPh)$_2$(PPh$_3$) (66.6 mg, 0.1 mmol ) in toluene (10 mL) at room temperature. After 2 h, the solution was concentrated to 1 mL, and hexane (10 mL) was layered. The resulting solution was kept in a freezer overnight. MeReO(edt)(PPh$_3$) was obtained in 60% yield.

*Anal.* Calc. for $C_{21.5}H_{23}ReOPS_2Cl$: C 42.0, H 3.97, S 10.4; Found: C 42.9, H 3.97, S 9.6. $^1$H NMR ($C_6D_6$): δ 7.74 (m, 6H), 6.94 (m, 9H), 3.60 (m, 1H), 3.31 (m, 1H), 2.88 (d, 3H, $J$ = 7.6 Hz), 2.73 (m, 1H), 2.40 (m, 1H). $^{13}$C NMR ($C_6D_6$): 134.57 (d, $J$ = 42 Hz), 131.13 (d, $J$ = 112.8 Hz), 130.45 (d, $J$ = 204 Hz), 128.76 (d, $J$ = 42.4 Hz), 46.32 (d, $J$ = 25.2 Hz), 43.50 (s) 11.64 (d, $J$ = 11.6).

*Procedure 3*

$$\{MeReO(SPh)_2\}_2 + 2\ (2\text{-}CH_3C_5H_4N) + 2\ edtH_2 \rightarrow 2\ [2\text{-}CH_3C_5H_4NH]^+\ [MeReO(edt)(SPh)]^- + 2\ PhSH$$

To a solution containing {MeReO(SPh)$_2$}$_2$ (87 mg, 0.1 mmol) and 2-picoline (2-CH$_3$C$_5$H$_4$N) (18.6 mg, 19.8 μL, 0.2 mmol) in toluene (20 mL) was added edtH$_2$ (18.8 mg, 16.8 μL, 0.2 mmol). The solution was stirred for 2 h; a dark red solid deposited at the bottom of the container which was rinsed by hexanes and dried under vacuum. Yield: 97%.

*Anal.* Calc. for $C_{15}H_{20}NOReS_3 \cdot C_6H_8N$: C 35.14, H 3.93, N 2.73, S 18.76; Found: C 35.30, H 4.05, N 2.71, S 19.08. $^1$H NMR ($CD_3CN$): δ 8.48 (d, 1H), 8.41 (m, 1H), 7.81 (m, 2H), 7.57 (m, 2H), 7.23 (t, 2H), 7.10 (t, 1H), 2.88 (m, 1H), 2.73 (s, 3H), 2.67 (m, 2H), 2.49 (m, 1H),

2.18 (s, 3H); $^{13}C$ NMR ($CD_3CN$): 150.0, 147.0, 133.9, 128.3, 127.5, 124.8, 124.7, 43.6, 43.4, 19.3, 7.2.

*Procedure 4*

$$\{MeReO(mtp)\}_2 + 2\ 4\text{-}Bu^t\text{-}Py \rightarrow 2\ MeReO(mtp)(4\text{-}Bu^t\text{-}Py)$$

$$MeReO(mtp)(4\text{-}Bu^t\text{-}Py) + 4,4'\text{-}Me_2\text{-}2,2'\text{-}Bpy \rightarrow MeReO(mtp)(4,4'\text{-}Me_2\text{-}2,2'\text{-}Bpy) + 4\text{-}Bu^t\text{-}Py$$

To a stirred solution containing $\{MeReO(mtp)\}_2$ (0.1 mmol) in toluene (10 mL), 4-*tert*-butylpyridine (1 mmol) was added. After 5 min, the color of the solution changed from yellow to green. Then 4,4'-dimethyl-2,2'-bipyridne (4,4'-$Me_2$-2,2'-bpy, 0.24 mmol) was added. A red solid precipitated and was collected by filtration and washed with hexane.

*Anal.* Calc. for $C_{20}H_{21}N_2OReS_2 \cdot C_7H_8$: C 50.06, H 4.51,N 4.32, S 9.76; Found: C 50.14, H 4.41, N 4.30, S 9.90.

An analog of one of these compounds, but with a terminal thio group in place of oxo has been prepared and characterized. It is $MeReS(mtp)PPh_3$.

*Procedure 5*

$$\{MeReO(mtp)\}_2 + 2\ PPh_3 \rightarrow 2\ MeReO(mtp)PPh_3$$

$$MeReO(mtp)PPh_3 + P_4S_{10} \rightarrow MeReS(mtp)PPh_3 + P_4S_9O$$

In 20 mL of toluene$\{MeReO(mtp)\}_2$ (150 mg, 0.2 mmol) was stirred with $PPh_3$ (121.8 mg, 0.46 mmol) at room temperature. The formation of the monomeric phosphine complex is indicated by the color of the solution changing from yellow to green. After 8 hours, $P_4S_{10}$ (143 mg) was added and stirred for another 2 hours. The color of the solution changed to red in this period. The reaction mixture was concentrated under vacuum to ca. 1 mL and chromatographed on silica (5% EtOAc in hexane). Yield: 147 mg (56%).

$^1H$ NMR($C_6D_6$): δ 7.73-7.41 (m, 15 H), 7.29 (t, 1H), 7.25 (m, 2H), 7.15(t, 1H), 4.98 (d, 1H), 3.75 (d, 3H), 2.63 (d, 1H); $^{13}C$ NMR($C_6D_6$): 146.74, 138.91, 134.58, 132.34, 131.61, 131.09, 128.83, 128.66, 128.41, 126.45, 49.66, 16.06; $^{31}P$ NMR($C_6D_6$): δ 23.42.

**Methyl(oxo)rhenium(V) complexes with two monoanionic bidentate ligands: [MeReO($\kappa^2$-chelate)$_2$]**

These compounds can be synthesized from MTO and the protonated bidentate ligand, with Re(VII) being reduced by a phosphane or sulfane. In the case of MeReO(dppba), where dppba is 2-phenylphosphinobenzoic acid, the ligand itself acts as the reducing agent. The other chelating ligands (X,Y$^-$, in general) are pa$^-$ (paH is 2-picolinic acid), hq$^-$ (hqH is 8-hydroxyquinoline) and mq$^-$ (mqH is 8-mercaptoquinoline).

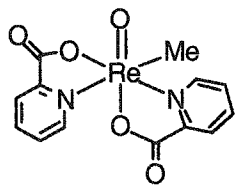

MeReO(pa)$_2$

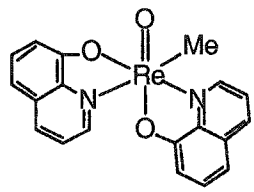

MeReO(hq)$_2$

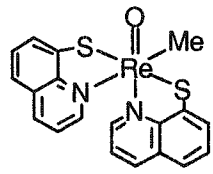

*trans*-MeReO(mq)$_2$

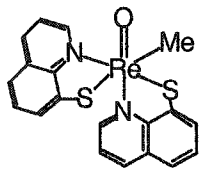

*cis*-MeReO(mq)$_2$

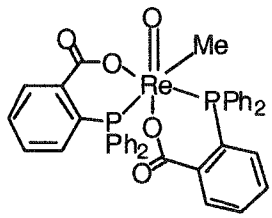

*cis*-MeReO(dppba)$_2$

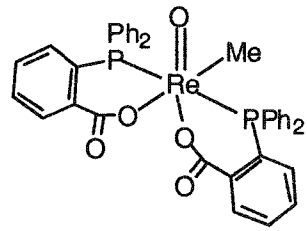

*trans*-MeReO(dppba)$_2$

*Procedure 1*

$$MTO + 2\ H(X,Y) + PPh_3/Me_2S \rightarrow MeRe(O)(X,Y)_2 + H_2O + Ph_3PO/Me_2SO$$

To a solution containing MTO (50 mg, 0.2 mmol) and the bidentate ligand (0.4 mmol) in $CH_2Cl_2$ (20 mL), $PPh_3$ (53 mg, 0.2 mmol) was added. The mixture was stirred for 12 h, layered with hexanes (20 mL) and placed in a freezer at ca. –12 °C. After 24 h a black powder had deposited; it was filtered and rinsed with hexanes. Dimethyl sulfide (19 mg, 0.3 mmol) can replace $PPh_3$.

MeReO(pa)$_2$ was synthesized from MTO and 2-picolinic acid (paH). Yield: 83% from $PPh_3$, 53% from dimethyl sulfide. The isomeric structure was established crystallographically.

*Anal.* Calc. for $C_{13}H_{11}N_2O_5Re$: C 33.84, H 2.40, N 6.07; Found: C 33.85, H 2.48, N 6.06. $^1$H NMR ($CDCl_3$): δ 8.84 (d, 1H), 8.52 (d, 1H), 8.44 (m, 1H), 8.29 (m, 1H), 8.19 (d, 1H), 7.77

(m, 3H), 4.43 (s, 3H); $^{13}C$ NMR ($CDCl_3$): 180, 163, 153, 150, 148, 146, 143, 130, 126, 125, 53, 29, 11. IR ($CHCl_3$): 1002.85 $cm^{-1}$ and, for the $^{18}O$-labeled compound, 950.75 $cm^{-1}$. UV-Vis ($CHCl_3$), $\lambda_{max}$/nm (log $\varepsilon$/L $mol^{-1}$ $cm^{-1}$): 568 (2.3), 396.5 (3.83) and 260 (4.14).

$MeReO(hq)_2$ was synthesized from MTO, 8-hydroxyquinoline (hqH) and $PPh_3$. Yield: 80%.

*Anal.* Calc. for $C_{19}H_{15}N_2O_3Re$: C 45.14, H 2.99, N 5.54; Found: C 44.64, H 2.92, N 5.29. $^1H$ NMR ($CDCl_3$): $\delta$ 8.56 (d, 1H), 8.36 (m, 1H), 8.21 (m, 1H), 7.66 (m, 4H), 7.40 (m, 3H), 7.07 (d, 1H) 6.46 (d, 1H), 4.53 (s, 3H). IR ($CHCl_3$): 979.86 $cm^{-1}$. UV-Vis ($CHCl_3$), $\lambda_{max}$/nm (log $\varepsilon$/L $mol^{-1}$ $cm^{-1}$): 470 (sh), 417 (3.70) and 360 (sh).

$MeReO(mq)_2$ was synthesized from MTO and 8-mercaptoquinoline (mqH). Yield: 50%.

*Anal.* Calc. for $C_{19}H_{15}N_2OReS_2$: C 42.44, H 2.81, N 5.21, S 11.93; Found: C 42.16, H 2.54, N 5.13, S 11.37. Two sets of $^1H$ NMR resonance peaks were found in solution in a 3:1 ratio. Two geometric isomers were assigned according to the x-ray structures and an earlier study of pyridine exchange reactions. In solution, the major species is *trans*-$MeReO(mq)_2$, $^1H$ NMR ($CDCl_3$): $\delta$ 10.88 (d, 1H), 8.39 (d, 1H), 8.34 (d, 2H), 8.06 (d, 2H), 7.80 (t, 1H), 7.74 (d, 1H), 7.58 (m, 1H), 7.74 (d, 1H), 7.41 (t, 1H), 6.95 (d, 1H), 6.75 (m, 1H), 4.95 (s, 3H). The minor solution species is *cis*-$MeReO(mq)_2$. Only three peaks are available due to broadening and overlap with peaks from **3a**. $^1H$ NMR ($CDCl_3$): $\delta$ 9.40 (s, 1H), 8.65 (s, 1H), 5.14 (s, 3H) ppm. $^{13}C$: too insoluble. IR ($CHCl_3$): **3a**, 985.46 $cm^{-1}$; **3b**, 998.96 $cm^{-1}$. UV-Vis ($CHCl_3$), $\lambda_{max}$/nm (log $\varepsilon$/L $mol^{-1}$ $cm^{-1}$): 699 (2.6), 432 (3.78) and 267.5 (4.43).

*Procedure 2*

$$MTO + 3\ dppbaH \rightarrow MeReO(dppba)_2 + dppbaH + H_2O$$

To a solution containing MTO (50 mg, 0.2 mmol) in $CH_2Cl_2$ (20 mL) 2-diphenylphosphinobenzoic acid (184 mg, 0.6 mmol) was added. The color of the solution changed to violet. After 12 h stirring the mixture was layered with hexanes and put into the freezer. A dark powder was isolated by filtration 24 h later and rinsed with hexanes. $MeReO(dppba)_2$ has two geometric isomers. Yield: 65% (total).

**Methyl(oxo)rhenium(V) complexes with tridentate ligands**

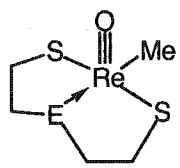


E = O, S

MeReO(SOS)

MeReO(SSS)

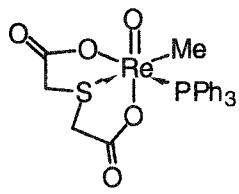


$MeReO(OSO)PPh_3$

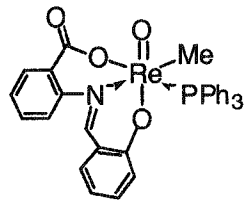


$MeReO(ONO)PPh_3$

Two methods have been used: ligand displacement from $\{MeReO(SPh)_2\}_2$ and reduction of MTO in the presence of $H_2(X,Y,X)$.

*Procedure 1*

$$\{MeReO(SPh)_2\}_2 + 2\ H_2XYX \rightarrow 2\ MeReO(XYX) + 4\ PhSH$$

$\{MeReO(SPh)_2\}_2$ (87 mg, 0.1 mmol) and the tridentate ligand (0.2 mmol) were mixed in toluene (20 mL), stirred for 4 hours, layered with hexane (20 mL) and placed in a freezer at ca. –12 °C. After 24 h a dark red powder had deposited; it was filtered and rinsed with hexanes.

MeReO(SSS): Yield: 84%.

*Anal.* Calc. for $C_5H_{11}OReS_3$: C 16.25, H 3.00, S 26.03; Found: C 16.36, H 2.82, S 26.15. $^1H$ NMR ($C_6D_6$): δ 3.55 (s, 3H), 3.28 (m, 2H), 2.42 (m, 2H), 2.25 (m, 2H), 0.56 (m, 2H); $^{13}C$ NMR ($C_6D_6$): 48.0, 43.5, 5.1. IR ($CHCl_3$): 983.53 $cm^{-1}$. UV-Vis ($CHCl_3$), $\lambda_{max}$/nm (log ε/L $mol^{-1}$ $cm^{-1}$): 252 (4.04) and 360 (sh).

MeReO(SOS): Yield: 66%.

*Anal.* Calc. for $C_5H_{11}O_2ReS_2$: C 16.99, H 3.14, S 18.14; Found: C 18.25, H 2.96, S 17.94. $^1H$ NMR ($C_6D_6$): δ 4.42 (s, 3H), 3.00 (m, 2H), 2.57 (m, 2H), 2.49 (m, 2H), 2.20 (m, 2H); $^{13}C$ NMR ($C_6D_6$): 85.1, 40.2, 4.0. IR ($CHCl_3$): 997.03 $cm^{-1}$. UV-Vis ($CHCl_3$), $\lambda_{max}$/nm (log ε/L $mol^{-1}$ $cm^{-1}$): 290 (sh).

*Procedure 2*

$$MeReO_3 + H_2XYX + PAr_3 \rightarrow MeReO(XYX) + H_2O + OPAr_3$$

MTO (250 mg, 1 mmol), the tridentate ligand (1 mmol) and a reducing agent such as triphenylphosphane or substituted triarylphosphanes (2 mmol) were mixed in $CH_2Cl_2$ (20

mL), stirred for 10 h, layered with hexane (20 mL) and placed in a freezer at ca. –12 °C. After 24 h a blue powder, $MeReO(OSO)PZ_3$, or dark red crystals, $MeReO(ONO)PPh_3$, had deposited. The solid was filtered and rinsed by hexane.

$MeReO(OSO)PPh_3$: Yield: 93%.

*Anal.* Calc. for $C_{23}H_{22}O_5PReS$: C 44.01, H 3.53, S 5.11, P 4.93; Found: C 43.97, H 3.51, S 4.66, P 4.30. $^1H$ NMR ($CDCl_3$): δ 7.47~7.70 (m, 15H), 4.58 (d, 3H), 3.61 (d, 1H), 3.36 (d, 1H), 2.89 (d, 1H), 1.38 (d, 1H); $^{13}C$ NMR ($CDCl_3$): 185.7, 177.8, 134.1 (d), 132.1 (d), 131.5 (d), 129.2 (d), 128.6 (d), 37.9, 36.6, 15.4; $^{31}P$ NMR ($CDCl_3$): δ 0.45. IR ($CHCl_3$): 1006.68 $cm^{-1}$. UV-Vis ($CHCl_3$), $\lambda_{max}$/nm (log ε/L $mol^{-1}$ $cm^{-1}$): 265 (sh) and 300 (sh).

The same procedure was successful for other triarylphosphanes, including $P(C_6H_4\text{-}4\text{-}OMe)_3$ and $P(C_6H_4\text{-}4\text{-}F)_3$.

$MeReO(ONO)PPh_3$: Yield: 93%.

*Anal.* Calc. for $C_{33}H_{27}NO_4PRe$: C 55.15, H 3.79, N 1.95, P 4.31; Found: C 53.83, H 3.59, N 1.85, P 4.02. $^1H$ NMR ($CD_2Cl_2$): δ 8.01 (m, 1H), 7.65 (s, 1H), 7.57 (m, 1H), 7.48 (m, 1H), 7.29 (d, 1H), 7.03 (m, 1H), 6.78 (m, 2H), 6.56 (d, 1H); $^{31}P$ NMR ($CD_2Cl_2$): –7.18. IR ($CHCl_3$): 983.58 $cm^{-1}$. UV-Vis ($CHCl_3$), $\lambda_{max}$/nm (log ε/L $mol^{-1}$ $cm^{-1}$): 300 (sh), 360 (sh) and 420 (sh).

**Complexes with N,N-diethylthiocarbamate (ddc) ligands**

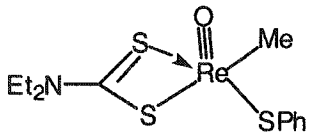


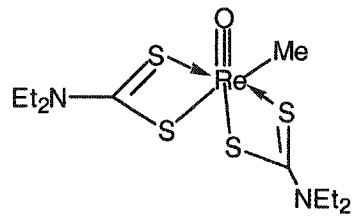


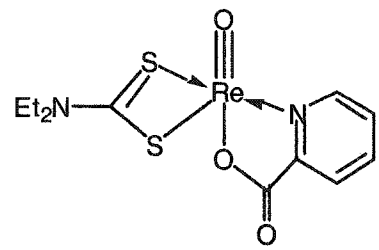


$MeReO(SPh)(ddc)$ $MeReO(ddc)_2$ $MeReO(pa)(ddc)$

The three methyl(oxo)rhenium(V) complexes shown were synthesized, either from Re(V) precursors, $\{MeReO(SPh)_2\}_2$ or $MeReO(pa)_2$, or by reduction of MTO with $PPh_3$ in the presence of $Na^+ddc^-$.

*Procedure 1*

$$\{MeReO(SPh)_2\}_2 + 2\ Na^+ddc^- \rightarrow 2\ MeReO(SPh)(ddc) + 2\ NaSPh$$

$\{MeReO(SPh)_2\}_2$ (1 mmol) mixed with $Na^+ddc^-$ (2 mmol) suspended in toluene (10 mL). The resulting mixture was stirred for 12 h and filtered. The filtrate was reduced to 1 mL by vacuum, layered with hexane (10 mL), and held at ca. –12 °C for 2 days. The red crystals that deposited were collected by filtration and washing with hexane. Yield: 73%.

*Anal.* Calc. for $C_{12}H_{18}NOReS_3$: C 30.36, H 3.82, N 2.95, S 20.27; Found: C 30.53, H 3.52, N 3.06, S 20.15. $^1H$ NMR ($C_6D_6$): 8.04(d, 2H), 7.25(m, 2H), 7.01(d, 1H), 4.06(s, 3H), 2.69(m, 1H), 2.56(m, 2H), 2.37(m, 1H), 0.40(t, 3H), 0.27(t, 3H)

*Procedure 2*

$$MTO + 2\ Na^+ddc^- + 2\ HOAc + PPh_3 \rightarrow MeReO(ddc)_2 + 2\ NaOAc + Ph_3PO$$

To the mixture of MTO (1 mmol) and acetic acid (2 mmol) in toluene (10 mL), $PPh_3$ (1 mmol) was added, stirred for 20 min as the color of the solution changed to red. Then $Na^+ddc^-$ (2 mmol) was added, stirred for 2 h until the color changed to green. The solution was filtered, layered with hexane (20 mL) and held at ca. –12 °C for 2 days. A green solid deposited on the bottom of the container, which was collected by filtration and washing by hexane. Yield: 81%.

$^1H$ NMR ($CDCl_3$): δ 4.74(s, 3H), 3.81(b, 8H), 1.36(b, 10H); $^{13}C$ NMR ($CDCl_3$): δ 45.1(b), 12.7, 5.0.

*Procedure 3*

$$MeReO(pa)_2 + Na^+ddc^- \rightarrow MeReO(pa)(ddc) + Na^+pa^-$$

$MeReO(pa)_2$ (1 mmol) was mixed with $Na^+ddc^-$ (1 mmol) suspended in toluene (10 mL). The resulting mixture was stirred for 4 h and filtered. The filtrate was layered with hexane (20 mL) and held at ca. –12 °C for 2 days. A violet solid was collected by filtration and washing with hexane. Yield: 92%.

*Anal.* Calc. for $C_{12}H_{17}N_2O_3ReS_2$: C 29.56, H 3.51, N 5.75, S 13.15; Found: C 29.44, H 3.32, N 5.62, S 12.82. $^1H$ NMR ($CDCl_3$): δ 8.84(d, 1H), 8.37(d, 1H), 7.84(t, 1 H), 7.63(t, 1H), 3.94(m, 2H), 3.85(m, 1H), 3.78(m, 1H), 3.66(s, 3H), 1.46(t, 3H), 1.42(t, 3H); $^{13}C$ NMR ( $CDCl_3$): 166.6, 149.2, 147.8, 141.7, 125.9, 125.8, 47.0, 45.7, 12.9, 12.6, 12.5.

**Oxorhenium(V) dithiolates**

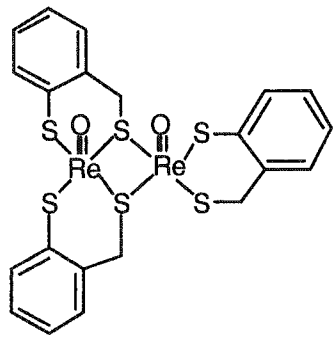

$\{ReO\}_2(mtp)_3$

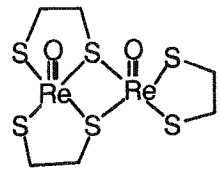

$\{ReO\}_2(edt)_3$

These two compounds are included, even though they formally lie outside the title of the chapter, because they are the most active Re(V) catalysts. They are prepared from $Re_2O_7$ and dithiols in two procedures, with and without benzene thiol.

*Procedure 1*

$$Re_2O_7 + 5\ mtpH_2 \rightarrow \{ReO\}_2(mtp)_3 + 2\ S,S'\text{-}mtp + 5H_2O$$

2-(Mercaptomethyl)thiophenol ($mtpH_2$, 3.0 g, 19 mmol) was added to a solution of dirhenium heptoxide (1.5 g, 3.1 mmol) in THF (20 mL). The dark brown solution was left to stand at room temperature for 2.5 h. Then hexane (70 mL) was added, and the reaction mixture kept at –11 °C for 2 days. After filtering and extensive washing with hexane, the product was isolated. Yield: 85%.

*Anal.* Calc. for $C_{21}H_{18}O_2Re_2S_6$: C 31.81, H 2.34, S 21.23; Found: C 31.70, H 2.45, S 21.03. $^1$H NMR ($CDCl_3$): δ 7.50-7.35 (m, 8H), 7.30-7.15 (m, 4H), 5.67 (d, 1H, $CH_2$, $J$ = 11.2), 5.21 (d, 1H, $CH_2$, $J$ = 11.2), 5.06 (d, 1H, $CH_2$, $J$ = 12.4), 4.30 (d, 1H, $CH_2$, $J$ = 11.6), 3.75 (d, 1H, $CH_2$, $J$ = 12.4), 3.62 (d, 1H, $CH_2$, $J$ = 11.2). $^{13}$C NMR ($CDCl_3$): 140.92, 140.36, 139.71, 139.02, 135.70, 135.47, 131.07, 130.94, 130.90, 130.58, 130.56, 130.38, 129.22, 128.97, 128.85, 128.70, 128.54, 128.42, 42.29, 40.92, 38.90.

*Procedure 2*

$$Re_2O_7 + 10\ PhSH \rightarrow \{ReO(SPh)_3\}_2 + 2\ S,S'\text{-}(SPh)_2 + 5\ H_2O$$

$$\{ReO(SPh)_3\}_2 + 3\ edtH_2 \rightarrow \{ReO\}_2(edt)_3 + 6\ PhSH$$

Benzenethiol (PhSH, 0.103 mL, 110 mg, 1.00 mmol) was added dropwise to a solution of rhenium(VII) oxide (48 mg, 0.1 mmol) in THF (20 mL). This mixture was stirred

for 6 h at room temperature. Hexane (40 mL) was layered on the top and the mixture was kept at ca. –12 °C for 2 days. A dark solid, believed to be $\{MeReO(SPh)_3\}_2$, was obtained. Its yield by this formula was 54%. It was then dissolved in toluene (20 mL), after which ethane-1,2-dithiol ($edtH_2$, 25 μL, 28 mg, 0.3 mmol) was added. This resulting solution was stirred for 2 h, concentrated to 2 mL under vacuum, layered by hexane (20 mL), and held at –12 °C for 2 days. Yield: 39%.

**References**

1. Y. Wang and J. H. Espenson, *Organic Letters* **2**, 3525-3526 (2000).

2. Y. Wang and J. H. Espenson, *Inorg. Chem.* **41**, 2266-2274 (2002).

3. Y. Wang, G. Lente and J. H. Espenson, *Inorg. Chem.* **41**, 1272-1280 (2002).

4. R. H. Holm, *Coord. Chem. Revs.* **100**, 183-221 (1990).

5. C. G. Young and A. G. Wedd, *Chem. Commun.* 1251-1257 (1997).

6. C. G. Young, in *Biomimetic Oxidations Catalyzed by Transition Metal Complexes*, B. Meunier (Ed.), Imperial College Press, 2000, 415-459.

7. W. A. Herrmann, R. M. Kratzer and R. W. Fischer, *Angew. Chem., Int. Ed.* **36**, 2652-2654 (1997).

8. M. M. Abu-Omar and J. H. Espenson, *Inorg. Chem.* **34**, 6239-40 (1995).

9. M. M. Abu-Omar, E. H. Appelman and J. H. Espenson, *Inorg. Chem.* **35**, 7751-7757 (1996).

10. J. H. Espenson and D. T. Y. Yiu, *Inorg. Chem.* **39**, 4113-4118 (2000).

11. J. H. Espenson, X. Shan, Y. Wang, R. Huang, D. W. Lahti, J. Dixon, G. Lente, A. Ellern and I. A. Guzei, *Inorg. Chem.* **41**, 2583-2591 (2002).

12. J. Jacob, I. A. Guzei and J. H. Espenson, *Inorg. Chem.* **38**, 1040-1041 (1999).

13. J. Takacs, M. R. Cook, P. Kiprof, J. G. Kuchler and W. A. Herrmann, *Organometallics* **10**, 316-20 (1991).

14. J. H. Espenson, X. Shan, D. W. Lahti, T. M. Rockey, B. Saha and A. Ellern, *Inorg. Chem.* **40**, 6717-6724 (2001).

15. J. Jacob, G. Lente, I. A. Guzei and J. H. Espenson, *Inorg. Chem.* **38**, 3762-3763 (1999).

16. G. Lente, J. Jacob, I. A. Guzei and J. H. Espenson, *Inorg. React. Mechs.* **2**, 169-177 (2000).

17. G. Lente, X. Shan, I. A. Guzei and J. H. Espenson, *Inorg. Chem.* **39**, 3572-3576 (2000).

18. J. Jacob, I. A. Guzei and J. H. Espenson, *Inorg. Chem.* **38**, 3266-3267 (1999).

19. X. Shan, A. Ellern and J. H. Espenson, *Inorg. Chem.* ACS ASAP.

20. X. Shan, A. Ellern, I. A. Guzei and J. H. Espenson, *Inorg. Chem.* manuscript submitted.

21. R. Huang and J. H. Espenson, *Inorg. Chem.* **40**, 994-999 (2001).

# GENERAL CONCLUSIONS

Oxidation of $MeReO(edt)PPh_3$ with sulfoxides and also the reaction of MTO with 1,2-ethanedithiol give rise to the methyl transfer product, $ReO(\kappa^2\text{-edt})(\kappa^2\text{-edtMe})$. Although the structure of this product was unsolved, evidence from NMR, UV spectra for oxidation products by $H_2O_2$ and structure of further ligand displacement product of $ReO(\kappa^2\text{-edt})(\kappa^1\text{-edtMe})TPA$ all proved that the methyl group, originally on rhenium in $MeReO(edt)PPh_3$ or MTO, transfers to thiolate sulfur. Kinetic study of reaction of MTO with 1,2-ethanedithiol ($edtH_2$) was carried out in DMSO, showing first-order dependences on both concentrations of MTO and $edtH_2$. Based on kinetic data and literature study, a mechanism was proposed, which consists of a reduction methyl transfer followed by two condensation steps.

Methyloxorhenium(V) complexes with monoanionic bidentate ligands were synthesized and characterized as: $MeReO(PA)_2$, $MeReO(HQ)_2$, $MeReO(MQ)_2$, and MeReO(diphenylphosphinobenzoate)$_2$. $MeReO(PA)_2$ catalyzes the sulfoxidation of thioethers by pyridine N-oxides and sulfoxides. The rate law for the former reaction shows a first-order dependence on the concentrations of pyridine N-oxide and $MeReO(PA)_2$. Correlation analysis by the Hammett LFER method showed a substantial pyridine N-oxide substituent effect, giving a large negative reaction constant, $\rho = -5.2$. The step involving sulfides is behind the rate controlling step, which was explored with competition experiments, giving $\rho = -1.9$, which is consistent with a nucleophilic attack of sulfide on the M=O. A mechanism proceeding by way of two intermediates was proposed. The first intermediate contains an opened PA-chelate ring; this allows the pyridine N-oxide to access the primary coordination sphere of rhenium. The second intermediate is a *cis*-dioxorhenium(VII) species, which the thioether then attacks. Oxygen-18 experiments showed that the two oxygen atoms of the latter intermediate are not equivalent; only the "new" oxygen is attacked by, and transferred to, $SR_2$.

Ionic rhenium compounds, containing $MeReO(edt)(SPh)^-$, were prepared and one was crystallographically characterized. A hydrogen bonded (N–H···S) interaction was recognized in the crystal of the ionic compound. Ligand displacement studies of PhSH by $PPh_3$ and pyridines were carried out in chloroform. On the basis of kinetic data, a structural

formula was proposed to be the molecular species MeReO(edtH)SPh, which exists in solution and can react with a Brönsted base to accelerate ligand displacement. The fast replacement of PhSH of MeReO(edtH)SPh with pyridine N-oxides lead to a direct observation of two intermediates, MeReO(edt)OPy and $MeReO_2$(edt)OPy, which play key role in catalyzed OAT from pyridine N-oxide to phosphane. Formation of each intermediate showed a large substituent effects, $\rho = -5.3$ and $\rho = -4.3$.

Since ligand displacement play important role in OAT catalytic cycle, Ligand displacement of MeReO(dithiolate)Py and ReO($\kappa^2$-edt)($\kappa^2$-edtMe) with phosphanes were studied. In both cases, equilibrium was formed and equilibrium constants were evaluated. Unlike all of the equilibrium constants following the Hammett equation, rate constants deviate markedly from Hammett behavior. This common feature for both cases has been interpreted in terms of a two step mechanism for ligand substitution reactions of these complexes. The rate controlling step varies as the Lewis basicity of phosphanes changed.

Both five and six-coordinate methyloxorhenium(V) compounds were synthesized and characterized when tridentate chelating ligands were used. The kinetics of oxidation of these compounds in chloroform with pyridine N-oxides differentiates as the coordination number changed. For the more steric demanding six-coordinate compounds, smaller species, like water, methanol, and $Cl^-$, were found to be involved in the reaction instead of pyridine N-oxide, which directly attack the rhenium of the five-coordinate compounds.

Generally, two criteria are essential for syntheses of rhenium complexes, reduction of rhenium(VII) to rhenium(V) by oxidation of thiols, phosphanes and sulfides; stabilization of rhenium(V) by using mono, bi, tridentate ligands, which contain coordinated N, O, P and S atoms.

## ACKNOWLEDGEMENTS

I would like to thank Professor James H. Espenson for guidance over my graduate career and encouraging my further pursuit in chemistry.

I am also thankful for Dr. Andreja Baca, Dr. Weidong Wang and group members, both past and present, for their assistance on daily work and insightful scientific discussion.

I appreciate the help from my committee members, Professor Gordon Miller and Professor Nenad M. Kostic.

In particular, I would like to thank my wife Huiyan and parents for their continuous support, inspiration and understanding.

This work was performed at Ames Laboratory under Contract No. W-7405-Eng-82 with the U. S. Department of Energy. The United States government has assigned the DOE Report number IS-T 1969 to this thesis.